

2012

Innovative composite materials application in the design of seats and interior parts

Gerardo Alvino

Follow this and additional works at: <http://scholar.uwindsor.ca/etd>

Recommended Citation

Alvino, Gerardo, "Innovative composite materials application in the design of seats and interior parts" (2012). *Electronic Theses and Dissertations*. Paper 5355.

This online database contains the full-text of PhD dissertations and Masters' theses of University of Windsor students from 1954 forward. These documents are made available for personal study and research purposes only, in accordance with the Canadian Copyright Act and the Creative Commons license—CC BY-NC-ND (Attribution, Non-Commercial, No Derivative Works). Under this license, works must always be attributed to the copyright holder (original author), cannot be used for any commercial purposes, and may not be altered. Any other use would require the permission of the copyright holder. Students may inquire about withdrawing their dissertation and/or thesis from this database. For additional inquiries, please contact the repository administrator via email (scholarship@uwindsor.ca) or by telephone at 519-253-3000ext. 3208.

**INNOVATIVE COMPOSITE MATERIALS APPLICATION IN THE DESIGN OF
SEATS AND INTERIOR PARTS**

by

Gerardo Alvino

A Thesis

Submitted to the Faculty of Graduate Studies
through Mechanical, Automotive and Materials Engineering
in Partial Fulfillment of the Requirements for
the Degree of Master of Applied Science at the
University of Windsor

Windsor, Ontario, Canada

2012

© 2012 Gerardo Alvino

Innovative composite materials application in the design of seats and interior parts

by

Gerardo Alvino

APPROVED BY:

Dr. Sreekanta Das, Outside Program Reader
Department of Civil and Environmental Engineering

Dr. Peter Frise, Program Reader
Department of Mechanical, Automotive and Materials Engineering

Dr. Vesselin Stoilov, Advisor
Department of Mechanical, Automotive and Materials Engineering

Dr. Andrzej Sobiesiak, Chair of Defense
Department of Mechanical, Automotive and Materials Engineering

September 14th, 2012

DECLARATION OF ORIGINALITY

I hereby certify that I am the sole author of this thesis and that no part of this thesis has been published or submitted for publication.

I certify that, to the best of my knowledge, my thesis does not infringe upon anyone's copyright nor violate any proprietary rights and that any ideas, techniques, quotations, or any other material from the work of other people included in my thesis, published or otherwise, are fully acknowledged in accordance with the standard referencing practices. Furthermore, to the extent that I have included copyrighted material that surpasses the bounds of fair dealing within the meaning of the Canada Copyright Act, I certify that I have obtained a written permission from the copyright owner(s) to include such material(s) in my thesis and have included copies of such copyright clearances to my appendix.

I declare that this is a true copy of my thesis, including any final revisions, as approved by my thesis committee and the Graduate Studies office, and that this thesis has not been submitted for a higher degree to any other University or Institution.

ABSTRACT

The constant increase of petroleum price and the always more strict regulations regarding the emissions level and environmental impact are today the main leading factors that drive worldwide car makers to make efforts in the research of lightweight solutions in order to decrease the fuel consumption and, as a consequence, to reduce the CO₂ amount released in the atmosphere. In this work the attention is focused on innovative materials, such as thermoplastic composites due to their low density, easiness of manufacturing and possibility to be recycled. The case study is geared towards the design of interior components, and in particular to the substitution of a current rear seat back steel structure, meeting stringent weight and stiffness requirements. Abaqus software is used in the conduction of Finite Element Analysis of the component. Cost and manufacturing aspects of the proposed design solution are investigated in order to provide a detailed feasibility overview.

DEDICATION

To my family, Jackie, and all the best friends that always supported me.

TABLE OF CONTENTS

DECLARATION OF ORIGINALITY	iii
ABSTRACT.....	iv
DEDICATION	v
LIST OF TABLES	ix
LIST OF FIGURES	xii
NOMENCLATURE	xx

CHAPTER

I. INTRODUCTION TO LIGHTWEIGHT VEHICLE STRUCTURES AND PROBLEM STATEMENT

1.1. Introduction and problem statement	1
1.2. History of composite materials	8
1.2.1. Lightweighting in the automotive sector	9

II. LITERATURE REVIEW: COMPOSITE MATERIALS, THEIR MANUFACTURING, END OF LIFE TREATMENT (LCA AND RECYCLABILITY) AND MARKET TREND

2.1. New material concepts and future trend.....	11
2.2. An overview on composite world.....	12
2.2.1. Fibrous reinforcement.....	13
2.2.1.1. Glass fiber reinforcement	14
2.2.1.2. Aramid fibers reinforcement.....	14
2.2.1.3. Carbon fibers reinforcement	15
2.2.1.3.1. Automotive challenges due to carbon fibers	17
2.2.2. Matrixes and their properties	21
2.2.3. Processing of product forms: fabrics and performs	23
2.2.4. Sheet molding compound (SMC) preparation.....	24
2.3. Design and structural simulation with composite materials	26
2.4. Composite materials modeling	26
2.5. Manufacturing aspects during composites production	28
2.5.1. Molding processes.....	30
2.5.2. Compression molding process	31
2.5.3. Resin transfer molding (RTM) process	32
2.5.4. Injection molding process.....	34

2.5.5. Injection charge compression molding (ICCM)	37
2.5.6. Part Fabrication Method	38
2.5.7. New advanced processes: Quickstep and melding	40
2.5.8. Resin spray technology (RST) process.....	43
2.5.9. Endless-LongFiberThermoplastic process.....	45
2.5.10. Part design with sandwich structures.....	48
2.5.11. Honeycomb design solution	51
2.5.12. Sandwich structures with corrugated core	52
2.5.13. Nano-tubes technology	55
2.6. Methods of composites repair.....	57
2.7. Life cycle assessment	58
2.8. Composite recycling methods.....	61
2.8.1. Mechanical recycling method.....	65
2.8.2. Fiber reclamation methods	65
2.8.3. Pyrolysis treatment	66
2.8.4. Oxidation treatment	67
2.8.5. Other chemical treatments	67
2.9. European composites market.....	72
2.9.1. BMW and SGL group joint venture	73
2.9.2. Audi and Voith partnership	74
2.9.3. Joint development agreement between Daimler and Toray	75
2.9.4. Composite materials application in Volvo V70 model.....	76
2.9.5. Ford partnership with North America universities	77
2.9.6. Joint effort between Toyota and Toray.....	77
2.9.7. GM Daewoo, Hyundai, Chrysler and Max Forma Plastics	77
2.9.8. BASF efforts to reduce manufacturing steps.....	81

III. DESIGN AND NUMERICAL RESULTS

3.1. Material selection and properties description	82
3.1.1. Thermoplastic and thermoset resins as matrix.....	82
3.1.2. Thermoset composites available on the market.....	85
3.1.3. Assumptions for thermoplastic composites properties evaluation.....	88
3.2. Design steps and proposed solutions	91
3.3. F.e.m. simulations set up in Abaqus environment.....	97
3.3.1. Model validation and comparison with available results	99
3.3.2. Behavior of components in PVC resin	102
3.3.3. Tests performed on components with thermoset constituent material.....	102

3.3.4. Tests results for thermoplastic composite components and material optimization	107
3.3.5. Results summary.....	129
3.4. Component stress analysis.....	135
3.5. Stiffness evaluation for the target design solutions..	146
IV. MATERIAL COSTS ANALYSIS AND COMPONENT PRICE ESTIMATION.....	147
V. DELAMINATION AND FAILURE MODES OF COMPOSITE MATERIALS	
5.1. Introduction to delamination.....	152
5.2. Different approaches to delamination analysis	155
5.2.1. Fracture mechanics approach	155
5.2.2. Cohesive or damage zone model	156
5.2. Analysis of fracture and debonding of seat back structure	157
VI. CONCLUSIONS AND RECOMMENDATIONS.....	164
APPENDICES	
Appendix A: A guide to composites analysis in Abaqus environment	169
REFERENCES.....	180
VITA AUCTORIS	184

LIST OF TABLES

CHAPTER III: DESIGN AND NUMERICAL RESULTS

Table 3-1. Thermoplastic and thermoset resins mechanical and physical properties.....	84
Table 3-2. Physical and mechanical properties of thermosets by Performance Composites.....	85
Table 3-3. Physical and mechanical properties of thermosets with glass fiber filler by AGY.....	87
Table 3-4. Physical and mechanical properties of NPL thermosets with carbon fiber filler.....	87
Table 3-5. Summary of physical and mechanical properties of thermosets selected for analysis.....	88
Table 3-6. Physical and mechanical properties estimation for fibers used with thermosets.....	89
Table 3-7. Thermoplastics properties after fibers and thermoplastic PVC resin combination.....	90
Table 3-8. Results obtained testing some design solutions in PVC material.....	102
Table 3-9. Results collection for thermoset with Std CF by Performance Composites.....	103
Table 3-10. Results collection for thermoset with HMCF by Performance Composites.....	103
Table 3-11. Results collection for thermoset with E-glass fiber by Performance Composites.....	104
Table 3-12. Results collection for thermoset with Kevlar fiber by Performance Composites.....	104
Table 3-13. Results collection for thermoset with UD Std CF by Performance Composites.....	105
Table 3-14. Results collection for thermoset with UD HMCF by Performance Composites.....	105
Table 3-15. Results collection for thermoset with UD E-glass fiber by Performance Composites.....	105

Table 3-16. Results collection for thermoset with UD Kevlar fiber by Performance Composites.....	106
Table 3-17. Results collection for thermoset with Epoxy resin and ‘S’ type glass fiber by AGY.....	106
Table 3-18. Results collection for thermoset with BMI resin and ‘S’ type glass fiber by AGY.....	106
Table 3-19. Results collection for thermoset with Epoxy resin and HS carbon fibers by NPL.....	107
Table 3-20. Results collection for thermoset with Epoxy resin and HM carbon fibers by NPL.....	107
Table 3-21. Results collection for PVC thermoplastic with Std CF by Performance Composites.....	108
Table 3-22. Results collection for PVC thermoplastic with HMCF by Performance Composites.....	110
Table 3-23. Results collection for thermoplastic with E-glass fiber by Performance Composites.....	112
Table 3-24. Results collection for thermoplastic with Kevlar fiber by Performance Composites.....	113
Table 3-25. Results collection for thermoplastic with UD Std CF by Performance Composites.....	115
Table 3-26. Results collection for thermoplastic with UD HMCF by Performance Composites.....	116
Table 3-27. Results collection for thermoplastic with UD E-glass by Performance Composites.....	118
Table 3-28. Results collection for thermoplastic with UD Kevlar by Performance Composites.....	119
Table 3-29. Results collection for PVC thermoplastic with ‘S’ type fiber glass by AGY.....	122
Table 3-30. Results collection for PVC thermoplastic with HS carbon fibers by NPL.....	124

Table 3-31. Results collection for PVC thermoplastic with HM carbon fibers by NPL.....	126
Table 3-32. Force and weight results for solutions with optimal performance and productivity.....	129
Table 3-33. Force and weight results for solutions with optimal performance.....	130
Table 3-34. Force and weight results for solutions with optimal lightweight and productivity.....	131
Table 3-35. Force and weight results for solutions with optimal lightweight.....	133
Table 3-36. Force and weight results for open structure satisfying the requirement.....	134
Table 3-37. Stresses evaluation on the component subject to positive displacement.....	143
Table 3-38. Stresses evaluation on the component subject to negative displacement....	143
Table 3-39. Stresses evaluation in the positive direction with modified boundary conditions.....	144
Table 3-40. Stresses evaluation in the negative direction with modified boundary conditions.....	144

LIST OF FIGURES

CHAPTER I: INTRODUCTION TO LIGHTWEIGHT VEHICLE STRUCTURES AND PROBLEM STATEMENT

Figure 1-1. Actual rear seat back in steel with peripheral reinforcement.....	2
Figure 1-2. Actual rear seat back main dimensions.....	2
Figure 1-3. Constraints and displacement application points.....	3
Figure 1-4. Aluminum sandwich structure solution A.....	4
Figure 1-5. Aluminum extruded structure solution B.....	4
Figure 1-6. Actual seat back.....	5
Figure 1-7. Force versus displacement in positive direction.....	6
Figure 1-8. Actual seat back.....	6
Figure 1-9. Force versus displacement in negative direction.....	7

CHAPTER II: LITERATURE REVIEW: COMPOSITE MATERIALS, THEIR MANUFACTURING, END OF LIFE TREATMENT (LCA AND RECYCLABILITY) AND MARKET TREND

Figure 2-1. Carbon fibers diffusion trend for several applications.....	16
Figure 2-2. Mechanical and physical properties comparison.....	19
Figure 2-3. Weight saving table in different vehicle systems.....	20
Figure 2-4. Weight saving chart in different vehicle systems.....	20
Figure 2-5. Examples of woven fibers with different texture.....	23
Figure 2-6. Pre-pregs production process scheme.....	24
Figure 2-7. Fibers rolling during SMC production.....	25
Figure 2-8. Resin infusion during SMC process.....	25
Figure 2-9. Compression molding process schematic.....	32
Figure 2-10. Resin transfer molding process illustration.....	33
Figure 2-11. Resin transfer molding cycle time reduction.....	34
Figure 2-12. Injection molding Temperature-Pressure graph.....	34
Figure 2-13. Injection molding process pressure and temperature treatment curves.....	35
Figure 2-14. Injection molding cost per hour as function of clamp force.....	36
Figure 2-15. Injection molding process.....	36

Figure 2-16. Example of a part obtained with injection molding process.....	37
Figure 2-17. Part fabrication method system layout.....	39
Figure 2-18. Melding process system configuration.....	41
Figure 2-19. Melding process control software.....	42
Figure 2-20. Pressure and temperature values during melding cycle.....	42
Figure 2-21. Example of parts joining with melding process.....	43
Figure 2-22. Resin spray during RST.....	44
Figure 2-23. Creation of vacuum bag.....	44
Figure 2-24. Part placement inside a pressure vessel during RST process.....	44
Figure 2-25. Endless fibers reinforcement strips.....	46
Figure 2-26. E-LFT manufacturing process illustration.....	46
Figure 2-27. Mechanical properties enhancement due to E-LFT process.....	47
Figure 2-28. Endless fibers application as reinforcement along main load path.....	47
Figure 2-29. Example of E-LFT application on rear seat back structure.....	48
Figure 2-30. Train front shield.....	49
Figure 2-31. Sandwich thickness scheme.....	49
Figure 2-32. Test equipment used for sandwich structure analysis.....	50
Figure 2-33. Load-Stroke graph from experimental test at different speed.....	50
Figure 2-34. Example of sandwich structure failure between external skin and core.....	51
Figure 2-35. Honeycomb core.....	52
Figure 2-36. Honeycomb layers.....	52
Figure 2-37. Test in parallel direction.....	53
Figure 2-38. Test in perpendicular direction.....	53
Figure 2-39. Load curves during tests on sandwich structure.....	54
Figure 2-40. Numerical results in the test of a sandwich structure with Abaqus software.....	54
Figure 2-41. Comparison between experimental and numerical results.....	55
Figure 2-42. Nano-tubes deposition method on pre-preg plies.....	55
Figure 2-43. Nano-tubes visualization between composite plies.....	56
Figure 2-44. Toray LCA analysis for planes and cars in Japan.....	59
Figure 2-45. Toray investigation of CO ₂ production for planes and cars in Japan.....	60

Figure 2-46. Example of recycling system from material collection to business potential.....	64
Figure 2-47. Technologies of mechanical recycling and fiber reclamation.....	66
Figure 2-48. SEM comparison between clean recycled and recycled with char residue fibers.....	67
Figure 2-49. Mechanical properties of recycled and virgin carbon fibers.....	68
Figure 2-50. Re-manufacturing processes summary analysis.....	69
Figure 2-51. Fiber glass production in Europe between 2007 and 2009.....	72
Figure 2-52. Fiber glass production in European countries between 2007 and 2009.....	73
Figure 2-53. Light weight rear seat back solution by Audi on TT model.....	75
Figure 2-54. Rear seat back in GMT application on Mercedes E-Class.....	76
Figure 2-55. GMT solution for rear seat back design on Volvo V70.....	76
Figure 2-56. Rear seat back solution for Daewoo Lacetti.....	78
Figure 2-57. Rear seat back solution for Hyundai Avante XD.....	78
Figure 2-58. Rear seat back solution for Hyundai Tuscani.....	79
Figure 2-59. Rear seat back solution for Hyundai Grandeur.....	79
Figure 2-60. Rear seat back solution for Hyundai HD Avante.....	80
Figure 2-61. Rear seat back solution for Chrysler 300C.....	80

CHAPTER III: DESIGN AND NUMERICAL RESULTS

Figure 3-1. Simple flat panel model respecting geometry requirements.....	91
Figure 3-2. Flat panel and peripheral rib.....	92
Figure 3-3. Panel with outer and internal rib.....	92
Figure 3-4. Panel with ribs grid.....	93
Figure 3-5. Panel with triangular ribs.....	93
Figure 3-6. Open structure with corrugated panel and peripheral reinforcement.....	94
Figure 3-7. Sandwich structure with corrugated panel as internal core.....	95
Figure 3-8. Vertical corrugated structure.....	95
Figure 3-9. Horizontal corrugated structure.....	95
Figure 3-10. Corrugated sandwich structure.....	96
Figure 3-11. Corrugated and ribbed structure.....	96
Figure 3-12. Extruded aluminum solution re-modeling with Abaqus software.....	99

Figure 3-13. Results comparison between models for extruded aluminum structure.....	100
Figure 3-14. Reinforced aluminum extruded structure re-modeling with Abaqus software.....	101
Figure 3-15. Results comparison between models for reinforced extruded aluminum structure.....	101
Figure 3-16. Optimized thickness of Std CF thermoplastic for lightweight and productivity.....	109
Figure 3-17. Optimized thickness of Std CF thermoplastic for lightweight.....	109
Figure 3-18. Optimized thickness of Std CF thermoplastic for performance and productivity.....	110
Figure 3-19. Optimized thickness of Std CF thermoplastic for performance.....	110
Figure 3-20. Optimized thickness of HMCF thermoplastic for lightweight.....	111
Figure 3-21. Optimized thickness of HMCF thermoplastic for lightweight and productivity.....	111
Figure 3-22. Optimized thickness of HMCF thermoplastic for performance and productivity.....	112
Figure 3-23. Optimized thickness of E-glass thermoplastic for lightweight.....	112
Figure 3-24. Optimized thickness of E-glass thermoplastic for lightweight and productivity.....	113
Figure 3-25. Optimized thickness of E-glass thermoplastic for performance.....	113
Figure 3-26. Optimized thickness of Kevlar thermoplastic for lightweight and productivity.....	114
Figure 3-27. Optimized thickness of Kevlar thermoplastic for performance and productivity.....	114
Figure 3-28. Optimized thickness of Kevlar thermoplastic for performance.....	115
Figure 3-29. Optimized thickness of UD Std CF thermoplastic for lightweight and productivity.....	115
Figure 3-30. Optimized thickness of UD CF thermoplastic for performance and productivity.....	116

Figure 3-31. Optimized thickness of UD CF thermoplastic for performance.....	116
Figure 3-32. Optimized thickness of UD HMCF thermoplastic for lightweight and productivity.....	117
Figure 3-33. Optimized thickness of UD HMCF thermoplastic for performance and productivity.....	117
Figure 3-34. Optimized thickness of UD HMCF thermoplastic for performance.....	118
Figure 3-35. Optimized thickness of UD E-glass thermoplastic for lightweight and productivity.....	118
Figure 3-36. Optimized thickness of UD E-glass thermoplastic for performance and productivity.....	119
Figure 3-37. Optimized thickness of Kevlar thermoplastic for lightweight.....	120
Figure 3-38. Optimized thickness of Kevlar thermoplastic for lightweight and productivity.....	120
Figure 3-39. Optimized thickness of Kevlar thermoplastic for performance and productivity.....	121
Figure 3-40. Optimized thickness of Kevlar thermoplastic for performance.....	121
Figure 3-41. Optimized thickness of S glass thermoplastic for lightweight.....	122
Figure 3-42. Optimized thickness of S glass thermoplastic for lightweight and productivity.....	122
Figure 3-43. Optimized thickness of S glass thermoplastic for performance and productivity.....	123
Figure 3-44. Optimized thickness of S glass thermoplastic for performance.....	123
Figure 3-45. Optimized thickness of HS fibers thermoplastic for lightweight and productivity.....	124
Figure 3-46. Optimized thickness of HS fibers thermoplastic for performance and productivity.....	125
Figure 3-47. Optimized thickness of HS fibers thermoplastic for performance.....	125
Figure 3-48. Optimized thickness of HM fibers thermoplastic for lightweight and productivity.....	127
Figure 3-49. Optimized thickness of HM fibers thermoplastic for performance and productivity.....	127

Figure 3-50. Optimized thickness of HM fibers thermoplastic for performance.....	128
Figure 3-51. Force values graph for design solutions with optimal lightweight and productivity.....	131
Figure 3-52. Weight values graph for solutions with optimal lightweight and productivity.....	132
Figure 3-53. Load to weight ratio for the materials presenting best lightweight and manufacturing performance.....	133
Figure 3-54. In plane max principal stress distribution on front side for positive displacement.....	136
Figure 3-55. In plane max principal stress distribution on rear side for positive displacement.....	136
Figure 3-56. Maximum principal stress distribution on front side for positive displacement.....	136
Figure 3-57. Maximum principal stress distribution on rear side for positive displacement.....	137
Figure 3-58. S_{11} stress distribution for positive displacement.....	137
Figure 3-59. S_{22} stress distribution on front side for positive displacement.....	138
Figure 3-60. S_{22} stress distribution on rear side for positive displacement.....	138
Figure 3-61. S_{12} stress distribution for positive displacement.....	139
Figure 3-62. In plane max principal stress on front side for negative displacement.....	140
Figure 3-63. In plane max principal stress on rear side for negative displacement.....	140
Figure 3-64. Maximum principal stress distribution on front side for negative displacement.....	140
Figure 3-65. Maximum principal stress distribution on rear side for negative displacement.....	141
Figure 3-66. S_{11} stress distribution on front side for negative displacement.....	141
Figure 3-67. S_{11} stress distribution on rear side for negative displacement.....	141
Figure 3-68. S_{22} stress distribution on front side for negative displacement.....	142
Figure 3-69. S_{22} stress distribution on rear side for negative displacement.....	142
Figure 3-70. S_{12} stress distribution for negative displacement.....	142
Figure 3-71. Model of a joint allowing seat back folding.....	145

Figure 3-72. Maximum principal stress distribution on the rotation hinge.....	145
Figure 3-73. Force-Displacement trend for target design solutions compared to the current one.....	146

CHAPTER IV: MATERIAL COSTS ANALYSIS AND COMPONENT PRICE

ESTIMATION

Figure 4-1. Interpolation of carbon fibers cost per kilogram as a function of Young's modulus.....	148
Figure 4-2. Glass and Kevlar fibers cost per kilogram as a function of Young's modulus.....	148
Figure 4-3. Fibers cost per kilogram estimation for the selected materials.....	149
Figure 4-4. Thermoplastic and thermoset resins average cost per kilogram.....	149
Figure 4-5. PVC thermoplastic composites cost per kilogram considering plies production.....	150
Figure 4-6. Component price estimation for each of the selected materials.....	151

CHAPTER V: DELAMINATION AND FAILURE MODES OF COMPOSITES

MATERIALS

Figure 5-1. Inner delamination for flat (a) and curved (b) sections.....	152
Figure 5-2. Illustration of delamination failure modes.....	153
Figure 5-3. Mode II delamination crack formation (a), growth (b) and coalescence (c).....	153
Figure 5-4. Schematic of a double cantilever beam test device.....	154
Figure 5-5. Schematic of end-notch flexure test device.....	154
Figure 5-6. Schematic of a mixed mode test device.....	154
Figure 5-7. Energy release rate for Mode I, II and III.....	155
Figure 5-8. VCCT model finite element mode after crack propagation.....	155
Figure 5-9. Traction in the cohesive zone ahead of the crack tip.....	156
Figure 5-10. Comparison between physical and numerical cohesive model.....	157
Figure 5-11. Illustration of single end-notched specimen and its dimensions.....	159
Figure 5-12. Fracture toughness as a function of Young's modulus for several materials.....	160

CHAPTER VI: CONCLUSIONS AND RECOMMENDATIONS

Figure 6-1. Component weight comparison between steel and composites.....	165
Figure 6-2. Component stiffness comparison between steel and composites.....	165
Figure 6-3. Component price comparison between carbon, glass and Kevlar fiber composites.....	166
Figure 6-4. Safety coefficient comparison between carbon, glass and Kevlar fiber composites.....	167

APPENDIX A: A guide to composites analysis in Abaqus environment

Figure A-1. Abaqus software part creation window.....	169
Figure A-2. Example of sketch drawing.....	170
Figure A-3. Example of component design.....	170
Figure A-4. Composite material input data parameters.....	171
Figure A-5. Composite section creation command window.....	171
Figure A-6. Composite lay-up definition during section creation.....	172
Figure A-7. Regions selection to assign the desired section.....	172
Figure A-8. Independent instance creation window.....	173
Figure A-9. Static load step creation command window.....	173
Figure A-10. Independent mesh “seed” command window.....	174
Figure A-11. Mesh control definition in terms of shape, technique and algorithm.....	174
Figure A-12. Mesh elements definition default parameters.....	175
Figure A-13. Visualization of the component meshed with Quad elements.....	175
Figure A-14. Boundary conditions category and type definition command window.....	176
Figure A-15. Creation of boundary conditions selecting displacement and rotation.....	176
Figure A-16. Boundary conditions visualization on the component.....	177
Figure A-17. Edit job command window.....	177
Figure A-18. Output visualization for displacement field.....	178
Figure A-19. Command window for output evaluation in correspondence of nodes.....	179
Figure A-20. Output visualization for reaction forces on the whole structure.....	179

NOMENCLATURE

PE: Polyethylene
PP: Polypropylene
PS: Polystyrene
PC: Polycarbonate
PA: Polyamide
PVC: Polyvinylchloride
PAN: Polyacrylonitrile
PET: Petra Thermoplastic Polyester
ABS: Acrylonitrile butadiene styrene
Std: Standard
UD: Unidirectional
HM: High modulus
HS: High strength
vCFs: Virgin carbon fibers
rCFs: Recycled carbon fibers
CFRP: Carbon fibers reinforced polymers
GFRP: Glass fibers reinforced polymers
CAFE: Corporate Average Fuel Economy
DOE: U.S. Department of Energy
ANL: Argonne National Laboratory
 P_{acc} : Power required during acceleration
 P_{hill} : Power required to climb the hill
LCA: Life cycle assessment
 T_g : Glass transition temperature
 t_{cool} : Mold cooling temperature
SMC: Sheet Molding Compound
BMC: Bulk Molding Compound
GMT: Glass Mat Thermplastic
IM: Injection Molding

RTM: Resin Transfer Molding

E-LFT: Endless Long Glass Fiber Thermoplastic

ICCM: Injection Charge Compression Molding

AVACS: Advanced Volume Automotive Composite Solutions

RST: Resin Spray Technology

CNTs: Carbon Nano-Tubes

EoL: End of Life

FBP: Fluidized bed process

E_1 : Elastic modulus in the main direction

E_2 : Elastic modulus in the transverse direction

E_f : Fiber elastic modulus

E_m : Matrix elastic modulus

G_{12} : Shear modulus in the x-y plane

G_{13} : Shear modulus in the x-z plane

G_{23} : Shear modulus in the y-z plane

G_f : Fiber shear modulus

G_m : Matrix shear modulus

ν_m : Matrix Poisson ratio

ν_f : Fiber Poisson ration

ν_{12} : Poisson ratio in the x-y plane

ν_f : Fiber volume content

ρ : Density

F.E.M.: Finite Element Method

BCs: Boundary Conditions

U_1 : Displacement in x direction

U_2 : Displacement in y direction

U_3 : Displacement in z direction

UR_1 : Rotation around x axis

UR_2 : Rotation around y axis

UR_3 : Rotation around z axis

RF_1 : Reaction force in x direction

RF_2 : Reaction force in y direction
 RF_3 : Reaction force in z direction
 S_{11} : Principal stress in x direction
 S_{22} : Principal stress in y direction
 S_{33} : Principal stress in z direction
 S_{12} : Principal stress in x-y plane
 K : Module of stiffness
DCB: Double Cantilever Beam
VCCT: Virtual Crack Closure Technique
 G_c : Critical energy release rate
 G_I : Energy release rate for Mode I delamination
 G_{II} : Energy release rate for Mode II delamination
 G_{III} : Energy release rate for Mode III delamination
 G_T : Total energy release rate
 τ^0 : Maximum traction allowed before damage in cohesive zone model
 K_I : Local stress intensity factor
 K_{Ic} : Local threshold stress intensity factor
 σ_{tr} : Threshold stress before fracture
UTS: Ultimate Tensile Strength
 $\sigma_{MaxPrinc}$: Maximum principal stress
SC: Safety Coefficient

CHAPTER I

INTRODUCTION TO LIGHTWEIGHT VEHICLE STRUCTURES AND PROBLEM STATEMENT

1.1. Introduction and problem statement

The scope of this work is related to the investigation of new lightweight materials that would be able to reduce vehicle weight and as consequence a reduction in CO₂ emissions that can be considered the most important issue in order to respect the new environmental regulations, reduce the fuel consumption and increase the vehicle performance. Nowadays many car makers are investigating and trying to find new solutions in order to both satisfy the new standards and the customer's expectations. The research is focused on new kinds of composite materials with particular attention to thermoplastic composites due to their low specific weight and recyclability aspects. The main issues are related to the actual lack of knowledge in this field and the need of relevant investments in research and manufacturing for large scale production. All these advantages and drawbacks will be analyzed during the development of the project and the target will be to find the best compromise.

The first task will be to provide a general overview about lightweight solutions, their advantages and consequences; a short description about the material selection will be provided as well in order to choose the one presenting the best suitable properties for our purpose. Once the material is known the next step will be to select the production method; a list and a short explanation of the most common and also innovative processes is given. Before starting with the design phase and structural simulation a benchmark analysis has been conducted, whose purpose is to understand how different car makers are moving in this new field and which kind of solution are going to be adopted. This scenario will give a clear idea about what could be the future development and at the same time will help in deciding which strategies to adopt in the design. After a benchmark analysis of the materials provided by several companies the target will be to find suppliers able to provide material with the required properties in terms of weight, costs and mechanical properties.

The research will be mainly focused on composite materials made with carbon or glass fibers and polymeric matrix.

At this point the design phase can start. The component to replace is a rear seat back for a medium segment car. The current solution consists of a metal panel joined with a steel reinforcement running around the panel profile whose purpose is to increase the whole structure stiffness. Dimensions represent one of the first constraints, the maximum length and height should not exceed 550 mm thus allowing a surface area around 0.3 m² while the depth has to be lower than 30 mm. Other design parameters such as thickness, round corners and all available methods to improve stiffness are not constrained and so these solutions will be tested during the design phase with an iterative procedure according to the results obtained during simulation steps. Weight is the second constraint; the best case scenario would be to create a component lighter or at least not heavier than the current solution, with mass of 3.11 kg. Figures 1-1 and 1-2 give an illustration of the actual solution realized by Fiat Automobiles.



Figure 1-1: Actual rear seat back in steel with peripheral reinforcement

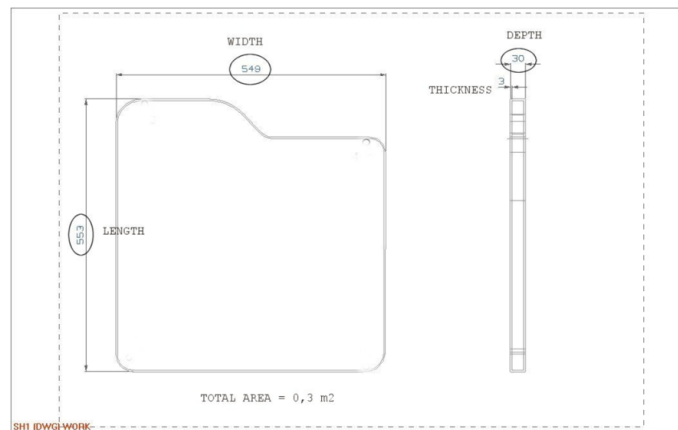


Figure 1-2: Actual rear seat back main dimensions

The component presented in Figure 1-1 is able to rotate along an axis passing through the lower points; this axis is better known as “Y axis” or “transverse axis” in the vehicle reference system. The right upper point represents a lock that when opened allows the seat folding. The upper left point is the force application point and will be discussed in details in the following section. The design phase will start from a simple flat panel as illustrated in Figure 1-3.

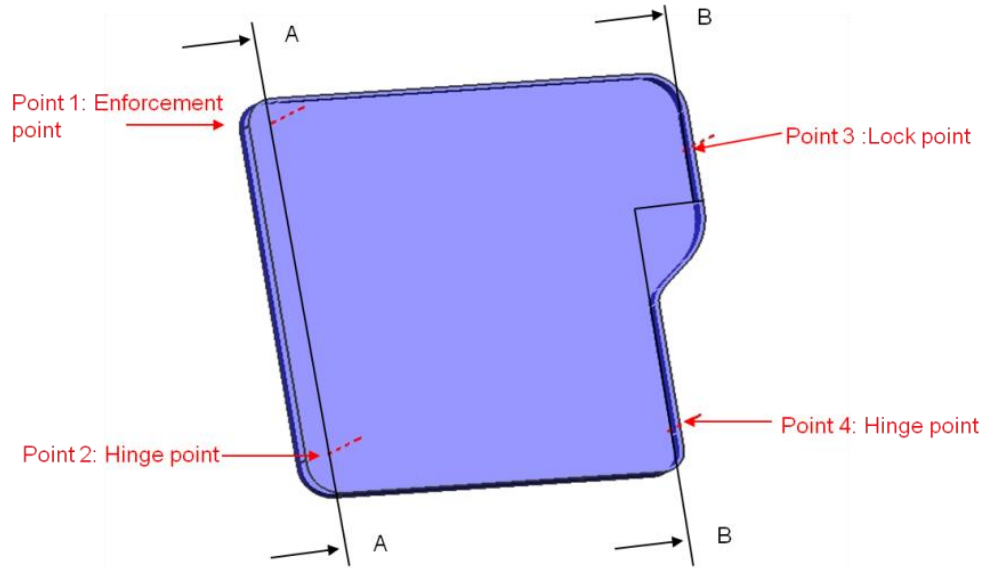


Figure 1-3: Constraints and displacement application points

Some solutions have been investigated by Fiat Research Centre (CRF) in the past and a list is presented below:

- ✓ Sandwich structure with external skins and aluminum honeycomb core
- ✓ Sandwich structure with external composite multi-layer with polyethylene PE matrix and fiber glass
- ✓ Sandwich structure with external steel skins 0.5 mm thick and honeycomb polypropylene PP core
- ✓ Extruded aluminum with peripheral aluminum reinforcements
- ✓ Frame obtained by using blowing process and PC or ABS as constituent materials
- ✓ PBT or PET thermoplastics with fiber glass reinforcement obtained via compression process
- ✓ Polypropylene tissue woven spun and warped and then manufactured through compression process.

Figures 1-4 and 1-5 give an idea of the solution described above for extruded aluminum case.



Figure 1-4: Aluminum sandwich structure solution A

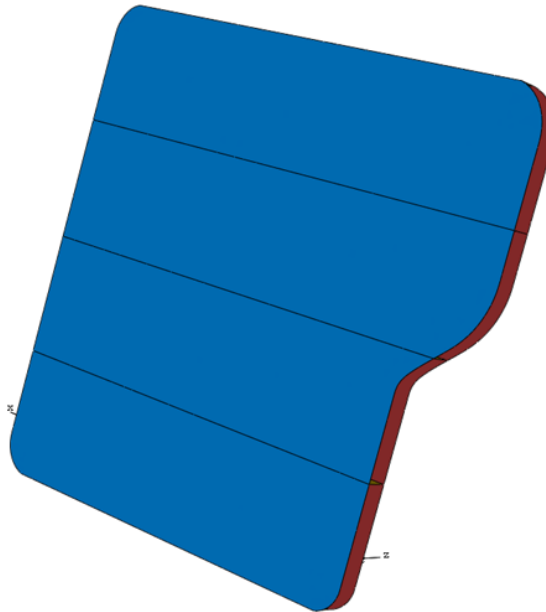


Figure 1-5: Aluminum extruded structure solution B

The solution A in yellow is made by two external skins plus an undulating panel in the middle; the overall weight is 7.49 kg with 3 mm thickness and 4.99 kg with 2 mm thickness. The example in blue is a sandwich structure with honeycomb core and 5.06 kg as weight with 3 mm thickness.

Both solutions comply with the stiffness requirements but not with the weight required since they are much heavier than the original solution with only 3.11 kg. Once a new solution will be designed and modeled the results have to be compared to the properties of the original component; in fact the main purpose of the research is to replace the whole original structure with a new one built in single piece of composite material without external reinforcements. The new design should be with reduced weight, having the same stiffness and to be produced in faster and cheaper way due to the fact that the new component is intended for high volume production. An overview about life cycle assessment and recyclability aspects will be provided in the following sections.

The mechanical response of the current model is experimentally measured as force versus displacement, and it is obtained at two different conditions. First applying a load in the upper left corner in order to allow a 100 mm displacement in both positive and negative direction with respect to the “longitudinal” or ”X” axis in the vehicle reference system as illustrated in Figures 1-6 and 1-7.

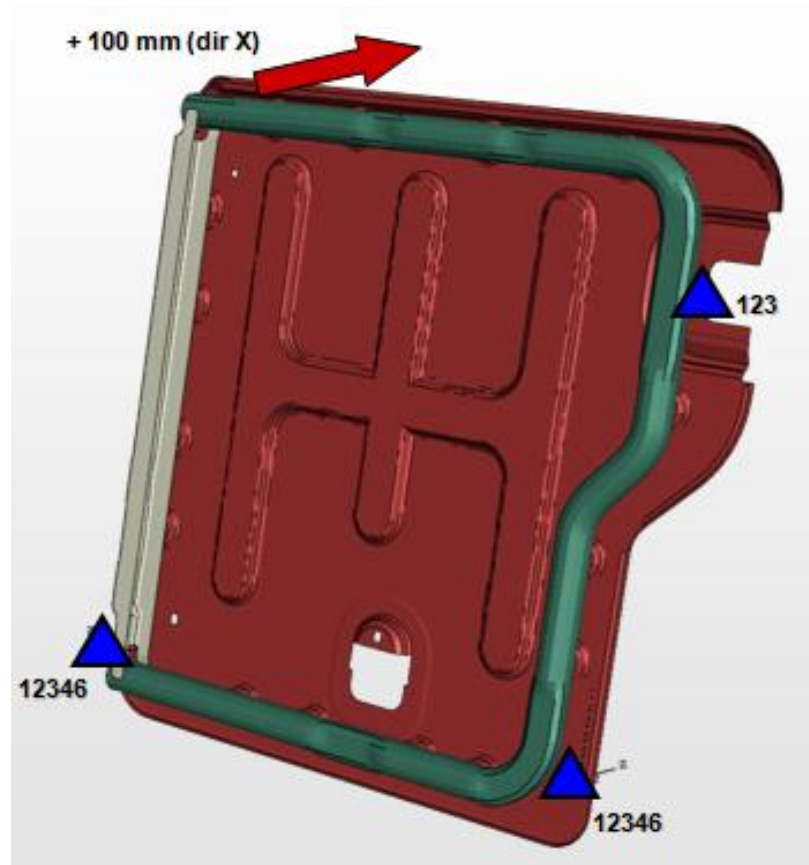


Figure 1-6: Actual seat back

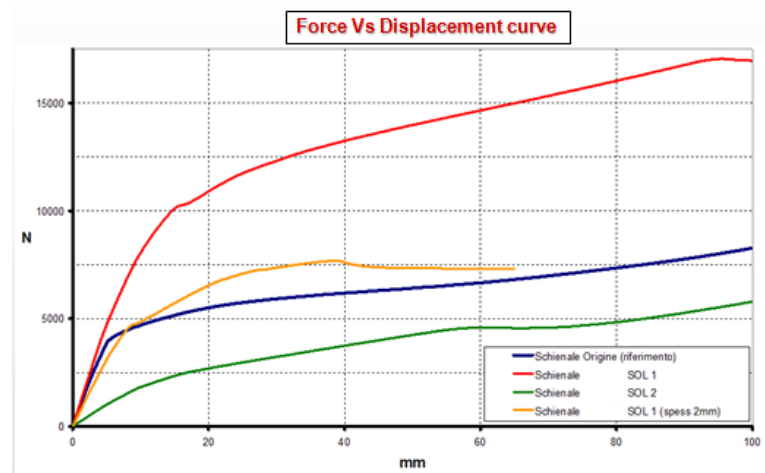


Figure 1-7: Force versus displacement in positive direction

The reference curve is the blue one for the current seat design and the maximum force value corresponding to 100 mm displacement in the positive direction is about 8,300 N. The red curve corresponding to the higher force and stiffness represents the undulated panel in the middle. However the weight of this design will exceed the target one. The green curve refers to the same solution but with lower thickness, 2 mm instead of 3 mm, but this time the values of the force and stiffness are too low and so not comparable to the original design. The yellow case refers to the blue sandwich structure; in the first stage the stiffness values are better than the original ones, but the component fails at 65 mm before reaching the required displacement. The results in Figures 1-8 and 1-9 come from the load application in the negative longitudinal direction.

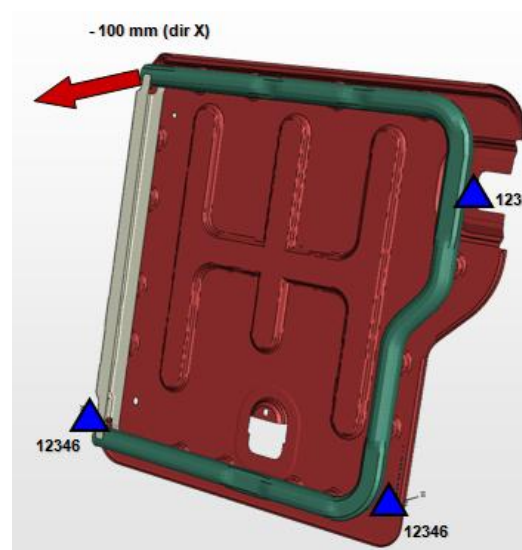


Figure 1-8: Actual seat back

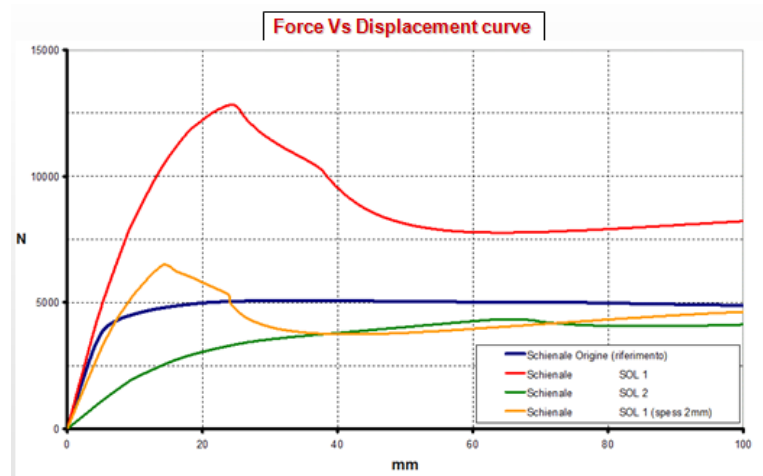


Figure 1-9: Force versus displacement in negative direction

The consideration in this case are the same as in the case of load applied in positive x direction; the only exception is that the final force values are lower in proposed solutions, in fact the maximum force value for the original design is around 5,000 N. The red curve reaches its maximum around 25 mm displacement and the curve in yellow does not show any failure in correspondence with 65 mm but reaches the final displacement even if with a force value lower than the original solution. In any case the values are almost always higher than the green curve.

For all cases present in Figure 1-9 the force versus displacement trend is not linear. The observed ductility is an important property to be considered in the production of metallic components, through stamping process for instance. At the same time the ductility and the corresponding toughness has to be considered in the case of impact, where high energy absorption and material deformation are desired. An example is the crash test for the rear seat back in accordance with the U.S. regulation; it consists in throwing a block at the rear side, and the test is considered successful if no failure in the component is observed.

Other two aspects should be considered to have a complete overview on the project; they are fatigue behavior and fire resistance that need experimental tests to be evaluated properly. Since it will not be possible to do this kind of work during the research they will not be discussed here.

1.2. History of composite materials

It is thought that the birth of composites in the automotive sector arises to 1953 when GM tried the first application in the Chevrolet Corvette which was the first car to employ structural polymer composites fiberglass as the body of the car. However, this solution was not suitable for high volume production at that time since the production process was relatively long, raw materials as resins and fibers were quite expensive and there were some difficulties to achieve high surface quality. Some issues related to stiffness, durability and UV ray degradation had to be considered as well.

The composite materials industry after more than fifty years is still limited in the adoption of structural composites in high volume car production. In the main part of automotive applications steel and aluminum alloys remain the best choice due to the deep knowledge level and the continuous innovation and improvements introduced by the manufactures during this time. The introduction of composites requires to identify and cross the critical technical barriers that could bring lightweight, durability and ease of formability in the automotive industry [1].

Lightweight is the key factor to reduce fuel consumption and at the same time CO₂ emissions. The transportation sector always requires more petroleum, compromising national security and creating a strong dependency on unstable geopolitical regions. For example, the United States imports 53 % while Europe imports 76 % of the needed petroleum from the Middle East. The same trend can be seen in developing countries as in the case of China that imports 30 % of its petroleum but the vehicle sales are increasing of 10 % every year and it will be higher than 50 % in the next years and so reaching the same conditions as Europe and North America. The global auto industry recognizes this need and because of this a lot of research and development have been done on cleaner engines, driveline efficiency and lightweighting. The adoption of high-strength steel, aluminum, magnesium, plastics and composites in different ways enables the achievement of modest weight saving, but more technical progress is necessary to improve fuel economy and reduce emissions. Hybrid-electric vehicles and fuel-cell drive systems are two examples of solutions on which car makers are focusing their attention. These solutions require many changes on the whole platform to be cost effective and so advanced composites represent a challenge in the near and midterm.

Advanced composites are engineering polymers presenting high performance reinforcements via fibers such as carbon. The industrial adoption has been limited for some of the following reasons:

- ✓ Lack of experience and knowledge in how to design with advanced composites
- ✓ High cost of the raw materials
- ✓ No affordable process for producing advanced-composite parts in high volume to automotive production standards [2].

1.2.1. Lightweighting in the automotive sector

The use of composites in the automotive industry is driven especially by lightweighting. The benefits differ according to the vehicle category. In the case of trucks for example a reduction in weight allows to increase the payload mass even if the overall mass remains the same. In the case of sports car a weight reduction means an increase in performance such as acceleration and top speed. For mass production vehicles the benefits can be classified in terms of fuel consumption and emission reduction. In order to reduce the greenhouse gas emission strict regulations have been introduced during the years. In 1975 CAFE (corporate average fuel economy) regulations were introduced in the USA; currently the CO₂ emission targets are 167.5 g/km in 2003, 140 g/km in 2008, and 120 g/km in 2012. The common opinion between car manufacturers is that the development of low emission engines will not be sufficient to meet the regulation targets. At the same time, zero emission engines such as fuel cells are far from high volume production; so the implementation of lightweighting materials and design has to play a key role in meeting the environmental regulations. In addition to light weight design other factors must also be considered.

- ✓ An optimum compromise between weight saving and additional cost (with a suggested threshold for the automotive sector of around 2.5 \$/kg)
- ✓ Passenger comfort, leading to heavier feature loaded vehicles
- ✓ High passive safety standards
- ✓ Class-A surface finishes
- ✓ Proven manufacturing technologies for body in white components.

During steady state driving conditions vehicles require only a small part of the available maximum power to maintain the speed. The maximum peak power is useful during acceleration and high-load driving conditions such as during passing maneuvers or hill climbing. The required power to achieve a given acceleration is determined by the vehicle's rate on change of the kinetic energy without considering other factors such as aerodynamic drag, rolling resistance and motor efficiency.

$$P_{acc} = 0.5m(v_1^2 - v_0^2)/t \text{ [1]},$$

where m is the vehicle mass, v_0 is the starting velocity, v_1 is the final speed and t is the time required to reach v_1 from v_0 . From this equation it can be seen that reducing the vehicle mass leads to a reduction in the required peak power. Mass has also a great contribution in determining the needed power during climbing; the effect is related to the potential energy variation.

$$P_{hill} = mgsin(\theta) \text{ [2]},$$

where g is the gravitational acceleration and θ is the angle of the incline. Rolling resistance is proportional to the mass. It can be assumed that by decreasing the vehicle mass by 50 % that compensates for the higher costs in the production of hybrid electric vehicles and fuel-cell drive system [2].

CHAPTER II

LITERATURE REVIEW: COMPOSITE MATERIALS, THEIR MANUFACTURING, END OF LIFE TREATMENT (LCA AND RECYCLABILITY) AND MARKET TREND

2.1. New material concepts and future trend

A list of future materials to be used in the automotive sector will now be presented. A new approach in material developing and evaluation is the life cycle assessment or LCA. This method keeps tracks of all stages of the product life of the material starting from raw material production until the end of the material life such as disposal, recycling or energy recovery. New composites based on natural materials provide an innovative solution in the LCA. The term natural was to be joined to the term environmentally friendly. For examples, polymers derived from plant oils, are potentially biodegradable and it is possible to improve their properties through genetic engineering. The negative aspect related to their use is in the application of toxic pesticides, quality control, and weather uncertainties.

One of the main issues in composites recycling consists in separating the reinforcement from the matrix. One adopted solution was to use the same material for both the matrix and the reinforcement as in the case of polypropylene with the same constituent fibers. Other solutions consist in orienting the material macro-molecules in certain a way. These materials are also known as “self-reinforced” and have the advantage of presenting molecular continuity and easy recyclability. Optimal development perspectives have been seen in carbon fibers; they have been recently employed in the aerospace industry and they found several applications especially in high performance cars where they present the principal structural material. The fluctuating price and the availability create some concerns regarding a wider industrial application and presenting a commercial risk in the vehicle production. In the resin fabrication system the addition of small hollow glass spheres has been studied to achieve a lower density and lower weight. The resulting composite has high surface finishing, paintability and high melting temperature. The limitations are driven by the difficulties of recyclability.

An emerging class of new composites is constituted by material based on nano-technologies such as carbon nano-tubes and inorganic nano-particles. They can be added to the conventional resins with the scope to create unique characteristics of mechanical and thermal properties, reduced flammability, and increase in thermal and electrical conductivity. Interesting application examples are the GMC Safari and the Chevrolet Astro 2002 vans that present a polypropylene material reinforced with clay nano-particles [1].

2.2. An overview on composite world

In order to better understand the function of this material class and their utility it is useful to discuss their main properties and characteristics. A composite material is constituted by two or more phases of different components so that it's possible to identify an interface at a macroscopic level. This definition enables identification of natural composite materials such as wood that is a cellulose fiber reinforced phenolic matrix, or other material used for construction such as reinforced concrete; in this case the steel rods act as fillers. The properties of a composite material are not only defined taking into account the physical and mechanical properties of each constituent, but also considering their concentration, shape, dimension, distribution and orientation. The discontinuous phase dimension is the main factor that allows to determine the entity of interface area between the components and has a principal role to describe their interaction and as a consequence to define the behavior of the composite material. These kinds of materials present properties completely different from those of the original components; in general sometimes a good relation to predict the properties is based on the weighted average of the properties related to each element and is called "rule of mixtures". Some interaction between the materials can make this rule invalid. Furthermore, the concentration does not have to be evaluated just considering the "composite average" since, even if the ratio between the materials is the same the concentration distribution can be different; this way there could be areas with different mechanical resistance or brittleness according to the concentration of reinforce or matrix. The reinforce orientation plays a fundamental role and can give an anisotropic behavior in the case of long fibers application with a certain preferential direction, or isotropic behavior when the reinforcement is uniformly dispersed inside the matrix as in the case of short fibers.

A common method to classify the composite materials is considering the form and orientation of the fibrous reinforcement, this way it's possible to distinguish between materials reinforced with fibers or particles.

The second category contains also materials with particles oriented randomly or preferentially. The most interesting category for the current application is given by composites with fibrous reinforcement [24, 28].

2.2.1. Fibrous reinforcement for composites

The main advantage of fibrous reinforcement is in its high specific resistance, that means a high resistance/weight ratio due especially to the fibers resistance and the low specific weight of the component materials. Experimentally can be proven that the material resistance increases considerably if it is produced in thin fiber form; different explanations exist for this phenomenon but it is mainly due to the specific characteristics of the material. For example, in the case of glass fibers the starting material presents an amorphous shape and when it becomes fiber the resistance increase is mainly due to the defect reduction in number and size. The fiber production allows a better defects control and so better mechanical properties. In crystalline materials the fiber production brings a preferred orientation of the crystals that stretch along the fiber orientation; this way the resistance increases in the direction along the fiber and the material shows anisotropic behavior. This phenomenon can be seen in both traditional materials such as steel, or carbon used to produce fibers for composites. In between the fibrous composites the most interesting category is the one of long fiber composites; in this case the fiber can be easily detected and have dimensions comparable to the one of the component they belong to. This way the applied load can be considered entirely along the fiber and completely supported by it. The matrix has the role to hold the fibers together, distribute the load and protect the fibers from the external elements. The resistance and the fracture are strictly linked to fiber characteristics. Usually long fiber composites are produced as laminas, then overlapped to form a laminate structure; a single lamina has thickness between 0.1 and 1 mm and cannot be used as structural element. So it's not only important to choose the composite but also the number of layers and their orientation; this way the material will be able to support the expected loads.

To produce laminates semi finished products called “pre-pregs” are adopted; they are made by thin laminas impregnated with not totally polymerized matrix. These products are then overlapped with fixed orientation (single-layer) or multiple orientations (multiple-layer) before they complete the polymerization phase at room temperature or with heating.

At the end of the polymerization phase laminates in composite material are obtained. With unidirectional fiber the material has anisotropic behavior; to overcome this problem it is possible to create multi-layers laminates with overlapped laminas according to the main loads directions; sometimes tissues with intertwined fibers can be created and are called “woven-fabrics”. Each solution has been studied according to the advantages that can be carried for the particular application. In composite materials production different kinds of fibers can be used and the most common are listed below.

2.2.1.1. Glass fibers reinforcement

Glass fibers have high resistance (almost twice that of the best steels), good stiffness (similar to aluminum), low cost, low electrical and thermal conductivity, high maximum operation temperature between 500 and 1000 °C.

In the composite production two different kinds of glass fiber exist:

- ✓ E-glass: The most employed due to the lower cost; made by 50 % silica, 15 % alumina, calcium and boron oxides. It has low electrical conductivity and was adopted for electrical purpose; this is the reason why it is called “E”.
- ✓ S-glass: Made by 65 % silica, 25 % alumina and 10 % magnesia. “S” stands for high strength.

Other special types of fibers are used for dedicated scopes.

2.2.1.2. Aramid fibers reinforcement

Aramid fibers are constituted by molecular chains with amidic joints with aromatic rings. They have optimal mechanical properties under tension, good resistance to chemical agents, excellent toughness and creep resistance. Being polymers, they have a very low specific weight; even lower than carbon fibers. Kevlar fibers are in between the best aramid fibers, presenting optimal mechanical properties, good impact resistance but very high cost.

2.2.1.3. Carbon fibers reinforcement

Carbon fibers have high resistance, a little bit less than glass fibers, but at the same time higher stiffness. They have high thermal and electrical conductivity and very good corrosion resistance. The negative thermal expansion coefficient allows them to have thermal dilatation equal to zero.

These materials are expensive but their diffusion in the market is increasing always more not only in aerospace but also in automotive and civil applications. The higher cost is due to the production process for the fibers that will be briefly described.

The starting point to produce carbon fibers is given by organic substances precursors rich in carbon. The most common precursors are rayon, polyacrylonitrile (PAN) and pitch. The production phases from rayon or PAN are almost identical. The fibers obtained from PAN have lower cost and so are more competitive on the market. Independently from the starting material the following production phases can be defined:

- ✓ Spinning
- ✓ Stabilization to avoid fibers melting in the next high temperature steps; the temperature depends on the base material adopted
- ✓ Carbonization (1000-1500 °C), to remove element different from carbon inside the molecular chain
- ✓ Graphitization (2700-2800 °C), to increase the carbon amount in crystalline state and hexagonal form.

It should be kept in consideration that to orient different graphite layers along the fiber axis all processes are performed with tensile loads with variable magnitude according to the starting material. Carbon fibers are also easily flammable and have high electrolytic potential; higher than aluminum. This is the reason why attention has to be paid to presence of corrosive agents. Two types of carbon fibers can be distinguished; each one showing particular characteristics suitable for dedicated applications:

- ✓ High Strength fibers: High resistance up to 7000 MPa, 10 times higher than a good steel
- ✓ High Modulus fibers: High stiffness up to $E = 960,000$ MPa, 5 times higher than steel.

Composite materials and carbon fibers (CFs) in particular, are subject to a tremendous surge in industrial usage. The CF industry is predicted to continue to have a strong growth for the next 4–5 years. Much of this growth has been sponsored for defense applications and commercial aircraft programs from Airbus, SAS and Boeing Company. Non-aerospace CF markets are also growing rapidly and applications will surely increase beyond high-end sporting goods, construction, and civil engineering. The automotive industry in particular is a large attractive potential market for car makers and suppliers. However, the CF industry as it currently exists is not properly structured to infiltrate the automotive industry [2]. Figure 2-1 represents the carbon fiber trend over the period from the introduction in the 70's until the future predictions in 2020 [4]. In the next years a tremendous expansion, especially for industrial application, is expected.

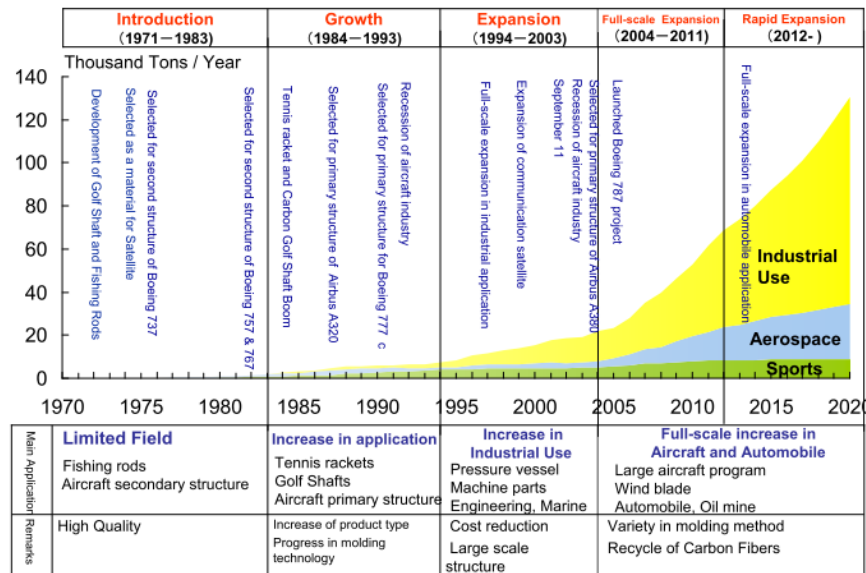


Figure 2-1: Carbon fibers diffusion trend for several applications [4]

Aerospace-grade carbon fibers of 4 to 7 GPa tensile strength and 275 GPa to 413 GPa modulus are in the range of 33 to 110 \$/kg (USD). While standard-grade carbon fibers of 3.8 to 4.5 GPa tensile strength and 220 to 250 GPa modulus are available at 15 to 30 \$/kg, the need is great for higher performance at lower cost [34].

The main factor that limited carbon fibers use in the automotive industry was the variable and unstable price. The Freedom CAR program has been promoted by the U.S. Department of Energy's (DOE) with the main purpose to find low-cost carbon fibers during the material research.

Both aluminum and magnesium offer probability of weight reduction but only carbon fibers can guarantee to reach weight saving up to 50 % in the construction of body and chassis components.

These improvements can bring up to 30 % reduction in fuel consumption, improve the ease of assembly and improve the safety.

Many industrial partners take part in the program and the investments are more than 8 million dollars every year. The program target is to develop high volume carbon fiber production with a price range varying from 6.6 and 11 \$/kg (USD).

Some requirements on the mechanical performance have to be achieved; in particular 1.72 GPa tensile strength, 172 GPa modulus, and 1% strain to failure [2].

2.2.1.3.1. Automotive challenges due to carbon fibers

Although prohibitively high, CF cost is often considered as the most difficult challenge that must be overcome before carbon-fiber-reinforced polymers (CFRP) can be widely adopted in the automotive sector, there are several other technical and market barriers that must be overcome:

- ✓ Supply chain maturity; long-term stable prices and supply
- ✓ Increased confidence and experience with CFRP design (design data, analytic tools)
- ✓ Development of robust joining, testing, and non-destructive evaluation techniques
- ✓ Development of short cycle time, high yield, molding technology
- ✓ Demonstration of cost-effective recycling/recovery and repair methods.

Carbon fibers reinforced polymers represent an attractive for designers in the study of structural automotive part, but a great competition exists with other materials such as aluminum and magnesium that have been studied and tested during the years, thus having high affordability about the design, fabrication, assembly and recycling that constantly improve. Recent data shows that aluminum use in North America automotive industries surpassed iron with an average of 14 kg application per vehicle. About magnesium the current application is between 4.5 and 5.4 kg per vehicle, but the trend is expected to increase by 5-7 %. China emerged in the recent years as a low cost magnesium producer and so this material application is expected to extend beyond the automotive field.

The DOE is spending several million dollars per year on research in support of automotive magnesium utilization.

Several high profile automotive applications are already in production: the front fenders and floor of the Corvette Z06, BMW M6 roof, Dodge Viper front fender support, Ford GT rear deck lid inner structure, Goodyear Eagle tires, and also numerous cosmetic and trim pieces that are available in the after-market [3].

More applications such as drive shafts, spoilers, A-pillars, underbody structures, and various body panels are adopted on other high-performance, low-volume cars. These exclusive, high-performance vehicles provide automotive design experience and, importantly, a growing base of knowledge with issues during the usage.

These examples refer to a vehicle production volume lower than 20,000 units /year and so they provide a negligible or small improvement to the carbon fiber future market. Increasing the carbon fiber volume during the years the cost is expected to be reduced to a range from 2 to 10 \$/kg [3]. Advanced composites, such as carbon fibers reinforced polymers, represent the most logical replacement for steel in vehicle structures where significant weight reduction greater than 60 % is desired to be achieved.

As said previously the two most widely diffused obstacles to the use of carbon composites in automotive structures are the high cost of the raw materials in between 11 and 22 \$/kg compared to 1.3 \$/kg for steel, and the high labor required to produce advanced composite parts. Cost is a key challenge factor in all of automotive design, especially for composites.

In the past despite their higher materials costs relative to steel, plastics and composites have been justified since their application was limited to non-structural or semi-structural components due to fabrication or assembly cost savings achieved typically through parts consolidation, less expensive tooling, and direct and indirect cost savings resulting from lighter weight.

A similar case can be made for using advanced composites in the vehicle's main structure. In a car body, the main design criteria are based on stiffness, as the body typically has adequate strength if it respects its stiffness and stability targets.

Thus, the best alternatives to steel considering a cost per unit specific stiffness perspective are carbon fiber composites and aluminum.

Although its cost per specific stiffness is higher than aluminum's, other important factors such as overall weight savings potential, cost savings for parts consolidation, functional integration, and lower tooling and equipment costs make carbon composites potentially cost-competitive in many applications. Figure 2-2 summarizes the properties of stiffness, density and cost for steel, aluminum glass and carbon fiber composites.

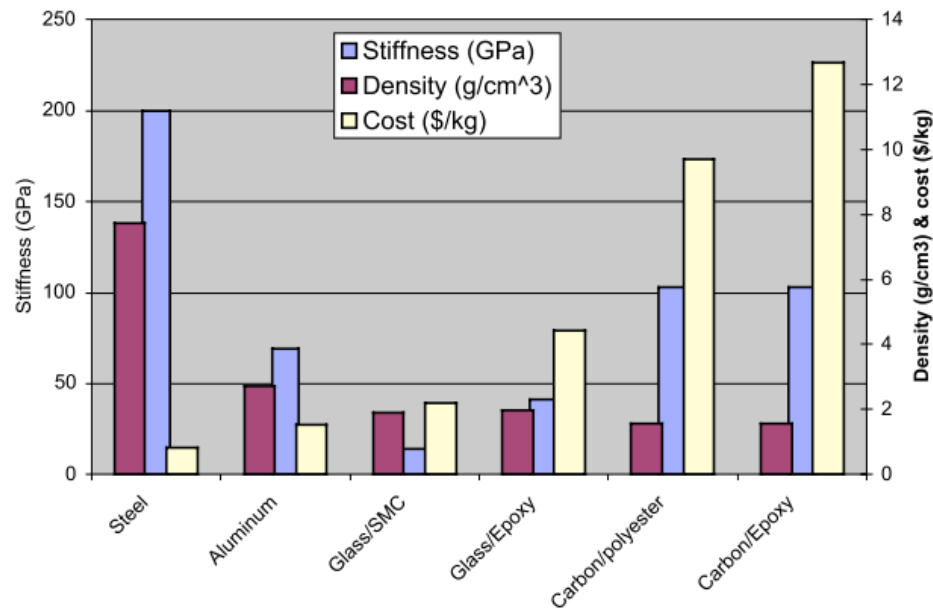


Figure 2-2: Mechanical and physical properties comparison [3]

Steel presents the best values of stiffness and cost but the highest density values; on the contrary carbon fiber composites have very low density, medium stiffness but very high cost. Aluminum and glass fiber composites have properties in between those of steel and carbon fiber composite.

An example of weight improvement is showed in hypercar project where every system is significantly lighter than conventional systems. Different techniques were used for each system to achieve this type weight savings. The body structure achieved almost 60% mass reduction compared to steel by using a combination of carbon fiber composites, aluminum, and unreinforced thermoplastic. Carbon fiber composites were used in the passenger safety cell and in dedicated composite energy absorbing members. Aluminum was used primarily in a front-end sub-frame, and unreinforced composite panels form the vehicle's skin.

The aluminum sub-frame and plastic skin are made with standard production techniques and will thus not be discussed in detail here. All the improvements are presented in Figure 2-3.

System	Benchmark mass (kg)	Revolution mass (kg)	Difference (%)
Structure	430	186.5	-57 %
Propulsion	468	288.3	-38 %
Chassis	306	201.2	-34 %
Electrical	72	33.4	-54 %
Trim	513	143.2	-72 %
Fluids	11	4.1	-63 %
Total	1,800	856.6	-52 %

Figure 2-3: Weight saving table in different vehicle systems [3]

The same data can be visualized in form of pie graph in Figure 2-4.

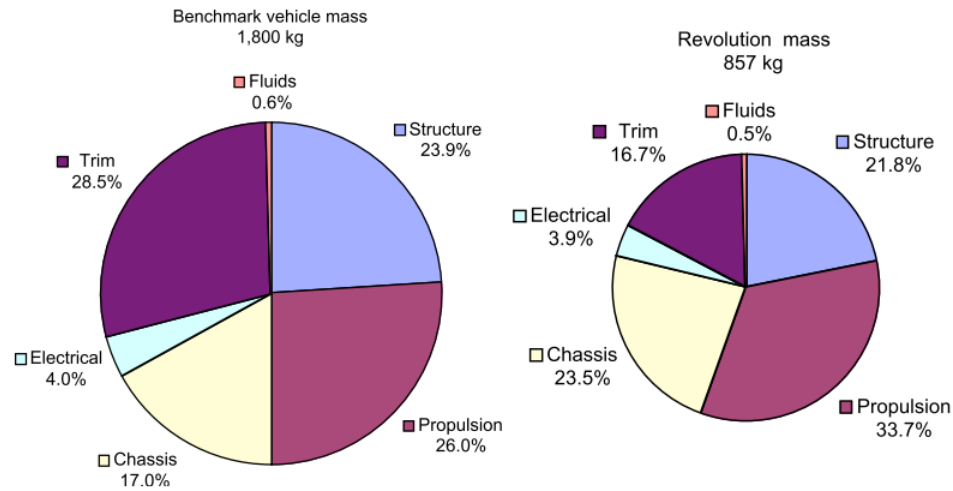


Figure 2-4: Weight saving chart in different vehicle systems [3]

The weight improvement range lies in between 34 and 72 %. The challenge in using lightweight materials is cost effective. As carbon fiber composites cost significantly more per kilogram and per unit stiffness than steel, cost savings must be found in the structural design and manufacturing methods in order to make composites economically feasible. The design strategy that Hypercar project adopted consists in minimizing the total amount of material following its idea of ensuring most effective use of the material used through concentrated, highly effective use whenever used; then simplifying assembly, tooling, parts handling, inventory, and processing costs through design.

2.2.2. Matrixes and their properties

Only fibers are not able to support compression or shear loads and so they could not have structural utility if not surrounded by a material that would act as a matrix in order to create a composite material. The matrix functions are listed as follow:

- ✓ Keep the fibers joined each other
- ✓ Transfer the outside load to the fibers
- ✓ Protect the fibers from environmental factors such as UV rays, corrosion etc.

According to the final purpose different categories of materials can be used as matrixes, for example:

- ✓ Polymer-matrix composites or PMCs
- ✓ Metal-matrix composites or MMCs
- ✓ Ceramic-matrix composites or CMCs

Initially MMCs were developed to improve the mechanical properties of traditional metals; they are mainly made by isotropic materials who present dispersed particles or short ceramic fibers inside the metal matrix. These materials have very high cost. CMCs are employed to resist in high temperature environments.

The most interesting category is the PMCs. The presence of polymers decreases the mechanical resistance with respect to the fibers, but gives the advantages of good corrosion resistance, low specific weight and easier formability. Even if the polymer decreases the resistance, the overall resistance is higher than the traditional materials. The polymers used as matrixes can be thermoplastics or thermosets; in prototype production only thermoset resins are used and these can be listed according to the chemical composition:

- ✓ Polyester resins
- ✓ Vinyl ester resins
- ✓ Epoxy resins
- ✓ Phenol resins
- ✓ Polyamide resins
- ✓ Silicon resins.

Polyester resins are among the most common used polymers, they are produced through polycondensation process and can have variable molecular weight and composition since can be produced starting from different raw materials and different reticulation agents.

The advantages can be summarized as follows:

- ✓ Low viscosity: Allows to easily complete the fiber reinforcement impregnation process
- ✓ Easy manufacturing
- ✓ Low cost, especially with respect to epoxy resins
- ✓ Possibility to stock pre-impregnated tissues due to lower reaction than epoxy resins.

The main problems in using this kind of material is dimension change between 4 and usually 8 percent that cannot be neglected. This issue can be overcome with an accurate mold design that takes into account the shrinkage effect too.

Epoxy resins are the most commonly used in composites with high mechanical properties and can be treated at temperatures and pressures not very high. The main features are:

- ✓ High mechanical and fracture resistance
- ✓ Optimal joint between fiber and matrix, that means high delamination resistance
- ✓ Resistance to chemical agents better than the other thermoset resins
- ✓ Shrinkage values lower than 2 percent.

Epoxy resins have higher viscosity than polyester resins and so are more difficult to manufacture; which is associated with higher costs. This is the reason why their usage is limited to those applications in which more care is given to the weight performance rather than the cost as in the case of aerospace applications.

Vinyl ester resins reach the compromise between manufacturing (typical of polyester resins) and mechanical properties (as for epoxy resins); the shrinkage however can reach around 5 to 10 percent.

Thermoplastic resins, known as thermo-softening plastics, can be in a liquid state when heated or solid state if cooled under a certain temperature. In contrast with thermosets they can be melted and molded several times which makes them recyclable. The process varies according to the material type. They become elastic and flexible for temperatures equal or higher than the glass transition temperature T_g .

Semi-crystalline thermoplastic have a portion of their volume that is with a crystalline morphology while the remaining volume is amorphous and has a random molecular orientation. Representatives of these materials are PE, polypropylene PP and polyamide PA. They can be produced in this films, powder or filaments and can be used in processes as compression or injection molding. These materials show good mechanical properties and high impact damage resistance. The material and tooling costs are higher than epoxy resins, but due to the faster production process the end product cost is lower. This material is treated at temperatures between 260 and 370 °C, so care should be taken to mold design with pressure values higher than 34 MPa in case of stamp molding. These materials offer several options to be joined, such as ultrasonic welding, infrared heating, vibration, hot air and gas, resistance heating, melding or conventional adhesives. The amorphous thermoplastics have random molecular orientation and can be manufactured the same way as crystalline plastics. Their properties are quite close with the exception of a higher melting and glass transition temperature in amorphous resins [24, 28].

2.2.3 Processing of product forms: fabrics and preforms

There are several ways to manufacture both fibers and matrixes and the most common are fabrics and preforms. Woven fabrics are produced before the impregnation step, they offer good opportunities to create complex shape lay-up with better mechanical properties than the unidirectional types. Usually the fibers used are the same in both longitudinal and transverse direction. The production process for a fabric layer consists of putting each fiber up and then under another one alternating in order to create a fabric. The length of each intertwining can vary according to the specific design as can be seen in Figure 2-5.

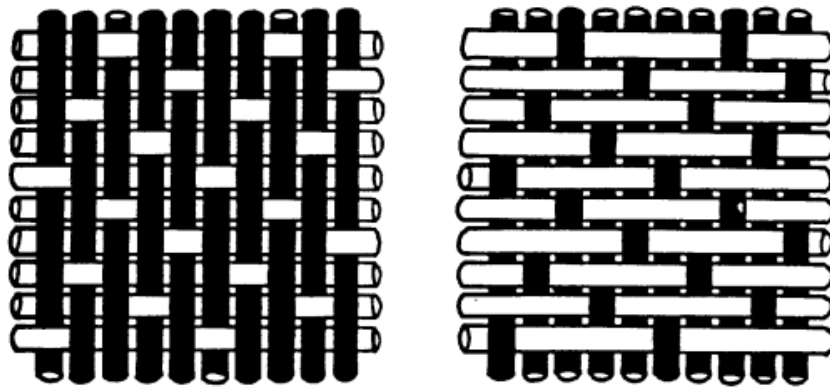


Figure 2-5: Examples of woven fibers with different texture [24]

The production of preforms consists of placing raw fibers with unidirectional orientation as a continuous strand. The next step is spreading the not completely cured resin whose purpose is to create a joint between all the fibers and then to have the tape of the final product. A special machine provides heat and pressure in order to keep the fibers aligned, inserts the melted resin and controls the thickness and resin distribution. A visual inspection helps to identify defects on the line.

Figure 2-6 gives an idea of pre-pregs production process [24].

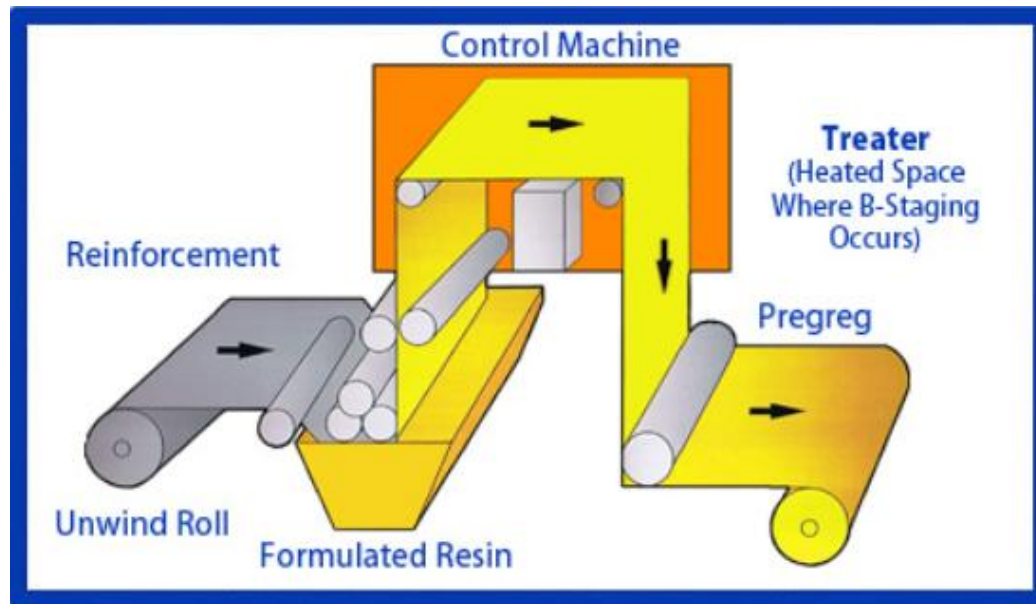


Figure 2-6: Pre-pregs production process scheme [24]

2.2.4. Sheet molding compound (SMC) preparation

In compounding process a selected glass fabric is fed into a SMC compounder between one or two resin layers. The SMC works the resin into the fabric, and in a few days after maturation a moldable material is available. The selected material is a glass fabric that has 0/90 degree oriented fibers. The material is compounded on a standard SMC compounding machine, except that the glass chopper was replaced with a roller for the fabric. One main issue in the SMC is keeping the fiber bundles that run perpendicular to the compounder straight during the compounding.

If the strand alignment during roll winding had accumulated an off-angle error, this off-angle is an input to the roll feeding into the compounder where it is very hard to correct.

Figure 2-7 provides an example of roll placement with the correct angle and direction.



Figure 2-7: Fibers rolling during SMC production [20]

In Figure 2-8 the fiber roll has been stretched and impregnated with the resin.

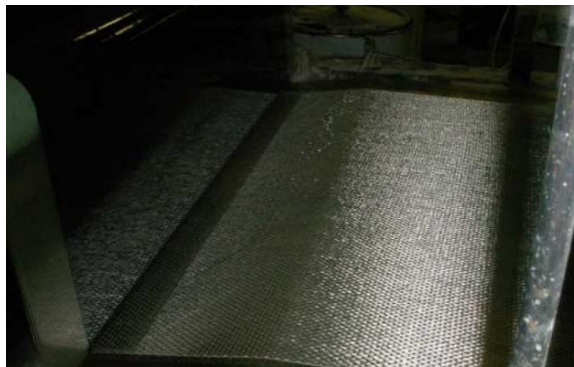


Figure 2-8: Resin infusion during SMC process [20]

Another issue in the SMC process is maintaining the correct proportion between resin and fabric. For compounding a structural fabric material it is necessary to use the minimum resin needed to fully wet the fabric, which proved to be a very delicate balance. The compounded material needs a minimum of 48 hours to mature and then it can be shipped for molding. It is possible to lay out templates on the compounded sheet and cut the charges by hand. This solution is extremely slow, but it allows to optimize the patterns, including trimming the edges and also wrinkles or overlaps. Charge preparation can be improved by automating the cutting of the charges. The plies can be sealed in styrene-resistant bags, and shipped for molding [20].

2.3. Design and structural simulation with composite materials

When composite materials were introduced to the automotive industry, they were not always completely appreciated by designers. Traditionally, the automotive sector has adopted isotropic sheets of metal that are joined by welding processes.

Composites, on the contrary, require specific knowledge of both the materials and the manufacturing processes if the opportunities they present in terms of functional integration, lightweighting, and styling freedom are to be properly exploited.

It is important that vehicle designers understand composite manufacturing processes and how they relate to the components they are going to develop. In the first days of composite use, there was often a big gap between the expectations of the vehicle designers and those of the composite manufacturers, and this often resulted in the poor use of materials and delays in production.

Nowadays, a major challenge relating to automotive composite design is the availability of simulation tools and a general lack of composite material characterization. Another drawback is the computational time required to model composite structures and components. The most of composite material models within commercial design software require very long solution times. These times are usually too long for the first phase of vehicle development, during which many different options have to be analyzed in a period of just a few months.

For composites to be properly evaluated at these beginning stages, the automotive industry needs a factor of ten reduction in solution times. The commercial software developers have not yet solved this problem, so some of the more advanced research and design centers are developing their own methodologies, which usually remain confidential. In summary, the automotive designers of today have an understanding of composites but there is a lack of a proper simulation software for all design phases [1].

2.4. Composite materials modeling

Modeling and numerical simulation are fundamental aspects of today's automotive sector. They are useful in order to reduce the time-to-market for new products and the costs associated with experimental testing. There are two general zones in which simulation is conducted and they are vehicle design and manufacturing processes.

In terms of vehicle design, the automotive sector has been undertaking structural analyses (static, dynamic, safety, noise and vibration, handling, etc.) for many years. During the time, models have increased in their precision and accuracy, but until recently they have only involved metals and a few polymer components.

The latter, in the most of cases, have only been modeled as isotropic materials. However, as the use of structural composite materials in the automotive sector has increased especially for sports cars, it has now become necessary to model composites with more accuracy. To a certain extent, the automotive industry has been able to pull out the experiences of the aerospace sector.

However, in many cases the materials and design targets are sufficiently divergent that a direct technology transfer is not always convenient. While modeling composites, one of the key challenges is to balance the sophistication of the materials models against reasonable computational solution times.

The composite manufacturing processes that are currently used for medium to high volume automotive production are injection molding (IM), Glass Mat Thermoplastic (GMT), Sheet Molding Compound (SMC), and Resin Transfer Molding (RTM) and are all supported by numerical codes and it is possible to simulate them.

It should be remembered that high volume production requires the best kind of optimization in order to reduce cycle time, scrap and the number of rejected parts. In the example of vehicle designers, the process analyst has to face the twin problems of material characterization and solution times.

One of the difficulties with material characterization consists in creating new materials. In terms of solution time computing power has increased, so have the quality, precision and size of the process models. In general, there is no doubt that the importance of modeling and simulation in the automotive sector will continue to increase [1].

2.5. Manufacturing aspects during composites production

Manufacturing is an issue for composites in the automotive sector when the high production volume required has to be considered. One of the reasons why composites are not widely used in mass production automotive applications is the cost of the raw materials, but the main reason is the lack of suitable manufacturing processes.

Currently, the choice of manufacturing process is driven strongly by the required rate of production. A typical truck application could have a volume of between 5,000 and 20,000 units/year, while in the case of cars it could be from 80,000 to 500,000 units/year, or even more. Further aspects that have to be considered are tooling costs, scrap production and cycle time. Tools for composite production are much cheaper than tools for sheet metal forming. This is because composite processes are single operations, while sheet metal forming requires from five to six separate tools on each component line.

These savings in tool costs are very influential at low production volumes, but this advantage is lost at higher volumes where part costs dominate. The only and best available composite manufacturing processes for high production volumes are short fiber reinforced thermoplastic injection molding and bulk molding compound (BMC) processes. However, these types of composite are not widely used for structural applications.

With the development of long fiber reinforced thermoplastic injection processes, high volume materials will come similar to what can be considered a “structural” fiber reinforced polymer. The main advantage of injection molding is that it produces little scrap and that it has very short cycle times; for example 90 seconds are required for a dashboard molding. At this time there are very few processes for medium volume composite production.

Compression molding using sheet molding compound (SMC) or glass mat thermoplastic (GMT) are the two most commonly diffused. Both have become highly automated over the last years and are currently used for cars and trucks with cycle times in the order of few minutes. Many of the problems originally faced with these materials, including high density, surface finish and paintability, have now been solved. However, a still present problem for both SMC and GMT is the requirement for post-machining and the associated production of scrap [1].

A truck bumper produced in SMC, for example, requires the milling of holes for light assembly, generating scrap that must be properly considered. Among the emerging materials that appear interesting for medium volume production, thermoplastics reinforced with continuous fibers are able to combine reasonable stiffness and strength with short cycle times. Another process for medium volume composite production is resin transfer molding (RTM). It can be used for structural applications and it is of growing interest for its potential for automation, good tolerances and good achievable mechanical properties. The surface finishing of RTM parts is also quite good. The disadvantages of RTM are: relatively high tooling costs, high levels of material waste and relatively long cycle times.

The E-LFT (Endless Long Glass Fiber Thermoplastic) process has also to be mentioned. It combines good structural characteristics with complete process automation. Founded in 1989 by Ron Hawley (Composite Products Inc.), it is now considered one of the most promising processes for structural parts. A current drawback, however, is the necessity of using a film to achieve cosmetic surface finishes. Not many other composite manufacturing processes have also become automated, such as fiber braiding and fiber placement. They are becoming interesting for niche and low volume production. There is no doubt that composite manufacturers are working very hard to be more competitive in terms of production for the automotive industry.

Two other urgent priorities are further improvement in surface finish and paintability. In particular, there is a need for the clarification and harmonization of standards and measures for surface quality control [1].

Nowadays there is not yet a composite processing alternative to high-speed metal stamping. A group of industries needs to join together and attack the problem from all angles, which include improvements in dispensing technologies, curing chemistries and the energy sources that drive cure.

The most effort within the automotive composites sector is that of a Japanese consortium driven by Nissan, which has decreased the cycle time from 160 to 10 minutes for resin transfer molding (RTM) simple flat panels with carbon fibers and epoxy resin. The fact shows that the challenge is possible and that composites must increase manufacturing speed by almost an order of magnitude to become competitive [34].

2.5.1. Molding processes

It is important that the preform be placed fairly precisely into the tool because fabric SMC has little flow and to minimize issues that might arise from tool closing with out of place charges. With 100 % charge coverage, if the charge was out of place, die lock at the shear edges was a major issue. To avoid this, the tool has to be designed with sacrificial zones near the shear edges. This approach indicates that a certain percentage of the molding compound is always going to be scrap.

Also a trimming operation beyond standard deflashing must be taken into account. A multi-axis laser trimmer can be used to achieve great success. A major issue from the start of molding underbodies was achieving tool closure consistently across the part, and thus having the desired level of compaction or consolidation of the fabric SMC during the molding. This part is quite complex depending on the size, three-dimensional structure, and changing number of layers. Having multiple layers resulted in multiple thicknesses.

Pressure values collected during the early molding trial usually show significantly uneven pressure distribution indicating larger thickness variations within the part versus the designed thickness. The temperature is directly influenced by the thickness and it gives a good idea about the required molding degree of care.

Manufacturing costs consisted mainly of material costs and they are around 120 until 200 \$/part, which showed major cost savings would be available with a scrap reduction. Considering a baseline scrap case and comparing it to an ideal case it is possible to save up to 30 \$/part. In case of more parts to be joined a surprising assembly savings can be achieved through adhesive bonding due to its low cost, or spot welds with an average cost of almost 9 \$/part.

All together these studies showed an increase in manufactured part cost for the composite underbody system, but a slight savings in assembly time. The net cost at the end was a cost of about 5 \$/kg for each kilogram of mass saved. Of course, what is acceptable cost may vary with each manufacturer and each vehicle, and will be a combination of many factors, such as the vehicle architecture and volume, the manufacturing decisions, the assembly line on which the vehicle will be built, and on the cost of the fuel [21].

2.5.2. Compression molding process

The compression molding process consists of placing the molding material that is generally preheated inside the molding cavity. The mold is then closed and a plunger provides the required force to create a certain pressure inside the cavity and then all the mold areas are in strict contact with the material.

Heat and pressure are maintained until the material reaches the final cure state. This process allows high-volume production even for complex shapes; either thermoset or thermoplastic materials can be employed and the reinforcement can be made of glass or carbon fibers.

The main advantages related to this process are the low cost compared to other methods and the easiness of production. There are some disadvantages due to the poor product consistency and the difficulty to control flashing; this means that scrapes have to be accepted and the components require edge cutting and further finishing operations.

Both SMC and BMC materials can be used during the process, they are disposed inside the mold and then modeled through the application of pressure and temperature. At the end of the cycle the mold is cooled and the part is removed.

In mass production industries thermoplastics are the most adopted materials in addition with long fiber and glass fiber mat reinforcement.

There are some considerations to keep in mind about compression molding:

- ✓ The proper material amount has to be determined
- ✓ The minimum amount of energy to manufacture the material has to be determined
- ✓ The minimum time required to heat the material has to be predicted
- ✓ The appropriate heating technique has to be defined
- ✓ The required force to obtain the proper shape has to be evaluated
- ✓ The mold has to be designed for rapid cooling at the end of material compression.

A description of the process is provided in Figure 2-9.

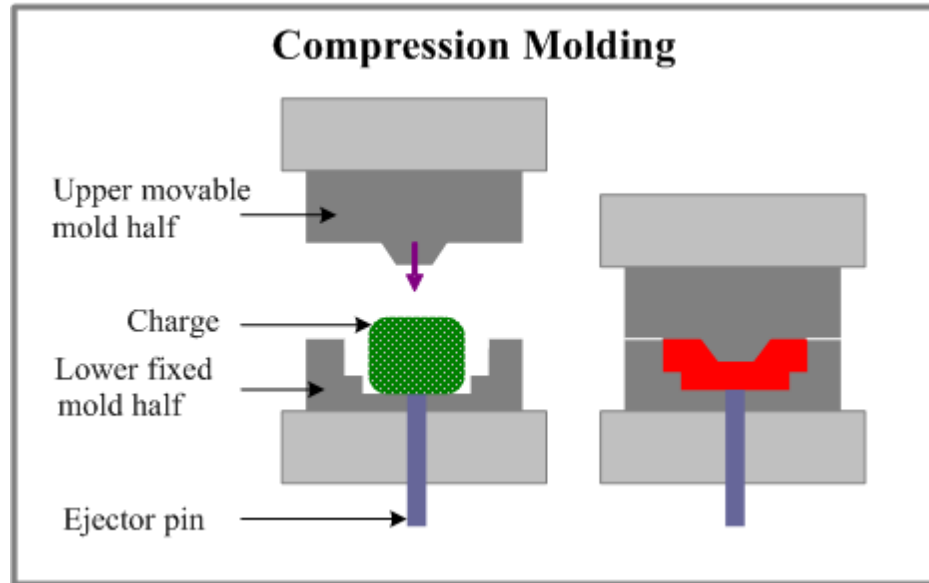


Figure 2-9: Compression molding process schematic [60]

In the automotive sector this process is diffused for the production of parts such as hoods, fenders, scoops, spoilers and some intricate parts [42].

2.5.3. Resin transfer molding (RTM) process

Resin transfer molding process is similar to compression molding, but this time the amount of molding material is measured before to be injected and the molding takes place. The material is preheated and then injected in a chamber better known as “pot”. A plunger has the function to force the material inside the mold cavity through runner systems; the material passes through a hole called “gate” before reaching the cavity. The walls of the cavity have temperature higher than the material melting temperature; this allows the material to flow and fill the cavity better. At the end of the process the mold is opened and the component is extracted. These operations are fully automated and guarantee good surface finish, dimensional stability and mechanical properties. The plastic can be used in form of powder, perform or granulated form before the treatment inside the mold.

Due to the short cycle time this process is optimal for high volume production and differently from compression molding the mold is closed allowing smaller tolerances and the production of more complex shapes.

The transfer molding process is a little bit more expensive than compression molding because of higher tooling costs, especially those related to the running system for the material to be injected. During the resin injection the fibers are already present inside the mold and they just need to be filled without need of further pressure. The mold is usually designed by using metals due to its better heat transfer that enhances resin flow and so quicker cycle duration, higher longevity, less deformation but higher cost. One of the disadvantages of this process similar to compression molding is the presence of air than can be trapped inside the mold and so also in this case an air vent system or vacuum creation must be studied.

A schematic of the process is provided in Figure 2-10.

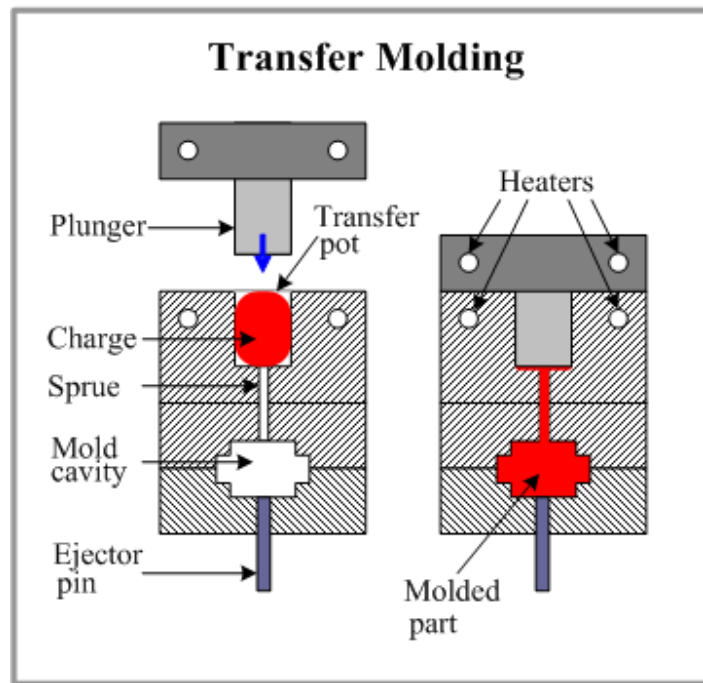


Figure 2-10: Resin transfer molding process illustration [61]

An example of RTM is provided in Figure 2-11 and is based on 25 minutes for base material setup, 35 minutes to inject the resin and about 90 minutes to cure it, finally the removal time is about 10 minutes. In overall the process takes about 160 minutes. With the new method the injection is done at high speed and the duration is less than 3 minutes, the curing time is reduced to 5 minutes and 1 minute is needed for both material set-up and removal.

The high speed is enhanced by a vacuum created inside a chamber that helps the resin flow. Figure 2-11 represents the cure degree as a function of the time; the advantages can be seen in terms of both time saving and cure degree improvement [42, 43].

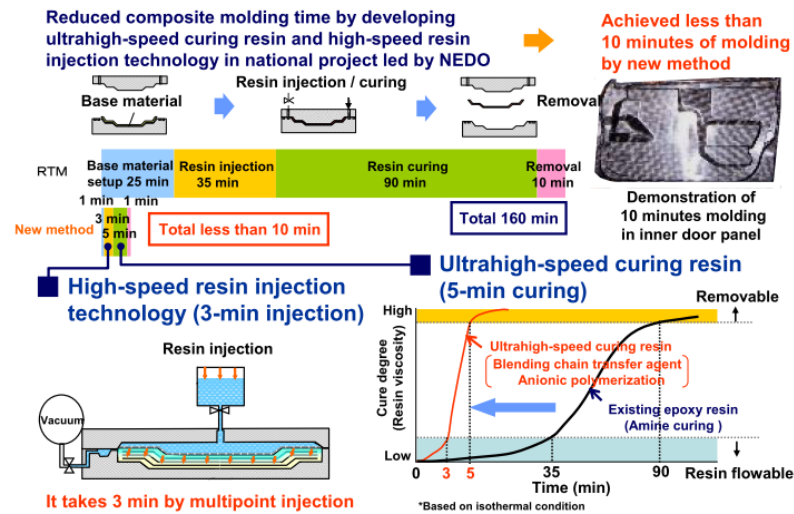


Figure 2-11: Resin transfer molding cycle time reduction [43]

2.5.4. Injection molding process

This process enables the production of both thermoset and thermoplastic materials. The procedure consists in feeding a heated barrel with a mix of different materials, usually in powder state. During the transfer the material is melted and forced inside a mold cavity by a screw-type plunger until it cools and can be removed. Figure 2-12 gives an overview of the processing window; too high temperatures could bring to thermal degradation while too high pressure could bring to flash and so material scrap and further finishing operation. The lower levels of temperature and pressure provide the limits for melting and short-shot [14].

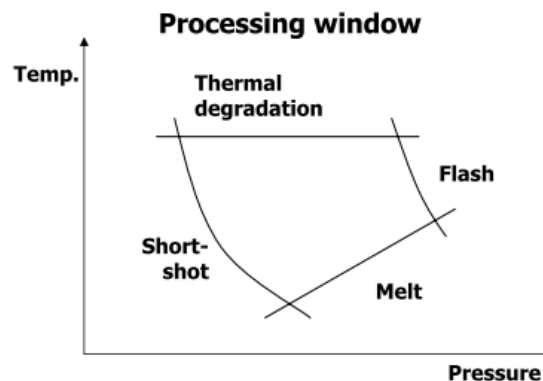


Figure 2-12: Injection molding Temperature-Pressure graph [14]

The cycle time is designed according to several rules; the most important part is the one related to the cooling effect. The cooling temperature can be set according to the following expression:

$$t_{\text{cool}} = (\text{half thickness})^2 / \alpha \text{ where } \alpha = 10^{-3} \text{ cm}^2/\text{s}$$

Figure 2-13 presents typical cycle pressure and temperature curves [14].

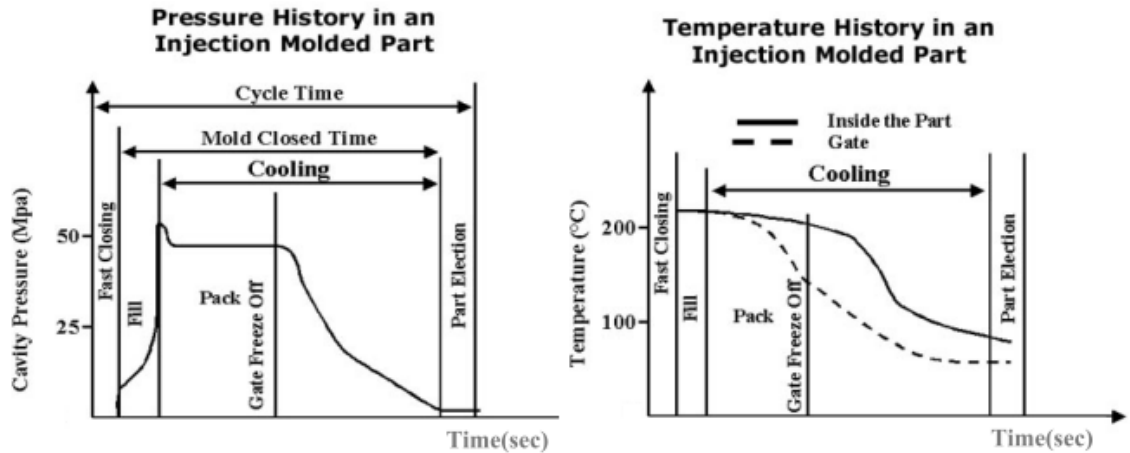


Figure 2-13: Injection molding process pressure and temperature treatment curves [14]

After the design phase the toolmaker creates the equipment by using metals such as steel or aluminum; the parts that can be manufactured vary from the smallest component to entire automotive body panels.

This method is an optimal way to produce high volumes of the same object. It has the advantages of high production rate, repeatability, tolerance control, wide range of materials applications, low labor cost, minimal scrap losses and little finishing part cure after the process.

The disadvantage lies in the high equipment investment and running costs; this is the reason why only high volume production is preferable. The forces required to keep the cavity closed vary from 5 to 6,000 tons and depends especially on the area of the part to mold.

As a rule of thumb 4 or 5 tons/in² can be used in almost all cases. This rule is no more valid for materials presenting higher stiffness values. The clamp force is strictly related to the machine rate in dollars per hour of working are showed in Figure 2-14 [14].

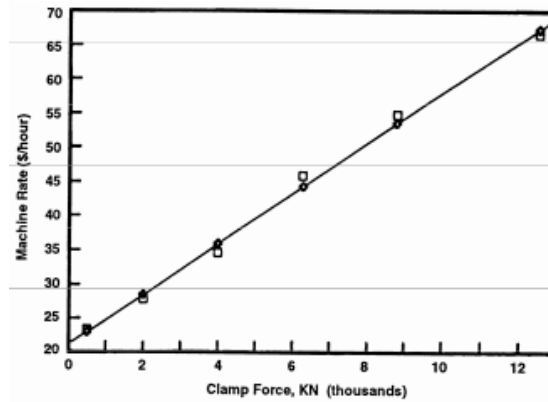


Figure 2-14: Injection molding cost per hour as function of clamp force [14]

The molds are produced by using materials as steel or aluminum that need high wear resistance due to the high capital investment. Systems able to let the trapped air to escape have to be kept into account otherwise it tends to accumulate in the corners of the cavity producing defects in the component. If the air is compressed it can ignite and burn the surrounding plastic. The cooling system is provided by a continuous path of holes running around the mold filled usually with water for economic reasons. There are some applications for high volume production presenting more than a single cavity; in some cases it is possible to have until 128 components with a single processing. They are better known as “family molds”. In part design a maximum thickness limit has to be set in order to stay within certain tolerance ranges; for both thermoplastics and thermosets typical values are between ± 0.2 and ± 0.05 mm. The power required during the process depends on the material specific gravity, melting point, thermal conductivity, part size and molding rate [44]. Figure 2-15 presents a system overview.

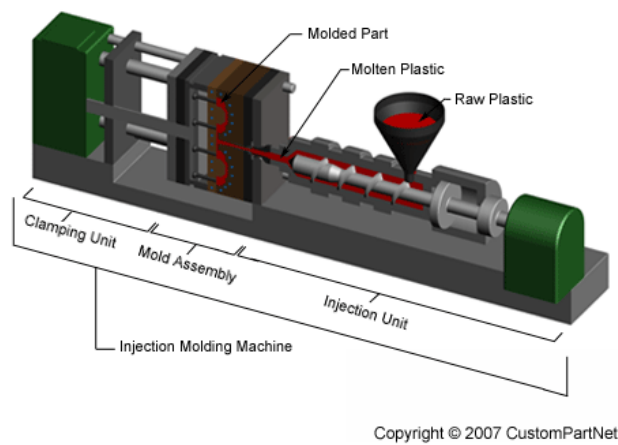


Figure 2-15: Injection molding process [62]

Several shapes can be modeled through injection molding such as bosses, ribs, through bosses for screw, bosses with gusset etc. Some examples are reported in Figure 2-16 [14].

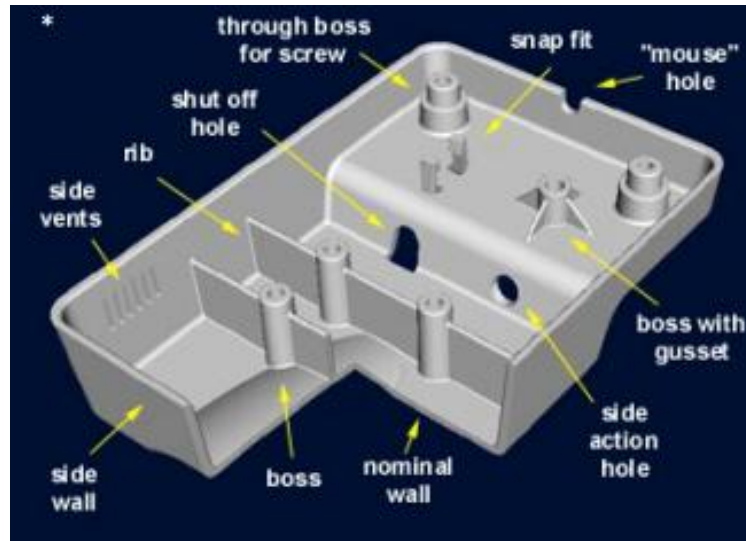


Figure 2-16: Example of a part obtained with injection molding process [14]

There are some guidelines in rib design, for example: the thickness of the rib at the intersection with the nominal wall should be from 50 to 60 of the nominal wall while the maximum rib height should be three times the nominal wall thickness; if the rib is too deep the filling process becomes difficult. In order to simplify the component extraction the draft should be in between 1 degree and 1.5 degree with a minimum value of 0.5 degree per each side. At the intersection between the rib and the wall there should be a radius in between 25 and 50 % of the wall thickness, also a minimum value of 0.381 mm is suggested.

These solutions eliminate sharp corners, reduce stress concentration and improve both flow and cooling. In between two subsequent ribs a minimum spacing of two times the wall thickness should be present to escape cooling problems. Finally the mold flow should be down inside the rib otherwise some gas could be trapped.

2.5.5. Injection charge compression molding ICCM

Injection charge compression molding is a new process and can be considered as the fusion of compression and injection molding processes. It consists of compressing the charge before filling is complete, the moldable cavity can be expanded during short-shot filling. After the charge is completely disposed a further compression is applied in order to improve material densification.

The process can be summarized in three main phases.

- ✓ Short-shot filling with injection
- ✓ Compression filling
- ✓ Compression and cooling.

Large BMC can be adopted and instead of been charged manually special injection unit can be designed thus providing automation and labor saving. The effects of process parameters such as delay, total time, pressure and distance on part quality can be summarized as follows:

- ✓ The mold cavity expansion during short-shot filling improves both the overall and local flow resistance
- ✓ ICCM has a positive effect on dimensional stability especially in the direction perpendicular to compression. This effect is provided by compression-based densification
- ✓ Two different orientation levels can be distinguished, one given by compression and the other given by injection. The shift between different levels put in evidence non uniform shrinkage and so a reduction in conformity to the cavity walls.
- ✓ An improvement in part quality, accuracy and conformity can be achieved through instant compression after short-shot, low compression pressure and long compression time and distance.
- ✓ Decreasing molding pressure, reducing residual stresses, minimizing molecular orientation, evenly packing, reducing shrinkages, reducing density variations [13].

The main factors affecting this process are compression speed and stroke; proper compression speed gives lower chamber pressure which results in lower residual stresses while higher stroke provides lower pressure distribution and so longer cycle time [12, 13].

2.5.6. Part Fabrication Method

The parts are designed for manufacture using a process under development by Hypercar project called Advanced Volume Automotive Composite Solution (AVACS). The AVACS process begins by creating a composite “tailored blank” from raw material inputs.

These blanks are then used in either a liquid infusion molding or a solid-state thermoplastic stamping process to create the final part. The tailored blanks are flat sheets made in the rough outline of each part with the fibers oriented as desired and in the appropriate thickness for the part.

Because the fiber form is long direction fibers, these flat sheets can be stamped to final shape or preformed for use in an infusion process. The main benefit of the AVACS process is that it breaks through the traditional cost-performance-production-rate tradeoff typical of composites to have a practical solution that meets automotive requirements. The main process steps are illustrated in Figure 2-17 [2].

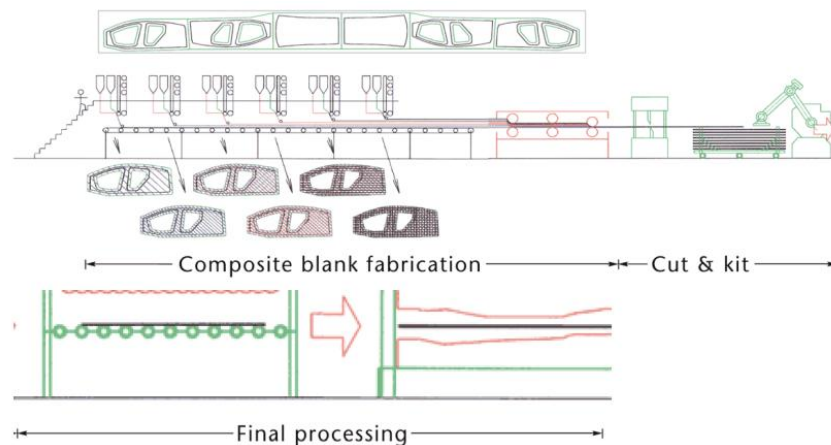


Figure 2-17: Part fabrication method system layout [2]

The first step in the AVACS process is creating a tailored blank for each composite part. This process places semi-consolidated layers of fiber and matrix on a flat conveyor, each layer with a specific fiber orientation. Consolidating the layers through a series of rollers finishes the blanks. This critical first step turns raw-material inputs (fiber and polymer matrix) into a form that can be stamped directly or preformed for resin infusion processes without more processing steps. The difference between the tailored blank in the case of stamping or resin infusion is simply the degree of resin impregnation and consolidation. Key benefits of tailored blanks include:

- ✓ Precise control of fiber alignment, angle, and thickness. Using computer control, the AVACS tailored blanking process can place highly aligned fibers that precisely match the load paths and geometry required for the part. This makes best use of the fibers, minimizing the material required to achieve the desired part performance.

- ✓ High fiber volume fraction parts. Since the fibers provide the bulk of the strength in composites and stiffness of the part, the higher volume fraction of fibers, the lighter the part. The AVACS process will produce parts with fiber volume fractions from 55 to 65 % depending on the final forming process but in any case much higher than typical SMC composites.
- ✓ Low scrap since the tailored blank fabrication process places material only where it is needed in the part, thus avoiding the need to cut out large holes or do extensive trimming.
- ✓ Flexible production equipment because AVACS equipment can make tailored blanks for any composite part that fits the equipment. Software control allows the equipment to make a variety of parts in series, continuously laying up part-specific blanks to the desired production volume without having to switch tools or forms. It is also easy to include special plies of different materials (such as insulation) or structural cores.

Once produced, the tailored blanks are sorted into kits and transferred to the final processing stations. This step allows for the blank fabrication to be physically separated from the final part manufacturing cells, if desired, thus enabling high machine utilization. The final processing step is determined by the specific application. The manufacturing process chosen for most of the composite parts is a resin transfer molding (RTM) variant using a nylon-12 "laurolactam" thermoplastic resin. In this step, the tailored blanks are preformed then placed in a mold along with any inserts and foam cores. The tool is then closed and resin is injected. Finally, the tool is cooled and the part is removed, trimmed to final shape, and moved to body assembly [2].

2.5.7. New advanced processes: Quickstep and melding

Adhesives are increasingly being used in industrial applications to replace and/or complement traditional fastening methods such as welding, bolts and rivets. The use of adhesives in these applications has the additional advantage of reducing the number of potential stress concentration sites caused by the presence of rivets. However limitations of adhesives are well known, such as susceptibility to peel forces and environmental attack by hydrolysis [9].

Advanced composites are usually cured by heating with air in an oven or in autoclave.

Air has low heat capacity so the heat rate to be induced in the composite and inside the tooling is limited. Furthermore the heat removal requires long time to be taken away. In 1990 a group of researchers from Australia realized that by using a liquid such as water as heat transfer medium, the process can be better controlled due to its higher thermal capacity. The humidity does not represent a problem since the cure is applied by using a vacuum bag.

This process allows high heating rates under control conditions inducing fast viscosity changes of resin. This way pre-pregs can be modeled and fast joining technique can be used. The composite material is laid up on the tool having thickness from 6 to 8 millimeters made by composite skins or metal sheets placed inside a vacuum bag. The tool has to be designed in order to transfer heat properly and it does not need stiffening elements and egg box like reinforcements as in the case of autoclave. The tool is placed in a pressure chamber where a Heat Transfer Liquid (HTL) is injected with temperature up to 180 °C. The vacuum bag provides separation between the liquid and the component even if they are in close thermal contact. The pressure inside the chamber is very modest, typically 25 Pa (a quarter of an atmosphere), that means a quarter of an atmosphere. On the top of the chamber a vibrating element produces favorable results. Due to the low pressure the chamber can be rectangular, welded from aluminum sandwich panels and designed in order to allocate more than one component for high volume production [8]. The component lies in a hydrostatic environment and so there are no forces that could deform the tool. The flow is managed through a series of baffles that avoid the formation of cold or hot spots. The whole system is presented in Figure 2-18. It is more simple, fast and cheap than autoclave [8].

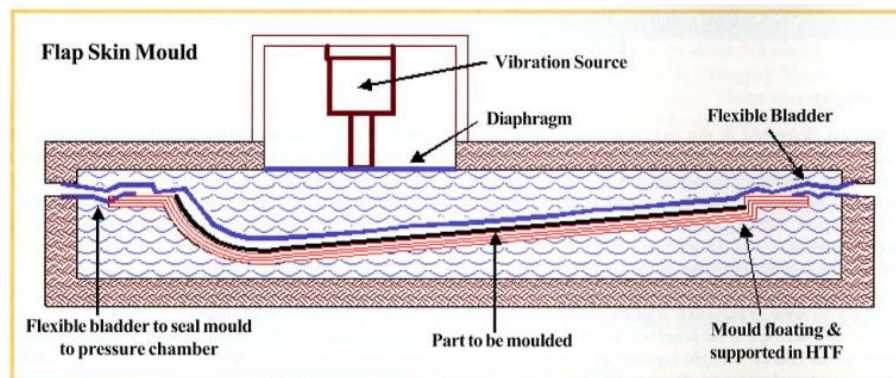


Figure 2-18: Melding process system configuration [8]

The temperature is controlled by some valves which select the liquid from three different tanks preheated at the maximum cure temperature, intermediate dwell temperature and room temperature. The cure process is monitored through the Quickstep software tool and it can be monitored through a computer monitor which illustrates the temperatures inside the system and is able to operate valves. An overview is given in Figure 2-19 [8].

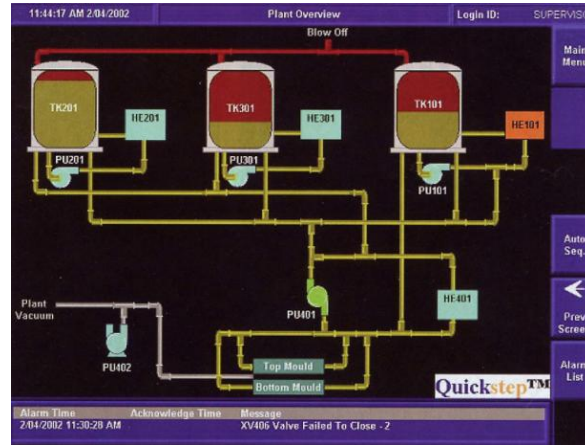


Figure 2-19: Melding process control software [8]

The curing cycle is reduced of a factor five with respect to the autoclave; in some cases the useful time can be just around 30 minutes. For high volume production the cycle time is too high; if we consider a typical daily production of an automotive plant the number of cars manufactured is between 1,000 and 2,000 units/day, this means a cycle time between 43 and 86 seconds. If this solution is adopted in future high scale production, according to the number of molds available and the fixed production amount, strong modifications and several innovations have to be achieved to reduce the cycle time about 30 times. A typical example of temperature and pressure trend versus time is shown in the graph of Figure 2-20.

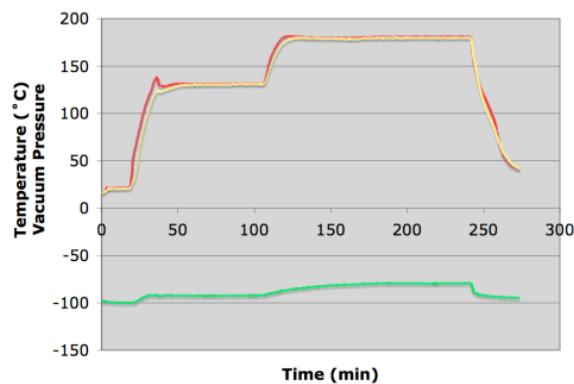


Figure 2-20: Pressure and temperature values during melding cycle [8]

The green line refers to pressure trend while the red and yellow ones represent the temperature monitored by two thermocouples; several sensors can be mounted in different areas in order to keep under control the cure state of each zone.

The new advantage of this process is given by the opportunity to stop the cycle at any time in order to have areas more or less cured.

This way two different parts can be joined by overlapping the partially cured areas and restart the cycle. Corbett et al. have successfully melded lap joints and it has been shown that the transition zone between the cured and uncured regions is less than 40 mm [9].

This process has been defined as “melding” even if it is more similar to welding than bonding [8].

No discontinuity has been evidenced in the component after this process, no porosity appears from x-ray analysis, mechanical properties remain unchanged and lap shearing test reveals that the joint has been successful [9]. Figure 2-21 provides a better description [9].

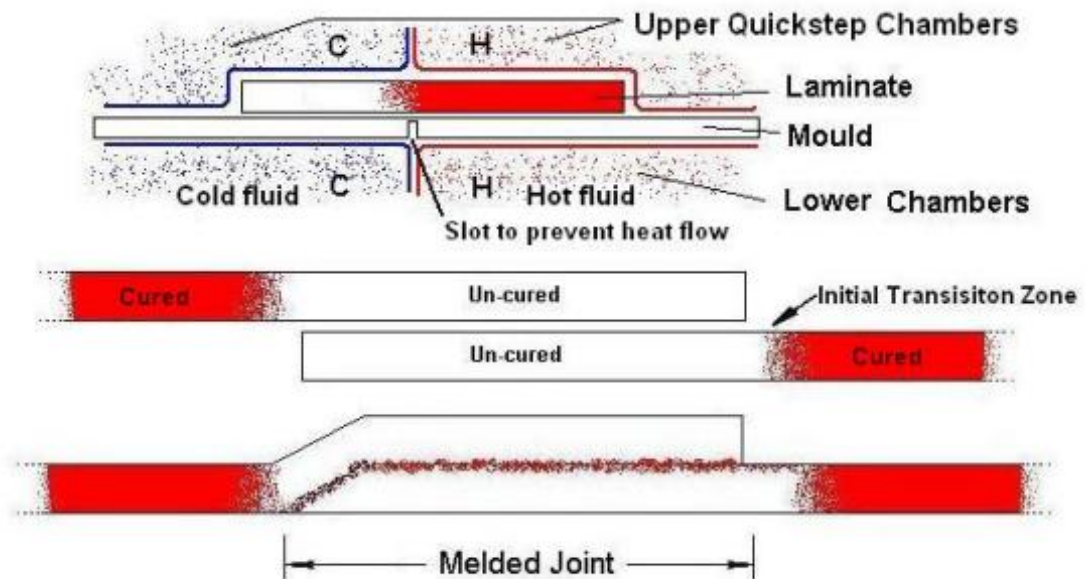


Figure 2-21: Example of parts joining with melding process [9]

2.5.8. Resin spray technology (RST) process

Almost all of the conventional processes use pre-pregs; RST process represents an innovation using various infusion processes to save costs. Instead of using several pre-preg layers it uses just a thick pre-form made by an automated process. The resin is sprayed into the tool by a gun manipulated by a robot.

The resin is heated and has low viscosity; after the injection the contact with the cold tool wall makes the resin to be like soft wax.

This way the resin can be deposited with different thickness. During the next step the preform is laid up the now solidified resin; in automotive high volume applications this step is made by robots. After that a vacuum bag is placed over the resin and the perform. All the components are transferred to a pressure vessel disposed with a certain angle in order to make the process faster; finally a heat treatment is applied.

The steps are summarized in Figures 2-22, 2-23 and 2-24.

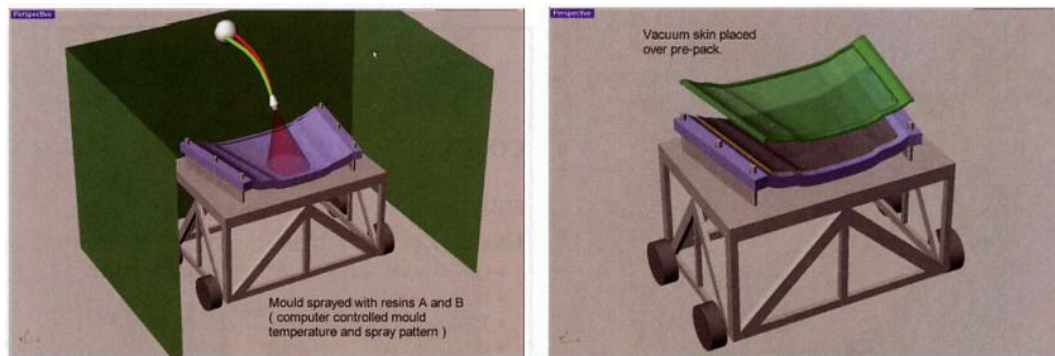


Figure 2-22: Resin spray during RST [9] Figure 2-23: Creation of vacuum bag [9]



Figure 2-24: Part placement inside a pressure vessel during RST process [9]

Too high resin viscosity does not allow it to infuse in the preform; this way the component will have zones rich in resins that require a good cosmetic finish.

The resin is also so reactive that cannot be cured in an oven because of its violent exothermal characteristics. However the liquid provides to carry away the heat and the cure can be controlled rapidly [9].

2.5.9. Endless-Long Fiber Thermoplastic process

E-LFT is a new mass production process that combines unidirectional-continuous or endless fibers and long fiber thermoplastic allowing the production of highly loaded components. The single step process comes from the LFT process and the new process for unidirectional continuous fibers thus providing low costs for complex structural lightweight parts to be produced at high volume. The continuous unidirectional fiber tapes EF can be inserted three-dimensionally along the main load paths enhancing the mechanical properties. The advantages are listed below:

- ✓ High performance: E-LFT parts have high mechanical properties and can replace metallic structures.
- ✓ Lightweight: The weight saving is about 30 to 45 percent compared to metallic solution.
- ✓ Cost efficient production: The process is fully automated, base material is at low cost and the cycle time is very short.
- ✓ Integration potential: The process enables high integration.
- ✓ Recycling: The components can be fully recycled.
- ✓ Short cycle times: The automated process and the thermoplastic matrix allow cycle times in between 30 and 60 seconds.

This process has been patented by Albert Weber GmbH in 1998, when there was the first idea. The serial production for the first part started in 2006. E-LFT stands for continuous or Endless fiber reinforced Long Fiber Thermoplastic and it is the combination of the LFT compression molding process with the local inlay of unidirectional continuous fiber tapes (EF).

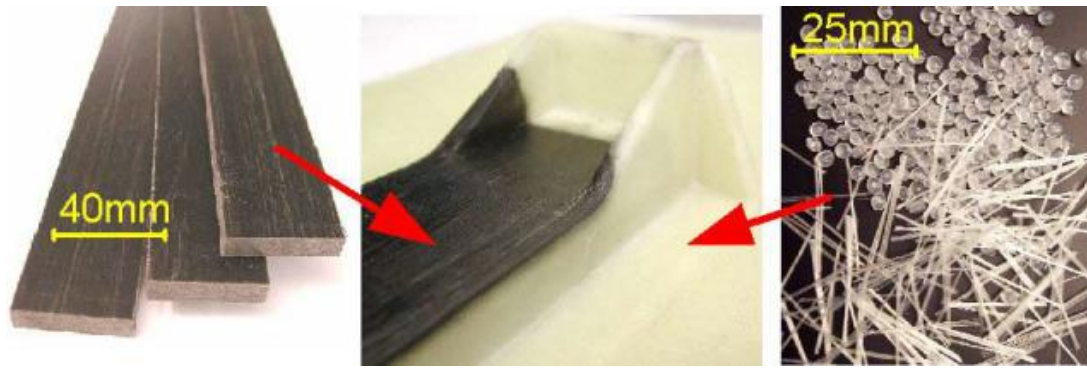


Figure 2-25: Endless fibers reinforcement strips [11]

The process is fully automated and the main steps are EF processing, LFT processing, robot handling and frame press. EF and LFT are processed in parallel way and disposed by a handling robot inside the tooling. The EF sticks are heated in an infra-red field while the LFT is processed with an extruder.

Both of them have to be compressed in the molten state in order to be properly joined each other. The material is placed in one shot in the exact place. The bonding is realized when the press is closed and the cavity of the mold are filled; no edge trimming is necessary.

Usually EF and LFT are made of the same material that is polypropylene and glass fibers, even if other fibers as aramid or carbon and other matrixes such as PET, PA and ABS can be employed.

During the process usually EF contains about 60 percent fiber while LFT contains only the 30 percent. Combining EF and LFT the mechanical properties can be enhanced of several hundred percents. EF have strength and rigidity much higher than LFT and can be placed in every place on the component following the load paths and reducing the overall weight.

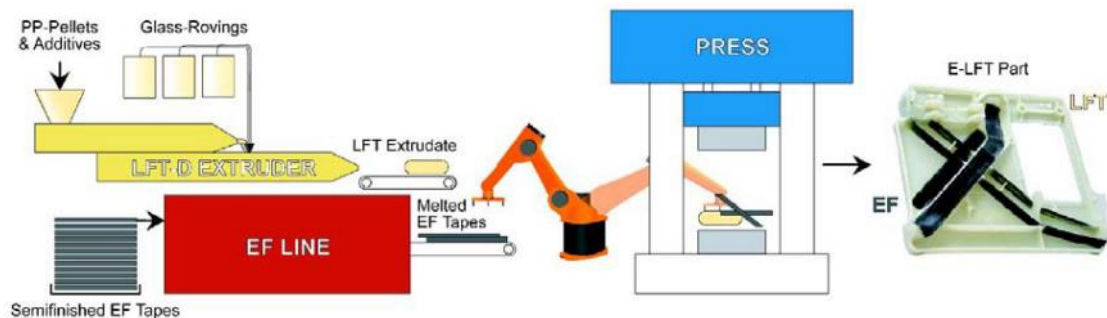


Figure 2-26: E-LFT manufacturing process illustration [11]

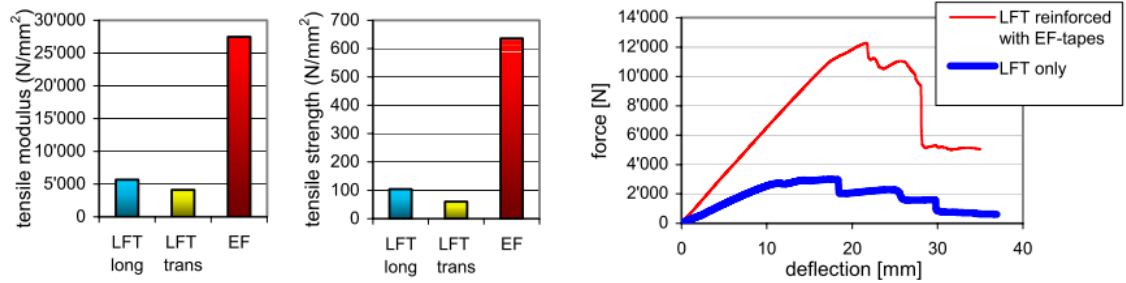


Figure 2-27: Mechanical properties enhancement due to E-LFT process [11]

The advantages for the component are:

- ✓ High stiffness and strength: Given by the excellent properties of EF.
- ✓ Nearly temperature independent material properties: Due to EF high fiber amount (> 60 %).
- ✓ Excellent crash properties: Impact resistance is much higher than the one of the single LFT.
- ✓ Good creep resistance: EF framework has very low creep.
- ✓ Design freedom: EF strips can be placed in 3D on the LFT geometry.
- ✓ Light weight: Specific reinforcement and low density material (LFT=1.12 g/cm³; EF=1.48 g/cm³).
- ✓ Resistance against dynamic load: Due to interface properties between EF and LFT.
- ✓ Integration potential: More than in case of metal parts.
- ✓ Reproducible component production: EF can be placed with high accuracy thus allowing optimal process control and so safety component production.



Figure 2-28: Endless fibers application as reinforcement along main load path [11]

Seating structures are target parts for this process. In Figure 2-29 a rear seat back with belt joint originally made by metal for a medium car has been completely substituted.

The target of the project were weight reduction, obtain the same stiffness and meet crash requirements.



Figure 2-29: Example of E-LFT application on rear seat back structure [11]

The seat is fixed at the bottom by pivot on both sides and with a lock at the top on the left side while in the middle of the top there is a joint for the belt. The component contains four EF strips connecting the main load joints, as can be seen in Figure 2-29. The obtained design is based on different studies and several simulation and first of all on a deep know-how. At the end this solution achieved 47 percent weight reduction and fulfilled all other requirements; a more performant component can be realized too. The costs are comparable to the metal solution [11].

2.5.10. Part design with sandwich structures

In the last years the application of the so called “sandwich structures” is always increasing, especially in the aerospace, automotive and naval sector for high performance requirements. The purpose is to create components with high bending stiffness and at the same time a reduction in weight with respect to the traditional materials. A sandwich structure is made by a central part better known as “core” and two external faces also known as “skins” usually made by laminates reinforced with fibers providing the material mechanical properties. The material applied as core requires low density in order to allow a certain lightness and keep the skins joined thus transferring properly the load. The idea is to have a light material with a high void percentage inside the core allowing high bending resistance.

The concept is that a material subject to bending is more solicited in the parts far from the neutral axis since the bending stiffness is directly proportional to the inertia moment of the beam section with respect to an axis lying on the neutral plane. This momentum increases exponentially increasing the material distance from the neutral axis.

This way it could be better to improve the external part stiffness and resistance at the expenses of the internal ones where it is better to lighten the structure. This solution finds many applications in structures with double T beams.

The usage of such solution allows a weight reduction between 50 and 70 % in comparison with typical materials such as metals, wood or glass fiber laminates. Some advantages related to sandwich structures are thermal and acoustic isolation, good crash and impact resistance, chemical agent resistance, atoxicity in case of thermoplastic materials application, recyclability and thermoformability.

Furthermore a sandwich structure can be formed easier than a simple single-skin laminate since the number of laminas to obtain the final stiffness is lower and the stiffeners can be eliminated thanks to the natural high stiffness of sandwich panels. Some disadvantages have to be considered such as production costs of the die material [45].

An example of sandwich structure is now presented; this solution was studied for a train face shield and the materials used are glass fibers and epoxy resin [46]. Figure 2-31 represents a typical sandwich structure where l is the length, t the single skin thickness, c is the core thickness and so the overall sandwich thickened will be $d=2t+c$. M and T refer to the flexural and torsion momentum [27].

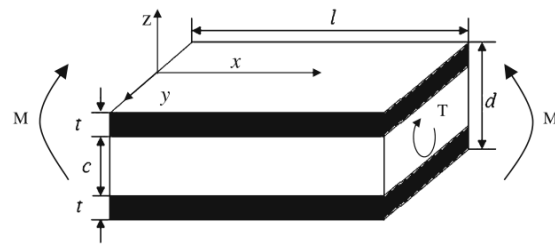


Figure 2-30: Train front shield [27] Figure 2-31: Sandwich thickness scheme [27]

The objective of this work is to investigate the panel behavior during frontal impact; this occurrence can be simulated through a bending loading. The load is applied in different conditions varying each time the load application speed. In Figure 2-32 the test equipment can be seen [46].

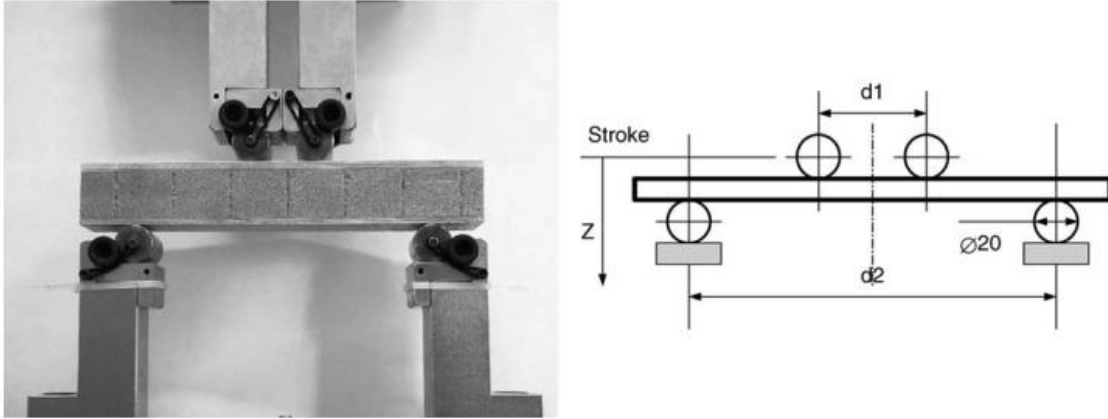


Figure 2-32: Test equipment used for sandwich structure analysis [46]

From the experimental set-up it is evident that the component reaches the failure point earlier by increasing the load application speed. This effect can be noticed in the curves belonging to Figure 2-33 [46].

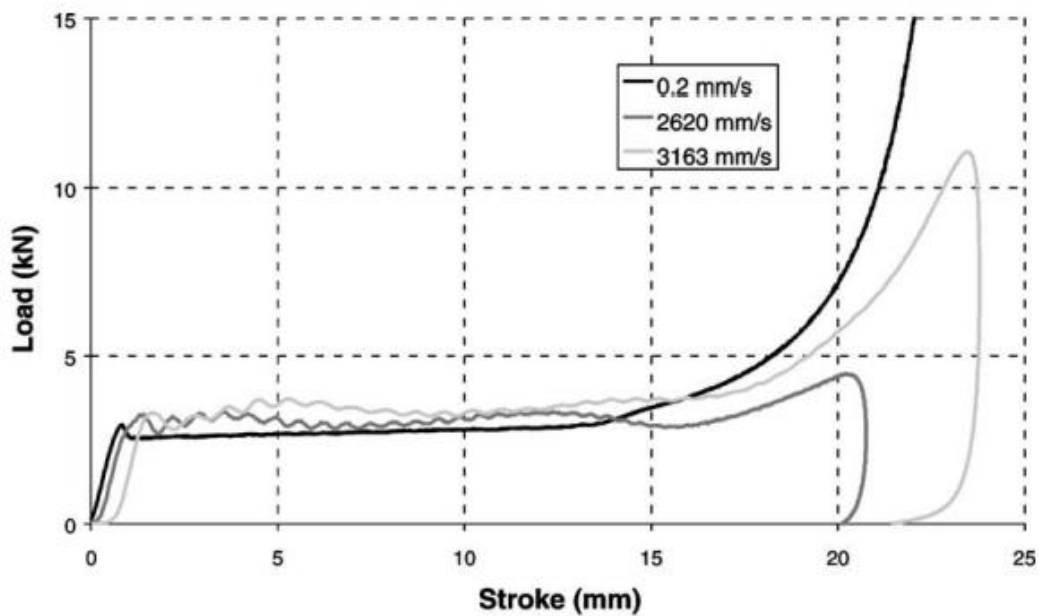


Figure 2-33: Load-Stroke graph from experimental test at different speed [46]

It has been pointed out that the main failure reason is due to the loss of contact between the interface belonging to the core structure and one of the external skins; in particular the fracture occurs in correspondence of the bearing support.

This phenomenon is better known as delamination and an example is provided in Figure 2-34 [46].

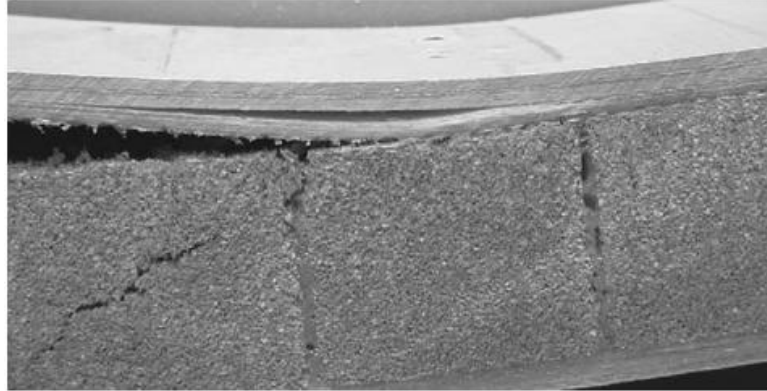


Figure 2-34: Example of sandwich structure failure between external skin and core
[46]

2.5.11. Honeycomb design solution

An optimal contact between external faces and core has to be always guaranteed in order to avoid skins sliding over the core when a shear load is applied at the interface. In presence of this kind of load it could be useful to have a structure able to resist along that direction.

One of the most common material structures used is called “honeycomb” and it takes the name for the alvear shape made by several cells with different form and dimension. The honeycomb structure density varies between 20 and 200 kg/m³ and can be produced from different materials as reinforced polymers and non metallic materials. One of the most diffused materials is the Nomex from DuPont industries, where the fibers are not made from cellulose but from aramid resin [45].

In metal honeycomb aluminum is the most diffused material. There are seven different processes to create a honeycomb structure depending on the materials used, but they are all expensive at the same way.

Nowadays some cheaper solutions have been proposed starting from cardboard or propylene sheets, but they can only be used for not primary applications. The properties vary according to the cell dimension and wall thickness. The main disadvantages are not only the difficulty in manufacturing, but also the complexity to join the alvear structure with the sandwich skins. Some properties such as drapability, sensibility to humidity conditions, and thermal isolation vary according to the adopted solutions.

The applications are limited to those fields where the costs have less importance than the performance requirements such as aerospace or sports good manufacturing.

From a theoretical analysis it can be concluded that in order to obtain the maximum flexural rigidity and bending strength the honeycomb weight should be in between 50 and 66.7 % of the panel's weight constituting the sandwich structure [45].

Figures 2-35 and 2-36 represent a honeycomb on the left and its application in a structure; the joining between the core and the skins is provided by adhesive bonding.

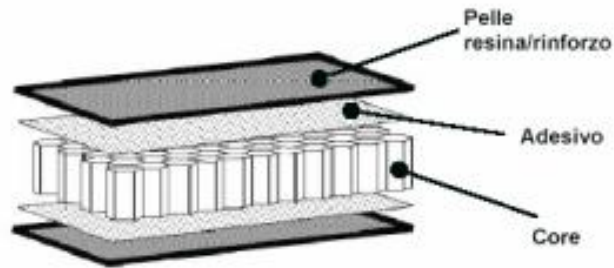
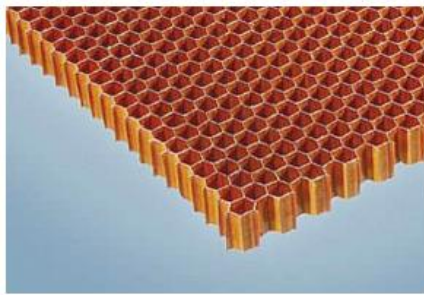


Figure 2-35: Honeycomb core [45] **Figure 2-36: Honeycomb layers [45]**

2.5.12. Sandwich structures with corrugated core

Sandwich structures with corrugated cores show better bending and twisting resistance than honeycomb core in addition to vertical shear. The results is that these structures having corrugated core provide optimal high flexural stiffness to weight ratio and are suitable in the production of components requiring high levels of stiffness and at the same time lightweight.

This solution has been thought to be adopted in the design of floor for hybrid vehicle; this way the batteries can be placed in a safe and secure location and at the same time space saving is obtained. The solution proposed adopts this technique and the constituent materials are epoxy resin and chopped glass fiber reinforcement due to their low cost. A three point bed test as the one described above has been performed to evaluate the component properties.

The specimen is supported in the lower part by two rigid bodies while a third moving element is placed in contact with the upper surface and then starts to move in order to reproduce the desired displacement or a certain load condition.

The equipment with the specimen installed is represented in Figures 2-37 and 2-38.

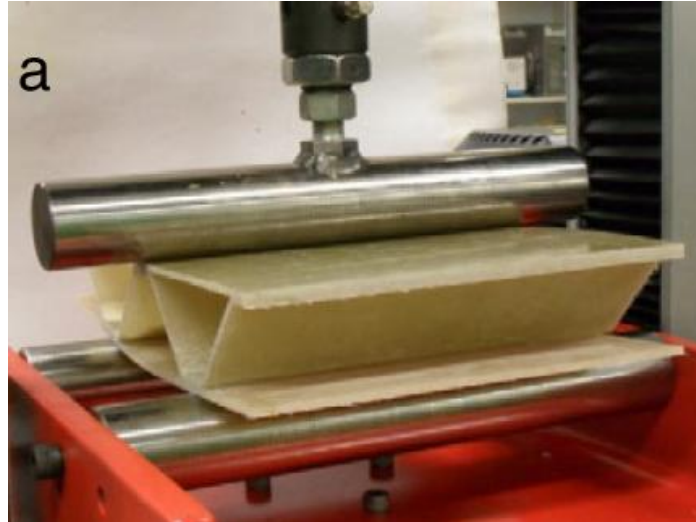


Figure 2-37: Test in parallel direction [19]

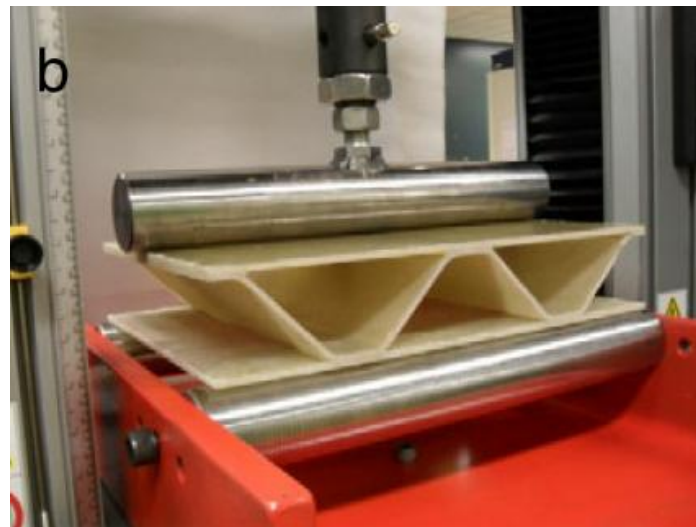


Figure 2-38: Test in perpendicular direction [19]

The test was conducted in two ways; numerically through Abaqus software and experimentally as explained above. The results were then compared. From the experimental test it was proved that the specimen has higher stiffness in the parallel direction (configuration a) since the final force value is higher before the failure occurs with the loss of contact between the external panel and the corrugated core. In the second configuration (b) the final stiffness is lower but the failure occurs later and a buckling phenomenon can be observed. Figure 2-39 shows the results.

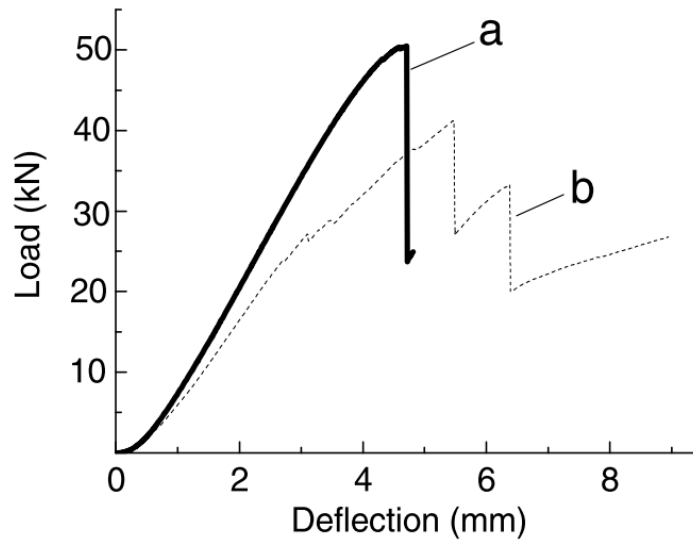


Figure 2-39: Load curves during tests on sandwich structure [19]

To reduce simulation times and costs a model was created in Abaqus environment even if the interaction between faces and core was ignored at this stage. The results of the simulation are presented in Figure 2-40.

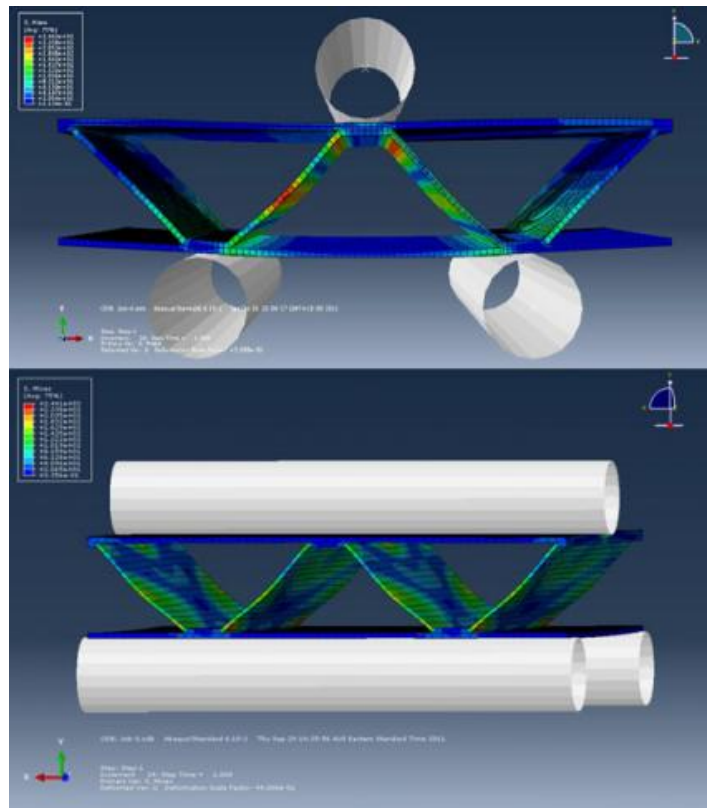


Figure 2-40: Numerical results in the test of a sandwich structure with Abaqus software [19]

From the analysis it can be noticed that the maximum stresses arise in correspondence of the corrugated core and on the faces where the contact between core and skins exist. The results were recorded during the simulations and comparing them to the experimental ones a good matching is evident as presented in Figure 2-41.

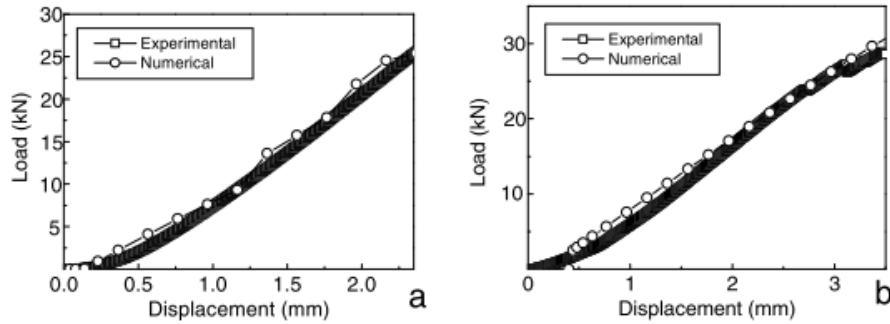


Figure 2-41: Comparison between experimental and numerical results [19]

Some factors such as corrugation angle, thickness of skins and core, fiber alignment and hybridization can be set iteratively until reaching the best compromise between bending performances and lightweight [19].

2.5.13. Nano-tube technology

A new kind of technology is presented by the application of carbon nano-tubes CNTs as interlaminar reinforcement. These tubes are aligned in vertical direction with respect to the lamina plane. They are grown at high temperatures and then transferred to pre-pregs at room temperature. The process of tubes deposition is based on a rolling transfer machine that aligns them on a pre-preg ply as can be seen in Figure 2-42.

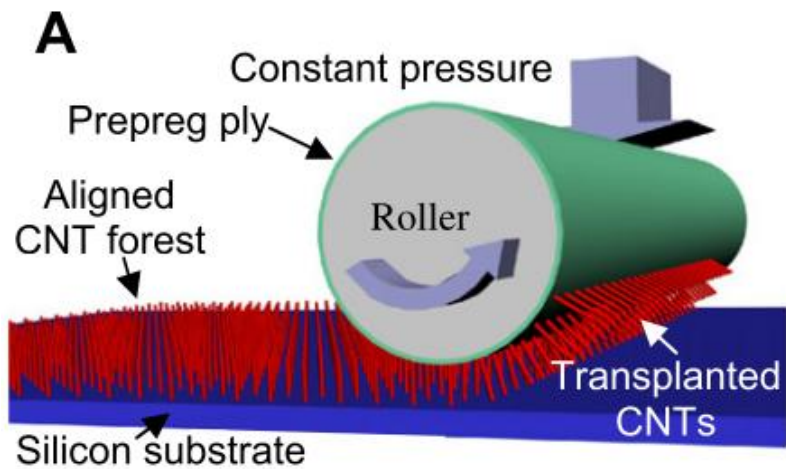


Figure 2-42: Nano-tubes deposition method on pre-preg plies [26]

The difficulties of this process lie in distributing and homogenizing the material in a proper way on the resin surface of the pre-preg. When the two external layers are put in contact to create the composite panel the overall structure can be schematized in Figure 2-43.

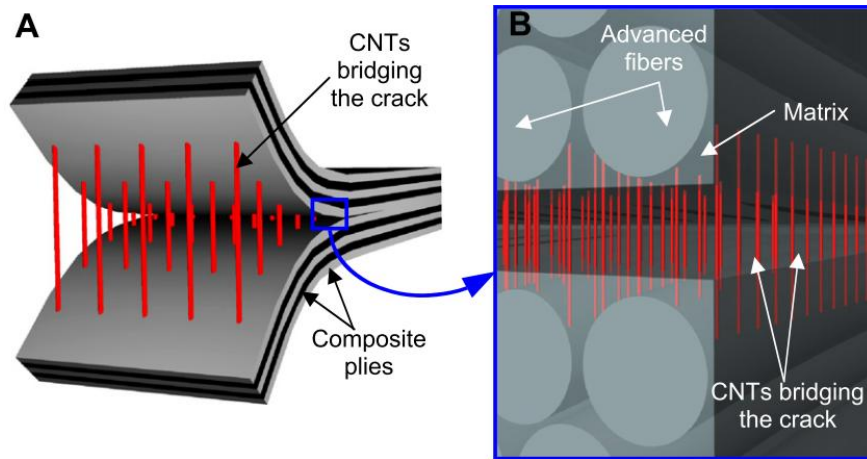


Figure 2-43: Nano-tubes visualization between composite plies [26]

This technology is still in experimental phase and a lot of work should be done before being accepted and diffused broadly but this could be in the future an optimal solution for bonded joints, composites repair and bonding of embedded or surface mounted devices [26].

2.6. Methods of composites repair

With respect to repair, the characteristics of the automotive field (in comparison to other transport modes) can be summarized as follows:

- ✓ Cars and trucks can be easily transported to a body workshop to be repaired
- ✓ Body workshops are usually well distributed throughout a territory
- ✓ Current structural composite repairs typically include panels, bumpers, a few supports and fewer chassis
- ✓ Composite components tend to be quite small (a big truck bumper weighs no more than 50 kg) and they are easily disassembled

According to these points, the logistics of performing composite repairs in the automotive sector shouldn't present any significant concern. Bumpers and panels are mainly fiber reinforced plastics and are designed to resist during low speed collisions, impacts due to small stones, and the weight of a leaning person.

For lighter energy impacts, bumpers typically break. Knowing the part dimensions and the assembly technologies, it is usually cheaper to replace a bumper than repair it. The situation is different for sports cars. Some high performance models employ a composite chassis structure that is usually manufactured in just one country and distributed worldwide.

The repair of the fully structural chassis part requires a deep knowledge of the component and the applied materials, as well as specialist equipment. If the damage is limited, it can often be repaired in a local authorized workshop. However, for more extensive damage, the vehicle must go back to the manufacturer.

Actually automotive composite repair is not currently a major issue because most applications allow direct part substitution. However, if the use of composites spreads to more diverse applications in the future, then the repair of difficult to replace parts will become a necessity [1].

2.7. Life cycle assessment

LCA was popularized decades ago, when some issues were raised about diminishing material and energy resources coupled with a growing world population. First used in the food and beverage industry, LCA was introduced in other sectors, driven in part by the European Commission's Environment Directorate, which requires manufacturers to keep under control energy and raw material consumption and solid waste generation.

Today, LCA methodology is discussed in the International Organization for Standardization (ISO) 14040 environmental management series standard, which is based on four major steps:

- 1) goal and scope definition (§4.2 ISO 14044);
- 2) inventory analysis (§4.3 ISO 14044)
- 3) impact assessment (§4.4 ISO 14044)
- 4) interpretation (§4.5 ISO 14044)

Each step, as noted in the following paragraphs, presents considerable challenges, as said by LCA practitioners [38].

Goal and scope definition: Each LCA starts by defining a goal and the “functional unit” of the study that is the service provided by the material, component or system and its performance characteristics.

Inventory analysis: Investigators must consider all of the possible inputs to and outputs from the functional unit that have an impact on the environment. Inputs include the upstream impacts of raw materials (e.g., sand for glass manufacture), the energy required to mine or extract the raw materials, the fuel costs to transport the raw materials to the manufacturing site, the energy used to transform the raw materials into the product (e.g., from natural gas or coal), the energy use associated with any recycled materials in the product and so forth.

Outputs include the downstream impacts of air pollutants (e.g., greenhouse gases), water pollutants, solid waste (e.g., disposal and/or recycling of the product itself), any co-products that can be beneficially reused and something more.

Impact assessment: Software is available to help LCA investigators explore the somewhat arduous process of the inventory analysis and assessment steps, including SimaPro and ECO-it from PRé Consultants (Amersfoort, The Netherlands) and GaBi from PE International (Stuttgart, Germany), among others.

Interpretation: This step is a challenge because assumptions about data input and the relative weight of impacts are different among those who use the software. “Interpretation of LCA results can vary,” confirms Mr. Bob Moffit, product manager at Ashland Performance Materials (Columbus, Ohio), who is the head of the company’s green resin efforts. Summarizing the term LCA stands for life cycle assessment and so an analysis on environmental impact due to the manufacturing of new products taking into account all the aspects from the raw material extraction, all the processes involved during the manufacturing and also the effect of that product during its life and also over; this means to evaluate all the aspects related to disassembling, recycling and after life treatment. In the picture below it can be seen a comparison between the impact of CO₂ due to both planes and cars during a 10 years period. In the first case it can be seen that the 99 % is due to flight operations while less than 1 % can be assigned to material and part production, assembly and disposal. In the case of cars the 84 % is given by driving operations, the 13 % to material and part production, the 4 % to assembly and finally the 1 % to disposal [4].

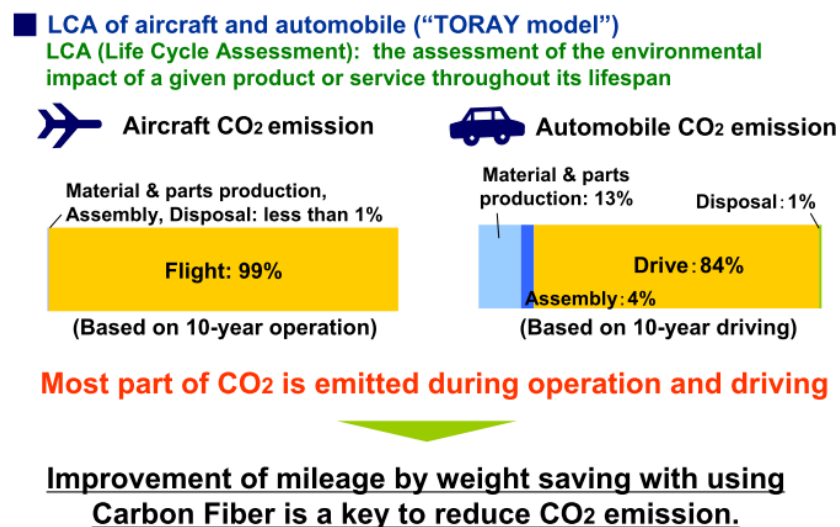


Figure 2-44: Toray LCA analysis for planes and cars in Japan [4]

Figure 2-45 gives a description of how carbon fiber reinforced polymer use helps for weight saving. In the case of planes a 50 % use means 20 % weight saving, while in the case of cars by using just the 20 % it is possible to have up to 30 % weight saving, this means that the potential is much higher in the second case even if the CO₂ reduction is much more evident in the case of planes as expected; comparing 2,700 to 0.5 tons reduction.

Toray industries studied the effect on CO₂ reduction based on a certain number of planes and cars sold in Japan; since the number of cars is higher than the number of planes the overall effect on the emission level is considerable and as it can be seen the CO₂ amount reduction is 20 times higher [4].

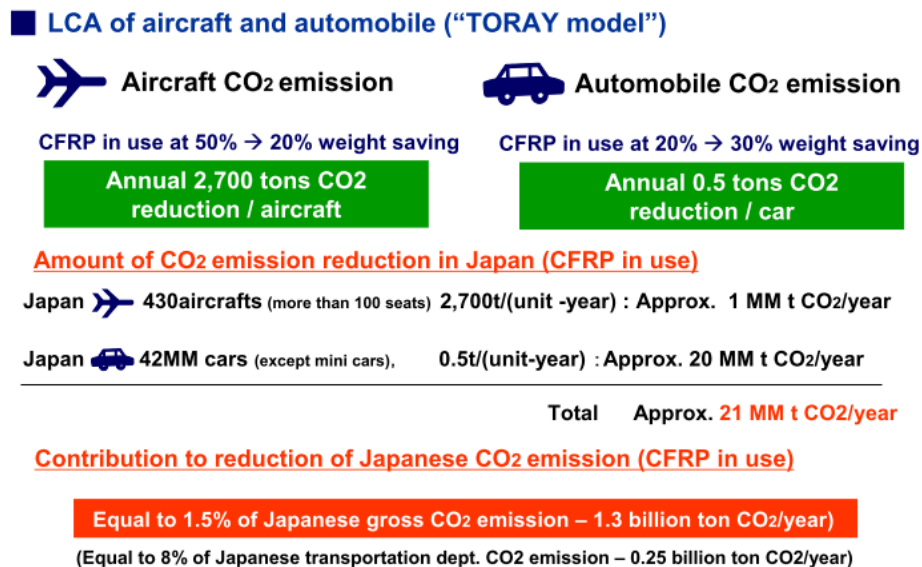


Figure 2-45: Toray investigation of CO₂ production for planes and cars in Japan [4]

2.8. Composite recycling methods

Recycling processes have been used in the automotive sector for many years and for economic reasons. Few years ago cars, buses and trucks were composed almost entirely of metal, and to recycle this material by melting it down to obtain new raw virgin product was the most economical and feasible way.

Metals are ideal for recycling because they lose memory with respect to the previous shape every time they are melted. Unfortunately, composites do not have the same characteristics, and it is common to query how easy it is to recycle composites.

In recent years, the number of different polymers employed by the automotive industry has been significantly reduced to facilitate recycling. Similarly, plastic components are now sold to ease identification and separation at the end of a vehicle's life. However, the overall number of cars that need to be recycled has increased up to 9 megatonnes per year, similarly the relative use of polymers in automotive applications.

Today, a car's overall weight is typically made up of about 75 % metal between ferrous and non-ferrous alloys and about 25 % of non-metal (plastic, glass, rubber and fabric). The need to treat and recycle all these different materials has led the European Council to issue Directive 2000/53/CE. To understand the content of this Directive it is necessary to be familiar with the terminology employed:

- ✓ Recovery: treatment of used materials for energy production
- ✓ Recycling: treatment of used materials for same or different production route (except energy)
- ✓ Re-use: use of an old vehicle component for the same application as the original

The Directive defines how end of life vehicles (ELVs) have to be managed as follows:

- ✓ Yesterday: landfill 25 %; re-use/materials recycling 75 % (the metal part)
- ✓ Today (2012): landfill 15 %; re-use/materials recycling 80 %; energy recovery 5 %.
- ✓ Tomorrow: landfill 5 %; re-use/materials recycling 85 %; energy recovery 10 %.

Today, the biggest obstacle to the recycling of composite components is not the recycling technologies but the lack of end-uses for, and the cost of the recycled material. The overall cost of recycled composite materials is considerably higher than their virgin equivalents. There is also no trust regarding the quality and technical performance of the recycled reinforcement or filler compared to virgin materials. As a result, there are very few automotive products that are manufactured predominantly from recycled composites. They also can be applied at an industrial level for cosmetic and semi-structural applications are natural fiber reinforcements (e.g. flax, hemp, coconut, abaca, basalt, animal hair, bird feathers, etc.). Although a lot of development work is still needed in this area, especially for applications where long fiber reinforcements are required, these materials seem to be promising from a recycling perspective because they can be burned and incinerated without forming any residues.

Another major issue associated with the recycling of composites is establishing equilibrium of the quantity thus preventing a growing mountain of recycled material. As an example, in theory short fiber reinforced thermoplastics can be easily recycled by re-melting and re-molding. Laboratory tests have demonstrated that it is possible to grind and re-melt these materials several times with little loss of structural performance. However during application reality is completely different. The average life of a car in the North Europe is 17 years. During this time it is exposed to sun, acid rains, dust, pollution and aggressive liquids. The result is that resinous materials become degraded over time, and when recycled their properties differ from the virgin products. For this reason, only a small amount of recycled material between 10 and 20 % is addresses to be added to virgin material for new components. The overall implication is that at every generation it is necessary to find applications that need much larger quantities of the material than the previous generation if all the recycled material is to be consumed. Whatever the future of materials in the automotive sector will be, a new global design approach is required, that is “design for recycling”.

As EoL (End of Life) recycling is no longer an option but a standard, it is necessary to consider it within a vehicle’s cost structure. This approach acts on different levels. Careful consideration needs to be given to material selection and design for separation.

Materials and components have to be classified in terms of re-use, energy recovery and recycling [2]. If CF is to be a suitable automotive material, then there will be a need for recycling and reclamation of the valuable fibers. Although there is no compulsory recycling standard in the United States, the European Union (EU) has a requirement that by 2015, more than 95 % of all vehicles by weight must be recycled. Today EU requirement is 85 %. If CFs were introduced in even modest amounts, from 4.5 to 5.4 kg/vehicle (comparable to magnesium content), then with current automotive scrap rates, approximately 45.3 tons of CF composite scrap would be disposed of from cars and light trucks every year. Economically viable means of reclaiming the fibers, maybe for less critical uses than virgin fibers (sporting goods, consumer products, and concrete reinforcement) must be made available.

Both an economical and environmentally friendly process for fiber reclamation and a market for recycled fibers would need to grow. Several efforts have been made in recent years to address the issue of recycling. Adherent Technologies of Albuquerque, New Mexico, investigated about a catalytic depolymerization process applied to a sample CF thermoset resin composite. Using this process, Adherent Technologies was able to reclaim more than 90 % of the CF in the composite and the recovered fibers only presented an 8.6 % reduction in strength. Argonne National Laboratory (ANL) conducted experiments with composite panels of known composition that showed that a single-step pyrolytic process is able to recover CF from thermoplastic and thermoset composites with very high yields. The recovered fibers were subsequently molded into flat panels and tested, with very good results. Oak Ridge National Laboratory also conducted tests of the recovered ANL fibers and discovered that the recovered fibers were of similar diameter, density, and morphology as virgin fibers. The recovered fibers also showed surface chemistry similar to virgin fibers, indicating that additional surface treatment might not be necessary for all downstream applications.

The ANL pyrolytic process is thought to be economically viable based on a nominal value of recovered fibers of 3 \$/kg [3].

Figure 2-46 [4] represents a recycling method used by Toray industries. In the first stage all the material is collected and filtered; after that it is cut, subjected to thermal cracking and finally milled. These are today's most common technologies.

The final products of this process are milled and chopped fibers, and carbon fibers for cement filling. All together they have to be studied in order to get potential business [4].

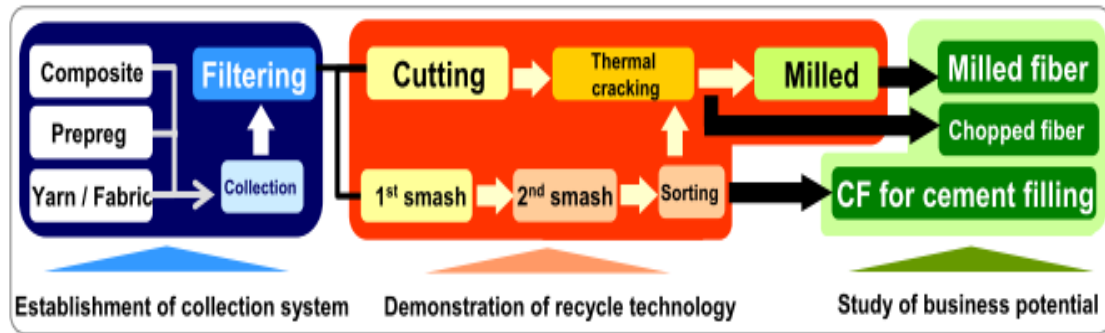


Figure 2-46: Example of recycling system from material collection to business potential [4]

Procedures and processes for dismantling and recycling need to be developed. It will also be necessary to include the end of life dismantling cost in a vehicle's purchase price, as the last owner will not want to pay and the number of old vehicles abandoned in European fields and woods will dramatically increase. The increasing presence of multi-material hybrid components is a recycling problem that has not yet been resolved by car manufacturers.

Currently there are two trends; to mill the component or to dismantle it. It is essential that research is focusing at a European level to investigate the management and recycling of hybrid material structures and components. Another worthwhile approach would be to combine the development of new recycling technologies and strategies with other different industrial sectors having the similar constraints. For example, electrical and electronic equipment manufacturers are now subject to the latest European directive that was approved in 2003. Issues such as identification, collection, transportation, dismantling and cleaning are important logistical matters that need to be solved in an economical way by both sectors [3]. A new process has been developed at Nottingham University where high quality fibers can be recovered from scrap thermoset composites by a fluidized bed combustion process. The method was first developed for glass fiber composites, but has been extended to carbon fiber composites.

The resin matrix is oxidized and partially combusted in the fluidized bed, thus liberating clean filaments of glass or carbon which are carried out of the fluidized bed in the flue gases.

They can then be collected in a cyclone and reused in other products. The process has been found to be highly effective for carbon fiber composites, creating carbon filaments of good quality and high value. It is therefore a viable means of treating composite propeller shafts when a vehicle is scrapped [6]. Two technology families have been proposed to recycle CFRPs; they are mechanical recycling and fiber reclamation. Both are explained in the next paragraphs. Most efforts have been done focusing on thermoset composites such as carbon–epoxy systems, as their cross-linked matrix cannot be reprocessed simply through re-melting. The process is easier in the case of thermoplastic resins.

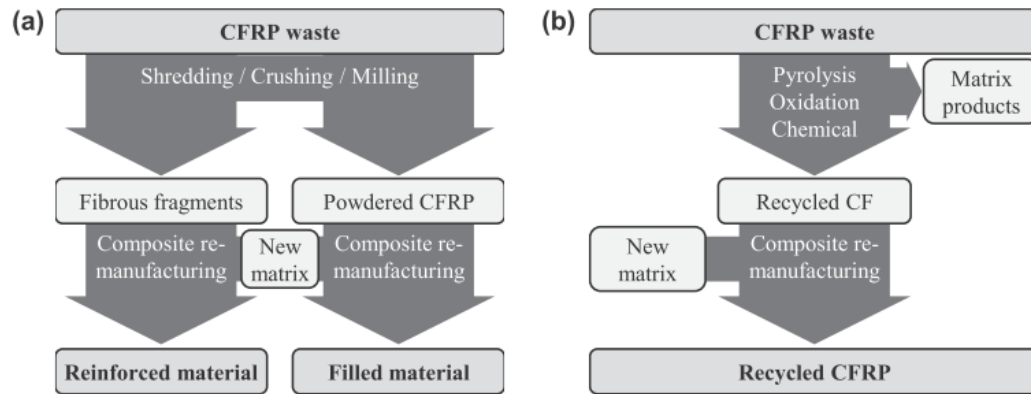
2.8.1.Mechanical recycling method

Mechanical recycling is constituted a component breakdown by shredding, crushing, milling, or other similar mechanical process; the resulting scrap pieces can then be segregated into powdered products rich in resin and fibrous products rich in fibers. Typical applications for mechanically recycled composites include their re-assembly in new composites as filler or reinforcement and use in construction industry, for example as fillers for artificial woods or asphalt, or as mineral-sources for cement. However, these products represent low value applications; mechanical recycling is therefore mostly used for glass fiber reinforced polymers, even though applications to reinforced thermoplastic and thermoset carbon fiber can be found as well. Because mechanical recycling does not recover individual fibers, the mechanical performance of the recyclates is evaluated at the composite level [7].

2.8.2.Fiber reclamation methods

Fiber reclamation consists on recovering the fibers from the CFRP, by employing an aggressive thermal or chemical process to break down the matrix that is typically a thermoset; the fibers are released and collected, and either energy or molecules can be recovered from the matrix. Fiber reclamation may be preceded by preliminary operations such as cleaning and mechanical size reduction of the waste. Fiber reclamation processes are particularly appointed to CFRPs: carbon fibers have high thermal and chemical stability, so usually their excellent mechanical properties are not significantly affected, especially the ones regarding stiffness.

Generally, the recycled CFs have a clean surface and mechanical properties comparable to the virgin products; nevertheless, some surface defects such as pitting, residual matrix and char and strength degradation have to be considered as well. After reclamation, the recycled fibers are usually re-impregnated with new resin in order to manufacture recycled CFRPs. Furthermore, recycled CFs have also been used in non-structural applications [7]. Figure 2-47 depicts the overall recycling scheme for both mechanical and fiber reclamation recycling.



Main technologies for CFRP recycling. (a) Mechanical recycling. (b) Fibre reclamation.

Figure 2-47: Technologies of mechanical recycling and fiber reclamation [7]

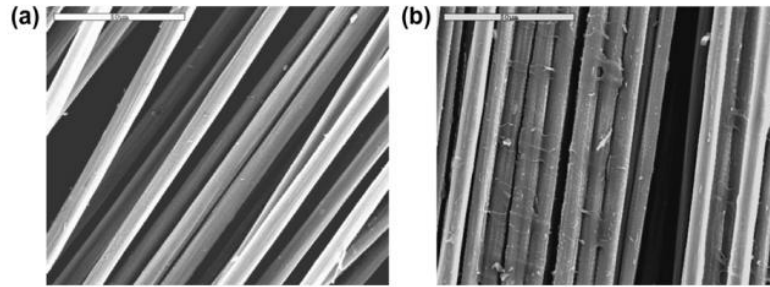
The most common fiber reclamation methods are:

- ✓ Pyrolysis
- ✓ Oxidation
- ✓ Other chemical treatments.

2.8.3. Pyrolysis treatment

Pyrolysis consists in the thermal decomposition of organic molecules in an inert atmosphere, for example N_2 , and it is one of the most widespread recycling processes for CFRP. During pyrolysis, the CFRP is heated up to 450 to 700 °C in the nearly absence of oxygen; the polymeric matrix is volatilized into lower weight molecules, while the carbon fibers remain inert and are eventually recovered.

This method includes a preliminary step of chopping the feedstock to a consistent length; after pyrolysis, an in-house developed manufacturing has proved to be particularly suitable for re-manufacturing [7]. A comparison between clean recycled fiber and fiber with some residuals after pyrolysis treatment is presented in Figure 2-48.



Scanning-electron microscopy of recycled (through pyrolysis) carbon fibres (Wong et al., 2009a). (a) Clean recycled fibres. (b) Recycled fibres with char residue.

Figure 2-48: SEM comparison between clean recycled and recycled with char residue fibers [7]

2.8.4. Oxidation treatment

Oxidation is another thermal process for CFRP recycling; it consists in the combustion of the polymeric matrix in a hot and oxygen-rich air flow at 450 to 550 °C temperature. This method has been used by a few researchers such as Jody et al., being the fluidized bed process (FBP) the most well-known implementation. During recycling, CFRP scrap is reduced to fragments approximately 25 mm large and is fed into a bed of silica on a metallic mesh.

As the hot air stream passes through the bed and decomposes the resin, both the oxidized molecules and the fiber filaments are carried up within the air stream, while heavier metallic components sink in the bed; this natural segregation makes the fluidized bed process particularly interesting for contaminated end of life components. The fibers are separated from the air stream in a vortex, and the resin is completely oxidized in an afterburner; energy recovery to feed the process is possible.

2.8.5. Other chemical treatments

Chemical methods for CFRP recycling are based on the use of a reactive medium such as a catalytic solution of benzyl alcohol, and supercritical fluids under low temperature typically less than 350 °C. The polymeric resin is decomposed into relatively large and therefore high value oligomers, while the CFs remain inert and are subsequently collected [7]. Injection molding (IM) and bulk molding compound (BMC) compression are two direct methods of remolding recycled CFs into recycled composites. During IM, a mixture of resin that is typically a thermoplastic, recycled CFs in short or milled form and fillers or additives are pre-compounded into pellets, which are subsequently injected into a mould with pressure range varying from 10 to 100 MPa.

The recycled products were 25 % less stiff than the virgin ones; strength reduction was less pronounced around 12 %, maybe due to an improved fiber to matrix adhesion in the recycled products.

Figure 2-49 gives an idea about the difference in mechanical properties between the virgin carbon fibers (vCFs) and the recycled ones (rCFs) according to the process used. Chemical process allows the highest values and at the same time the lowest difference compared to the virgin material. Pyrolysis has the advantage of providing high elastic modulus but the disadvantage of low strength and shear resistance.

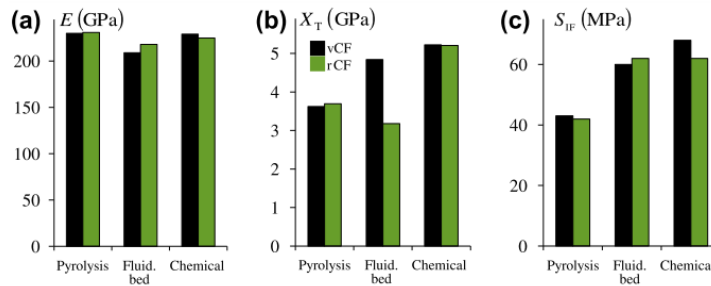


Fig. 5. Mechanical properties of recycled carbon-fibres and their virgin precursors. (a) Young's modulus. (b) Strength. (c) Interfacial shear strength with epoxy resin (Jiang et al., 2008; Jiang et al., 2009; Panesar, 2009); see Sections 2.2 (pyrolysis), 2.3 (fluidised bed process), and 2.4 (chemical).

Figure 2-49: Mechanical properties of recycled and virgin carbon fibers [7]

The main factors affecting the mechanical performance of the recycled CFRPs, especially the strength, are the fractions of fillers and of recycled carbon fibers. The mechanical performance of the recycled CFRPs was higher than that of commercial glass BMCs; however, it is not clear whether these recycled CFRPs can be competitive in price.

The production and subsequent re-impregnation of 2D or 3D recycled CF non-woven dry products with short and random reinforcement architecture is one of the most commonly used manufacturing processes for recycled CFRPs. Different methods are used to produce the intermediate dry non-woven product; the potential for fiber alignment is highlighted and put in evidence.

Many techniques are similar to the production of chopped fibers and are mostly applied to virgin GFRP or paper. The 2D or 3D non-woven dry products are then either compression molded with resin layers, or re-impregnated via liquid process.

Fiber alignment is a key point to improve the mechanical performance of composites manufactured with discontinuous recycled carbon fibers; in fact not only the composite's mechanical properties improve along preferential fiber orientation but also manufacturing requires lower molding pressures and smoother interactions between fibers.

A centrifugal alignment platform was presented by Wong et al. and it uses a rotating drum equipped with a convergent nozzle, which aligns a highly dispersed suspension of recycled carbon fibers. The use of fibers shorter than 5 mm improves the recycled CFRP alignment obtained up to a value of 90 %.

A spinning technique is under development by Wong et al. within the FibreCycle project. Wet dispersions of recycled CFs are moved through a pipe with an induced vortex; under optimized conditions, spun yarns with 50 filaments and 60 mm long are produced.

As some recycling processes can preserve the reinforcement architecture of the waste, it is possible to recover the structured tissue from large woven items, for example out of date pre-preg rolls, end of life aircraft fuselage, or pre-preg trimmings from large components. Re-impregnating through resin transfer molding (RTM) or resin infusion of the recycled tissue fabrics then produces woven recycled CFRPs.

With the actual available recycling processes, stiffness and strength could theoretically reach more than 70 GPa and 700 MPa respectively; in addition, fabrics reclaimed from pre-preg rolls would be fully traceable. The characteristics of some re-manufacturing processes are showed in Figure 2-50.

Summary analysis of different re-manufacturing processes.

Process	Advantages	Drawbacks	Implementation		
			Manufacturer	Matrix ^a	Focus ^b
Direct moulding (see Section 3.2)	<ul style="list-style-type: none"> Processes already established^c Mechanical performance compatible with low- or medium-end structural applications 	<ul style="list-style-type: none"> Very low fibre contents ($V^f < 20\%$) Reduced fibre length^d Difficult processing due to rCFs' filamentised form^{d,e,f} 	<ul style="list-style-type: none"> Wong et al. (2007a) – IM Connor (2008) – IM Pickering et al. (2006), Turner et al. (2009), Warrior et al. (2009) – BMC 	(PP) (PC) (EP,VE)	P,T T P,T,D
Compression moulding of non-woven products (see Section 3.3)	<ul style="list-style-type: none"> Processes requiring minor adaptations only^g Processes widely used for rCFRP and well documented Mechanical properties comparable to virgin structural materials^{h,j} Potential application in automotive and aircraft industries^{i,k} 	<ul style="list-style-type: none"> Common fibre damage during compression moulding^{h,j} Competing market dominated by relatively cheap materials^l 	<ul style="list-style-type: none"> Pickering et al. (2006), Turner et al. (2009), Wong et al. (2007b, 2009a) Janney et al. (2009) Nakagawa et al. (2009) Szpieg et al. (2009b) Cornacchia et al. (2009) 	(EP) (EP,UP) (UP) (rPP) (PP)	P,T,D P,T,D T,D P,T P
Compression moulding of aligned mats (see Section 3.4)	<ul style="list-style-type: none"> Improved uniaxial mechanical properties^m Possibility of tailoring the lay-up of rCFRP laminates Potential for preserving fibre length and achieving higher reinforcement fractions^{d,m} 	<ul style="list-style-type: none"> Need for nearly perfect alignment to significantly improve packability^d Need for substantial development of processes^{d,m} 	<ul style="list-style-type: none"> Turner et al. (2009), Howarth and Jeschke (2009), Wong et al. (2009b) – papermaking technique Janney et al. (2007) – 3-DEP Wong et al. (2009a) – centrif. align. rig Wong et al. (2009b) – yarn spinning 	(EP) (EP,UP) (un.) (un.)	P,T P P P
Impregnation of woven (see Section 3.5)	<ul style="list-style-type: none"> Structured architecture with continuous fibres and high reinforcement content Simplicity of manufacturing processes Applicable demonstrators already manufactured 	<ul style="list-style-type: none"> Applicability currently reduced to pre-preg EoL rolls Experimental realisation of theoretical mechanical properties still to be measured 	<ul style="list-style-type: none"> Allen (2008) Meredith (2009) George (2009) 	(EP) (un.) (un.)	T D D

Figure 2-50: Re-manufacturing processes summary analysis [7]

Three methods for recovering clean fibers through fiber alignment from CFRP waste were previously identified: pyrolysis, oxidation in fluidized bed, and chemical recycling.

Pyrolysis is currently the only process with high scale implementations; some chemical methods are advantageous considering the mechanical performance of the recycled CFs; while the fluidized bed process is particularly interesting for end of life components and contaminated waste. Mechanical degradation is usually minor in all optimized processes apart from the fluidized bed, even though it depends on fiber type and length. Current estimations suggest that reclaiming recycled CFs needs only a small fraction of the resources for producing virgin CFs, so recycling CFRP seems to be economically and environmentally viable. The main technical challenges are due now to waste preparation, recycling of end of life parts, and quality control of recycled CFs. Research on recycled CFRP manufacturing is still under development. Re-impregnating non-woven mats is one of the most effective techniques in terms of the mechanical performance of the composites. In addition to the technical challenges identified in the previous section, the biggest current challenge to CFRP recycling operations is the establishment of a CFRP recycling system chain supporting the effective commercialization of recycling processes and products. The main concerns to overcome, as identified by academics, recyclers, end-users and governments, are:

- ✓ Global strategy in organizing a network for recycling and so bringing together suppliers or users, recyclers and researchers so as to understand the current state of the art and plan for future developments on the topic according to industrial needs.
- ✓ Governments should support and give incentives to the option of recycling; this could involve not only penalties for who does not recycle but also direct privileges for companies applying in recycling their waste.
- ✓ Implementing suitable legislation because there is currently a lack in specific legislation regarding the recycling operations. For example, the classification of pyrolysis processes for recycling should be distinguished from that of traditional pyrolysis processes.
- ✓ Logistics and cooperation in the supply chain between waste suppliers and recyclers, which considers supplying the waste in a continued and suitable way, and providing the recyclers with material certificates when possible.

At the same time recyclers must guarantee that materials and components supplied will not undergo reverse engineering.

- ✓ Market identification and product pricing needs that characteristics and properties of different recycled products are known, their processing times and costs are assessed, and the value of the recycled label is established.
- ✓ LCA of the environmental, economic and technical advantages of recycled materials over other ones and disposal methods should be estimated only through cradle to grave analyses of the whole life cycle.
- ✓ Market establishment for the recyclates; this is approved by leading researchers, CF recyclers, CF users, and analysis. A market creation requires all the previous issues to be overcome, so recycled materials are accepted as an environmentally friendly and cost effective.

One of the most promising applications for recycled CFRPs is based on non critical structural components; structural applications would completely exploit the mechanical performance of the fibers, thus increasing the final value of recycled products. The aeronautics industry is particularly interested in incorporating recycled CFRPs in the interior design of aircraft. Certification of recycled materials might not be available in the short term, and it is recognized that recycled CFRPs should be allowed to mature in non-aeronautical applications first. There is also scope to produce automotive components with recycled materials, not only for technical or economic reasons, but also to boost green credentials. Even if legislation does not concern about recyclability and sustainability the automotive industry grew always more interest for natural composites, which are nowadays widely used in mass production despite some associated problems, for example consistency of feedstock. Recycled CFRPs could follow as an environmentally friendly material with improved mechanical performance. However, more detailed, multi-scale and systematic studies on the mechanical performance of recycled CFs and recycled CFRPs are useful in order to increase the acceptance of recyclates as structural materials by engineers and designers. It is also essential to perform life cycle analyses of the several recycling and re-manufacturing methods, to evaluate cost effectiveness and environmental impact of using recycled carbon fibers. All these considerations are not only addressed to CFs and CFRPs but can be extended to all the types of thermoplastic and thermoset fiber reinforced composites.

2.9. European composites market

In 2009 glass fibers production volumes in Europe was 815,000 tons and was reduced by about thirty percent as compared to 2007.

Despite the detailed representation of individual years in this context, it is suggested to consider a period of three years as entities.

Over shorter time periods, information obtained from raw materials producers in the composites may deviate from the volumes actually processed during this time window.

Especially at the beginning of the economic and financial crisis in 2008, the end of stocks amount by companies caused the reduction in raw material sales initially to exceed the decline in composites production.

The second half of 2009 in particular, however, is characterized by noticeable sales increases as compared to the first six months.

A slightly increased decline in production relative to the decrease of the entire European plastics production in 2008 is to be attributed especially to the reduced contribution of composites to the commodity market, which did not suffer quite as much of a slump as it happened for the industrial business.

The European glass fiber market trend can be better understood in Figure 2-51.

	2009* kt	2009/08* %	2008 kt	2008/07 %	2007 kt
SMC	160	-23.8	210	-7.1	226
BMC	56	-20.0	70	-10.3	78
Σ SMC/BMC	216	-22.9	280	-7.9	304
Hand lay-up	123	-39.1	202	-17.2	244
Spray lay-up	74	-28.2	103	-16.9	124
Σ Open mould	197	-35.4	305	-17.1	368
RTM	94	-11.3	106	-13.1	122
Sheets	56	-18.8	69	-21.6	88
Pultrusion	39	-15.2	46	-8.0	50
Σ Continuous processing	95	-15.7	115	-16.7	138
Filament winding	69	-12.7	79	-1.3	80
Centrifugal casting	55	-11.3	62	-6.1	66
Σ Pipes and Tanks	124	-12.1	141	-3.4	146
GMT/LFT	75	-21.1	95	-4.0	99
Others	14	-12.5	16	-11.1	18
Sum:	815	-23.0	1058	-11.5	1195

Fig. 1: GFR production volumes in Europe, itemised by techniques / components (2009* = estimated)

Figure 2-51: Fiber glass production in Europe between 2007 and 2009 [32]

Figure 2-52 provides similar information but the data refers to several European countries.

	2009* Kt	2009/08* %	2008 Kt	2008/07 %	2007 Kt
UK / Ireland	106	-13.8	123	-14.6	144
Belgium / Netherlands / Luxembourg	31	-18.4	38	-7.3	41
Finland / Norway / Sweden / Denmark	52	-24.6	69	-13.8	80
Spain / Portugal	188	-20.3	236	-12.6	270
Italy	122	-33.3	183	-12.9	210
France	87	-24.3	115	-12.2	131
Germany	118	-18.6	145	-6.5	155
Austria / Switzerland	13	0.0	13	-23.5	17
Eastern Europe**	98	-27.9	136	-7.5	147
Sum:	815	-23.0	1058	-11.5	1195

Fig. 3: GFRP production volumes in Europe, broken down by country / group of countries. (2009**= estimated, Eastern Europe**= Poland, the Czech Republic, Hungary, Romania, Serbia, Croatia, Macedonia)

Figure 2-52: Fiber glass production in European countries between 2007 and 2009
[32]

2.9.1. BMW and SGL group joint venture

In July 2010 the BMW Group (Bayerische Motoren Werke) declared that the Megacity Vehicle (MCV) was available on the market in 2013 under a BMW sub-brand. This revolutionary vehicle will be the world's first mass produced vehicle with a passenger cell made from carbon. BMW's LifeDrive architecture is helping them to open up a new chapter in lightweight automotive design history. The LifeDrive concept is made of two horizontally separated, independent modules. The Drive module includes the battery, drive system and structural and crash functions into a single construction inside the chassis. The second one, the Life module, consists primarily of a high-strength, extremely lightweight passenger cell made of CFRP offering many advantages over steel: while it is at least as strong as steel, it is also around 50 % lighter. Aluminum, on the contrary, would save "only" 30 % weight over steel.

This makes CFRP the lightest material that can be used in body construction without compromising safety requirements. Furthermore, the new vehicle architecture opens the door to totally new manufacturing processes which are both simpler and more flexible, and use less energy. The MCV's new architecture also gives vehicle designers additional freedom in creating new aesthetics for sustainable urban mobility solutions.

Thanks to this innovative program, BMW Group established a joint venture with SGL Group in October 2009 to cooperate for the production of carbon fibers and textile semi-finished products for these new vehicle concepts.

The two groups have worked together for many years in the area of carbon fiber composites. The total investment volume is 90 millions of Euro during the first development phase. The joint venture operates through two companies, one based in the USA, that is SGL Automotive Carbon Fibers LLC, and the other one in Germany, that is SGL Automotive Fibers GmbH & Co KG. SGL Group holds 51 % of the shares and the BMW Group owns the 49 %. This joint venture is designed to be a classic double win situation. BMW is getting pioneering future technologies and raw materials needed for the Megacity Vehicle on competitive terms, while the SGL Group is moving into the automobile business with BMW as a strong partner.

2.9.2. Audi and Voith partnership

The planned long term and exclusive partnership between Audi and Voith putting its attention on the further development and highly automated production of fiber reinforced materials for use in future automotive projects. The idea is to use the high potential of this innovative material to benefit lightweight construction and efficiency. With a focus on implementation in volume production, Audi and Voith are looking to work together in developing new, innovative high-tech materials, in addition to industrialization and process engineering for conventional fiber reinforced polymers.

One approach involves environmentally compatible fiber composite materials that provide ideal properties for use in the automotive industry as a complement to existing materials, with respect to both total energy balance and process engineering. For many years Voith GmbH has been intensively involved with the use of CFRPs in industrial plant design, such as in lightweight construction components in paper machines or in drive engineering. With the contribution of the development partnership being announced, the Company will now be able to furnish its technological know-how to the automotive sector as well. Voith strongly believes in the growth potential in the use of fiber reinforced polymers in high volume production, especially in this market [31].

One example of rear seat back in composite material is presented on the Audi TT; the overall weight is 3.5 kg keeping into account steel frame and carpet [18]. Figure 2-53 shows the seat back structure.



Figure 2-53: Light weight rear seat back solution by Audi on TT model [18]

2.9.3. Joint development agreement between Daimler and Toray

Under the Joint Development Agreement signed, Toray, in addition to developing optimal carbon fiber intermediate materials for CFRP, has been working on the design and molding processes with Daimler, taking responsibility for designing parts and developing technologies for joining of the parts. Thus bringing together their respective strengths, the companies have succeeded in developing an innovative technology for mass production of CFRP parts with a significantly shorter molding cycle. The partners plan to start supplying the mass-produced CFRP parts utilizing Short Cycle Resin Transfer Molding (RTM), an innovative CFRP molding process technology developed by Toray for Daimler's Mercedes-Benz passenger vehicles that will be launched in 2012. Lightweight construction is a fundamental aspect of Daimler's strategy towards sustainable mobility. The company has set a development goal to reduce the body-in-white weight up to 10 % compared with the preceding model for all Mercedes-Benz vehicles with the purpose of further improving fuel efficiency and reducing exhaust gas emissions. In order to achieve this goal, Daimler is working on the developments of technologies based on the principle of allocating the right material in the right place. As part of this move, the company thinks to actively adopt CFRP parts and increase the number of models using such parts. The joint venture will manufacture and market CFRP parts to further promote the introduction of carbon fiber composite materials in the automotive field, not only in the current applications for sport cars [33].

The Mercedes E-Class gives a further example of composite application on rear seat back. The weight is only 2.5 kg for the left part and 6 for the right one. The component is one shell design and the production volume is higher than 90,000 units/year. The material adopted includes 30 percent of chopped fibers and 40 percent of unidirectional glass fibers plus a steel frame. The results are high strength performance, integrated third safety belt and high integration depth. The system supplier is the German company Rutgers [17-18].



Figure 2-54: Rear seat back in GMT application on Mercedes E-Class [17-18]

2.9.4. Composite materials application in Volvo V70 model

On the Volvo V70 a composite material with 30 percent of glass fiber and polypropylene matrix with steel reinforcement has been adopted. The overall weight is 5.2 kg and so the advantaged are in terms of weight saving, crash resistance, easy of assembly, integration of adjustable head resets, seat back and load floor functionality. The production volume is 15,000 units/year and the system supplier is the same as in the case of Mercedes, that means Rutgers [17-18].



Figure 2-55: GMT solution for rear seat back design on Volvo V70 [17-18]

2.9.5. Ford partnership with North America universities

The Ford Motor Company is the first company to develop and use an environmentally friendly wheat straw reinforced plastic in a vehicle. This was achieved by working in close contact with academic researchers and one of its suppliers. The first application of the plastic based on natural fibers containing 20 % bio-filler is on the 2010 Ford Flex's third-row interior storage bins. This application alone reduces petroleum consumption by some 9 metric tons per year and CO₂ emissions by 13.5 metric tons per year. Ford researchers were approached with the wheat straw-based plastic formulation by the University of Waterloo in Ontario, Canada, as part of the Ontario BioCar Initiative, an effort between Waterloo University, the University of Guelph, University of Toronto and University of Windsor. Ford works in close relation with the Ontario government on the BioCar project, which is seeking to advance the use of more materials based on plants in the auto and agricultural industries.

The opportunity for using wheat straw to reinforce plastics in high volume, high content applications is a strong desire for many industries. In Ontario alone for example, where Flex is built, more than 28,000 farmers grow wheat, along with corn and soybeans. Wheat straw, the byproduct of growing and processing wheat, is generally discarded. Ontario, for example, has some 30 million tons of available wheat straw waste at any given time. Today Ford and its suppliers are working with four southern Ontario farmers for the wheat straw needed to mould the Flex's two interior storage bins [30].

2.9.6. Joint effort between Toyota and Toray

In Japan, in late 2010, carbon fiber supplier Toray and Toyota announced a joint effort to develop carbon composites and processes for body panels on some Lexus models [35].

2.9.7. GM Daewoo, Hyundai, Chrysler and Max Forma Plastics

Some companies such as Daewoo, Hyundai, Kia and Chrysler adopted some composite solutions on several car models; having as one of their main suppliers Max Forma Plastics, a manufacturer of automotive components made of glass fiber reinforced thermoplastic (GMT) and expanded polypropylene (EPP) foam. Current GMT components are rear bumpers, knee bolsters, underbody shields, load floors, seat back rests, seat cushion panels, battery trays, and spare tire wells.

GMT is supplied and machined in Korea by Hanwha. The company provides design, analysis, testing and manufacturing. In the following some examples related to a rear seat back will be provided. The objective is to reduce weight, have a good fuel efficiency, integrate a third safety belt, assembly easily and possibility to restraint the luggage.

Figures 2-56 to 2-61 provide some cases of weight reduction.

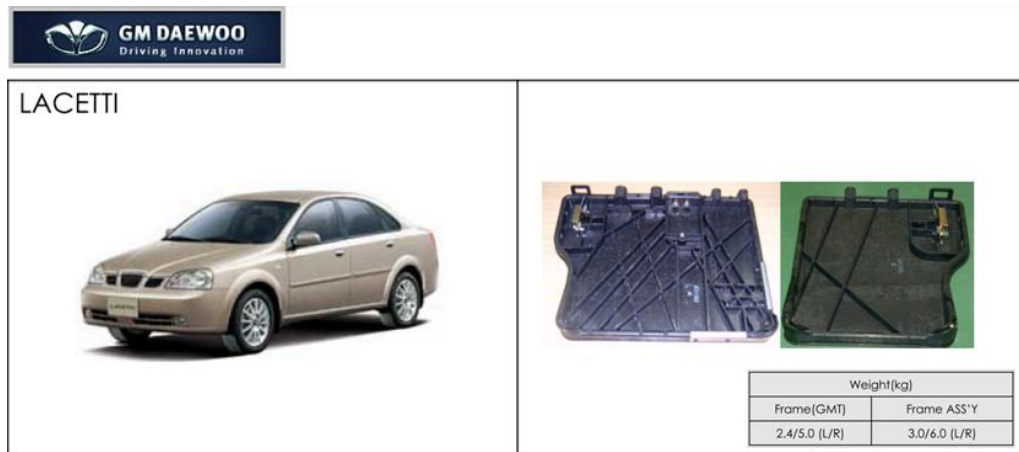


Figure 2-56: Rear seat back solution for Daewoo Lacetti [18]

In the Lacetti model there was a weight reduction from 3 to 2.4 kg for the left side and from 6 to 5 kg for the right one; the old frame has been substituted by a new one in glass fiber MAT. The seat panel is reinforced in the back through a system of ribs that have a more complex shape on the left side due to its dimension.

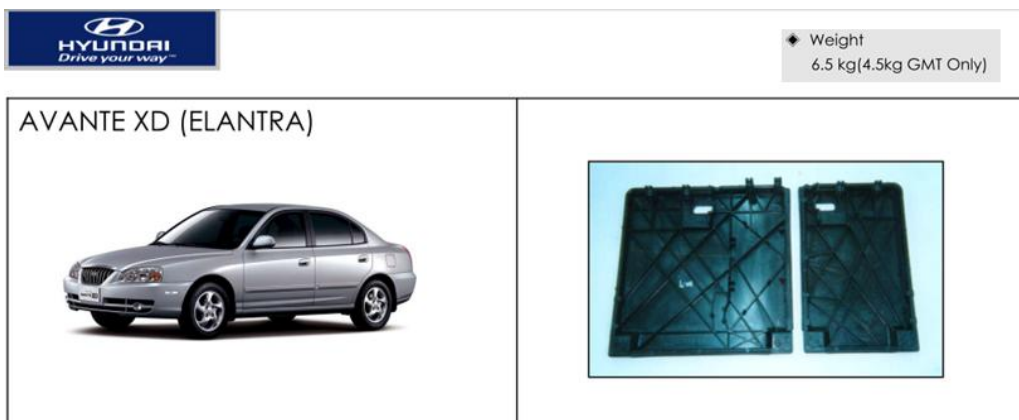


Figure 2-57: Rear seat back solution for Hyundai Avante XD [18]

In the Avante XD the weight shifted from 6.5 to 4.5 kg by using only GMT. The design solution is similar to the one presented above.



Figure 2-58: Rear seat back solution for Hyundai Tuscani [18]

For the Tuscani model the achievement was similar to the one obtained for Avante XD; this time the weight reduction is about 1.8 kg and the design is similar to the ones presented for the other models. Even the material remains the same.



Figure 2-59: Rear seat back solution for Hyundai Grandeur [18]

The grandeur reaches the same objectives by using similar solution. The components are very light even though the European version has higher weight to meet the different regulations requirements.



Figure 2-60: Rear seat back solution for Hyundai HD Avante [18]

Nothing more to say about the HD Avante, material and design solutions have been fully accepted by Hyundai in all the car models.

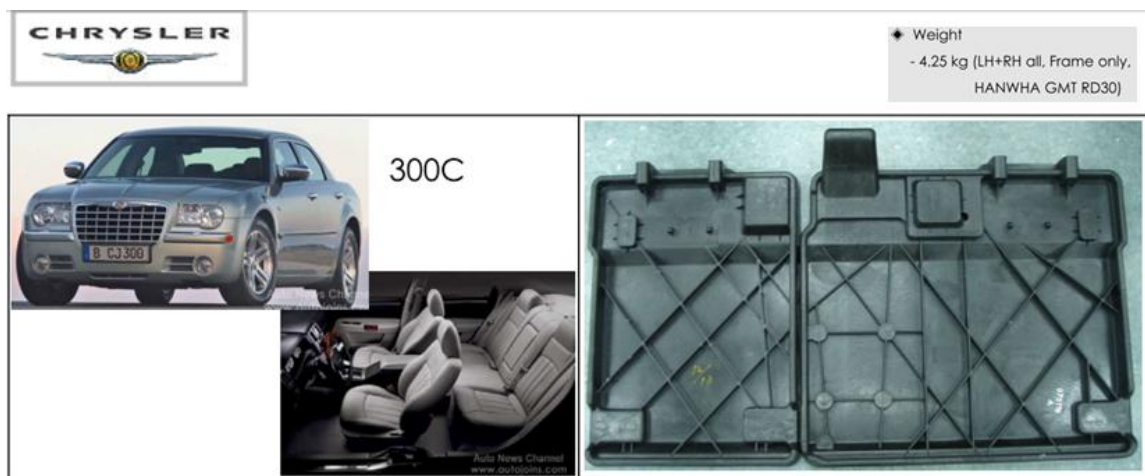


Figure 2-61: Rear seat back solution for Chrysler 300C [18]

Max Forma Plastic provides components also for Chrysler; the model adopting this solution is the 300C old version; in this case the overall final weight for both left and right side is 4.25 kg.

Information about older solutions is not available. All these examples want to demonstrate that new light material solutions can be adopted not only for low volume or sport cars but also for high volume and low-medium segment vehicles [18].

The advantages due to this solution can be summarized as:

- ✓ Weight reduction of about 40 to 50 percent compared to steel
- ✓ High integrated and D.O.F. design allowing also hybrid solutions
- ✓ High mechanical properties with low density
- ✓ Excellence in toughness
- ✓ No splintering under crash loads or tests
- ✓ High energy absorption
- ✓ No need to paint or treat surface for anticorrosion or heavy metal
- ✓ Recyclable and eco-friendly material
- ✓ Meet of international regulations

2.9.8. BASF efforts to reduce manufacturing steps

In September 2004 BASF introduced a new one-piece seating structure that is going to be widely accepted in the U.S. automotive industry market. The typical automotive seating parts are composed by several elements that need to be assembled by hand. With the BASF structure all these pieces are held together in a way that with respect to a standard metal base structure there are about 15 pieces and 10 assembly step less. The benefits are not only in terms of economic convenience, production time and efficiency but also in terms of weight saving since the reduction could be around the 50 percent according to component design and platform without compromising the performances. This method eliminates bumps, squeaks and rattles occurring in multiple component structures because of localized fatigue. The material used is Ultramid, Petra Thermoplastic Polyester (PET) and Nypel Polyamide Nylon for seat cushion pans and back frames, seat track adjuster and transmissions, lumbar handles and supports, and recliner handles. The structure has commercial application in domestically produced vehicles. This process eliminates further operations on the components such as welding, finishing, painting and coatings due to the fact that this kind of material is not prone to corrosion and presents excellent surface appearance. Plastics are also easier to manage, handle and assemble for workers safety due to the removal of sharp weight and the noticeable weight reduction [16].

CHAPTER III

DESIGN AND NUMERICAL RESULTS

3.1. Material selection and properties description

In this part of the work the research will be focused on the finding and description of different kinds of materials that will be used in the next stages of the component design and structural analysis. The first materials analyzed are the plastics, both thermoplastics and thermosets. Next data related to thermoset composites will be presented and according to their properties each material will be used in a new composite. The main properties considered are density, in order to evaluate the component weight, price, to have an idea about material costs, and more important, mechanical properties such as Young's modulus (E), shear modulus (G) and Poisson ratio (ν) to have a complete set of data allowing to run the simulations and compare the different solutions.

3.1.1. Thermoplastic and thermoset resins as matrix

A complete set of data related to these kind of polymers has been provided by CES; all the data related to material density, price, Young's and shear moduli, Poisson's ratio are given in a certain range of values so the average value of each one has been considered. The considered thermoplastic polymers will be shortly described.

- ✓ Polyethylene (PE): Inert and extremely resistant to fresh and salt water, food, and most water-based solutions. This is one of the main reasons why it is used as food container. It is cheap and easy to mold and fabricate.
- ✓ Polystyrene (PS): Optically clear, cheap and easy to mold. It is brittle and the mechanical properties can be enhanced by blending it with polybutadiene but losing optical transparency even if the impact resistance is improved at low temperatures. It is used for foam packaging.

- ✓ Polypropylene (PP): It is produced in very large quantities; more than 30 million tons per year in 2000. The trend is increasing of about 10 % every year. In pure form it is flammable and degradable in sunlight. Fire retardants are useful to reduce the burning time and stabilize it in order to have better resistance to UV rays and solutions presenting salt and water.
- ✓ Polyvinylchloride (PVC): It is one of the cheapest, most commonly used and versatile polymer. In its pure form it is rigid and not very tough; due to the low price the material is very cost-effective for non extreme engineering applications. Glass fiber reinforcement makes the material sufficiently strong, stiff and tough to be used for roofs, flooring and building panels. It can be also foamed to design lightweight components for automotive applications.

Next a description of thermoplastic engineering polymers will be provided.

- ✓ Acrylonitrile butadiene styrene (ABS): Tough, resilient and easy to mold. It is usually opaque even if some grades can be transparent or furnished with vivid colors. This material is used for power tools casing.
- ✓ Polyamides (Nylon, PA): Nylon can be drawn in fibers as fine as silk and in the last years it was a substitute in the texturing industry. These fibers have been replaced by new materials but it is still possible to find some applications, for example as rubber reinforcement in car tires.
- ✓ Polycarbonate (PC): This engineering thermoplastic presents properties better than the commodity polymers; it has optical transparency and good toughness and rigidity, even at relatively high temperatures. Glass fiber reinforcement gives better mechanical properties at high temperatures.

Then some examples of thermoset resins are described.

- ✓ Epoxies: These resins present excellent mechanical, electrical and adhesive properties and good resistance to heat and chemical attack. They are used as adhesives, coatings and can be filled with other materials such as carbon or glass fibers to create a composite.

As adhesive they provide high strength bonding between different materials; as coating they are used to encapsulate electrical coils and electronic components; as composites they are used for low molding volume of thermoplastics.

- ✓ Phenolics: Stiff, strong, easy to mold and colored. Once its production exceeded the one of PE, PS and PVC combined. They are still widely used due also to their chemical stability, electrical properties, fire resistance and low price.
- ✓ Polyester: Can be also thermosets or elastomers. The unsaturated polyester resins are thermosets. These resins are used as matrixes for glass fibers but present lower mechanical properties than epoxy resins; at the same time the cost is lower.

A collection of the main properties belonging to the materials described above is presented in the Table 3-1.

Thermoplastics	Density [g/cm3]	Price [USD/Kg]	Young modulus Em [GPa]	Shear modulus Gm [GPa]	Poisson ratio vm
Polyethylene PE	0,95	1,81	0,76	0,27	0,43
Polystyrene PS	1,04	1,53	1,90	0,70	0,39
Polypropylene PP	0,90	1,48	1,22	0,43	0,42
Polyvinylchloride PVC	1,44	1,36	3,14	1,13	0,40

Thermoplastics engineering	Density [g/cm3]	Price [USD/Kg]	Young modulus Em [GPa]	Shear modulus Gm [GPa]	Poisson ratio vm
Acrylonitrile butadiene styrene ABS	1,11	2,73	2,00	0,68	0,41
Polyamides Nylons, PA	1,13	3,38	2,91	1,08	0,35
Polycarbonate PC	1,17	3,96	2,22	0,83	0,40

Thermosets	Density [g/cm3]	Price [USD/Kg]	Young modulus Em [GPa]	Shear modulus Gm [GPa]	Poisson ratio vm
Epoxy	1,25	2,34	2,71	0,97	0,40
Phenolic	1,28	1,76	3,79	1,37	0,39
Polyester	1,22	1,93	3,24	1,17	0,39

Table 3-1: Thermoplastic and thermoset resins mechanical and physical properties


In Table 3-1 it can be seen that PE presents the lowest density with a quite low price; the only disadvantage is its mechanical properties. In fact the Young's and shear moduli are the lowest between all the polymers present. Phenolic polymers have the highest Young's and shear moduli and at the same time low density and price. Between all the materials PVC has the lowest price and the best mechanical properties between the thermoplastics, both commodity and engineering; the only disadvantage lies in the relatively high density [53].

3.1.2. Thermoset composites available on the market

In this paragraph some data related to thermoset composites with carbon, Kevlar and glass fibers as fillers will be presented. The information has been provided by some of the largest companies for composites production such as Performance Composites, AGY and NPL. The set of mechanical properties necessary for computer aided design, estimation of the component weight and material costs consists of:

- ✓ E_1 : Elastic modulus in the main direction
- ✓ E_2 : Elastic modulus in the transverse direction
- ✓ G_{12} : Shear modulus in the x-y plane
- ✓ G_{13} : Shear modulus in the x-z plane
- ✓ G_{23} : Shear modulus in the y-z plane
- ✓ ν_{12} : Poisson ratio in the x-y plane
- ✓ ρ : Density

All the information by Performance Composites is summarized in Table 3-2 [54].

															
Mechanical Properties of Carbon Fibre Composite Materials, Fibre / Epoxy resin (120°C Cure)															
Fibres @ 0° (UD), 0/90° (fabric) to loading axis, Dry, Room Temperature, Vf = 60% (UD), 50% (fabric)															
	Symbol	Units	Std CF Fabric	HMCF Fabric	E glass Fabric	Kevlar Fabric	Std CF UD	HMCF UD	M55** UD	E glass UD	Kevlar UD	Boron UD	Steel S97	Al. L65	Tit. dtd 5173
Young's Modulus 0°	E1	GPa	70	85	25	30	135	175	300	40	75	200	207	72	110
Young's Modulus 90°	E2	GPa	70	85	25	30	10	8	12	8	6	15	207	72	110
In-plane Shear Modulus	G12	GPa	5	5	4	5	5	5	5	4	2	5	80	25	
Major Poisson's Ratio	ν_{12}		0.10	0.10	0.20	0.20	0.30	0.30	0.30	0.25	0.34	0.23			
Ult. Tensile Strength 0°	Xt	MPa	600	350	440	480	1500	1000	1600	1000	1300	1400	990	460	
Ult. Comp. Strength 0°	Xc	MPa	570	150	425	190	1200	850	1300	600	280	2800			
Ult. Tensile Strength 90°	Yt	MPa	600	350	440	480	50	40	50	30	30	90			
Ult. Comp. Strength 90°	Yc	MPa	570	150	425	190	250	200	250	110	140	280			
Ult. In-plane Shear Stren.	S	MPa	90	35	40	50	70	60	75	40	60	140			
Ult. Tensile Strain 0°	ext	%	0.85	0.40	1.75	1.60	1.05	0.55		2.50	1.70	0.70			
Ult. Comp. Strain 0°	exc	%	0.80	0.15	1.70	0.60	0.85	0.45		1.50	0.35	1.40			
Ult. Tensile Strain 90°	eyt	%	0.85	0.40	1.75	1.60	0.50	0.50		0.35	0.50	0.60			
Ult. Comp. Strain 90°	eyc	%	0.80	0.15	1.70	0.60	2.50	2.50		1.35	2.30	1.85			
Ult. In-plane shear strain	es	%	1.80	0.70	1.00	1.00	1.40	1.20		1.00	3.00	2.80			
Thermal Exp. Co-ef. 0°	Alpha1	Strain/K	2.10	1.10	11.60	7.40	-0.30	-0.30	-0.30	6.00	4.00	18.00			
Thermal Exp. Co-ef. 90°	Alpha2	Strain/K	2.10	1.10	11.60	7.40	28.00	25.00	28.00	35.00	40.00	40.00			
Moisture Exp. Co-ef 0°	Beta1	Strain/K	0.03	0.03	0.07	0.07	0.01	0.01		0.01	0.04	0.01			
Moisture Exp. Co-ef 90°	Beta2	Strain/K	0.03	0.03	0.07	0.07	0.30	0.30		0.30	0.30	0.30			
Density		g/cc	1.60	1.60	1.90	1.40	1.60	1.60	1.65	1.90	1.40	2.00			

** Calculated figures

Table 3-2: Physical and mechanical properties of thermosets by Performance Composites [54]

All the materials have Epoxy resin matrix cured at 120 °C and the filler is either in fabric form, with fiber orientation of 0/90 ° with respect to the loading direction axis or in unidirectional form, with fiber orientation at 0° . In the case of fabric filler the fiber volume fraction is 50 % while in the case of unidirectional materials the volume fraction is increased up to 60 %. Between all materials present the ones selected are: Standard carbon fiber (StdCF) fabric, high modulus carbon fiber (HMCF) fabric, E-glass fiber fabric, Kevlar fiber fabric, unidirectional UD StdCF, UD HMCF, UD E-glass fiber and UD Kevlar fiber composites.

The materials provided as fabrics have the same Young's moduli E_1 and E_2 in both directions; this means that they have isotropic behavior. On the contrary unidirectional composites present a principal modulus E_1 which is much higher than the transverse one E_2 and so orthotropic behavior. It is important to point out how the Young's modulus E_1 for unidirectional fiber orientation is much higher than E_1 for fabric products considering the same material.

Considering only the Young's modulus in the principal direction it is clear why the HMCF composites, especially unidirectional ones, have properties exceeding the other composites reinforced with different fillers such as UD Kevlar fiber, UD glass fiber, Kevlar fiber fabric and E-glass fiber fabric. As described in the literature review section, usually "E" glass fibers are used for electrical purpose, but considering applications that are not highly structural these fibers are not necessarily limited to their original sector and can be widely employed. In case of applications with high stiffness requirements, if glass fibers would be adopted it is suggested to adopt high strength ("S") glass fibers. This is just a simple consideration, in fact to evaluate the mechanical behavior all the other parameters have to be considered according to the design solution, load distribution and so on. In Table 11-2 some data are missing, such as G_{13} and G_{23} . In general it can be considered that $G_{13}=G_{12}$ and $G_{23}=0.5G_{12}$ [54]. The data about high strength "S" glass fiber composite have been provided by AGY. Here the fibers are embedded not only in Epoxy resin as in the previous examples but also in BMI resin. The data is again present as a range of values and in order to be used; the average values have been considered. A list of the material properties is shown in Table 3-3 [55].

S-2 Glass Fiber Unidirectional Composite Properties



Property	ASTM Standard	Epoxy		BMI	
Elastic Constants (22°C/75°F)		GPa	Msi	GPa	Msi
Longitudinal modulus, E_L	D3039	53 – 59	7.7 – 8.5	59 – 70	8.6 – 10.1
Transverse modulus, E_T	D3039	16 – 20	2.3 – 2.9	17 – 21	2.5 – 3
Axial Shear modulus, G_{LT}	D3518	6 – 9	0.9 – 1.3	11 – 21	1.6 – 3.1
Poisson's ratio, ν_{LT}	D3039		0.26 – 0.28		0.27 – 0.31
Strength Properties		MPa	Ksi	MPa	Ksi
Longitudinal tension, F_L^{tu}	D3039	1540 – 2000	230 – 290	1930 – 2200	280 – 320
Longitudinal compression, F_L^{tc}	D3410	690 – 1240	100 – 180	1240 – 1516	180 – 220
Transverse tension, F_T^{tu}	D3039	41 – 82	6 – 12	62 – 96	9 – 14
Transverse compression, F_T^{tc}	D3410	110 – 200	16 – 29	138 – 207	20 – 30
In-plane shear, F_{LT}^{tu}	D3518	62 – 165	9 – 24	124 – 221	18 – 32
Interlaminar shear F^{su}	D2344	55 – 103	8 – 15	69 – 124	10 – 18
Longitudinal flexural	D790	1240 – 1720	180 – 250		
Longitudinal bearing	D653	464 – 552	68 – 80		
Ultimate Strain					
Longitudinal tension, ϵ_L^{tu}	D3039		2.7 – 3.5%		3.2 – 3.6%
Longitudinal compression, ϵ_L^{tc}	D3410		1.1 – 1.8%		1.7 – 2.5%
Transverse tension, ϵ_T^{tu}	D3039		0.26 – 0.50%		0.4 – 0.6%
Transverse compression, ϵ_T^{tc}	D3410		1.1 – 2%		1.5 – 2.2%
In-plane shear ϵ_{LT}^{tu}	D3518		1.6 – 2.5%		2 – 2.5%
Physical Properties					
Fiber volume (%)	D2734		57 – 63		59 – 65
Density g/cm ³ (lb/in ³)	D792		1.96 – 2.02 (0.071 – 0.073)		(0.070 – 0.073)

Table 3-3: Physical and mechanical properties of thermosets with glass fiber filler by AGY [55]

It is clear that the BMI resin shows better mechanical properties than the Epoxy one. Unfortunately neither G_{13} nor G_{23} are provided. These values can be computed in the way presented earlier [54]. The elastic modulus for S glass fiber composite with Epoxy resin is lower compared to all carbon fibers and the UD Kevlar fiber composites presented before, while in the case of BMI the elastic modulus is higher than both UD or fabric E-glass and Kevlar fiber composites. It is important to stress that the S glass fiber composite has much higher elastic transverse and shear modulus than all of the UD materials described above. The last set of composites found refers to NPL and the data is related to high strength (HS) and high modulus (HM) carbon fiber composites with epoxy resin matrix. The data is present in Table 3-4 [56].

Elasticities of fibre-reinforced plastics – full set



Material	$\frac{E_{11}}{\text{GPa}}$	$\frac{E_{22}}{\text{GPa}}$	$\frac{E_{33}}{\text{GPa}}$	$\frac{G_{12}}{\text{GPa}}$	$\frac{G_{13}}{\text{GPa}}$	$\frac{G_{23}}{\text{GPa}}$	ν_{12}	ν_{21}	ν_{23}
High Modulus Carbon Fibre/Epoxy –unidirectionally reinforced specimen	287	7.80	7.75	6.7	6.7	2.5	0.30	0.01	0.55
High Strength Carbon Fibre/Epoxy –unidirectionally reinforced specimen	172	11.6	11.6	7.8	7.8	3.9	0.36	0.02	0.48

Elastic Constants measured at NPL by the Ultrasonic Technique (Read and Dean, 1978).

Table 3-4: Physical and mechanical properties of NPL thermosets with carbon fiber filler [56]

The HM fiber composite has the best mechanical properties among all the materials in terms of Young's modulus in the principal direction while the HS carbon fiber composites have E_1 that is a bit lower than the UD HMCF composite, but this is not for the elastic modulus in the transverse direction E_2 . Therefore the materials cannot be compared considering only these parameters.

The NPL materials have also the highest shear modulus between all the materials described so far. Based on the information available so far, it is possible to assume that NPL materials have the best performance during the analysis with a certain accuracy. This time all set of data is available but the fiber volume fraction has been considered 60 % and the density has been estimated to be 1.6 g/cm^3 .

All the data related to the materials presented above has been collected and it is shown in Table 3-5.

Thermoset composites	Density [g/cm ³]	E1 [GPa]	E2 [GPa]	G12 [GPa]	G13 [GPa]	G23 [GPa]	v12	Fiber volume [%]
StdCF Performance Composites	1,60	70,00	70,00	5,00	5,00	2,50	0,10	50
HMCF Performance Composites	1,60	85,00	85,00	5,00	5,00	2,50	0,10	50
E glass Performance Composites	1,90	25,00	25,00	4,00	4,00	2,00	0,20	50
Kevlar Performance Composites	1,40	30,00	30,00	5,00	5,00	2,50	0,20	50
UD StdCF Performance Composites	1,60	135,00	10,00	5,00	5,00	2,50	0,30	60
UD HMCF Performance Composites	1,60	175,00	8,00	5,00	5,00	2,50	0,10	60
UD E glass Performance Composites	1,90	40,00	8,00	4,00	4,00	2,00	0,25	60
UD Kevlar Performance Composites	1,40	75,00	6,00	2,00	2,00	1,00	0,34	60
S-2 glass fiber AGY with BMI	1,99	56,00	18,00	7,50	7,50	3,75	0,27	60
S-2 glass fiber AGY with Epoxy	1,99	64,50	19,00	16,00	16,00	8,00	0,29	62
HS carbon fiber NPL	1,60	172,00	11,60	7,80	7,80	3,90	0,36	60
HM carbon fiber NPL	1,60	287,00	7,80	6,70	6,70	2,50	0,30	60

Table 3-5: Summary of physical and mechanical properties of thermosets selected for analysis

3.1.3. Assumptions for thermoplastic composites properties evaluation

Currently thermoplastic composites don't have wide application in structural components and it is hard to find data related to mechanical properties as the ones showed in the previous section. Therefore the idea is to re-create a thermoplastic composite starting from the thermoset matrix.

The properties of the Epoxy matrix are well known and presented above. Even if the resin is not the one used for each of the desired materials, it is possible to use the data so that knowing both the matrix and the composite, the data related to the fiber can be extracted by inverting the following relationships.

A distinction has to be made in the case of isotropic and orthotropic material. In the case of isotropic material the following relations can be considered.

$$E_1 = E_2 = E_f v_f + E_m (1 - v_f)$$

$$v_{12} = v_f v_f + v_m (1 - v_f)$$

$$G_{12} = E_1 / [2 (1 + v_{12})]$$

For the orthotropic material the following relations have been used [57, 58].

$$E_1 = E_f v_f + E_m (1 - v_f)$$

$$E_2 = E_f E_m / [(v_f E_m + (1 - v_f) E_f)]$$

$$v_{12} = v_f v_f + v_m (1 - v_f)$$

$$G_{12} = G_f G_m / [(v_f G_m + (1 - v_f) G_f)]$$

Where:

E_f : Fiber elastic modulus along the main axis

E_m : Matrix elastic modulus

G_f : Fiber shear modulus

G_m : Matrix shear modulus

v_f : Fiber Poisson ratio

v_m : Matrix Poisson ratio

v_f : Fiber volume fraction

Some correction coefficients for each material have to be considered so that all the values are comparable. By inverting the formulas presented above, the fiber properties can be extracted and Table 3-6 below illustrates the values of the density, the Young's and shear moduli and the Poisson's ratio for all the materials fibers.

<i>Fibers</i>	<i>Density [g/cm3]</i>	<i>Ef [GPa]</i>	<i>Gf [Gpa]</i>	<i>vf</i>
<i>StdCF Performance Composites</i>	1,95	137	1,6	0,20
<i>HMCF Performance Composites</i>	1,95	167	1,6	0,20
<i>E glass Performance Composites</i>	2,55	47	1,9	0,15
<i>Kevlar Performance Composites</i>	1,55	57	1,6	0,30
<i>UD StdCF Performance Composites</i>	1,83	223	2,8	0,23
<i>UD HMCF Performance Composites</i>	1,83	290	2,8	0,23
<i>UD E glass Performance Composites</i>	2,33	65	3,7	0,15
<i>UD Kevlar Performance Composites</i>	1,50	123	6,8	0,30
<i>S-2 glass fiber AGY</i>	2,48	88	30,0	0,18
<i>HS carbon fiber NPL</i>	1,83	285	2,1	0,33
<i>HM carbon fiber NPL</i>	1,83	477	2,3	0,23

Table 3-6: Physical and mechanical properties estimation for fibers used with thermosets

Once the data for the fibers is known it can be used again with a new matrix employing the same relations. The PVC is the selected thermoplastic matrix due to its superior mechanical properties in term of Young's and shear moduli and very low price, although it was noted before that the density value is somewhat high. The new materials mechanical properties in thermoplastic PVC resin are illustrated in Table 3-7.

<i>Thermoplastic composites</i>	<i>Density [g/cm3]</i>	<i>E1 [GPa]</i>	<i>E2 [GPa]</i>	<i>G12</i>	<i>G13 [GPa]</i>	<i>G23 [GPa]</i>	<i>v12</i>	<i>Fiber volume [%]</i>
<i>StdCF Performance Composites</i>	1,70	70,20	70,20	7,81	7,81	3,91	0,10	50
<i>HMCF Performance Composites</i>	1,70	85,20	85,20	7,78	7,78	3,89	0,10	50
<i>E glass Performance Composites</i>	2,00	25,20	25,20	5,62	5,62	2,81	0,20	50
<i>Kevlar Performance Composites</i>	1,50	30,18	30,18	7,81	7,81	3,91	0,20	50
<i>UD StdCF Performance Composites</i>	1,68	135,16	11,42	7,62	7,62	3,81	0,30	60
<i>UD HMCF Performance Composites</i>	1,68	175,00	9,20	7,00	7,00	3,50	0,30	60
<i>UD E glass Performance Composites</i>	1,97	40,00	9,00	4,55	4,55	2,28	0,25	60
<i>UD Kevlar Performance Composites</i>	1,48	75,00	6,70	2,26	2,26	1,13	0,34	60
<i>S-2 glass fiber AGY</i>	2,00	56,50	19,94	8,50	8,50	4,25	0,27	60
<i>HS carbon fiber NPL</i>	1,68	172,00	13,00	14,36	14,36	7,18	0,36	60
<i>HM carbon fiber NPL</i>	1,66	287,00	8,93	10,91	10,91	5,46	0,30	60

Table 3-7: Thermoplastics properties after fibers and thermoplastic PVC resin combination

3.2. Design steps and proposed solutions

In this section the procedures and the ideas used to reach the final component design will be illustrated. Some constraints have been considered; the main ones are related to the available space.

The dimensions fixed for the component are 550 millimeters in length and width, and 30 millimeters in height. The round corners have been set to 30 millimeters and all the other parameters have been fixed so that a good compromise between design, weight and productivity could be reached.

Since the design phase requires high variability of the solutions adopted and need of several steps to reach the final target, it has been decided to keep a constant thickness of 3 millimeters for all the surfaces, and the overall surface area has been set around certain values in order to have a component weight as much close as possible to the target maximum weight of 3.11 kg for each of the materials presenting different density values. The software used for the design in FEM simulation phase is Abaqus and all the surfaces have been created in 3D modeling space, deformable type, and with shell shape, both planar or extruded according to the surfaces mutual orientation within the preset.

The first design is a simple flat panel with dimensions satisfying the criteria described above. An example is provided in Figure 3-1.



Figure 3-1: Simple flat panel model respecting geometry requirements

Starting from this point several panel design solutions have been developed; the first one is the use of a rib perpendicular to the outer profile running around the component. After that a series of internal ribs has been introduced with different orientation; for example aligned at 45° and parallel to each other or aligned at 45° and -45° in order to create a grid, or oriented randomly in order to create a structure with triangular ribs concentrated in different areas with different density. Some examples are provided in Figures 3-2 to 3-5.

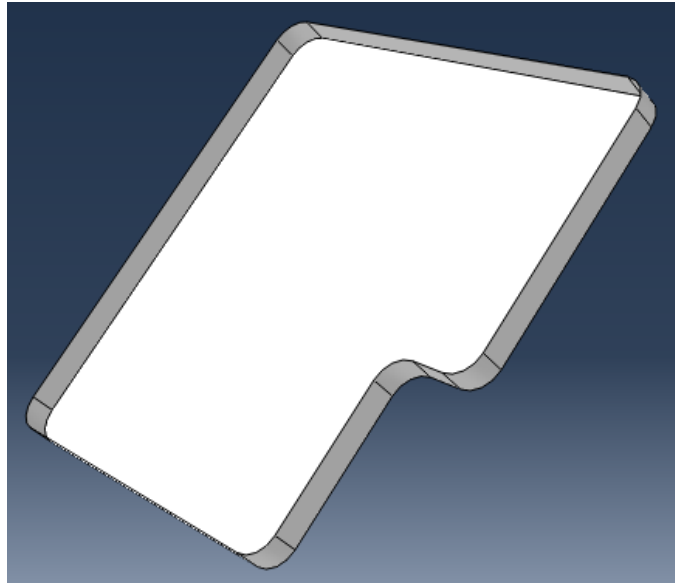


Figure 3-2: Flat panel and peripheral rib

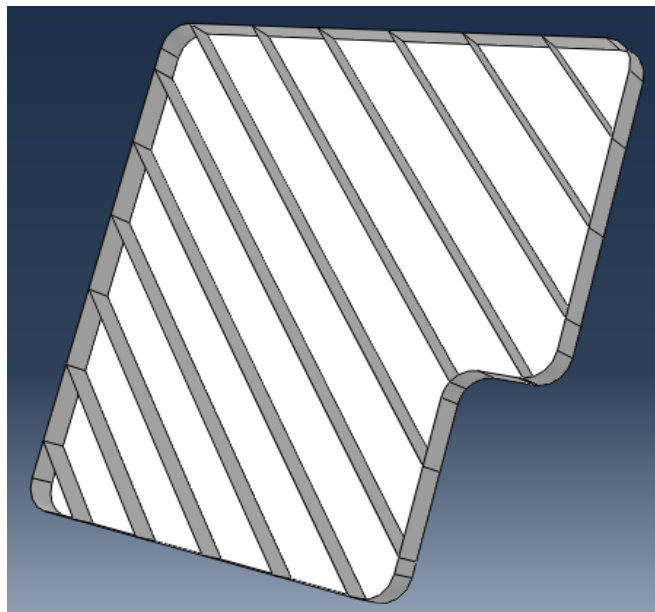


Figure 3-3: Panel with outer and internal ribs

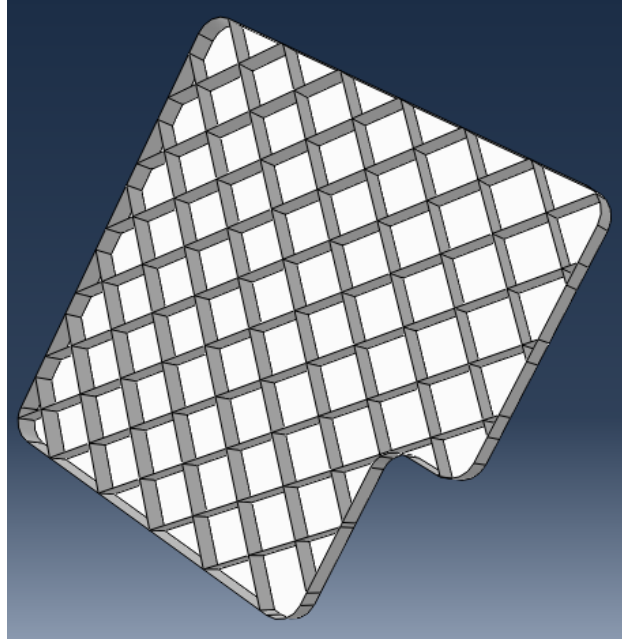


Figure 3-4: Panel with ribs grid

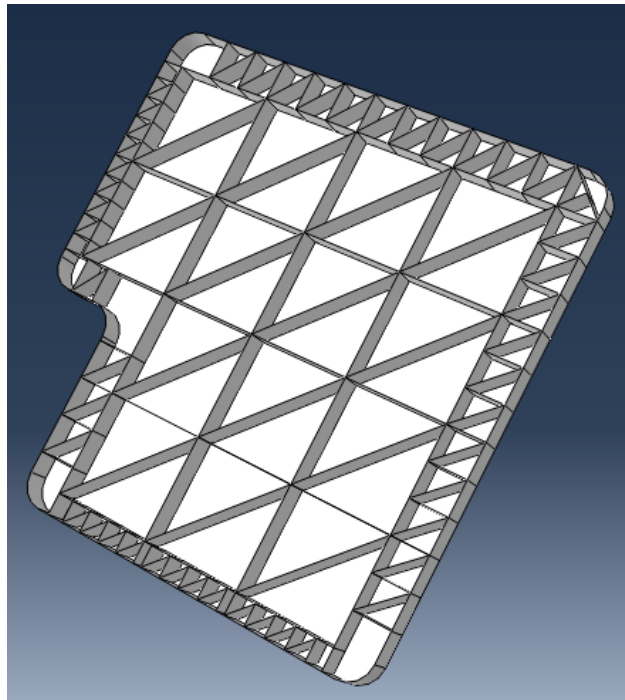


Figure 3-5: Panel with triangular ribs

These proposed design solutions have the advantage of allowing a good load distribution over the structure and therefore the capability to reach high stiffness values; at the same time a quick production phase can be employed by assuming the production of the flat panel and the outer rib by compression molding process.

The next step consists of the injection molding of the inner ribs that require more or less time according to the amount of material to be used. These steps will be described in more details in the next chapters. Next solution consists of the same flat panel with or without the outer rib reinforcement and a corrugated panel with enough flat surfaces to be joined with the panel at its end. The rib orientation then has been considered in vertical, horizontal and with 45° angle inclination. An example of the component with outer rib and vertical oriented corrugated panel is present in Figure 3-6.

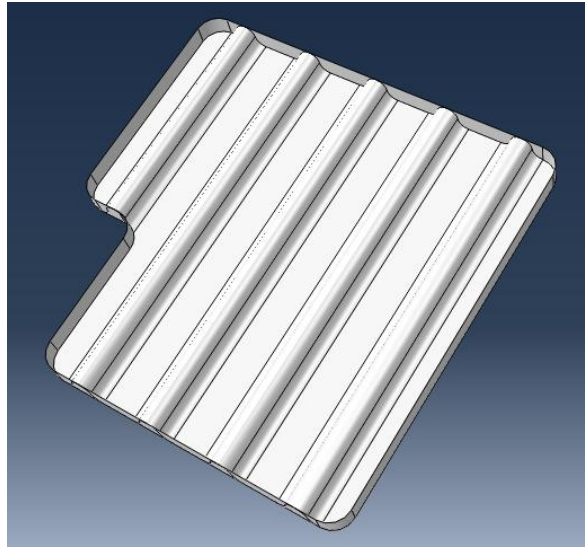


Figure 3-6: Open structure with corrugated panel and peripheral reinforcement

Similar to the solution presented before this one in Figure 3-6 allows a quick production once the flat and the corrugated panels are available. The challenge related to this process is the way to join both panels at the contact surfaces; not only the panel surfaces need to be joined but also they should establish a contact between the border profile of the corrugated panel and the outer reinforcement. All these design modifications enhance the structure stiffness. Their effect will be evaluated and analyzed in the simulation part. The solutions considered to join the panels will be selected between adhesive bonding, mechanical fastening and the new melding process described in the literature review part. A further improvement of the solution described above consists of placing the corrugated panel in between two flat panels instead of one. This time the corrugated panel needs to have flat surface areas on both sides in order to be joined to the two outer panels. A better visual description of the combined panels can be seen in Figure 3-7.

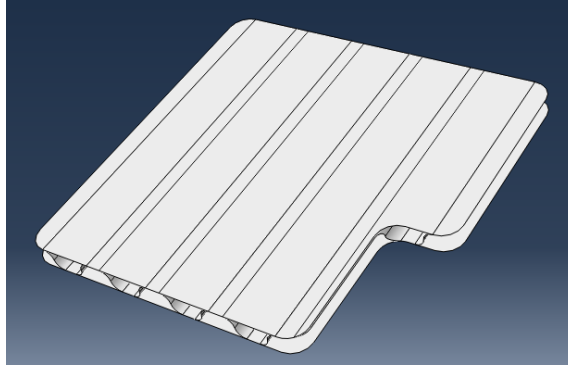


Figure 3-7: Sandwich structure with corrugated panel as internal core

To the base solution different tricks have been added, for example the addition of the outer rib running along the profile, different corrugated panel orientation as described for the open structure before, and further reinforcement inside the corrugated panel by putting ribs in between the waves. Figures 3-8 to 3-11 illustrate the described solution.

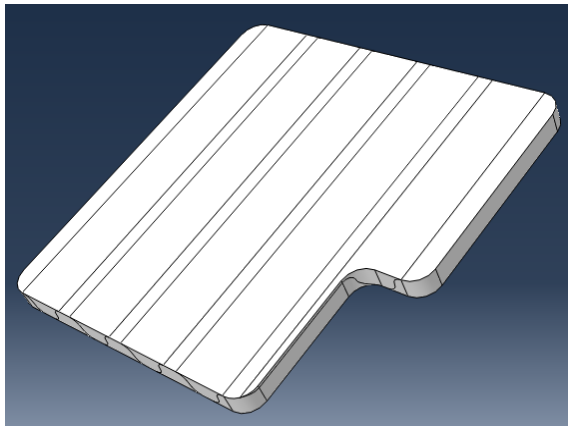


Figure 3-8: Vertical corrugated structure

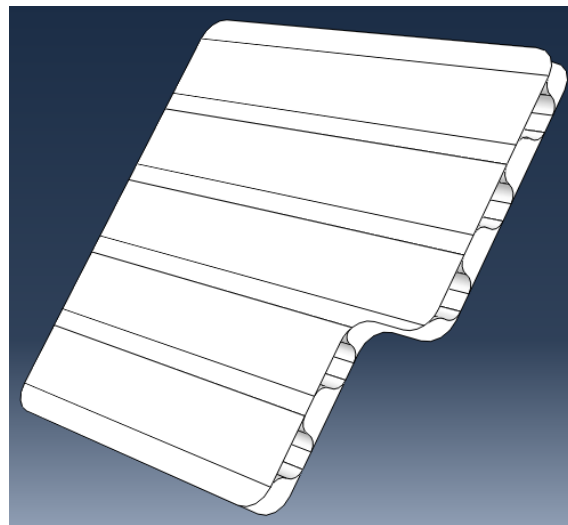


Figure 3-9: Horizontal corrugated structure

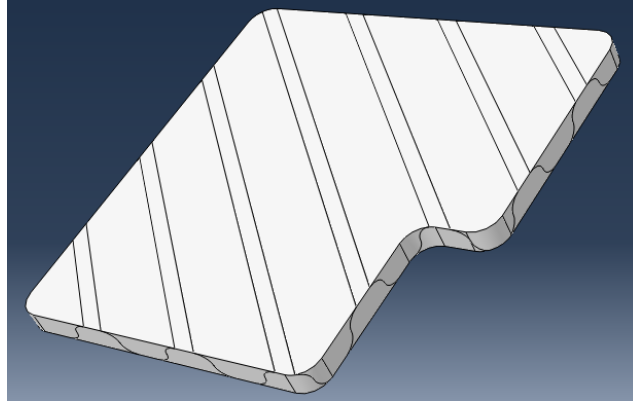


Figure 3-10: Corrugated sandwich structure

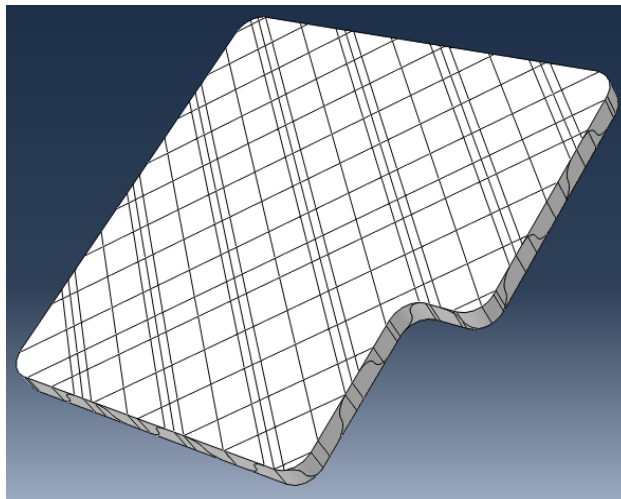


Figure 3-11: Corrugated and ribbed structure

During the analysis the set of the solutions was considered in order to better understand the effects of the different modifications and to find the best compromise. The production steps for these solutions are similar to the steps described for the open structure with some differences. The most important one is the fact that there should be a double bonding instead of a single one, so the required processing time can increase depending on the selected manufacturing process. Then the outer rib along the profile has to be molded with just one of the outer panels while the other one is to be used for just closing the box. In the case with inner ribs between the corrugated panel the process will take longer since the first step will be the injection molding of the ribs on the panel and then everything has to be placed inside the panel with presenting a cavity and closed by the flat panel. As in the previous case the assembly process has to guarantee an optimal bonding not only between the faces but also between the profile edges.

3.3. F.e.m. simulations set up in Abaqus environment

In this section the simulations set up will be described. The work consists of running the simulations for the selected set of different materials varying not only the component design, but also the thickness of the parts and the fiber orientation in the composite materials.

As it was noted earlier, working in Abaqus environment all parts are created as 3D models, deformable and as shell planar or extruded. Soon after, the material input data has to be provided and the set of data required for composites is composed by the parameters described in the materials description chapter, while by using an isotropic material without fibers, for example PVC, the required data are only the Young's and shear moduli and the Poisson's ratio.

In the section related to the material creation the mechanical properties are elastic and isotropic for materials such as resins, while the option "lamina" has to be selected in order to create a composite. Once the material properties are known the section has to be defined; for isotropic materials the shell surfaces selection is homogeneous and the thickness value has to be input; in the case of composite the option "composite" has to be selected and then the number of plies, the constituent material for each of them, their thickness, fiber orientation angle, integration points number and ply name has to be decided by the user. The section integration is done during analysis and Simpson rule is used for the thickness integration.

At this point the section assignment can be done and to each of the component faces a different section can be assigned thus allowing the component to have different thicknesses in different areas with different materials kind and different orientations in the case of composite materials.

The next step consists in creating an independent mesh so that the component meshing can be done directly and automatically on the instance. In the section "step" a new step called "load" has to be created together with the existing "initial" one; the step is set as static and general, the incrementation type is automatic with a maximum of 100 increments. The initial and maximum incremental size is one while the minimum one is $1e-5$. The equation solver method is set as direct by default and full Newton solution technique is used.

The load variation is ramp linearly over step by default too. Other parameter can be set but they have secondary importance. All this data allows to create the boundary conditions (BCs) of the component; in this case study they can be set as mechanical and displacement/rotation type for the selected step that is usually the load one. This set-up allows to analyze the component behavior not through forces or pressures application but by imposing certain displacements. Before setting the conditions, the faces, edges or nodes to apply the BCs have to be defined; after that it is possible to pick between three displacements U_1 , U_2 and U_3 along the x, y and z axis and three rotations about the same axes UR_1 , UR_2 and UR_3 . If one of the parameters is not picked it means that the component is free to move and is not constrained; just picking one of them means to impose a constraint with a null displacement or rotation, 0 value is imposed by default and it can be modified in order to have the desired movement. The amplitude is set as ramp by default. The model to analyze needs the constraints to be set as points since it is necessary to evaluate the reaction forces in each point and in every direction and then all the values related to a certain direction have to be summed before the reaction force magnitude in the displacement application point is known. The boundary conditions description has been provided in the problem statement; the rotation along the Y axis in the car reference system has been simplified and modeled with three points along the lower seat back by picking all the parameters except UR_1 that allows the seat to rotate about the X axis in the component reference system. The lock condition has been applied to the right upper corner in one fixed point and U_1 , U_2 and U_3 have been constrained with 0 displacement so that the component is able to rotate around that point as if it was a spherical joint thus giving freedom to UR_1 , UR_2 and UR_3 . The displacement point instead has been fixed in the upper left corner and the only parameter modified is U_2 whose value is set to +/-100 in order to let the seat back bend along the positive and negative x direction in the car reference system; all the other movements are allowed and not constrained. The next step consists in creating the component mesh; the instance is sized by selecting the “seed” option and an approximated global size is set to 10. The minimum size factor as a fraction of global size is set to 0.1 by default. Quad elements with linear geometric order and finite membrane strain are used; all the parameters have been kept constant as provided by default.

Several iterations have been performed varying the mesh size until mesh independent solution has been achieved and the results were not affected by further increase of mesh density.

The component is ready to be analyzed, but before running the simulation the information to check have to be decided and selected by modifying the “field output request”; the data useful for the project purposes is stresses, strains, displacements and forces/reactions. Before launching the simulation a job needs to be created with full analysis type, all the parameters have not been changed. The output results are monitored after submitting the job created and accessing to the visualization it is possible to evaluate the reaction forces RFs in the three directions x, y and z illustrated as RF_1 , RF_2 and RF_3 . Using the tools query it is possible to pick in the constraint point and read the exact force value; after applying the equilibrium on the structure the reaction force in correspondence of the displacement point is known and can be useful to evaluate the stiffness in that point.

3.3.1. Model validation and comparison with available results

Before running the simulations for the design solutions presented in the previous section some of the old solutions tested in the past by Fiat automobiles have been reproduced in Abaqus environment in order to see if it is possible to have a matching between the two models and validate the new one. The solution used to test the developed model is an extruded aluminum structure with inner horizontal ribs perpendicular to the panel surface. The design is provided in Figure 3-12.

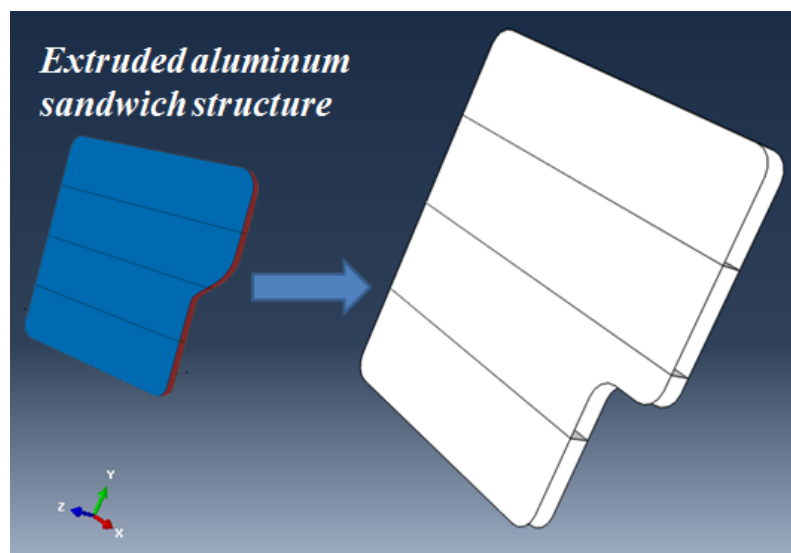


Figure 3-12: Extruded aluminum solution re-modeling with Abaqus software

Both solutions have 5.06 kg weight with 3 mm thickness constant for all the regions; the material applied is aluminum with 2.7 kg/dm^3 density and 70 GPa Young's modulus. The results for the two models are overlapped and can be visualized in Figure 3-13.

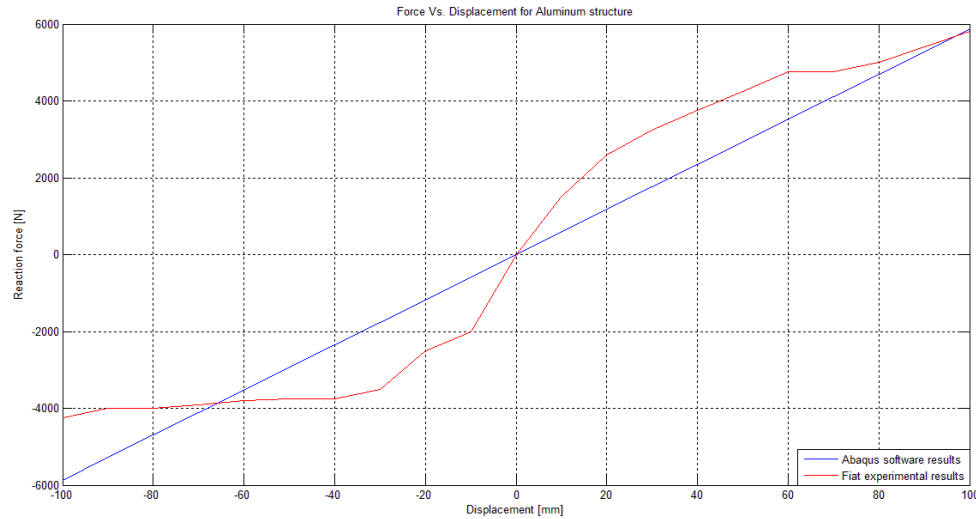


Figure 3-13: Results comparison between models for extruded aluminum structure

The final force value is almost the same in both cases and the component stiffness is about 58 N/mm. The Abaqus model has a linear trend with constant slope and so stiffness, while the solution provided by Fiat has no-constant shape but can be well fitted and approximated by the linear model.

Furthermore Fiat data shows a clear elastic-plastic behavior, with linear region between -30 mm and 40 mm, and plastic regions above 40 mm and below -30 mm. The presented model simulates a composite material with aluminum material properties with purely elastic response, which is evident in Figure 3-13. Although both the model and the experimental data represent different materials behavior the stress-displacement trends are consistent, which is a proof for the accuracy of the model.

The same procedure has been used for another extruded aluminum structure similar to the one presented earlier, but with more reinforcement planes displaced sidelong between the external skins. The material used is the same described in the previous case. The analyzed designs are two; the first one has 7.49 kg weight and 3 mm thickness while the second is lighter and thinner presenting 4.99 kg weight and 2 mm thickness. The design is the same for both structure and it is shown in Figure 3-14.

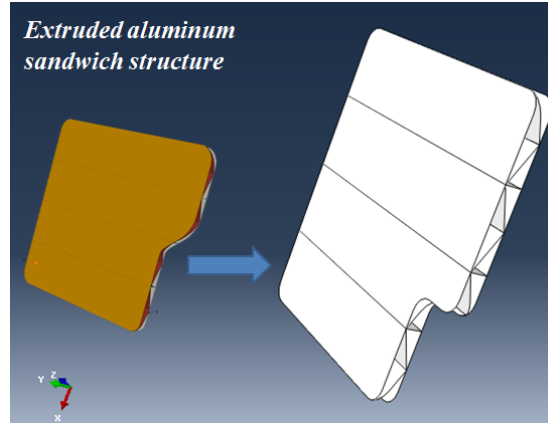


Figure 3-14: Reinforced aluminum extruded structure re-modeling with Abaqus software

The structure with 3 mm thickness has the same force value in correspondence of 100 mm displacement but during all the displacement range the model obtained from Fiat has not a constant shape, while Abaqus model has linear trend and so constant thickness. In the case with 2 mm thickness it is not possible to compare the force values since the Fiat model analysis is limited up to 60 mm displacement. In both cases Abaqus models approximate and fit the non-linear results in proper way creating a matching and a certain correspondence. The considerations are similar to those previously described. The results have been summarized in Figure 3-15.

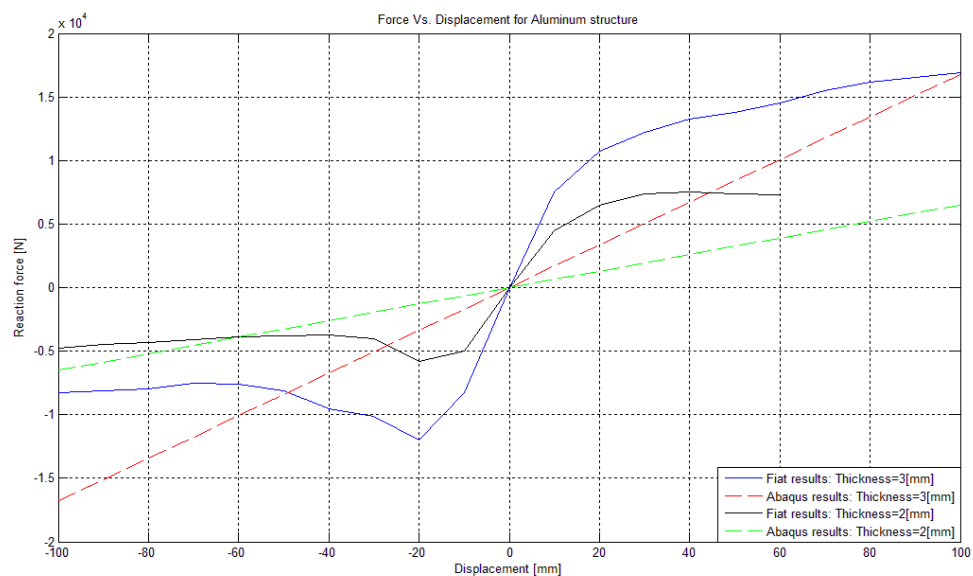


Figure 3-15: Results comparison between models for reinforced extruded aluminum structure

3.3.2. Behavior of components in PVC resin

The design solutions introduced in the previous sections have been analyzed considering always the PVC thermoplastic matrix due to its better mechanical properties and lower cost. The isotropic behavior allows for better comparison between the stiffness values obtained step by step introducing modifications in the component. In these first simulations the component thickness has been set constant for all the surfaces and the variations are related only to the geometrical dimensions in order to meet the weight requirements. Table 3-8 summarizes the results.

PVC	Thickness [mm]	Maximum RF [N]	Resultant [N]	Weight [Kg]
Panel	3 pan / 3 rib	4	3	1,20
Panel with triangular ribs	3 pan / 3 rib	755	220	2,88
Closed structure with corrugated panel	2 fpan / 2 rpan / 2 corr / 2 rib	3753	1177	2,79

Table 3-8: Results obtained testing some design solutions in PVC material

The presented results refer to three conditions reached for a simple flat panel, the panel with triangular ribs and the closed structure with corrugated and the two external panels. Not only the reaction force in the displacement application point but also the maximum reaction force on the structure has been evaluated in order to have an idea about the maximum stiffness value in a certain point that is one of the constraint points. In the first case, as expected, the force values are in the order of few Newton while the improvement is evident by adding ribs that allow to reach values in the order of hundred Newton even if only the solution with corrugated panel allows to reach values over 1000 N. The thickness has not been increased since for the hypothesis of constant thickness the weight requirement would not be satisfied and at the same time the improvement would have been negligible.

3.3.3. Tests performed on components with thermoset constituent material

A similar approach as the one described above has been applied to each of the thermoset composites available. The components have the same thickness in all the parts with the exception of the closed structure with both corrugated panel and reinforcements inside. The new challenge consists of placing the fiber in the proper way; in fact several solutions such as displacing the ply fibers at $0^\circ/90^\circ$, $45^\circ/-45^\circ$, increasing the angle by 45° each step, trying with symmetrical lay-up have been evaluated. The results presented in Table 3-9 refer to the Std CF composite by Performance Composites.

StdCF Performance Composites with Epoxy resin	Thickness [mm]	Fiber orientation [°]	Maximum RF [N]	Resultant [N]
Panel	3 pan / 3 rib	0/90	20	15
Panel	3 pan / 3 rib	45alt	682	50
Panel	3 pan / 3 rib	45/-45	109	82
Open structure with corrugated panel	3 fpan / 2 corr / 3 rib	0/90	6866	762
Panel with triangular ribs	3 pan / 3 rib	45/-45	3693	1586
Open structure with corrugated panel	3 fpan / 2 corr / 3 rib	45alt	11270	2278
Panel with triangular ribs	3 pan / 3 rib	45alt	9913	3259
Panel with triangular ribs	3 pan / 3 rib	0/90	21150	3425
Open structure with corrugated panel	3 fpan / 2 corr / 3 rib	45/-45	10590	3431
Closed structure with corrugated panel and ribs	2 fpan / 2 rpan / 1,5 corr / 2 rib	0/90	31090	5533
Closed structure with corrugated panel	2 fpan / 2 rpan / 2 corr / 2 rib	0/90	35420	6770
Closed structure with corrugated panel and ribs	2 fpan / 2 rpan / 1,5 corr / 2 rib	45alt	49570	13228
Closed structure with corrugated panel	2 fpan / 2 rpan / 2 corr / 2 rib	45alt	54630	19799
Closed structure with corrugated panel and ribs	2 fpan / 2 rpan / 1,5 corr / 2 rib	45/-45	52120	24910
Closed structure with corrugated panel	2 fpan / 2 rpan / 2 corr / 2 rib	45/-45	52950	27973

Table 3-9: Results collection for thermoset with Std CF by Performance Composites

The reaction force range varies from about 15 N for the flat panel up to 28,000 N for the corrugated structure. Only this kind of structure for this material is able to satisfy the force requirements above 8,000 N without exceeding the weight limit. The reason for that is due to the fact that the design has been developed considering as reference density the one of composites with carbon fibers since they are in between the ones of glass and Kevlar fiber composites. It is important to stress that the solution with corrugated panel and inner ribs is weaker than the one with just the corrugated panel since the material quantity has been removed from the panel in order to build the ribs. This means that the influence of the panel is much stronger than the one of the ribs. The values in Table 3-9 refer to the best solution; it can be noted that in all cases the higher values are obtained displacing the ply fibers at 45°/-45° with respect to the load direction; this is satisfied only for the structures with corrugated panel since for the panel and the panel with ribs the optimal values are achieved at 0°/90° orientation. These results are the same for the other materials even if some exceptions are observed and will be pointed out. Table 3-10 is related to the HMCf by Performance Composites.

HMCf Performance Composites with Epoxy resin	Thickness [mm]	Fiber orientation [°]	Maximum RF [N]	Resultant [N]
Panel	3 pan / 3 rib	0/90	20	15
Panel	3 pan / 3 rib	45alt	86	59
Panel	3 pan / 3 rib	45/-45	130	98
Open structure with corrugated panel	3 fpan / 2 corr / 3 rib	0/90	7330	774
Panel with triangular ribs	3 pan / 3 rib	45/-45	3952	1688
Open structure with corrugated panel	3 fpan / 2 corr / 3 rib	45alt	13200	2686
Panel with triangular ribs	3 pan / 3 rib	45alt	11740	3879
Panel with triangular ribs	3 pan / 3 rib	0/90	25657	3987
Open structure with corrugated panel	3 fpan / 2 corr / 3 rib	45/-45	12050	4038
Closed structure with corrugated panel and ribs	2 fpan / 2 rpan / 1,5 corr / 2 rib	0/90	33500	5664
Closed structure with corrugated panel	2 fpan / 2 rpan / 2 corr / 2 rib	0/90	38520	6943
Closed structure with corrugated panel and ribs	2 fpan / 2 rpan / 1,5 corr / 2 rib	45alt	58320	15420
Closed structure with corrugated panel	2 fpan / 2 rpan / 2 corr / 2 rib	45alt	64600	23436
Closed structure with corrugated panel and ribs	2 fpan / 2 rpan / 1,5 corr / 2 rib	45/-45	60420	29775
Closed structure with corrugated panel	2 fpan / 2 rpan / 2 corr / 2 rib	45/-45	60900	33072

Table 3-10: Results collection for thermoset with HMCf by Performance Composites

The results are similar to the ones presented for Std CF composite since the materials have the same density but this time the force values are higher since E_1 and E_2 are higher. The maximum reaction force value in correspondence of the displacement application point is around 3,300 N.

Some differences are present by using E-glass fiber composite by Performance Composites.

<i>E glass Performance Composites with Epoxy resin</i>	<i>Thickness [mm]</i>	<i>Fiber orientation [°]</i>	<i>Maximum RF [N]</i>	<i>Resultant [N]</i>
Open structure with corrugated panel	3 fpan / 2 corr / 3 rib	0/90	4030	571
Open structure with corrugated panel	3 fpan / 2 corr / 3 rib	45alt	4730	922
Panel with triangular ribs	3 pan / 3 rib	45/-45	2345	970
Open structure with corrugated panel	3 fpan / 2 corr / 3 rib	45/-45	4760	1266
Panel with triangular ribs	3 pan / 3 rib	45alt	4241	1301
Panel with triangular ribs	3 pan / 3 rib	0/90	7020	1433
Closed structure with corrugated panel and ribs	2 fpan / 2 rpan / 1,5 corr / 2 rib	0/90	17870	4032
Closed structure with corrugated panel	2 fpan / 2 rpan / 2 corr / 2 rib	0/90	19370	4888
Closed structure with corrugated panel and ribs	2 fpan / 2 rpan / 1,5 corr / 2 rib	45alt	20940	5780
Closed structure with corrugated panel	2 fpan / 2 rpan / 2 corr / 2 rib	45alt	22420	7867
Closed structure with corrugated panel and ribs	2 fpan / 2 rpan / 1,5 corr / 2 rib	45/-45	22400	8814
Closed structure with corrugated panel	2 fpan / 2 rpan / 2 corr / 2 rib	45/-45	23200	10300

Table 3-11: Results collection for thermoset with E-glass fiber by Performance Composites

The overall behavior of the several solutions tested is similar to the previous case but this time the material has lower mechanical properties and higher density thus having weight up to 3.69 kg with only two solutions able to satisfy the force requirements.

The Kevlar fiber composite by Performance Composites have some interesting properties as evidenced in Table 3-12.

<i>Kevlar Performance Composites with Epoxy resin</i>	<i>Thickness [mm]</i>	<i>Fiber orientation [°]</i>	<i>Maximum RF [N]</i>	<i>Resultant [N]</i>
Closed structure with corrugated panel and ribs	2 fpan / 2 rpan / 1,5 corr / 2 rib	0/90	21930	5016
Closed structure with corrugated panel	2 fpan / 2 rpan / 2 corr / 2 rib	0/90	23700	6077
Closed structure with corrugated panel and ribs	2 fpan / 2 rpan / 1,5 corr / 2 rib	45alt	25440	7053
Closed structure with corrugated panel	2 fpan / 2 rpan / 2 corr / 2 rib	45alt	27180	9547
Closed structure with corrugated panel and ribs	2 fpan / 2 rpan / 1,5 corr / 2 rib	45/-45	27700	10608
Closed structure with corrugated panel	2 fpan / 2 rpan / 2 corr / 2 rib	45/-45	28200	12409

Table 3-12: Results collection for thermoset with Kevlar fiber by Performance Composites

The material is able to satisfy the requirements; the force values are better compared to the ones obtained for the E-glass fiber composite with the advantage of a noticeable weight reduction with component weight of 2.72 kg. The Young's and shear moduli values are a bit higher than the ones for E-glass composite. The next results are obtained from the same materials introduced above but with unidirectional ply fiber alignment; the example below is for UD Std CF by Performance Composites.

UD StdCF Performance Composites with Epoxy resin	Thickness [mm]	Fiber orientation [°]	Maximum RF [N]	Resultant [N]
Closed structure with corrugated panel and ribs	2 fpan / 2 rpan / 1,5 corr / 2 rib	90	19960	4927
Closed structure with corrugated panel and ribs	2 fpan / 2 rpan / 1,5 corr / 2 rib	0	24610	5142
Closed structure with corrugated panel	2 fpan / 2 rpan / 2 corr / 2 rib	90	22060	5857
Closed structure with corrugated panel	2 fpan / 2 rpan / 2 corr / 2 rib	0	27070	6308
Closed structure with corrugated panel and ribs	2 fpan / 2 rpan / 1,5 corr / 2 rib	-45	26840	8756
Closed structure with corrugated panel	2 fpan / 2 rpan / 2 corr / 2 rib	-45	25990	9596
Closed structure with corrugated panel and ribs	2 fpan / 2 rpan / 1,5 corr / 2 rib	45	27660	9827
Closed structure with corrugated panel	2 fpan / 2 rpan / 2 corr / 2 rib	45	29000	11389

Table 3-13: Results collection for thermoset with UD Std CF by Performance Composites

The results are in between the ones obtained for E-glass and Kevlar fiber composites but much lower than the ones obtained for the same materials provided as fabric; the reason is given by the E_2 modulus that is very low compared to the one for fabric plies even if the value of E_1 is much higher and the shear behavior is the same. The maximum values in this case are given again by fibers with 45° angle orientation. The weights are the same as the previous carbon fiber composites. Similar considerations can be done for the UD HMCf composite always by Performance Composites.

UD HMCf Performance Composites with Epoxy resin	Thickness [mm]	Fiber orientation [°]	Maximum RF [N]	Resultant [N]
Closed structure with corrugated panel and ribs	2 fpan / 2 rpan / 1,5 corr / 2 rib	90	19010,00	4867,00
Closed structure with corrugated panel and ribs	2 fpan / 2 rpan / 1,5 corr / 2 rib	0	24870,00	5149,50
Closed structure with corrugated panel	2 fpan / 2 rpan / 2 corr / 2 rib	90	20870,00	5767,32
Closed structure with corrugated panel	2 fpan / 2 rpan / 2 corr / 2 rib	0	26880,00	6311,20
Closed structure with corrugated panel and ribs	2 fpan / 2 rpan / 1,5 corr / 2 rib	-45	24820,00	7741,93
Closed structure with corrugated panel	2 fpan / 2 rpan / 2 corr / 2 rib	-45	23770,00	8411,70
Closed structure with corrugated panel and ribs	2 fpan / 2 rpan / 1,5 corr / 2 rib	45	25680,00	8780,82
Closed structure with corrugated panel	2 fpan / 2 rpan / 2 corr / 2 rib	45	26800,00	10104,60

Table 3-14: Results collection for thermoset with UD HMCf by Performance Composites

It is important to notice that the results are worse than the ones obtained for the previous material even though the E_1 modulus is much higher and the shear moduli are the same with UD Std CF composite. The influence is due to the lower E_2 value that plays a fundamental role as it was explained before. UD E-glass composite is not able to satisfy the requirements even if the values are very close to the target ones.

UD E glass Performance Composites with Epoxy resin	Thickness [mm]	Fiber orientation [°]	Maximum RF [N]	Resultant [N]
Closed structure with corrugated panel and ribs	2 fpan / 2 rpan / 1,5 corr / 2 rib	90	14080	3808
Closed structure with corrugated panel and ribs	2 fpan / 2 rpan / 1,5 corr / 2 rib	0	15530	3885
Closed structure with corrugated panel	2 fpan / 2 rpan / 2 corr / 2 rib	90	15070	4525
Closed structure with corrugated panel	2 fpan / 2 rpan / 2 corr / 2 rib	0	16550	4739
Closed structure with corrugated panel and ribs	2 fpan / 2 rpan / 1,5 corr / 2 rib	-45	17320	5691
Closed structure with corrugated panel and ribs	2 fpan / 2 rpan / 1,5 corr / 2 rib	45	17350	6162
Closed structure with corrugated panel	2 fpan / 2 rpan / 2 corr / 2 rib	-45	16750	6267
Closed structure with corrugated panel	2 fpan / 2 rpan / 2 corr / 2 rib	45	18290	7220

Table 3-15: Results collection for thermoset with UD E-glass fiber by Performance Composites

In the case of UD Kevlar composite the results are still unsatisfactory but the lower material weight allows for further optimization to reach the target weight value additional more material can be employed. The mechanical properties are lower than in the case of UD E-glass composite, especially for E_2 values while E_1 are almost the same in both cases.

UD Kevlar Performance Composites with Epoxy resin	Thickness [mm]	Fiber orientation [°]	Maximum RF [N]	Resultant [N]
Closed structure with corrugated panel and ribs	2 fpan / 2 rpan / 1,5 corr / 2 rib	90	94060	2061
Closed structure with corrugated panel and ribs	2 fpan / 2 rpan / 1,5 corr / 2 rib	0	11540	2150
Closed structure with corrugated panel	2 fpan / 2 rpan / 2 corr / 2 rib	90	10660	2461
Closed structure with corrugated panel	2 fpan / 2 rpan / 1,5 corr / 2 rib	0	13050	2644
Closed structure with corrugated panel and ribs	2 fpan / 2 rpan / 1,5 corr / 2 rib	-45	13960	4890
Closed structure with corrugated panel	2 fpan / 2 rpan / 2 corr / 2 rib	-45	13080	5369
Closed structure with corrugated panel and ribs	2 fpan / 2 rpan / 1,5 corr / 2 rib	45	14550	5478
Closed structure with corrugated panel	2 fpan / 2 rpan / 2 corr / 2 rib	45	15360	6372

Table 3-16: Results collection for thermoset with UD Kevlar fiber by Performance Composites

The glass fiber composites with Epoxy and BMI resin provided by AGY have noticeable mechanical properties, much higher than the values found for the previous E-glass composites. This fact is also due to the better properties of the “S” type fibers over “E” type. The results can be compared in the Tables 3-17 and 13-18.

S-2 glass fiber AGY with Epoxy resin	Thickness [mm]	Fiber orientation [°]	Maximum RF [N]	Resultant [N]
Closed structure with corrugated panel and ribs	2 fpan / 2 rpan / 1,5 corr / 2 rib	0/90	29960	7339
Closed structure with corrugated panel	2 fpan / 2 rpan / 2 corr / 2 rib	0/90	31680	8851
Closed structure with corrugated panel and ribs	2 fpan / 2 rpan / 1,5 corr / 2 rib	45alt	32400	9473
Closed structure with corrugated panel	2 fpan / 2 rpan / 2 corr / 2 rib	45alt	35600	12862
Closed structure with corrugated panel and ribs	2 fpan / 2 rpan / 1,5 corr / 2 rib	45/-45	35520	13799
Closed structure with corrugated panel	2 fpan / 2 rpan / 2 corr / 2 rib	45/-45	36750	16285

Table 3-17: Results collection for thermoset with Epoxy resin and ‘S’ type glass fiber by AGY

S-2 glass fiber AGY with BMI resin	Thickness [mm]	Fiber orientation [°]	Maximum RF [N]	Resultant [N]
Closed structure with corrugated panel and ribs	2 fpan / 2 rpan / 1,5 corr / 2 rib	0/90	46750	14560
Closed structure with corrugated panel and ribs	2 fpan / 2 rpan / 1,5 corr / 2 rib	45alt	45750	14975
Closed structure with corrugated panel and ribs	2 fpan / 2 rpan / 1,5 corr / 2 rib	45/-45	46700	16231
Closed structure with corrugated panel	2 fpan / 2 rpan / 2 corr / 2 rib	0/90	47570	17287
Closed structure with corrugated panel	2 fpan / 2 rpan / 2 corr / 2 rib	45alt	48530	18351
Closed structure with corrugated panel	2 fpan / 2 rpan / 2 corr / 2 rib	45/-45	48790	19392

Table 3-18: Results collection for thermoset with BMI resin and ‘S’ type glass fiber by AGY

The disadvantage related to both materials is due to the high density value that is even more than the one of E-glass composites so that the overall weight is about 3.86 kg; but, since the force values exceed the required one the component can be easily improved to meet the target result.

The last materials tested are both high strength and high modulus carbon fiber composites by NPL; all the mechanical properties are better than the ones found for all the materials described so far. Only the value of E_2 for both HS and HM material is lower than the one of S-2 glass fiber composites. The results are presented in Table 3-19 and 3-20.

HS carbon fiber NPL with Epoxy resin	Thickness [mm]	Fiber orientation [°]	Maximum RF [N]	Resultant [N]
Closed structure with corrugated panel and ribs	2 fpan / 2 rpan / 1,5 corr / 2 rib	0/90	44930	8391
Closed structure with corrugated panel	2 fpan / 2 rpan / 2 corr / 2 rib	0/90	50130	10244
Closed structure with corrugated panel and ribs	2 fpan / 2 rpan / 1,5 corr / 2 rib	45alt	57750	16092
Closed structure with corrugated panel	2 fpan / 2 rpan / 2 corr / 2 rib	45alt	74880	27107
Closed structure with corrugated panel and ribs	2 fpan / 2 rpan / 1,5 corr / 2 rib	45/-45	71130	32905
Closed structure with corrugated panel	2 fpan / 2 rpan / 2 corr / 2 rib	45/-45	72400	38440

Table 3-19: Results collection for thermoset with Epoxy resin and HS carbon fibers by NPL

HM carbon fiber NPL with Epoxy resin	Thickness [mm]	Fiber orientation [°]	Maximum RF [N]	Resultant [N]
Open structure with corrugated panel	3 fpan / 2 corr / 3 rib	0/90	10370	1048
Panel with triangular ribs	3 pan / 3 rib	0/90	42790	6455
Open structure with corrugated panel	3 fpan / 2 corr / 3 rib	45/-45sym	18540	6853
Open structure with corrugated panel	3 fpan / 2 corr / 3 rib	45/-45	19050	6958
Open structure with corrugated panel	3 fpan / 2 corr / 3 rib	45/-45 inv	19960	6960
Closed structure with corrugated panel and ribs	2 fpan / 2 rpan / 1,5 corr / 2 rib	0/90	44860	7717
Closed structure with corrugated panel	2 fpan / 2 rpan / 2 corr / 2 rib	0/90	55560	9478
Closed structure with corrugated panel and ribs	2 fpan / 2 rpan / 1,5 corr / 2 rib	45alt	76980	21536
Closed structure with corrugated panel	2 fpan / 2 rpan / 2 corr / 2 rib	45alt	99500	39346
Closed structure with corrugated panel and ribs	2 fpan / 2 rpan / 1,5 corr / 2 rib	45/-45	96850	50307
Closed structure with corrugated panel	2 fpan / 2 rpan / 2 corr / 2 rib	45/-45	96920	56506

Table 3-20: Results collection for thermoset with Epoxy resin and HM carbon fibers by NPL

Both materials have the best performance between all of the adopted ones; the maximum force is about 38 kN for HS carbon fiber composite and 56 kN for HM carbon fiber composite. The weight requirement is satisfied and the value is exactly 3.11 kg for the same reasons discussed previously. From all the data presented it can be concluded that the best material is the last one presented, and only the closed structure with corrugated panel can satisfy the force requirements. The open structure with corrugated panel and HS carbon fiber composite is not able to exceed 7 kN in correspondence of the displacement node.

3.3.4. Tests results for thermoplastic composite components and material optimization

According to the results obtained for the thermoset composites and since the purpose of the project is to replace the rear seat back with a thermoplastic material it has been decided to take into account only the best configurations found during the simulations.

The work consisted in optimizing the component by varying the thickness in all four major parts: front flat panel, rear flat panel, middle corrugated panel and external rib profile.

It has been assumed that the component will be built by having a set of plies with 0.5 mm thickness in order to reduce the number of possible combinations. The way used to obtain the mechanical and physical properties of each material has been described in the previous section. The results are provided as tables similar to the ones for thermoset composites with the addition of a column for the component weight and one dedicated to additional notes with the following notation meaning:

- ✓ W: Best solution found for weigh saving between all the ones computed
- ✓ W+P: Best solution found for weight saving and productivity easiness
- ✓ P+P: Best solution found for performance and productivity easiness
- ✓ P: Best solution found for performance

The evaluation of the maximum performance is not the main project task, but it has been considered at the same time with the purpose to have an idea about the maximum stiffness levels that can be reached by exploiting all the amount of material available up to 3.11 kg component weight.

In the case of Std CF the results are showed in Table 3-21.

StdCF Performance Composites with PVC resin	Thickness [mm]	Fiber orientation [°]	Maximum RF [N]	Resultant [N]	Weight [Kg]	Notes
Closed structure with corrugated panel	0,5 fpan/ 0,5 rpan / 0,5 corr / 0,5 rib	45/-45	13920	6876	0,83	
Closed structure with corrugated panel	0,5 fpan/ 0,5 rpan / 1 corr / 0,5 rib	45/-45	14370	7051	1,12	
Closed structure with corrugated panel	0,5 fpan/ 0,5 rpan / 0,5 corr / 2,5 rib	45/-45	17950	8397	1,03	W
Closed structure with corrugated panel	1 fpan/ 0,5 rpan / 0,5 corr / 0,5 rib	45/-45	16440	8729	1,06	W+P
Closed structure with corrugated panel	1 fpan/ 1 pan / 0,5 corr / 1 rib	45/-45	26210	13825	1,35	
Closed structure with corrugated panel	1 fpan/ 1 rpan / 1 corr / 1 rib	45/-45	27890	14163	1,65	
Closed structure with corrugated panel	1 fpan/ 1 rpan / 1 corr / 1,5 rib	45/-45	29480	14480	1,94	
Closed structure with corrugated panel	1,5 fpan/ 1,5 rpan / 1 corr / 1,5 rib	45/-45	41540	21330	2,17	
Closed structure with corrugated panel	1,5 fpan/ 1,5 rpan / 1,5 corr / 1,5 rib	45/-45	43520	21788	2,47	
Closed structure with corrugated panel	2 fpan/ 2 rpan / 1,5 corr / 2 rib	45/-45	55730	29141	2,99	
Closed structure with corrugated panel	2 fpan/ 2 rpan / 2 corr / 2 rib	45/-45	59970	29666	3,29	
Closed structure with corrugated panel	3 fpan/ 2,5 rpan / 0,5 corr / 2 rib	45/-45	66740	36301	3,11	P+P
Closed structure with corrugated panel	2,5 fpan/ 2,5 rpan / 0,5 corr / 4 rib	45/-45	71800	37519	3,09	P

Table 3-21: Results collection for PVC thermoplastic with Std CF by Performance Composites

The best solution for weight saving allows to create a component with mass of 1.03 kg with global thickness of 0.5 mm and 2.5 mm of the outer reinforcement thickness; this means that four more strips with 0.5 mm thickness have to be added to the outer rib with an additional manufacturing step. Figure 3-16 provides an example of parts thickness for the solution presented above.

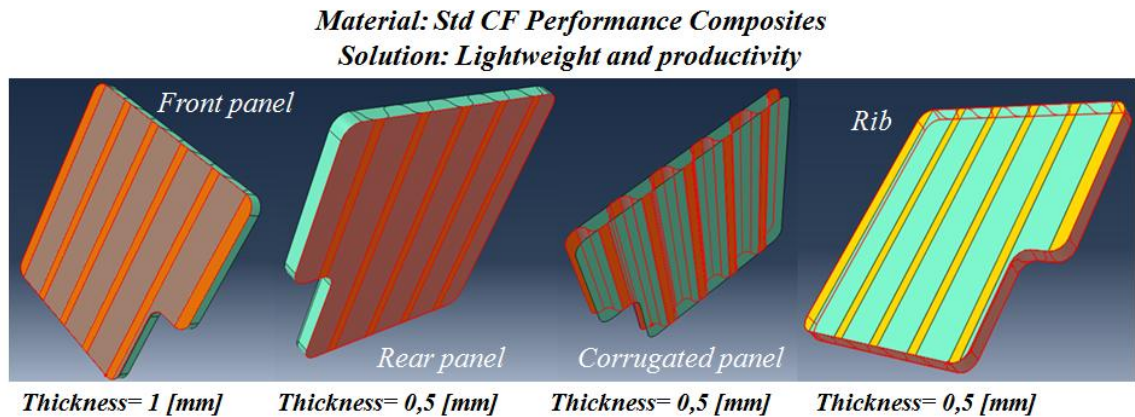


Figure 3-16: Optimized thickness of Std CF thermoplastic for lightweight and productivity

The easier way to produce it consists of having a component with 0.5 mm thickness in all its parts with the exception of the front panel that has to be 1 mm thick and so the outer rib has to be molded together with the thinner flat panel; the total mass is 1.06 kg and so 30 grams more than the other solution but the force increase is more than 3 kN. Figure 3-17 illustrates this solution.

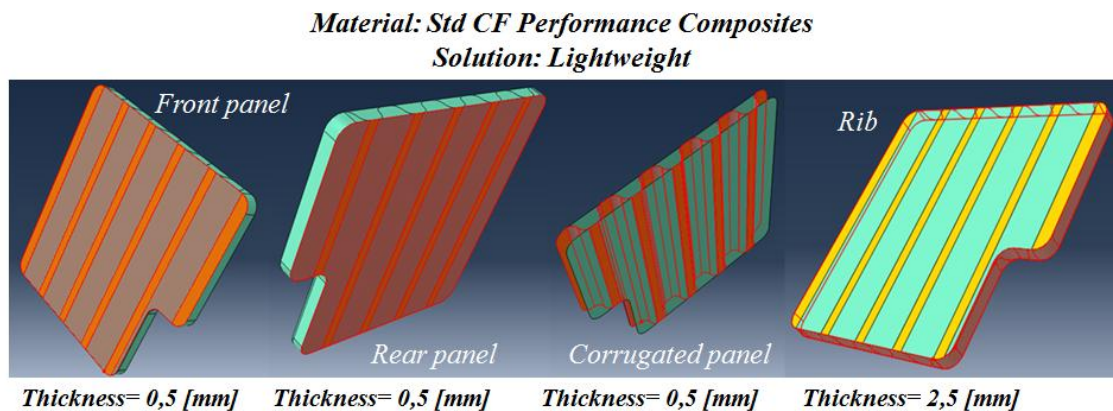


Figure 3-17: Optimized thickness of Std CF thermoplastic for lightweight

Exploiting all the material available the force can reach values as high as 36 kN. In the case with best performance and production since the thinner flat panel is 2.5 mm while the outer rib has to be 2 mm thick it is necessary to place inside the mold a panel cut with just the panel shape. The thickness values are presented in Figure 3-18.

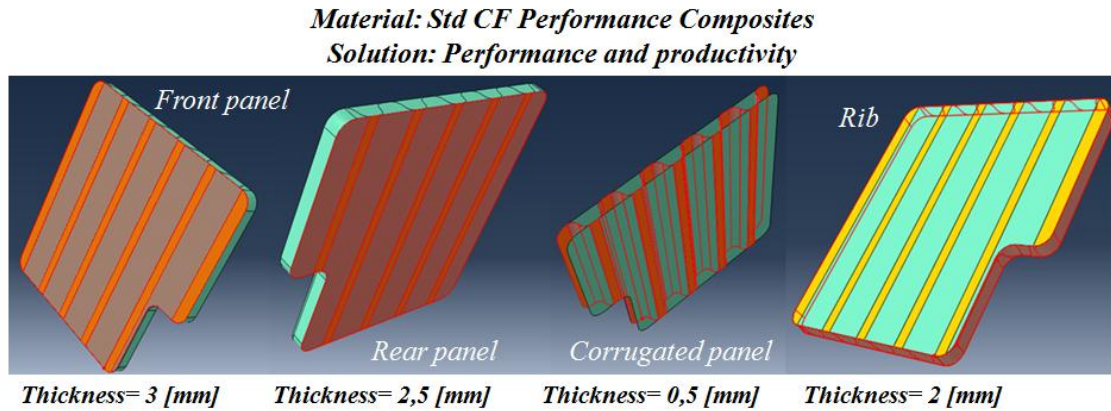


Figure 3-18: Optimized thickness of Std CF thermoplastic for performance and productivity

To have the best performances 3 more strips have to be over the rib belonging to the thicker panel molded with the external reinforcement; the force improvement is more than 1.2 kN. Figure 3-19 shows the parts thickness values.

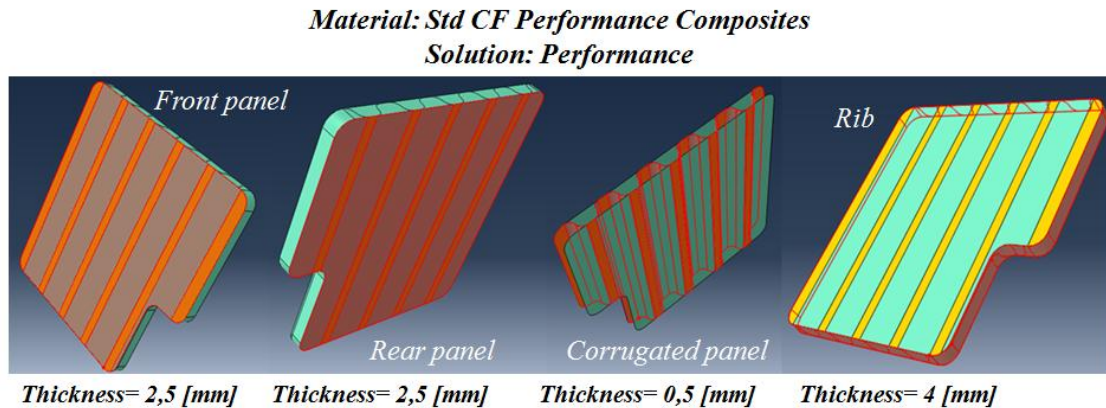


Figure 3-19: Optimized thickness of Std CF thermoplastic for performance

The HMCf material allows to have better weight saving and mechanical behavior than the previous one.

HMCf Performance Composites with PVC resin	Thickness [mm]	Fiber orientation [°]	Maximum RF [N]	Resultant [N]	Weight [Kg]	Notes
Closed structure with corrugated panel	0,5 fpan/ 0,5 rpan / 0,5 corr / 0,5 rib	45/-45	15320	8102	0,83	
Closed structure with corrugated panel	0,5 fpan/ 0,5 rpan / 1 corr / 0,5 rib	45/-45	16530	8323	1,12	
Closed structure with corrugated panel	0,5 fpan/ 0,5 rpan / 0,5 corr / 1 rib	45/-45	17710	8947	0,88	W
Closed structure with corrugated panel	1 fpan/ 0,5 rpan / 0,5 corr / 0,5 rib	45/-45	19000	10229	1,06	W+P
Closed structure with corrugated panel	1 fpan/ 1 pan / 0,5 corr / 1 rib	45/-45	30260	16306	1,35	
Closed structure with corrugated panel	1 fpan/ 1 rpan / 1 corr / 1 rib	45/-45	32130	16735	1,65	
Closed structure with corrugated panel	1,5 fpan/ 1,5 rpan / 1,5 corr / 1,5 rib	45/-45	50110	25800	2,47	
Closed structure with corrugated panel	2 fpan/ 2 rpan / 1,5 corr / 2 rib	45/-45	66340	34335	2,99	
Closed structure with corrugated panel	2 fpan/ 2 rpan / 2 corr / 2 rib	45/-45	68960	35180	3,29	
Closed structure with corrugated panel	3 fpan/ 2,5 rpan / 0,5 corr / 2 rib	45/-45	77260	42993	3,11	P+P

Table 3-22: Results collection for PVC thermoplastic with HMCf by Performance Composites

The best weight of 0.88 kg is again reached by adding one strip over the molded panel with external rib while it is possible to have the best productivity with a weight of 1.06 kg and a force increment of about 3 kN. Figure 3-20 and 3-21 show the thickness values.

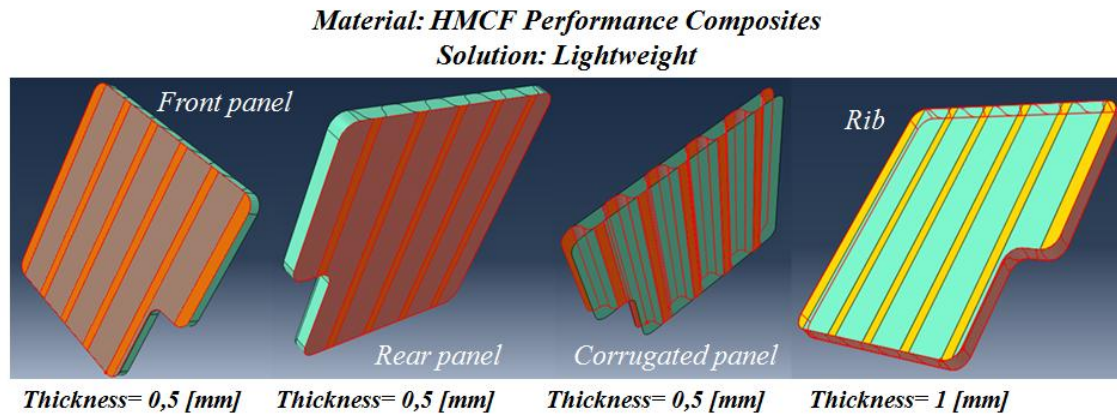


Figure 3-20: Optimized thickness of HMCF thermoplastic for lightweight

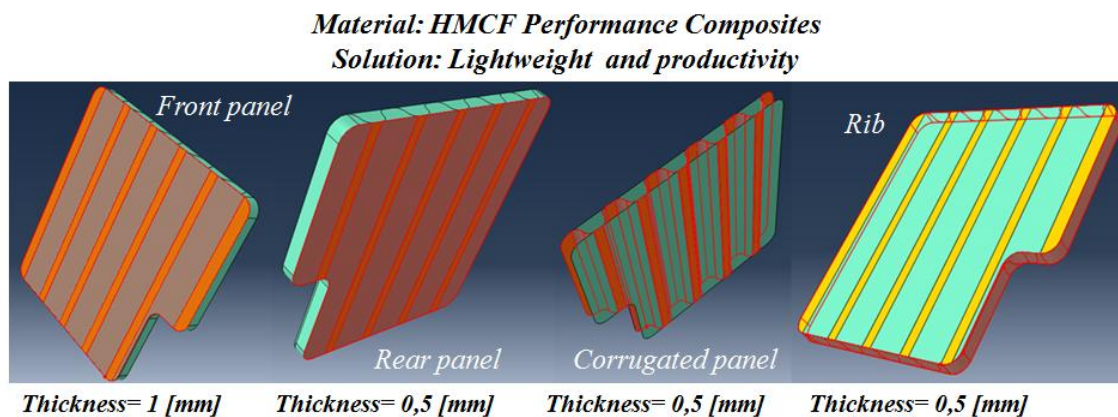


Figure 3-21: Optimized thickness of HMCF thermoplastic for lightweight and productivity

The best performance and productivity are reached having a 3 mm front panel, 2.5 mm rear panel, 0.5 mm corrugated panel and 2 mm outer rib.

The value of force obtained is almost 43 kN and it is necessary to place inside the mold just one ply cut with the panel shape and put it over the thinner panel without increasing the rib thickness. The values of thickness are evidenced in Figure 3-22.

Material: HMCF Performance Composites
Solution: Performance and productivity

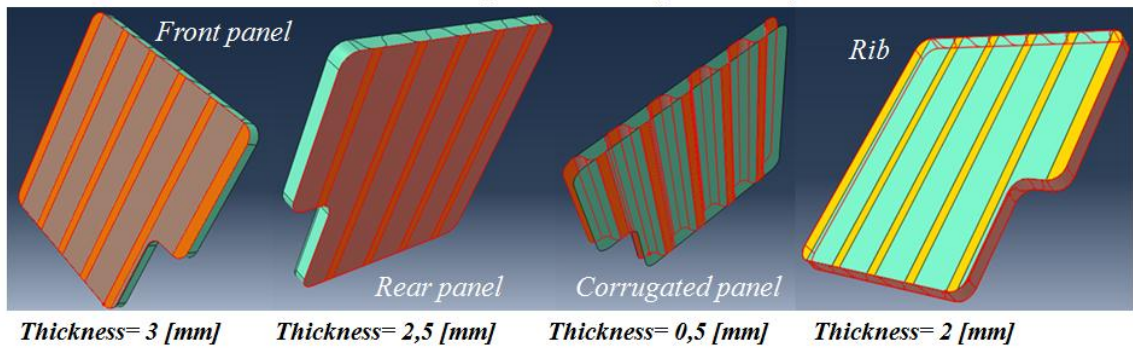


Figure 3-22: Optimized thickness of HMCF thermoplastic for performance and productivity

The E-glass composite enables the target value to be attained but with the disadvantages of lower mechanical properties and higher weight compared to carbon fiber composites.

E glass Performance Composites with PVC resin	Thickness [mm]	Fiber orientation [°]	Maximum RF [N]	Resultant [N]	Weight [Kg]	Notes
Closed structure with corrugated panel	1,5 fpan/ 1,5 rpan / 2 corr / 1,5 rib	45/-45	15560	7363	3,25	
Closed structure with corrugated panel	1,5 fpan/ 1,5 rpan / 1,5 corr / 1,5 rib	45/-45	18370	7904	2,90	
Closed structure with corrugated panel	1,5 fpan/ 1 rpan / 0,5 corr / 3 rib	45/-45	19010	8329	2,39	W
Closed structure with corrugated panel	2 fpan/ 1,5 rpan / 0,5 corr / 1,5 rib	45/-45	18020	8461	2,49	W+P
Closed structure with corrugated panel	2 fpan/ 2 rpan / 1,5 corr / 2 rib	45/-45	20180	9752	3,52	
Closed structure with corrugated panel	2 fpan/ 2 rpan / 2 corr / 2 rib	45/-45	25640	10722	3,87	
Closed structure with corrugated panel	2,5 fpan/ 2 rpan / 0,5 corr / 3 rib	45/-45	23550	11064	3,10	P

Table 3-23: Results collection for thermoplastic with E-glass fiber by Performance Composites

The best configuration for weight saving allows to have a component of 2.39 kg and it is necessary to add a manufacturing step to add three strips over the panel with 1.5 mm thickness as can be seen in Figure 3-23.

Material: E Glass fiber Performance Composites
Solution: Lightweight

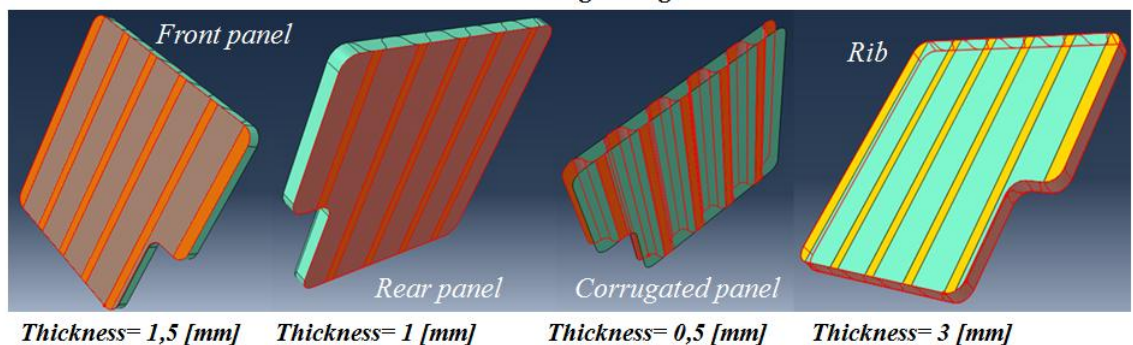


Figure 3-23: Optimized thickness of E-glass thermoplastic for lightweight

With 0.1 kg of weight addition it is possible to have the rib thickness by placing directly three plies inside the mold; the force improvement is more than 100 N. Parts thickness is evidenced in Figure 3-24.

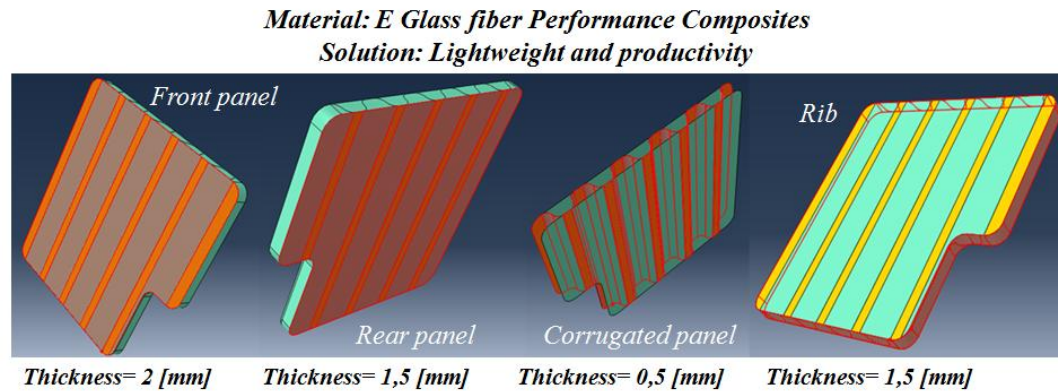


Figure 3-24: Optimized thickness of E-glass thermoplastic for lightweight and productivity

Exploiting all the material available the force value is higher than 11 kN and one strip has to be added to the thicker panel. Figure 3-25 illustrates the values of thickness for the different component parts.

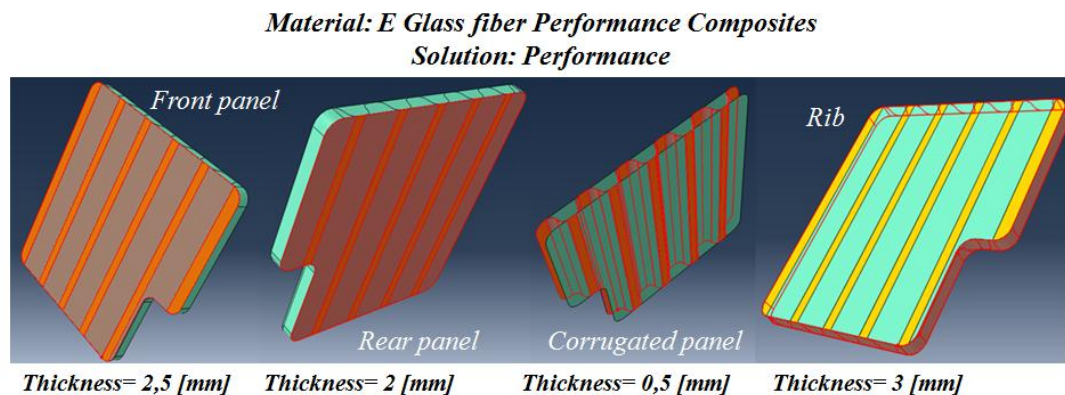


Figure 3-25: Optimized thickness of E-glass thermoplastic for performance

The Kevlar composite gives interesting results in terms of both weight and stiffness.

Kevlar Performance Composites with PVC resin	Thickness [mm]	Fiber orientation [°]	Maximum RF [N]	Resultant [N]	Weight [Kg]	Notes
Closed structure with corrugated panel	1 fpan/ 1 rpan / 1 corr / 1 rib	45/-45	14760	6277	1,45	
Closed structure with corrugated panel	1 fpan/ 1 rpan / 1,5 corr / 1 rib	45/-45	15760	6394	1,71	
Closed structure with corrugated panel	1,5 fpan/ 1 rpan / 0,5 corr / 3,5 rib	45/-45	19870	8277	1,63	
Closed structure with corrugated panel	1,5 fpan/ 1,5 rpan / 0,5 corr / 1 rib	45/-45	18800	8626	1,61	W+P
Closed structure with corrugated panel	1,5 fpan/ 1,5 rpan / 1 corr / 0,5 rib	45/-45	21840	9421	1,92	
Closed structure with corrugated panel	1,5 fpan/ 1,5 rpan / 1,5 corr / 1,5 rib	45/-45	23150	9597	2,18	
Closed structure with corrugated panel	2 fpan/ 2 rpan / 2 corr / 2 rib	45/-45	31980	13013	2,90	
Closed structure with corrugated panel	3 fpan/ 3 rpan / 0,5 corr / 3 rib	45/-45	41050	18626	3,05	P+P
Closed structure with corrugated panel	3 fpan/ 3 rpan / 0,5 corr / 3,5 rib	45/-45	42510	19052	3,09	P

Table 3-24: Results collection for thermoplastic with Kevlar fiber by Performance Composites

The requirements are satisfied with 1.61 kg of material; the production steps are very simple and it is necessary to cut one ply with the panel shape. Thickness values are shown in Figure 3-26.

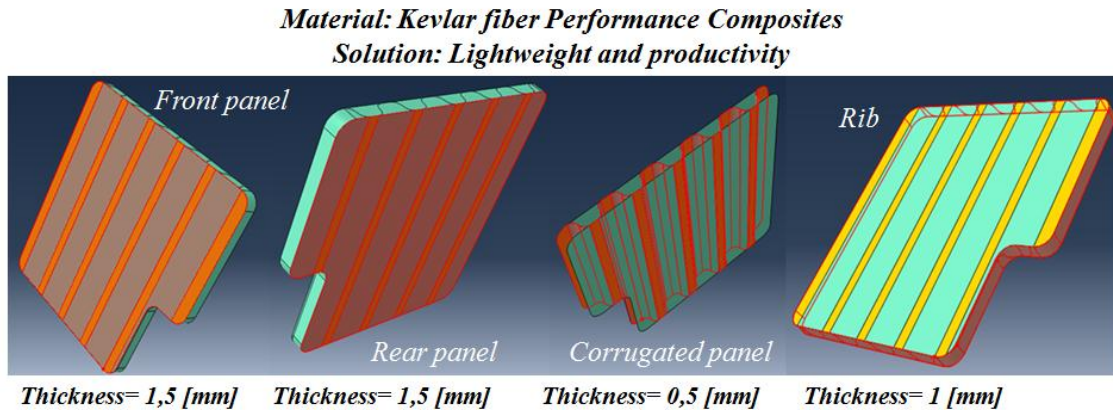


Figure 3-26: Optimized thickness of Kevlar thermoplastic for lightweight and productivity

The best performance with a fast production is over 16 kN and the rib profile is built directly placing the plies inside the mold during the production of the panels. If a strip is added to the molded panel it is possible to reach the best performance of 19 kN for this material. These solutions are illustrated in Figures 3-27 and 3-28.

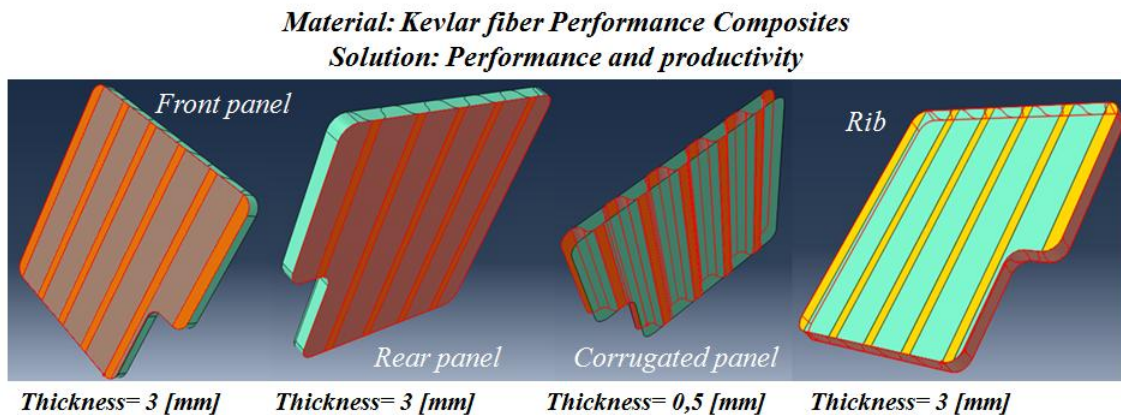


Figure 3-27: Optimized thickness of Kevlar thermoplastic for performance and productivity

Material: Kevlar fiber Performance Composites
Solution: Performance

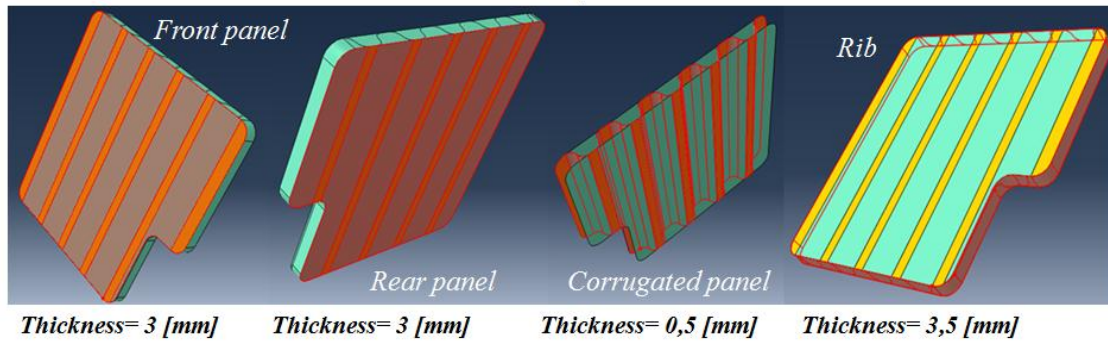


Figure 3-28: Optimized thickness of Kevlar thermoplastic for performance

The UD Std CF composite results are presented in Table 3-25.

UD StdCF Performance Composites with PVC resin	Thickness [mm]	Fiber orientation [°]	Maximum RF [N]	Resultant [N]	Weight [Kg]	Notes
Closed structure with corrugated panel	1 fpan/ 1 rpan / 1 corr / 1 rib	45/-45	15130	6272	1,63	
Closed structure with corrugated panel	1 fpan/ 1 rpan / 1,5 corr / 1 rib	45/-45	16780	6524	1,92	
Closed structure with corrugated panel	1,5 fpan/ 1,5 rpan / 1 corr / 1,5 rib	45/-45	22400	9318	2,15	
Closed structure with corrugated panel	1,5 fpan/ 1,5 rpan / 1,5 corr / 1,5 rib	45/-45	24550	9637	2,45	
Closed structure with corrugated panel	1 fpan/ 1 rpan / 0,5 corr / 0,5 rib	45/-45	20220	9984	1,28	W+P
Closed structure with corrugated panel	2 fpan/ 2 rpan / 2 corr / 2 rib	45/-45	34970	13092	3,26	
Closed structure with corrugated panel	3 fpan/ 2,5 rpan / 0,5 corr / 2 rib	45/-45	67920	37954	3,08	P+P
Closed structure with corrugated panel	2,5 fpan/ 2,5 rpan / 0,5 corr / 4,5 rib	45/-45	75160	40085	3,11	P

Table 3-25: Results collection for thermoplastic with UD Std CF by Performance Composites

It is possible to have a component with 1.28 kg of weight and a value of force higher than the one required; it has not been possible to find a configuration able to reduce both the force and the weight for this kind of material. The only modification during the production consists of placing inside the mold a ply that does not contribute to the increase of the outer rib thickness. The component thickness is shown in Figure 3-29.

Material: UD Std CF Performance Composites
Solution: Lightweight and productivity

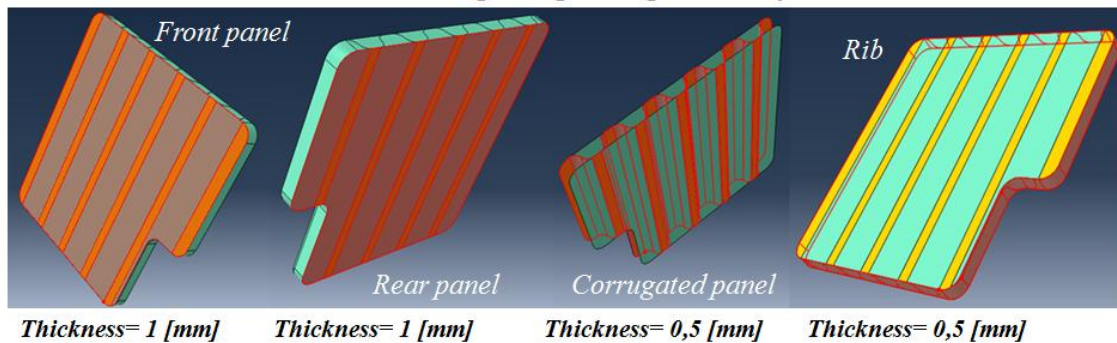


Figure 3-29: Optimized thickness of UD Std CF thermoplastic for lightweight and productivity

Optimal values of performance and easiness of production can be obtained by placing one ply over the thinner panel inside the mold that does not increase the outer rib thickness. Figure 3-30 illustrates the thickness values.

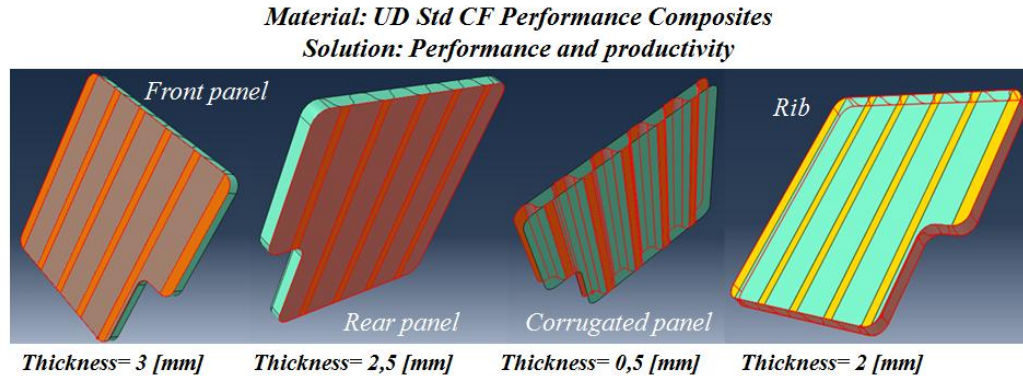


Figure 3-30: Optimized thickness of UD CF thermoplastic for performance and productivity

To have the best performance of 40 kN four strips have to be put over the molded panel outer reinforcement. In Figure 3-31 the component parts thickness can be seen.

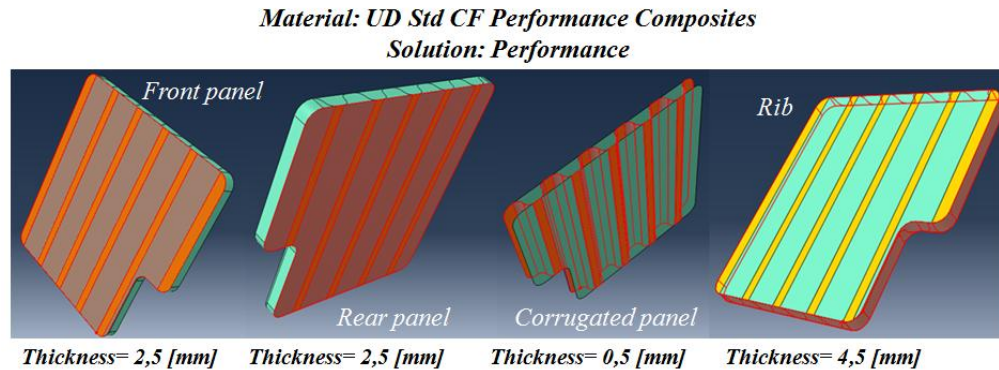


Figure 3-31: Optimized thickness of UD CF thermoplastic for performance

The UD HMCf composite allows performance slightly better than that of UD Std CF composite even if the weights are around the same values. In Table 3-26 the data is summarized.

UD HMCf Performance Composites with PVC resin	Thickness [mm]	Fiber orientation [°]	Maximum RF [N]	Resultant [N]	Weight [Kg]	Notes
Closed structure with corrugated panel	1 fpan/ 1 rpan / 1 corr / 1 rib	45/-45	13660	5579	1,63	
Closed structure with corrugated panel	1 fpan/ 1 rpan / 1,5 corr / 1 rib	45/-45	15320	5837	1,92	
Closed structure with corrugated panel	1,5 fpan/ 1,5 rpan / 1 corr / 1,5 rib	45/-45	20190	8265	2,15	
Closed structure with corrugated panel	1,5 fpan/ 1,5 rpan / 1,5 corr / 0,5 rib	45/-45	22340	8585	2,45	
Closed structure with corrugated panel	1 fpan/ 1 rpan / 0,5 corr / 0,5 rib	45/-45	21600	10719	1,28	W+P
Closed structure with corrugated panel	2 fpan/ 2 rpan / 2 corr / 2 rib	45/-45	31770	11664	3,26	
Closed structure with corrugated panel	3 fpan/ 2,5 rpan / 0,5 corr / 2 rib	45/-45	78140	45574	3,08	P+P
Closed structure with corrugated panel	2,5 fpan/ 2,5 rpan / 0,5 corr / 4,5 rib	45/-45	86820	48385	3,11	P

Table 3-26: Results collection for thermoplastic with UD HMCf by Performance Composites

The optimal configuration to have good weight saving and easiness of production is given by a component with 1 mm thickness front and rear panels, and 0.5 mm corrugated panel and external rib. Since the rib thickness is lower than the thickness of the panels it is necessary to insert a ply cut with the panel shape that does not contribute to the increase of the rib thickness. The weight is 1.28 kg and the force value is over 10 kN, which is 2 kN more than required but no further improvement is possible due to material properties and form availability. The thickness values are shown in Figure 3-32.

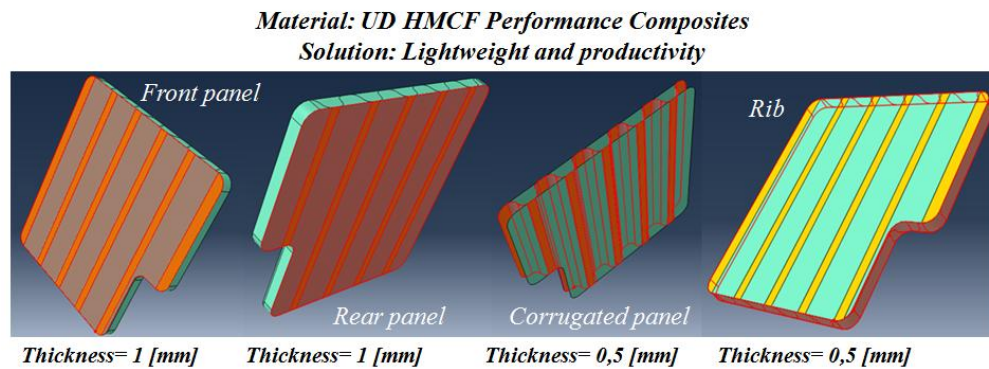


Figure 3-32: Optimized thickness of UD HMCF thermoplastic for lightweight and productivity

The best results of performance together with a reduction in production step are provided by a 3 mm thick front panel, 2.5 mm thick rear panel, 0.5 mm corrugated and 2 mm external rib. The molding phase has to be done again by inserting one ply that has no influence on the external reinforcement and enabling 0.5 mm less than the thinner panel. Figure 3-33 shows the thickness values for the different parts.

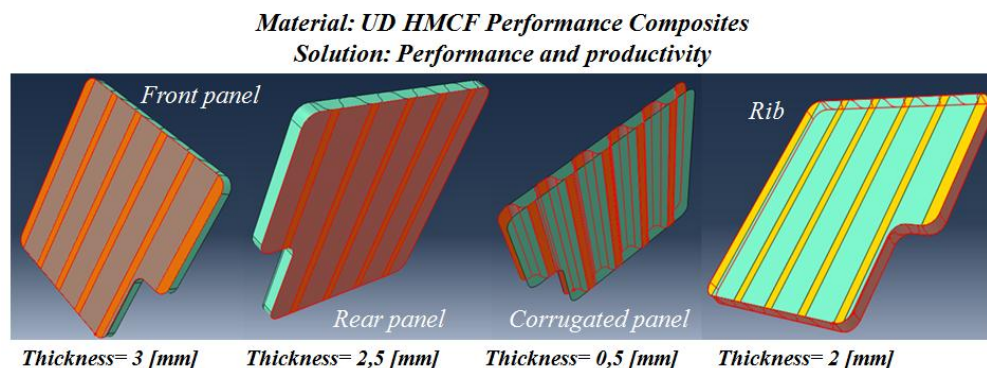


Figure 3-33: Optimized thickness of UD HMCF thermoplastic for performance and productivity

In order to have the best performance instead, 4 plies have to be added on the rib thus the thickness can be increased from 2.5 mm to 4.5 mm; the force values are above 48 kN. Figure 3-34 provides the component parts thickness.

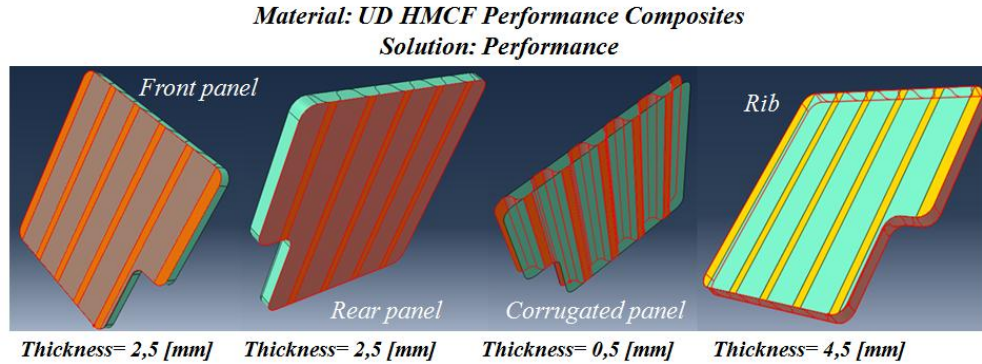


Figure 3-34: Optimized thickness of UD HMCF thermoplastic for performance

Table 3-27 presents the results obtained in the case of UD E-glass fiber composite; this material with thermoset matrix was not able to satisfy the requirements. Even though the force value was close to the target one, the mass was higher than 3.11 kg.

<i>UD E glass Performance Composites with PVC resin</i>	<i>Thickness [mm]</i>	<i>Fiber orientation [°]</i>	<i>Maximum RF [N]</i>	<i>Resultant [N]</i>	<i>Weight [Kg]</i>	<i>Notes</i>
<i>Closed structure with corrugated panel</i>	<i>2 fpan / 2 rpan / 2 corr / 2 rib</i>	<i>45/-45</i>	<i>19940</i>	<i>7832</i>	<i>3,83</i>	
<i>Closed structure with corrugated panel</i>	<i>2 fpan / 1,5 rpan / 0,5 corr / 1,5 rib</i>	<i>45/-45</i>	<i>17110</i>	<i>8555</i>	<i>2,46</i>	<i>W+P</i>
<i>Closed structure with corrugated panel</i>	<i>2,5 fpan / 2 rpan / 0,5 corr / 2 rib</i>	<i>45/-45</i>	<i>21930</i>	<i>11264</i>	<i>3,07</i>	<i>P+P</i>

Table 3-27: Results collection for thermoplastic with UD E-glass by Performance Composites

The component has been optimized and now the requirements are fulfilled with 8.5 kN as reaction force and a weight of 2.46 kg. During the production it could be easier to create the external rib during the thinner panel molding. The part thickness is shown in Figure 3-35.

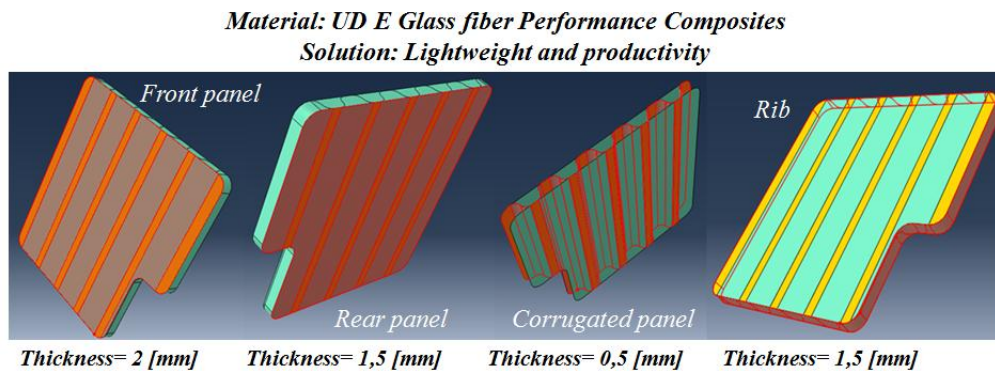


Figure 3-35: Optimized thickness of UD E-glass thermoplastic for lightweight and productivity

By exploring all the material available the force value can be increased up to 11 kN and as in the previous case it is better to have the outer reinforcement in the same step with the thinner rear panel during molding. Figure 3-36 provides the thickness values in the different regions.

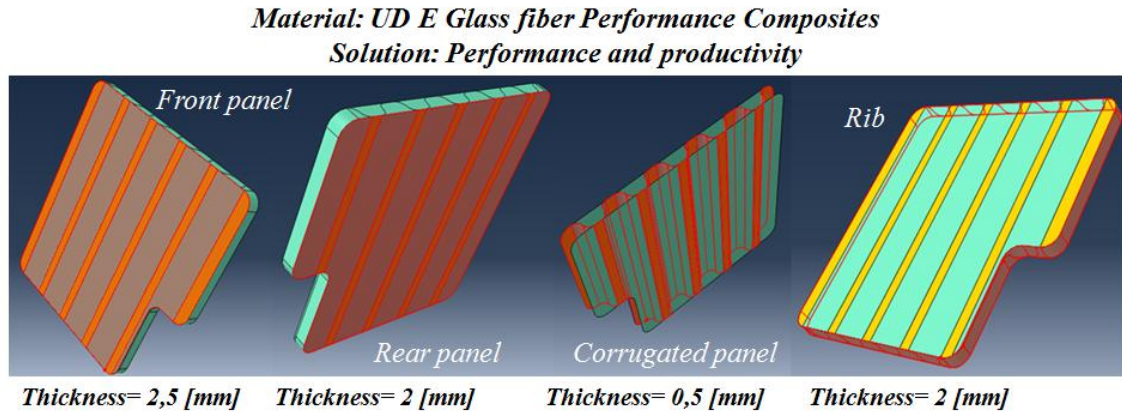


Figure 3-36: Optimized thickness of UD E-glass thermoplastic for performance and productivity

During the thermosets analysis, the Kevlar composite was not able to satisfy the requirements but its light weight makes the material easier to be optimized. The results collection is showed in Table 3-28.

UD Kevlar Performance Composites with PVC resin	Thickness [mm]	Fiber orientation [°]	Maximum RF [N]	Resultant [N]	Weight [Kg]	Notes
Panel	6,5 pan	45/-45	977	726	3,09	
Panel with triangle ribs	3,5 pan / 2,5 rib	0/90	11310	1777	2,88	
Open structure with corrugated panel	2 fpan / 4 corr / 1,5 rib	45/-45	5614	1791	3,12	
Panel with triangle ribs	3 pan / 3 rib	0/90	12260	1891	2,96	
Open structure with corrugated panel	2,5 fpan / 3,5 corr / 2 rib	45/-45	6378	2118	3,10	
Panel with triangle ribs	2,5 pan / 3,5 rib	0/90	13910	2178	3,04	
Panel with triangle ribs	2 pan / 4,5 rib	0/90	13740	2201	3,00	
Panel with triangle ribs	2 pan / 4 rib	0/90	14410	2220	3,12	
Open structure with corrugated panel	2 fpan / 3,5 corr / 4 rib	45/-45	7158	2296	3,08	
Closed structure with corrugated panel	1,5 fpan / 1 rpan / 0,5 corr / 1 rib	45/-45	14070	8147	1,38	
Closed structure with corrugated panel	1 fpan / 1 rpan / 0,5 corr / 3 rib	45/-45	15100	8419	1,36	W
Closed structure with corrugated panel	1 fpan / 1,5 rpan / 0,5 corr / 1,5 rib	45/-45	15320	8866	1,43	W+P
Closed structure with corrugated panel	1,5 fpan / 1 rpan / 0,5 corr / 1,5 rib	45/-45	15320	8866	1,43	
Closed structure with corrugated panel	1,5 fpan / 1,5 rpan / 0,5 corr / 1,5 rib	45/-45	18640	10681	1,63	
Closed structure with corrugated panel	1,5 fpan / 1,5 rpan / 1 corr / 1,5 rib	45/-45	19370	11050	1,89	
Closed structure with corrugated panel	2 fpan / 2 rpan / 1,5 corr / 2 rib	45/-45	27780	15668	2,61	
Closed structure with corrugated panel	2 fpan / 2,5 rpan / 1,5 corr / 2 rib	45/-45	29770	17149	2,81	
Closed structure with corrugated panel	2,5 fpan / 2,5 rpan / 1,5 corr / 3 rib	45/-45	36200	20402	3,11	
Closed structure with corrugated panel	3 fpan / 3 rpan / 0,5 corr / 3 rib	45/-45	37990	22370	3,01	P+P
Closed structure with corrugated panel	3 fpan / 3 rpan / 0,5 corr / 4 rib	45/-45	40130	23443	3,10	P

Table 3-28: Results collection for thermoplastic with UD Kevlar by Performance Composites

The number of numerical tests is higher than the previous cases, this is due to the fact that it has been chosen to simulate the open rib structure with corrugated and the panel with rib added that gave unsatisfactory results when used with thermoset composites without optimization.

These operations have been done not only for Kevlar fiber composite but also for the best glass and carbon fiber materials in order to make sure that the weaker materials would never reach the desired target. Unfortunately the open structure with corrugated panel and the one with ribs are not able to reach the force values over 8 kN and so the only solution is to create a corrugated closed structure. The best weight achieved is 1.36 kg with a force value of 8.4 kN; the external reinforcement is much thicker than the panels and in this case 4 strips have to be added to the molded panel that can be either front or rear panel. Figure 3-37 illustrates the thickness values.

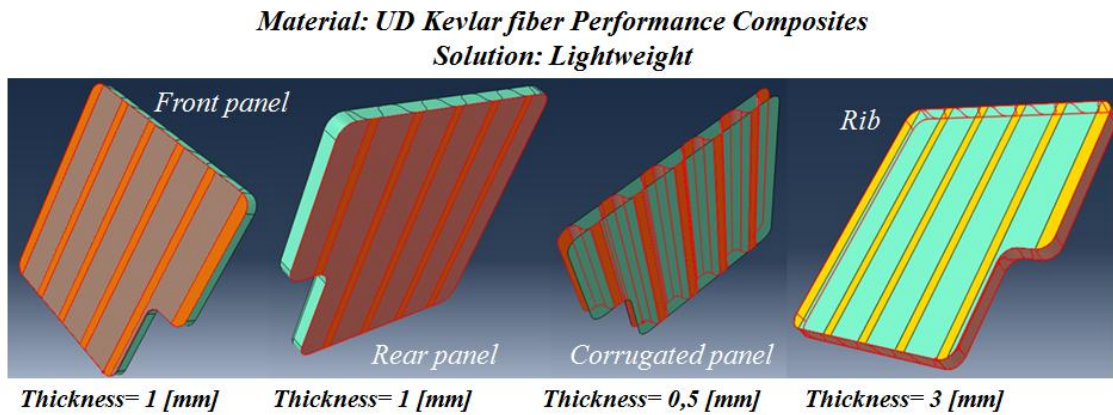


Figure 3-37: Optimized thickness of Kevlar thermoplastic for lightweight

The condition for the best production has a slightly heavier weight of 1.43 kg but at the same time almost 300 N more for the reaction force. During the molding the external rib has to be built together with the rear panel with 1.5 mm thickness. The component parts thickness can be seen in Figure 3-38.

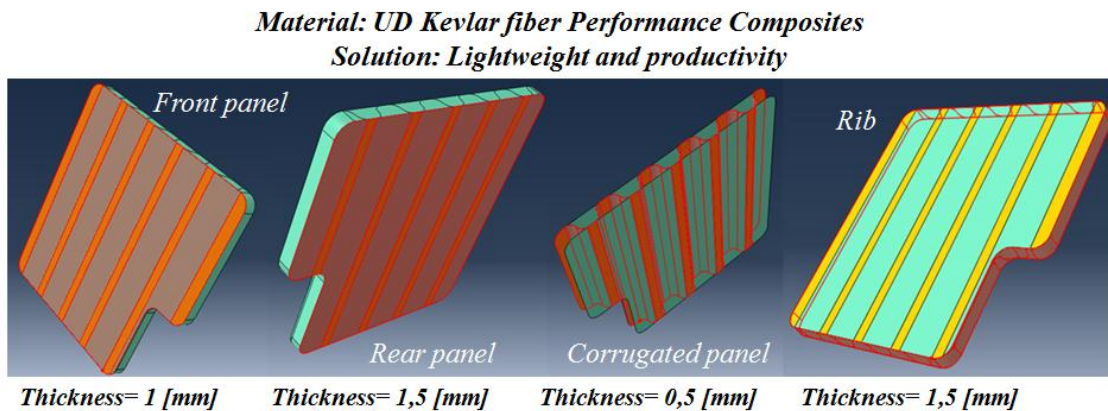


Figure 3-38: Optimized thickness of Kevlar thermoplastic for lightweight and productivity

By increasing the weight up to 3.01 kg it is possible to reach more than 22 kN force and create the panel in simpler way; the reinforcement on the outside profile does not need to have different thickness with respect to the front or the rear panel. Figure 3-39 illustrates the thickness values in the component regions.

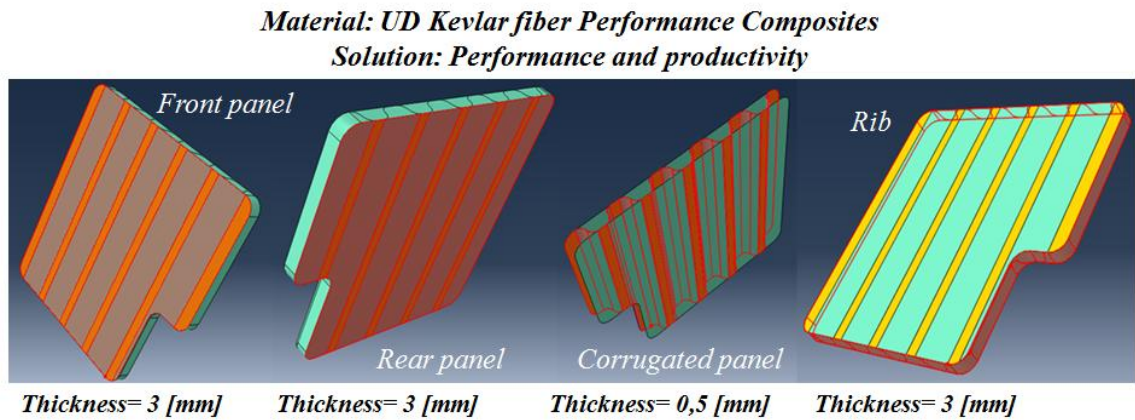


Figure 3-39: Optimized thickness of Kevlar thermoplastic for performance and productivity

The best case for performance allows to reach more than 23 kN force with the application of 3.10 kg of material; the production requires an additional step by adding two strips to the cavity obtained after molding. Figure 3-40 put in evidence the thickness values.

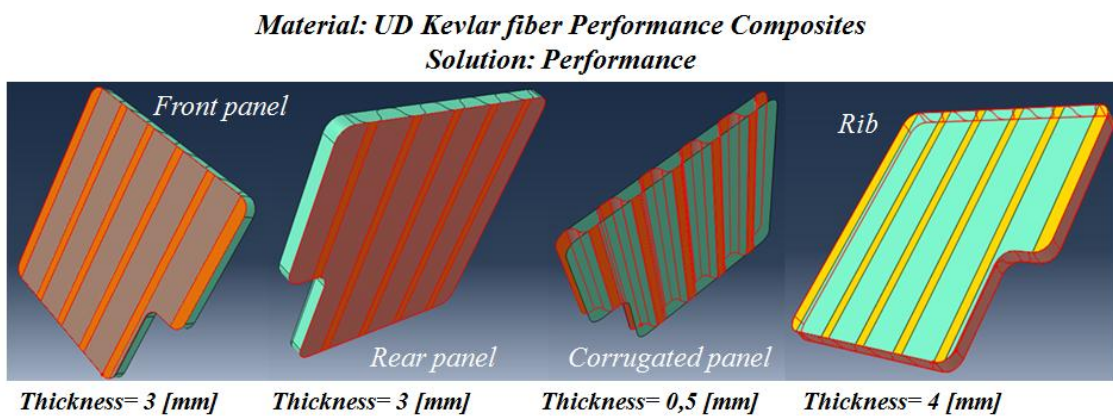


Figure 3-40: Optimized thickness of Kevlar thermoplastic for performance

Different design solutions have been tested also for S-2 glass fiber with PVC matrix composite since this material has the best properties among all the glass fiber composites. The results are showed in Table 3-29.

S-2 glass fiber AGY with PVC resin	Thickness [mm]	Fiber orientation [°]	Maximum RF [N]	Resultant [N]	Weight [Kg]	Notes
Panel	6,5 pan	45/-45	376	282	3,07	
Panel with triangular ribs	2,5 pan / 2 rib	0/90	5520	1368	2,95	
Panel with triangular ribs	2 pan / 2,5 rib	0/90	7631	1766	3,06	
Open structure with corrugated panel	1,5 fpan / 2,5 corr / 3,5 rib	45/-45	8935	1822	3,10	
Open structure with corrugated panel	2,5 fpan / 2 corr / 2 rib	45/-45	7773	1836	3,11	
Closed structure with corrugated panel	1,5 fpan / 1 rpan / 0,5 corr / 0,5 rib	45/-45	16960	7775	1,81	
Closed structure with corrugated panel	1 fpan / 1 rpan / 0,5 corr / 1 rib	45/-45	16520	7886	1,59	
Closed structure with corrugated panel	1 fpan / 1 rpan / 1 corr / 1 rib	45/-45	17720	8047	1,94	
Closed structure with corrugated panel	1 fpan / 1 rpan / 1,5 corr / 1 rib	45/-45	19070	8213	2,29	
Closed structure with corrugated panel	1 fpan / 1 rpan / 0,5 corr / 1,5 rib	45/-45	18040	8379	1,65	W
Closed structure with corrugated panel	1 fpan / 1 rpan / 1 corr / 1,5 rib	45/-45	19310	8559	2,00	
Closed structure with corrugated panel	1,5 fpan / 1 rpan / 0,5 corr / 1 rib	45/-45	18690	9123	1,87	W+P
Closed structure with corrugated panel	1,5 fpan / 1,5 rpan / 1 corr / 1,5 rib	45/-45	26750	12137	2,56	
Closed structure with corrugated panel	1,5 fpan / 1,5 rpan / 1,5 corr / 1,5 rib	45/-45	28530	12383	2,91	
Closed structure with corrugated panel	2 fpan / 2 rpan / 2 corr / 2 rib	45/-45	38820	16861	3,88	
Closed structure with corrugated panel	2,5 fpan / 2 rpan / 0,5 corr / 2 rib	45/-45	35730	17391	3,11	P+P
Closed structure with corrugated panel	2 fpan / 2 rpan / 0,5 corr / 4 rib	45/-45	38250	17570	3,08	P

Table 3-29: Results collection for PVC thermoplastic with ‘S’ type fiber glass by AGY

Again the only design solution able to satisfy the requirements is by creating a component with a closed and corrugated structure. The other solutions are not able to exceed 2 kN resultant force. The combination allowing the best weight reduction is 1.65 kg heavy and the force is slightly lower than 8.4 kN; the disadvantage of this solution lies in the production phase; in fact one more stripe has to be added along the external rib profile after the molding panel is extracted. Figures 3-41 and 3-42 illustrate the thickness values in case of optimal lightweight and optimal lightweight combined with easiness of manufacturing.

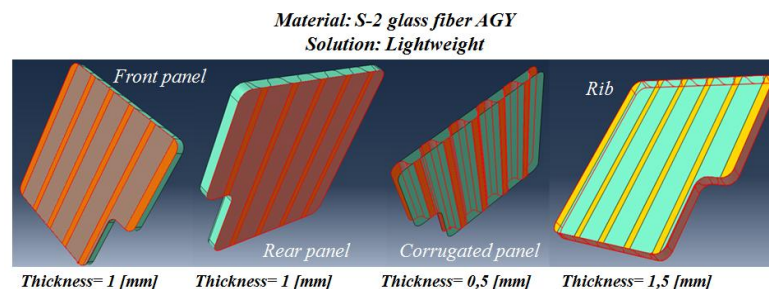


Figure 3-41: Optimized thickness of S glass thermoplastic for lightweight

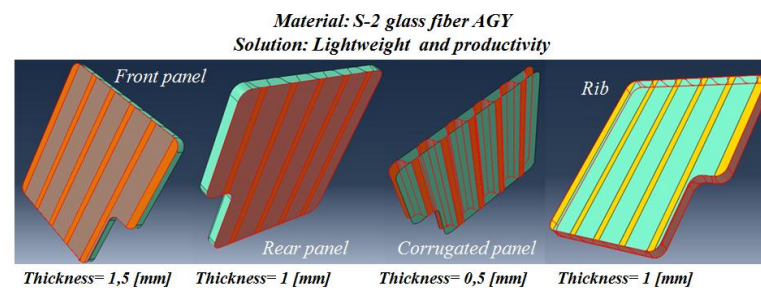


Figure 3-42: Optimized thickness of S glass thermoplastic for lightweight and productivity

Exploring all the 3.11 kg of material available the best performance and productivity conditions are met; the force values are higher than 17 kN and there is no need to cut or add strips or plies but it is enough just molding the external reinforcement together with the thinner 2 mm rear panel. This solution is shown in Figure 3-43.

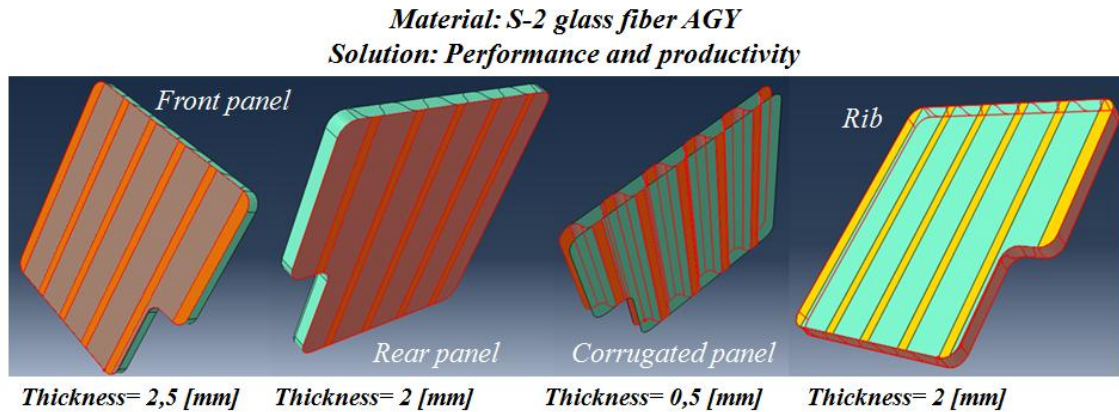


Figure 3-43: Optimized thickness of S glass thermoplastic for performance and productivity

With 3.08 kg instead, the best performance of 17.5 kN is achieved even though during the production it is necessary to bring the outer rib thickness from 2 mm to 4 mm by adding four strips on the molded piece. The component thickness values are evidenced in Figure 3-44.

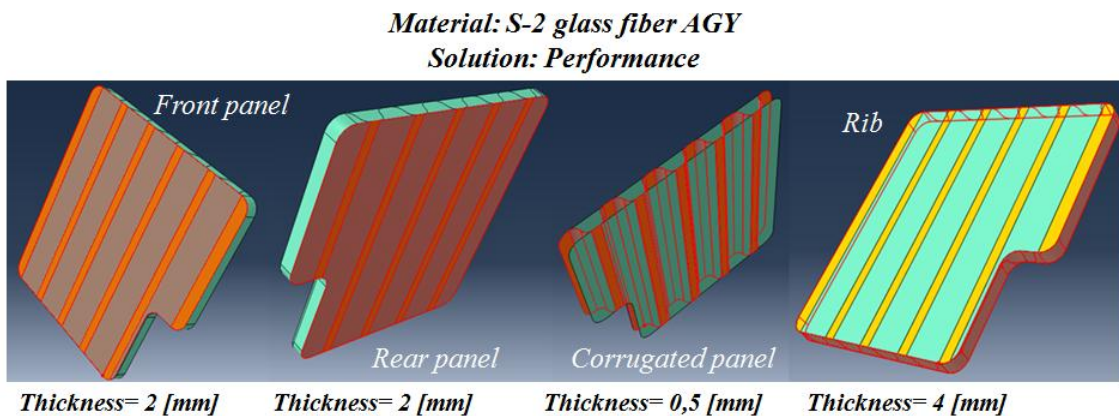


Figure 3-44: Optimized thickness of S glass thermoplastic for performance

The last results refers to HS and HM carbon fiber composites with PVC resin; in the previous simulations on thermosets these materials showed the best results and for this reason it has been decided to test one more design solution in order to check if the project is feasible or not at least with the best performance material.

The high strength fibers are not sufficient to reach the desired values in fact the best condition is obtained by analyzing the open structure with corrugated panel whose overall weight is 3.13 kg and so over the limit and at the same time the force monitored in correspondence of the displacement application point is around 5.1 kN. Even if the target values are not reached, the results are much better, as expected, than the ones obtained with the previous material. In order to meet the desired condition it is necessary to have a higher performance composite. The results for HS carbon composite are presented in Table 3-30.

HS carbon fiber NPL with PVC resin	Thickness [mm]	Fiber orientation [°]	Maximum RF [N]	Resultant [N]	Weight [Kg]	Notes
Panel	6,5 pan	0/90	569	422	3,04	
Panel	6,5 pan	45alt	2326	726	3,04	
Panel	6,5 pan	45/-45	1573	1176	3,04	
Closed structure with corrugated panel	0,5 fpan / 0,5 rpan / 0,5 corr / 0,5 rib	45/-45	9025	3713	0,81	
Closed structure with corrugated panel	0,5 fpan / 0,5 rpan / 1 corr / 0,5 rib	45/-45	10600	4110	1,11	
Panel with triangular ribs	1,5 pan / 3,5 rib	45sym	14530	4929	2,98	
Panel with triangular ribs	2,5 pan / 3 rib	0/90	24990	5101	3,13	
Open structure with corrugated panel	3 fpan / 2 corr / 4,5 rib	45/-45	19670	5550	3,10	
Closed structure with corrugated panel	1 fpan / 0,5 rpan / 0,5 corr / 2,5 rib	45/-45	17600	7881	1,26	
Closed structure with corrugated panel	1 fpan / 1 rpan / 0,5 corr / 0,5 rib	45/-45	28550	13341	1,28	W+P
Closed structure with corrugated panel	1 fpan / 1 rpan / 1 corr / 0,5 rib	45/-45	33770	18488	1,33	
Closed structure with corrugated panel	1 fpan / 1 rpan / 1 corr / 1 rib	45/-45	37120	19060	1,63	
Closed structure with corrugated panel	1,5 fpan / 1,5 rpan / 1,5 corr / 1,5 rib	45/-45	62330	29724	2,44	
Closed structure with corrugated panel	2 fpan / 2 rpan / 2 corr / 2 rib	45/-45	85440	41518	3,25	
Closed structure with corrugated panel	3 fpan / 2,5 rpan / 0,5 corr / 2 rib	45/-45	94050	50394	3,08	P+P
Closed structure with corrugated panel	2,5 fpan / 2,5 rpan / 0,5 corr / 4,5 rib	45/-45	105100	53035	3,10	P

Table 3-30: Results collection for PVC thermoplastic with HS carbon fibers by NPL

The best combination to have optimal weight reduction, easiness of productivity and force requirements satisfied consists of creating a structure with 1.28 kg mass with external panels 1 mm thick and 0.5 mm thick corrugated panel and outer reinforcement. Since the rib thickness is lower than the flat panels one, inside the mold a single ply has to be placed without increasing the rib thickness. The component parts thickness is shown in Figure 3-45.

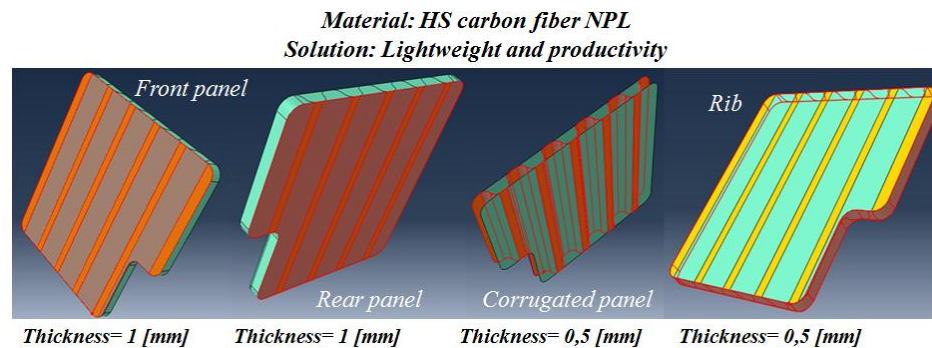


Figure 3-45: Optimized thickness of HS fibers thermoplastic for lightweight and productivity

The best absolute performance results are given by 3.10 kg of material and creating a component with 2.5 mm thick external panels, 0.5 mm thick corrugated panel and 4.5 mm thick external reinforcement that has to be created with an additional production step by placing four strips above the molded panel and around its profile. The force values obtained are above 53 kN. This solution can be better seen in Figure 3-46.

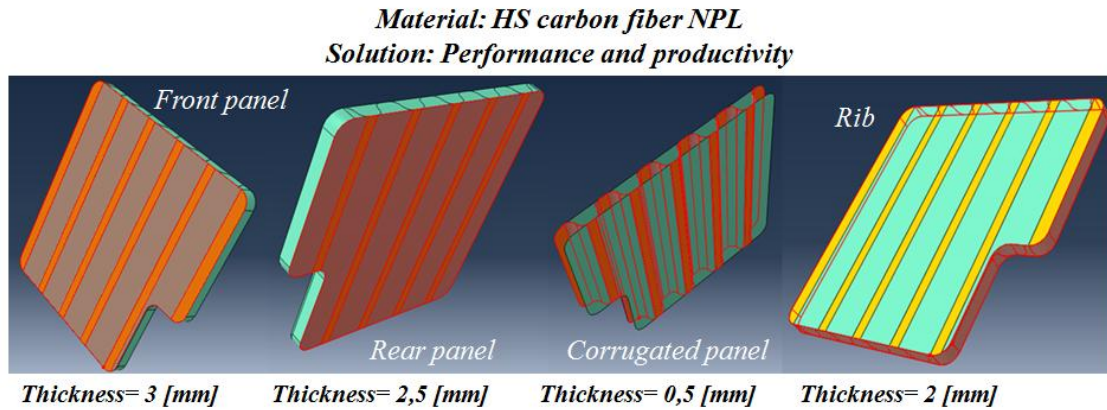


Figure 3-46: Optimized thickness of HS fibers thermoplastic for performance and productivity

With a different combination it is possible to have the best performance together with the easiness of productivity; the seat back needs to have a 3 mm front panel thickness, 2.5 mm rear panel thickness, 0.5 mm corrugated panel thickness and 2 mm external reinforcement thickness that means to place inside the mold cavity a ply with a different cut in order to keep the rib thickness constant. The overall weight is 3.08 kg and the reaction force in correspondence of the displacement application point is higher than 50 kN. Figure 3-47 provides an example for the solution described above.

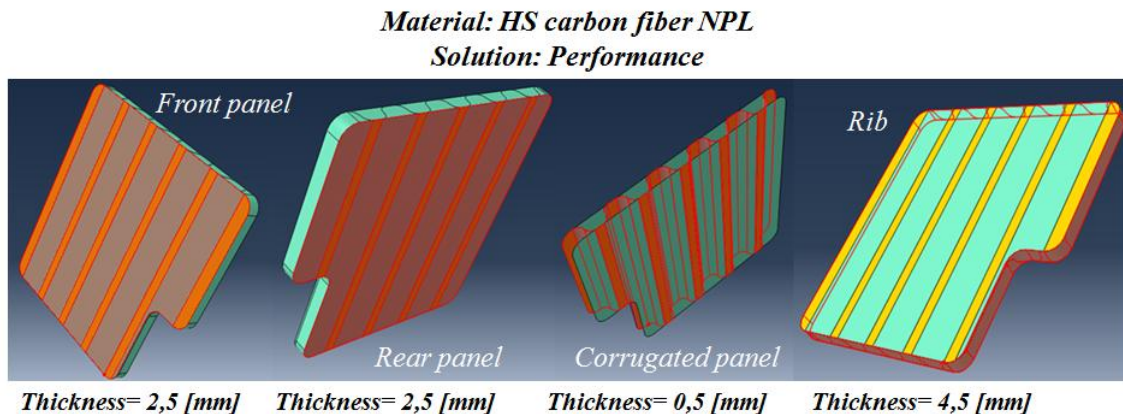


Figure 3-47: Optimized thickness of HS fibers thermoplastic for performance

The final results refers to the HM carbon fiber composite with PVC matrix by NPL; this material is the one presenting the best properties between all the ones available and so more simulations have been conducted to determine which of the design ideas are feasible. In the optimal case the solution with triangular ribs is not able to exceed 7 kN force and the weight is at the limit of 3.09 kg so that further improvements will not bring noticeable results. In the case of open structure with corrugated panel the weights are between 3.06 and 3.11 kg while the reaction forces have values in between 8.3 and 8.5 kN.

The parameters combined are front panel, corrugated panel and rib thickness. Even if the requirements are satisfied the material needed is much more than the one used for a closed structure. At this point of the analysis it is difficult to conclude which solution is better between the open and the closed structure since the first has the advantage of faster and easier production while the second has the advantage of more than 50 % weight saving. More details about material and production costs will be provided in the next steps so that a better comparison can be done.

The results are collected in Table 3-31.

HM carbon fiber NPL with PVC resin	Thickness [mm]	Fiber orientation [°]	Maximum RF [N]	Resultant [N]	Weight [Kg]	Notes
Panel	6,5 pan	0/90	4418	326	3,01	
Open structure with corrugated panel	5 fpan / 0,5 corr / 4,5 rib	0/90	4990	741	3,08	
Open structure with corrugated panel	5 fpan / 0,5 corr / 4,5 rib	45alt	2676	1133	3,08	
Open structure with corrugated panel	5 fpan / 0,5 corr / 4,5 rib	45/-45	3925	1617	3,08	
Panel	6,5 pan	0/90	2488	1809	3,01	
Panel with triangular ribs	3 pan / 2,5 rib	45/-45	6029	2774	3,00	
Panel with triangular ribs	3 pan / 2,5 rib	45sym	65400	2850	3,00	
Closed structure with corrugated panel	0,5 fpan / 0,5 rpan / 0,5 corr / 0,5 rib	45/-45	7023	2955	0,80	
Closed structure with corrugated panel	0,5 fpan / 0,5 rpan / 1 corr / 0,5 rib	45/-45	8577	3427	1,09	
Open structure with corrugated panel	4,5 fpan / 1 corr / 4 rib	45/-45	16110	6112	3,10	
Panel with triangular ribs	3 pan / 2,5 rib	0/90	39340	6626	3,00	
Panel with triangular ribs	1,5 pan / 3,5 rib	45sym	23930	6783	2,95	
Panel with triangular ribs	3 pan / 2,5 rib	45alt	17140	6851	3,00	
Open structure with corrugated panel	4 fpan / 1,5 corr / 3,5 rib	45/-45	18870	6956	3,12	
Panel with triangular ribs	2,5 pan / 3 rib	45alt	26760	6956	3,09	
Panel with triangular ribs	2,5 pan / 3 rib	0/90	42520	6990	3,09	
Closed structure with corrugated panel	1 fpan / 0,5 rpan / 0,5 corr / 2,5 rib	45/-45	15280	7219	1,24	
Panel with triangular ribs	3 pan / 3 rib	45/-45	44070	7259	3,32	
Open structure with corrugated panel	3 fpan / 2,5 corr / 2 rib	45/-45	22700	7646	3,11	
Open structure with corrugated panel	2 fpan / 2 corr / 2 rib	45/-45	23790	7650	2,91	
Open structure with corrugated panel	3,5 fpan / 2 corr / 2,5 rib	45/-45	22560	7922	3,09	
Open structure with corrugated panel	2,5 fpan / 2 corr / 6 rib	45/-45	24900	8280	2,99	
Open structure with corrugated panel	3 fpan / 2 corr / 4,5 rib	45/-45	24370	8320	3,06	ok
Open structure with corrugated panel	2,5 fpan / 2 corr / 6,5 rib	45/-45	25430	8434	3,04	ok
Open structure with corrugated panel	3 fpan / 2 corr / 5 rib	45/-45	24770	8502	3,11	ok
Open structure with corrugated panel	2,5 fpan / 2 corr / 7 rib	45/-45	25830	8581	3,09	ok
Closed structure with corrugated panel	1 fpan / 1 rpan / 0,5 corr / 0,5 rib	45/-45	31880	15281	1,27	W+P
Closed structure with corrugated panel	1 fpan / 1 rpan / 1 corr / 1 rib	45/-45	46880	26761	1,61	
Closed structure with corrugated panel	1,5 fpan / 1,5 rpan / 1,5 corr / 1,5 rib	45/-45	81830	43536	2,41	
Closed structure with corrugated panel	2 fpan / 2 rpan / 2 corr / 2 rib	45/-45	112300	61452	3,22	
Closed structure with corrugated panel	3 fpan / 2,5 rpan / 0,5 corr / 2,5 rib	45/-45	132100	76098	3,09	P+P
Closed structure with corrugated panel	2,5 fpan / 2,5 rpan / 0,5 corr / 4,5 rib	45/-45	137700	77351	3,07	P

Table 3-31: Results collection for PVC thermoplastic with HM carbon fibers by

NPL

The HM carbon fiber composite allows it to have a component 1.27 kg meeting the best conditions for weight saving and production easiness with a structure presenting 1 mm thick external panels and 0.5 mm thick corrugated panel and outer rib. As in the previous cases during the molding phase it is necessary to place a ply which does not increase the rib thickness inside the mold cavity. The force value is above 15 kN, so 7 kN more than the required one; but due to the material availability form and its properties it is not possible to lower the weight otherwise the requirements cannot be met. The component parts thickness is shown in Figure 3-48.

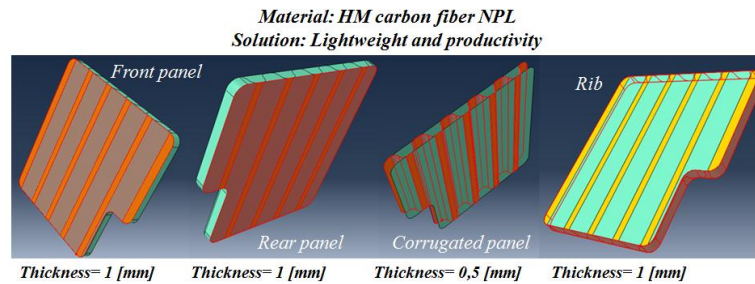


Figure 3-48: Optimized thickness of HM fibers thermoplastic for lightweight and productivity

A better performing design is given by combining 2.5 mm thick external panels with 0.5 mm corrugated panel and 4.5 mm thick external reinforcement. The use of strips is required to increase the rib thickness and so the production process will take longer time. The force result is more than 77 kN. With a different combination of thicknesses it is possible to have an easier manufacturing keeping almost the same weight, 3.09 kg instead of 3.07 kg, and a 1.2 kN lower force. The thickness values for the solutions with best performance and easiness of manufacturing and for just the best performance are provided in Figures 3-49 and 3-50.

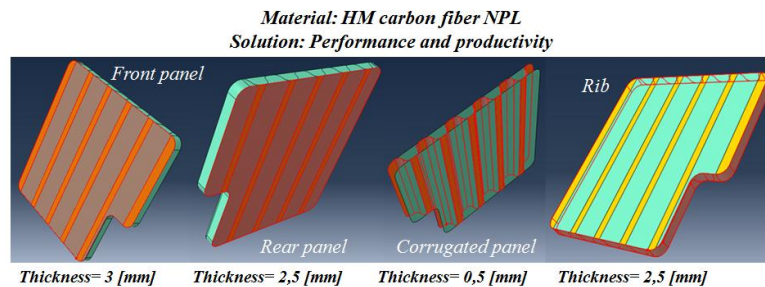


Figure 3-49: Optimized thickness of HM fibers thermoplastic for performance and productivity

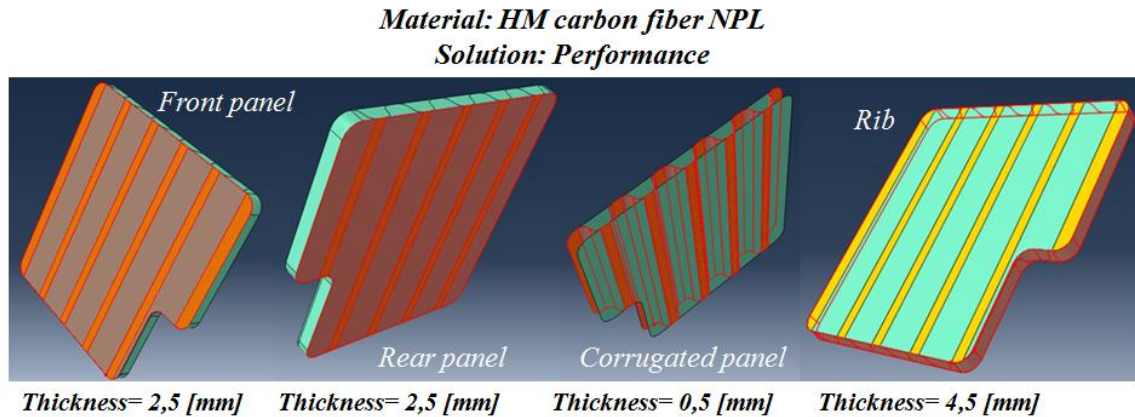


Figure 3-50: Optimized thickness of HM fibers thermoplastic for performance

The advantage lies in the production phase since the rib has the same thickness of the rear panel and so both can be produced inside the mold with a single step. HM carbon fiber composite shows higher performance than HS carbon fiber composite not only considering the closed structure but also in the case of open and ribbed structure that in the previous case were proved not feasible. The difference between the two materials is due to a much higher value of E_1 but lower values of E_2 , G_{12} , G_{13} and G_{23} for the HM carbon fiber composite compared to HS carbon fiber composite; this means that the elastic modulus in the principal direction has the main influence on the component mechanical behavior with respect to the other parameters.

After these considerations what can be pointed out is that all materials are able to satisfy the project requirements although with different design solutions, surface thickness, fiber orientation and weight. In particular it is shown that the greatest effect on stiffness is given by the front panel, followed by the external rib and then the corrugated panel that can be used with the minimum thickness of 0.5 mm. In general all materials and design solutions have common manufacturing steps. The base processes are the molding of both corrugated, flat and concave panel and the injection molding for the solutions presenting ribs inside the panel with cavity and so with outer reinforcement obtained in one step. According to the thicknesses combinations the difference in the manufacturing process is given by the outer rib thickness, in particular if the rib thickness is less than the thinner panel, both of them have to be produced inside the same mold but the plies have to be placed with different cut shape.

If the ribs have the same thickness as the thinner or thicker panel it has to be produced with the panel having the same thickness and the plies don't need any cut and can be provided with the same profile. In the case that the rib thickness is more than the thicker panel thickness it is necessary to add some strips above the existing rib obtained with the molding process until the desired value is achieved.

3.3.5. Results summary

According to the discussion present so far, all the data related to the best configuration of weight, performance and manufacturing have been collected and grouped in order to perform a better comparison between the different materials.

Table 3-32 is related to the best results available to have optimal performance and manufacturing.

Results collection for thermoplastics presenting best performance and productivity

<i>Materials list</i>	<i>Maximum force [N]</i>	<i>Resultant force [N]</i>	<i>Overall weight [Kg]</i>
<i>StdCF Performance Composites</i>	66740	36301	3,11
<i>HMCF Performance Composites</i>	77260	42993	3,11
<i>E glass Performance Composites</i>	23550	11064	3,10
<i>Kevlar Performance Composites</i>	41050	18626	3,05
<i>UD Std CF Performance Composites</i>	67920	37954	3,08
<i>UD HMCF Performance Composites</i>	78140	45574	3,08
<i>UD E glass Performance Composites</i>	21950	11264	3,07
<i>UD Kevlar Performance Composites</i>	37990	22370	3,01
<i>S-2 glass fiber AGY</i>	35730	17391	3,11
<i>HS carbon fiber NPL</i>	94050	50394	3,08
<i>HM carbon fiber NPL</i>	132100	76098	3,09

Table 3-32: Force and weight results for solutions with optimal performance and productivity

It is important to notice how the resultant forces in correspondence of the displacement application point have varied from 11 kN for UD E-glass composite up to 76 kN for HM carbon fiber composite while the weights are very close to each other within the range between 3.01 kg for UD Kevlar composite and 3.11 kg for Std CF, HMCF and S-2 glass fiber composite. At this point a classification of materials according to the performance can be done; the best performance is achieved in HM carbon fiber composite, followed by HS carbon fiber, UD HMCF, HMCF, UD Std CF, Std CF, UD Kevlar, Kevlar, S-2 glass, UD E-glass and E-glass composites.

In general it is possible to deduce that the best performance is achieved with carbon fiber composite followed by Kevlar and the glass fiber composite. On average Kevlar fiber composite has properties almost 60 % lower than carbon fiber composite while glass fiber composite is almost 75 % weaker than the carbon fiber composite. Table 3-33 is a collection of the best performance values without considering an optimal manufacturing process.

Results collection for thermoplastics presenting best performance

Materials list	Maximum force [N]	Resultant force [N]	Overall weight [Kg]
StdCF Performance Composites	71800	37519	3,09
HMCF Performance Composites	n.a.	n.a.	n.a.
E glass Performance Composites	n.a.	n.a.	n.a.
Kevlar Performance Composites	42510	19052	3,09
UD Std CF Performance Composites	75160	40085	3,11
UD HMCF Performance Composites	86820	48385	3,11
UD E glass Performance Composites	n.a.	n.a.	n.a.
UD Kevlar Performance Composites	40130	23443	3,10
S-2 glass fiber AGY	n.a.	n.a.	n.a.
HS carbon fiber NPL	105100	53035	3,10
HM carbon fiber NPL	137700	77351	3,07

Table 3-33: Force and weight results for solutions with optimal performance

This case some values are omitted since the best solution for performance is also the same for the manufacturing, and they have been discussed in the best performance and productivity section above. The weights fall in the same range described earlier and the considerations about the forces and the material classifications are close to the ones presented; the only exception is that the force values are slightly higher than before with a variation range between 500 N and 3 kN. The materials showing better performance are HS and UD HMCF composites while the ones with less force increase are Kevlar and UD Kevlar composites.

The weight variation range is from 0.02 kg for HM carbon fiber composite to 0.09 kg for UD Kevlar fiber composite and can be considered negligible. The values presented are useful to gain comprehension about material performance considering the same amount available, but what is actually interesting in this work is to understand which material permits the lowest weight and manufacturability while satisfying the stiffness requirements. The results for all the materials are listed in Table 3-34.

Results collection for thermoplastics presenting best lightweight and productivity

Materials list	Maximum force [N]	Resultant force [N]	Overall weight [Kg]
StdCF Performance Composites	16440	8729	1,06
HMCF Performance Composites	19000	10229	1,06
E glass Performance Composites	18020	8461	2,49
Kevlar Performance Composites	18800	8626	1,61
UD Std CF Performance Composites	20220	9984	1,28
UD HMCF Performance Composites	21600	10719	1,28
UD E glass Performance Composites	17110	8555	2,46
UD Kevlar Performance Composites	15320	8866	1,43
S-2 glass fiber AGY	18690	9123	1,87
HS carbon fiber NPL	28550	13341	1,28
HM carbon fiber NPL	31880	15281	1,27

Table 3-34: Force and weight results for solutions with optimal lightweight and productivity

In contrast from the previous case, where the purpose was to investigate the performance, in this case the force values are more or less higher than the target one but their variation is lower; the key factor is the component weight. Figures 3-51 and 3-52 give a better idea about force and weight results for all materials adopted.

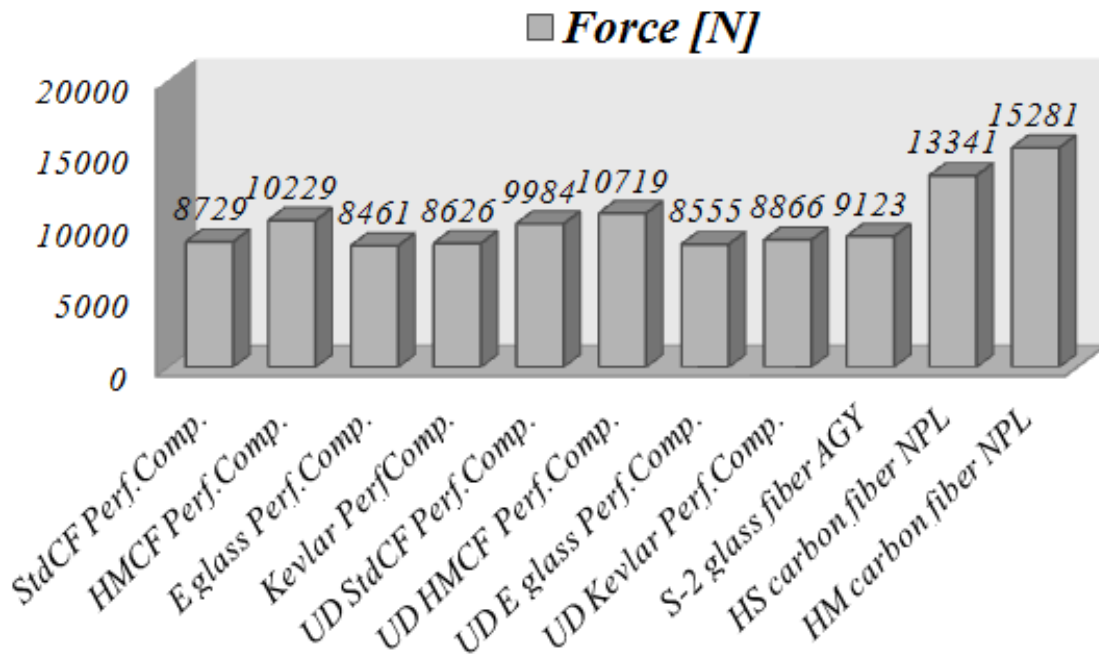


Figure 3-51: Force values graph for design solutions with optimal lightweight and productivity

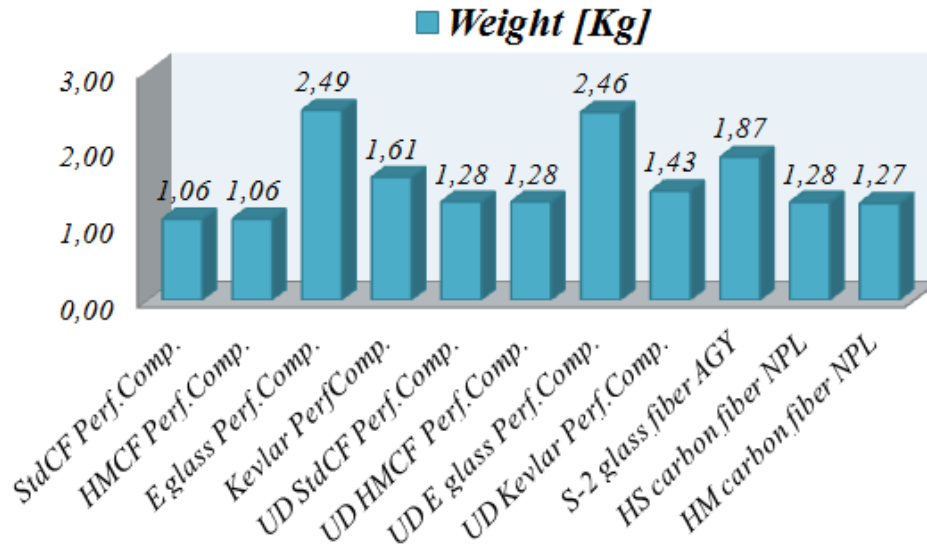


Figure 3-52: Weight values graph for solutions with optimal lightweight and productivity

Considering the resultant forces the classification of material is the following: HM carbon fiber, HS carbon fiber, UD HMCf, HMCf, UD Std CF, S-2 glass fiber, UD Kevlar, Std CF, Kevlar fiber, UD E-glass and E-glass composites.

The classification is slightly different from the previous one but the best and worst materials are always the same; the only exception is given by S-2 glass fiber composite that this time has a behavior better than UD Kevlar, Std CF, Kevlar and E-glass fibers. The force values vary from 8.4 kN for E-glass fiber composite to 15.3 kN for HM carbon fiber composites while the weights are from 1.06 kg for HMCf composite to 2.49 kg for E-glass composite.

On average it can be deduced that both glass and Kevlar fiber composites have the same behavior but they both have more than 20 % weaker results than the carbon fiber composites. The weight variation presents interesting values; in fact carbon fiber composites have the lowest weight, Kevlar fiber composites are more than 25 % heavier while glass fiber composites are about 90 % heavier than carbon fiber composites. Glass fiber composites are also about 50 % heavier than Kevlar fiber composites as well.

It is possible to better evaluate the materials properties by considering the combined results in terms of forces and weights, and in particular the ratio of load to weight which emphasizes the optimal solution with the highest force and the lowest weight.

The results are summarized in Figure 3-53.

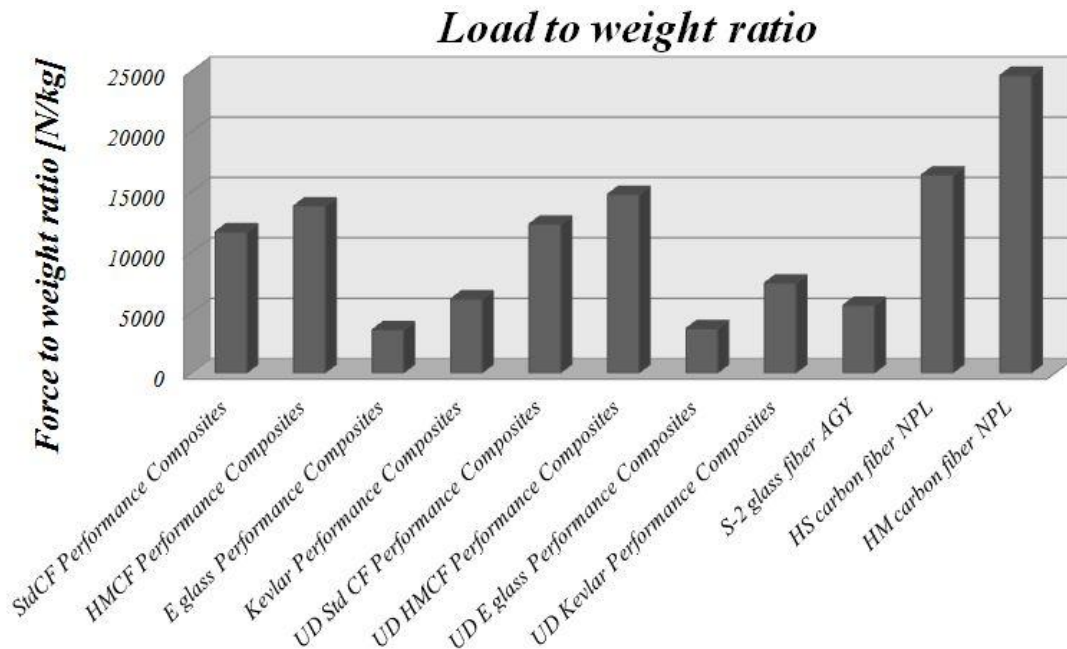


Figure 3-53: Load to weight ratio for the materials presenting best lightweight and manufacturing performance

The highest values of the load to weight ratio are obtained with high modulus and high strength carbon fiber composites by NPL, followed by UD and fabric standard and high modulus carbon fibers composites by Performance Composites. Kevlar fibers composites have values slightly higher than the glass fiber ones, but much lower with respect to the results obtained by using carbon fibers.

Table 3-35 summarizes the solutions found to have the lowest weight without considering the manufacturing aspects.

Results collection for thermoplastics presenting best lightweight

Materials list	Maximum force [N]	Resultant force [N]	Overall weight [Kg]
StdCF Performance Composites	17950	8397	1,03
HMCF Performance Composites	17710	8947	0,88
E glass Performance Composites	19010	8329	2,39
Kevlar Performance Composites	n.a.	n.a.	n.a.
UD Std CF Performance Composites	n.a.	n.a.	n.a.
UD HMCF Performance Composites	n.a.	n.a.	n.a.
UD E glass Performance Composites	n.a.	n.a.	n.a.
UD Kevlar Performance Composites	15100	8419	1,36
S-2 glass fiber AGY	n.a.	n.a.	n.a.
HS carbon fiber NPL	n.a.	n.a.	n.a.
HM carbon fiber NPL	n.a.	n.a.	n.a.

Table 3-35: Force and weight results for solutions with optimal lightweight

The omitted values have been presented before in the cases of the best lightweight and the optimal production process. In general it is possible to point out that the materials behavior follows the same rules described in the previous examples. The force variation range considering the same material is limited and is reduced of 130 N for E-glass fiber composite and of 1.2 kN for HMCF composite. The weight reduction is 0.03 kg for Std CF composite, which can be considered negligible, while it is 0.18 kg for HMCF composite. In the case of HMCF composite the weight reduction is noticeable and has a strong influence on the reaction force value even though the requirements remain satisfied. Table 3-36 refers to the solution found with different design concepts, such as open structure with corrugated panel, that satisfy the requirements with the material presenting the best performance.

Results collection for thermoplastics with open structure plus corrugated panel

<i>Materials list</i>	<i>Maximum force [N]</i>	<i>Resultant force [N]</i>	<i>Overall weight [Kg]</i>
HM carbon fiber NPL	24370,00	8320,42	3,06
HM carbon fiber NPL	25430,00	8434,48	3,04
HM carbon fiber NPL	24770,00	8502,04	3,11
HM carbon fiber NPL	25830,00	8580,92	3,09

Table 3-36: Force and weight results for open structure satisfying the requirements

In Table 3-36 only the reaction force values and the weights are presented. Each solution is related to a certain configuration of surface thicknesses. What is important to point out is that both the forces and the weights have close values for the various configurations, however all of them are able to satisfy the stiffness requirements. The disadvantage is due to the fact that these results cannot be compared to the ones obtained for the closed structure with corrugated panel since in the best case, considering that the stiffness values are almost similar, in the example with closed structure made by UD E-glass fiber composite the maximum achieved weight is 2.46 kg which is almost 25 % less than the lightest open structure solution of 3.04 Kg. The lowest mass of 0.88 kg in the closed structure with HMCF composite is 3.5 times lighter than the heaviest one of 3.11 kg among the open structure presented above. These considerations could lead to a conclusion that the design with open structure and corrugated panel is weaker than the one with closed structure; this is true considering the weights and the values of stiffness reached with a certain material amount usage.

At the same time this it is not true considering the manufacturing aspects because it is evident that the open structure requires less steps and less time to be manufactured. Before deciding what will be the winning material, design and manufacturing process it is useful to have a deeper knowledge about the material and production costs, the time required by each assembly and construction step, the life cycle analysis for each solution and the way to treat and recycle the component at the end of its life. Once all the data will be available a better scenario could bring to the final decision about how to obtain the desired seat back.

3.4. Component stress analysis

In this section a description of the stress behavior related to the component structure will be provided. The pictures present refer to standard carbon fiber composite material since for all the materials the stress distribution is the same with the only difference that their module is different.

The stresses analyzed are in plane maximum principal, maximum principal, stresses S_{11} and S_{22} in the main directions along the x and y axis in the component reference frame, and shear stresses S_{12} in the same plane. Stresses S_{33} along z axis are not presented due to their null value.

The first set of data is computed by applying the displacement in the positive y direction, perpendicular to the component panel. The distribution of the in plane maximum principal stress is uniform on part of the front structure while the highest stress values are concentrated in correspondence of the lower left and upper right constraint points. The range of values goes from 8736 MPa for high modulus carbon fiber by NPL, up to 707 MPa for E-glass fiber composite by Performance Composites.

Similar considerations can be done evaluating the maximum principal stresses, the difference is that this time most of the component surface is not loaded except in correspondence of the boundary regions and, as illustrated before, the stress values are higher in the rear part that is subject to compression. The range of values is from 8769 MPa for high modulus carbon fiber composite by NPL to 912 MPa in the case of E-glass fiber composite by Performance Composites. The distribution for the stresses described above is provided in Figures 3-54 to 3-57.

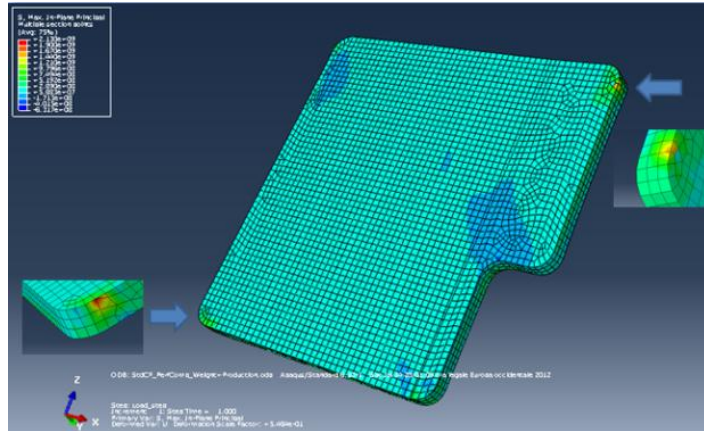


Figure 3-54: In plane max principal stress distribution on front side for positive displacement

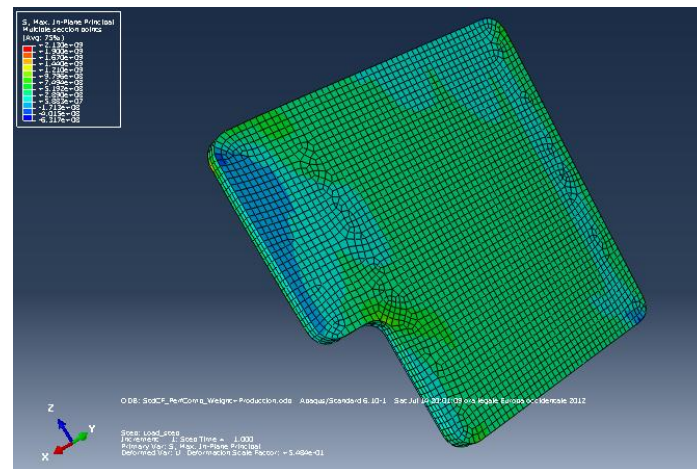


Figure 3-55: In plane max principal stress distribution on rear side for positive displacement

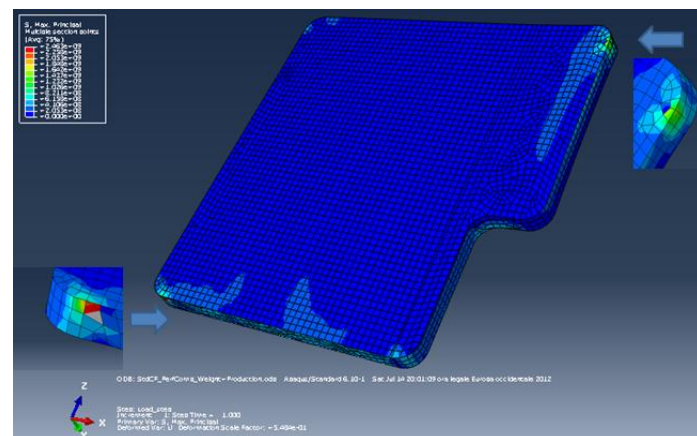


Figure 3-56: Maximum principal stress distribution on front side for positive displacement

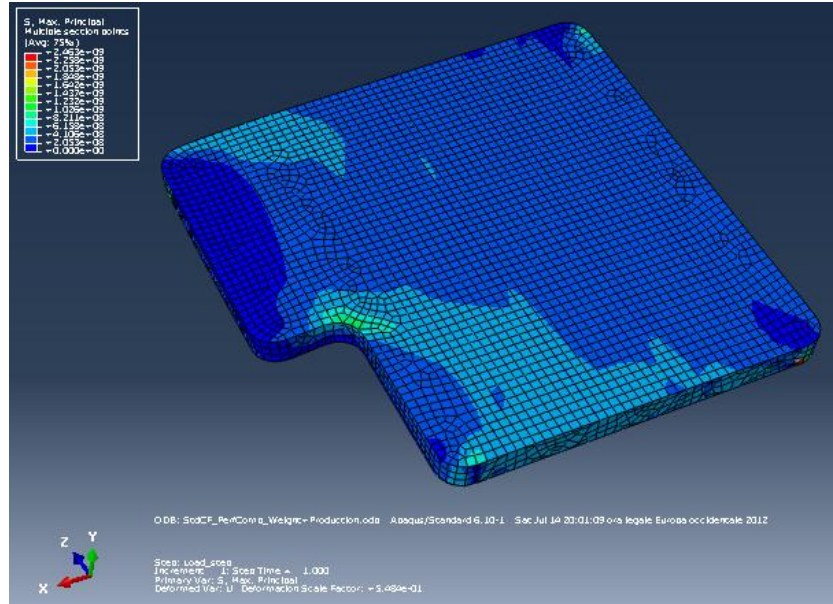


Figure 3-57: Maximum principal stress distribution on rear side for positive displacement

The stress S_{11} distribution along the x axis in the model reference frame has an uniform trend and very low values on both front and rear structure sides. Again, the points under maximum stress are in correspondence of the boundary conditions, especially in the lower left and upper right points. The values range goes from 5156 MPa for high modulus carbon fibers by NPL to 594 MPa for E-glass fiber composite by Performance Composites. Figure 3-58 gives an illustration of the stress distribution.

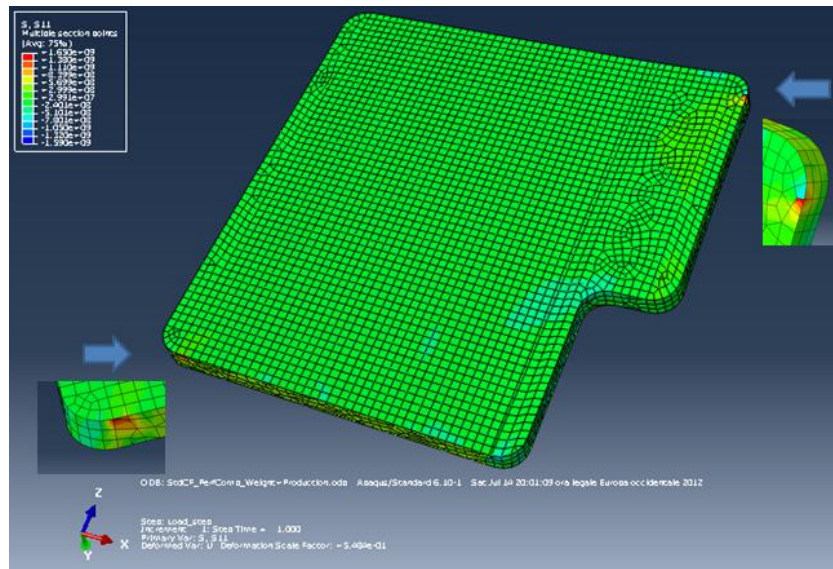


Figure 3-58: S_{11} stress distribution for positive displacement

Similar considerations can be done for the stress S_{22} along the y direction in the component reference system. This time the point with the highest load is the upper right hinge point. The load is more uniformly distributed on the front side while the compression stresses have higher values and more loaded areas on the back. The stress values are lower than S_{11} and their range is from 611 MPa for high modulus carbon fiber composite by NPL to 473 MPa for E-glass fiber composite by Performance Composites. Figures 3-59 and 3-60 provide an illustration of S_{22} stresses in both front and rear component side.

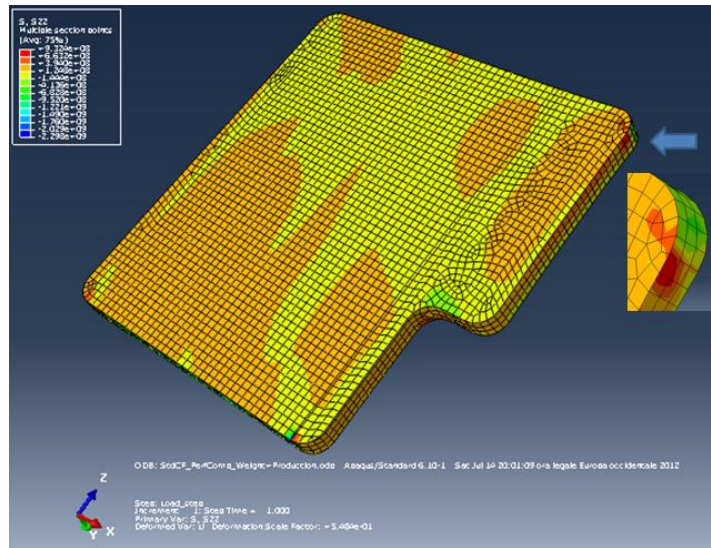


Figure 3-59: S_{22} stress distribution on front side for positive displacement

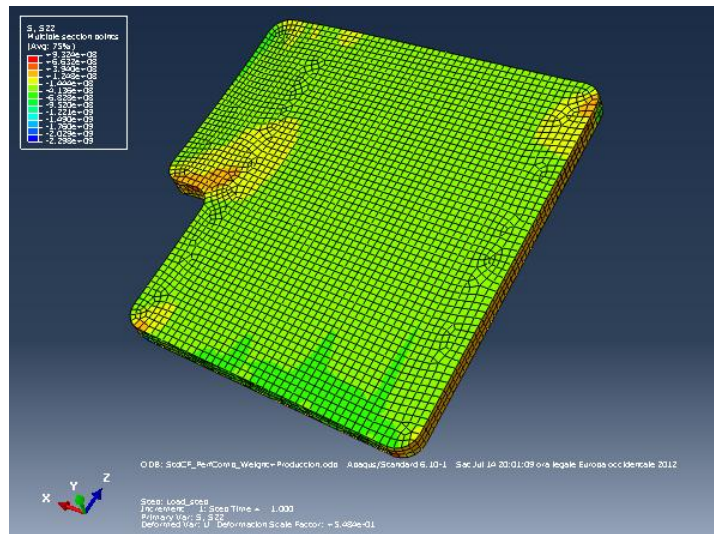


Figure 3-60: S_{22} stress distribution on rear side for positive displacement

The last stress component considered is S_{12} , which is the shear stresses in the x-y plane in the model reference system. The considerations for the stress distribution are the same provided so far, there are some more loaded areas on the surface, but the stress values are lower with respect to the ones evaluated in the constrained points, in particular the lower left and upper right corners. The values are much lower than the others presented above, and the range goes from 780 MPa for high modulus carbon fiber composite by NPL to 200 MPa for E-glass fiber composite by Performance Composites. The stress distribution is shown in Figure 3-61.

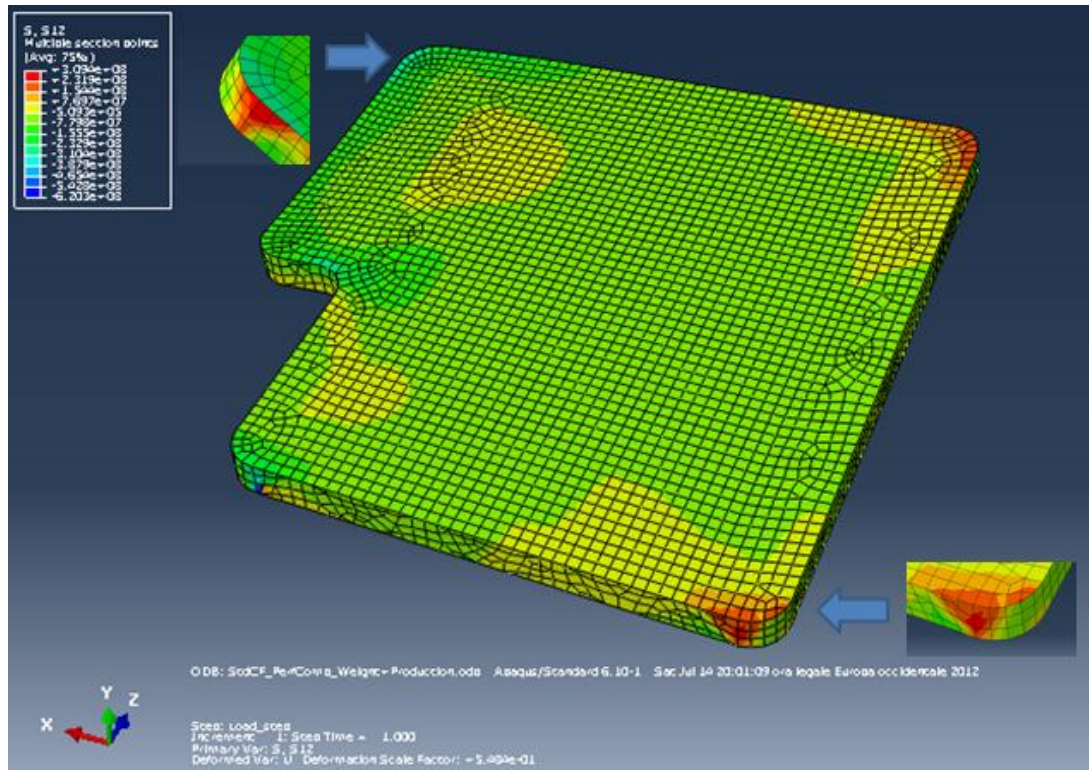


Figure 3-61: S_{12} stress distribution for positive displacement

In the case of displacement in the negative direction it has been observed that the stresses are lower for materials with unidirectional fiber orientation, while a stress increase has been witnessed for pre-preg composite materials.

The stress distribution has similar pattern as in the previous case, the sections with highest load remain the same. The only exception is that in this occurrence the point with highest stress is the lower right one instead of the lower left and upper right ones. The following Figures 3-62 to 3-70 show the stress behavior.

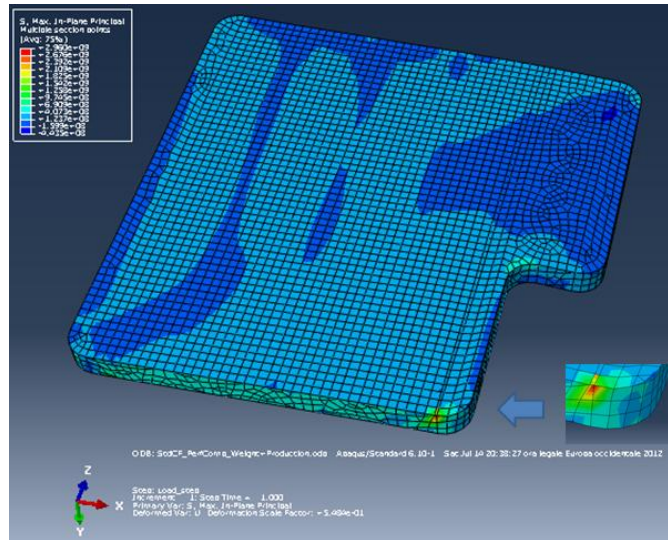


Figure 3-62: In plane max principal stress on front side for negative displacement

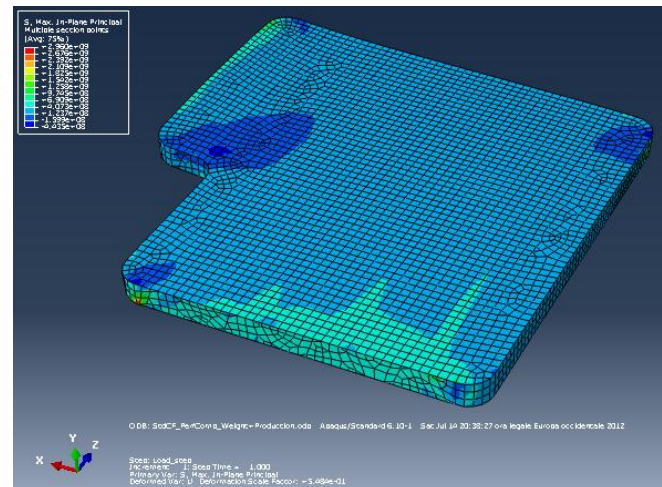


Figure 3-63: In plane max principal stress on rear side for negative displacement

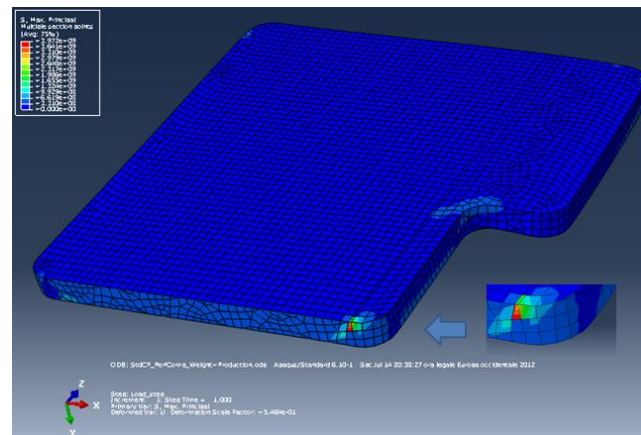


Figure 3-64: Maximum principal stress distribution on front side for negative displacement

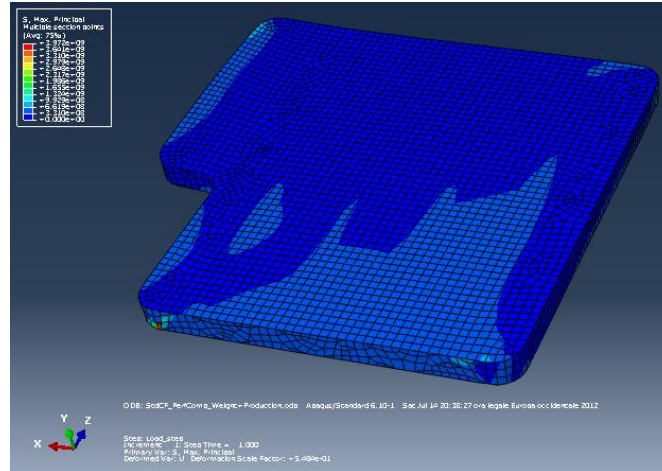


Figure 3-65: Maximum principal stress distribution on rear side for negative displacement

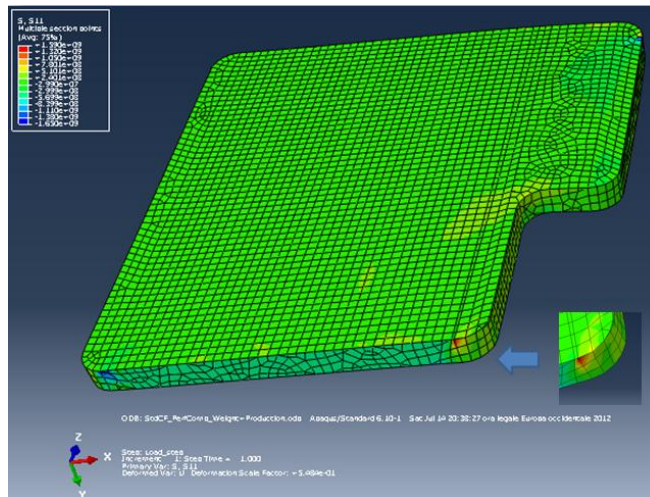


Figure 3-66: S_{11} stress distribution on front side for negative displacement

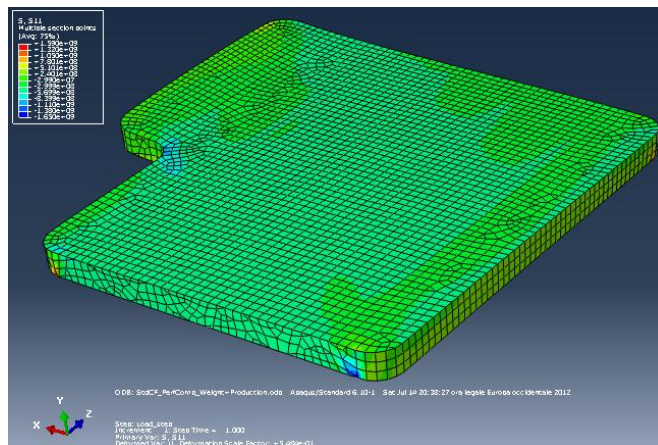


Figure 3-67: S_{11} stress distribution on rear side for negative displacement

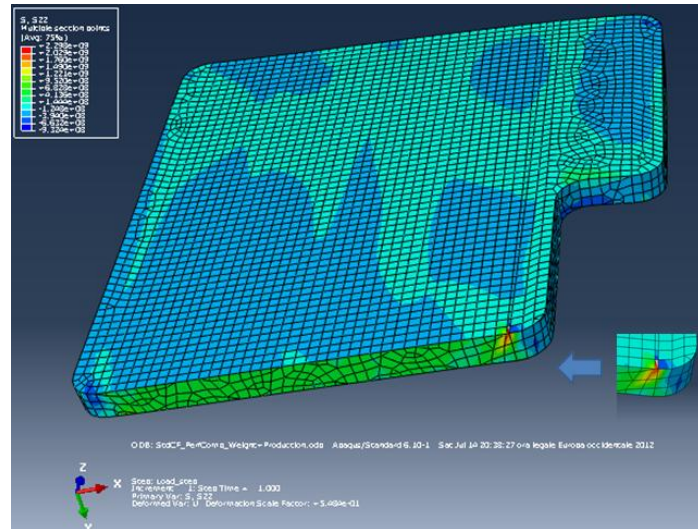


Figure 3-68: S_{22} stress distribution on front side for negative displacement

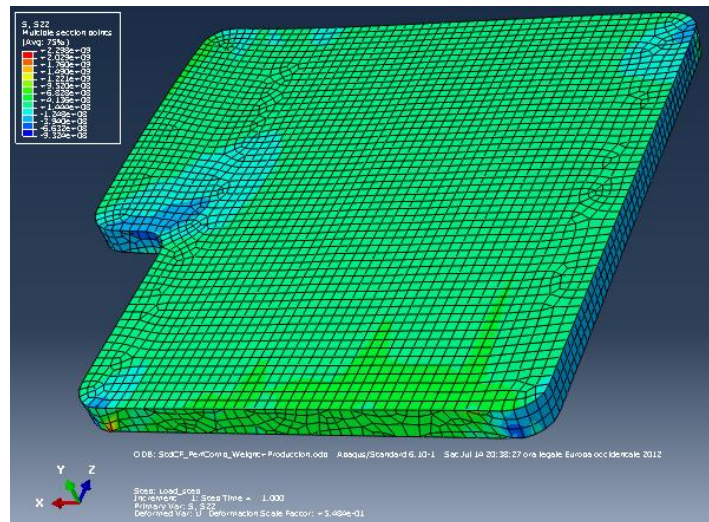


Figure 3-69: S_{22} stress distribution on rear side for negative displacement

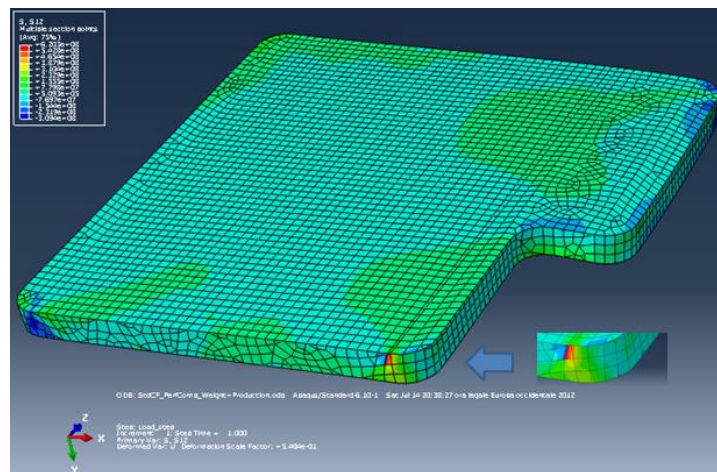


Figure 3-70: S_{12} stress distribution for negative displacement

The stresses distributions were evaluated for each of the materials at disposal and the results obtained by applying displacement in the positive x direction are summarized in Table 3-37.

Positive displacement	Max in plane principal [MPa]	Max principal [MPa]	S11 [MPa]	S22 [MPa]	S12 [MPa]
Std CF Performance Composites	2130	2463	1650	932	309
HMCF Performance Composites	2535	2978	1918	1105	357
E glass Performance Composites	707	912	594	473	200
Kevlar Performance Composites	1052	1302	843	659	301
UD Std CF Performance Composites	4658	4658	2838	552	514
UD HMCF Performance Composites	5467	5467	3300	516	507
UD E glass Performance Composites	1416	1416	1006	192	182
UD Kevlar Performance Composites	1316	1316	1185	119	126
S-2 glass fiber AGY	1804	1804	1201	381	285
HS carbon fiber NPL	6605	6605	3853	647	809
HM carbon fiber NPL	8736	8736	5156	611	780

Table 3-37: Stresses evaluation on the component subject to positive displacement

Table 3-38 shows the stresses obtained applying the displacement in the negative direction.

Negative displacement	Max in plane principal [MPa]	Max principal [MPa]	S11 [MPa]	S22 [MPa]	S12 [MPa]
Std CF Performance Composites	2960	3972	1590	2298	620
HMCF Performance Composites	3574	4823	1906	2685	698
E glass Performance Composites	899	1173	529	770	196
Kevlar Performance Composites	1368	1792	791	1202	328
UD Std CF Performance Composites	4398	4388	2990	1055	741
UD HMCF Performance Composites	5320	5320	3553	974	810
UD E glass Performance Composites	933	933	708	275	193
UD Kevlar Performance Composites	1035	1035	808	198	160
S-2 glass fiber AGY	1329	1345	1171	819	259
HS carbon fiber NPL	5867	5867	3792	1175	1002
HM carbon fiber NPL	8438	8438	5750	1019	1183

Table 3-38: Stresses evaluation on the component subject to negative displacement

According to the data presented in Table 3-37 and 3-38 it can be concluded that pre-preg laminates show higher stress values under negative displacement application; the opposite is observed in case of positive displacement. It can also be pointed out that high strength and high modulus carbon fibers by NPL have the highest stress values. This can be attributed to their higher mechanical properties in terms of Young's modulus. E-glass fiber composites instead present the lowest values of stresses. In general it can be summarized that the best performing carbon fiber composites are the standard and high modulus ones, whereas the best glass fiber composite is the E-glass by Performance Composite. According to these results a better comparison can be done in order to select from the available materials. In any case it can be noticed that the stress magnitudes are very high in the boundary regions, while a close to uniform distribution is present in the rest of the structure.

This means that the sandwich structure with the corrugated panel inside has an optimal behavior in distributing the load throughout the component. In order to decrease the stress concentration values two alternatives can be adopted. The first consists of changing the boundary constraints from points to distributed surface loads, the second, more efficient, consists of the design of physical joints that allow the component to be embedded in the car body.

Tables 3-39 and 3-40 represent a stresses collection similar to the one presented previously, but in this case the boundary conditions are modified. The rotation has been modeled selecting an edge along the lower component side while the upper hinge is modeled with a curved edge in the component rounded corner.

Positive displacement	Max in plane principal [MPa]	Max principal [MPa]	S11 [MPa]	S22 [MPa]	S12 [MPa]	Resultant force [N]
Std CF Performance Composites	3504	3504	2572	1617	830	12256
HMCF Performance Composites	4195	4195	3012	1839	894	14560
E glass Performance Composites	1595	1595	1051	705	364	11684
Kevlar Performance Composites	2187	2187	1445	947	542	12030
UD Std CF Performance Composites	4490	4502	3051	864	698	14117
UD HMCF Performance Composites	5454	5454	3501	790	671	15209
UD E glass Performance Composites	2009	2009	1371	247	302	11794
UD Kevlar Performance Composites	2122	2122	1469	137	199	12517
S-2 glass fiber AGY	2922	2922	2064	578	564	12543
HS carbon fiber NPL	6364	6364	4214	1107	978	19701
HM carbon fiber NPL	8833	8833	5540	914	894	21560

Table 3-39: Stresses evaluation in the positive direction with modified boundary conditions

Negative displacement	Max in plane principal [MPa]	Max principal [MPa]	S11 [MPa]	S22 [MPa]	S12 [MPa]	Resultant force [N]
Std CF Performance Composites	2287	2401	1268	1375	1375	12256
HMCF Performance Composites	2775	2921	1517	1676	635	14560
E glass Performance Composites	730	775	543	428	421	11684
Kevlar Performance Composites	1107	1181	795	640	640	12030
UD Std CF Performance Composites	2647	3797	2150	850	704	14117
UD HMCF Performance Composites	2932	4328	2386	845	644	15209
UD E glass Performance Composites	1099	1099	811	253	379	11794
UD Kevlar Performance Composites	1438	1438	878	203	249	12517
S-2 glass fiber AGY	1166	1667	1123	407	642	12543
HS carbon fiber NPL	3395	4941	2999	1016	1224	19701
HM carbon fiber NPL	4228	6429	3615	1077	1119	21560

Table 3-40: Stresses evaluation in the negative direction with modified boundary conditions

Applying these modifications, it can be seen that the materials behavior remains the same as described before; the difference is in the higher stress concentration in the upper component part and the hinge region.

This is due to a more uniform distribution in the lower component part with lower stress values in correspondence of the rotation constraint. The second solution to reduce and modify the stress distribution in the component has been tested as well.

The modification has been applied only to the rotational movement, and the constraint has been modeled as a tube joined to the back of the structure where at the inside a cylindrical pivot can be inserted thus allowing the seat to fold. Figure 3-71 shows the model of the joint.

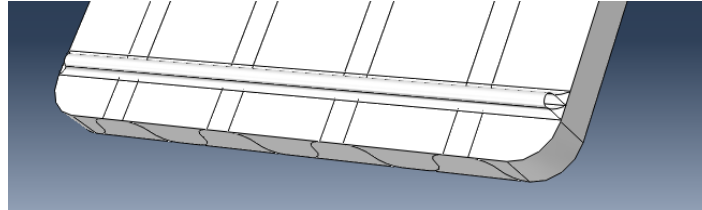


Figure 3-71: Model of a joint allowing seat back folding

The stress values have been analyzed and the results show a better and more uniform distribution of the load on the newly introduced part.

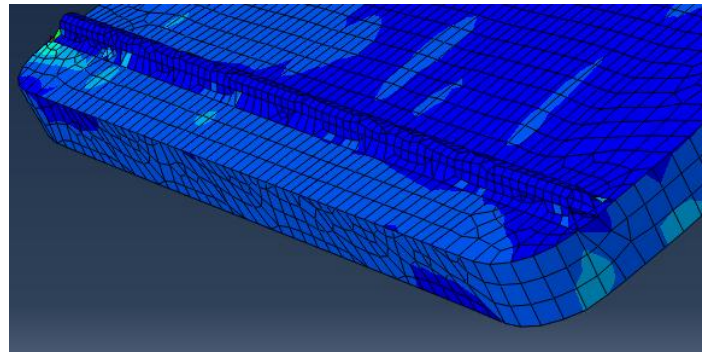


Figure 3-72: Maximum principal stress distribution on the rotation hinge

This example shows that it is possible to decrease the stress concentration on the component through simple modifications. Unfortunately the Abaqus software does not allow the design of complex shapes and at the same time the joints cannot be designed properly because there is no a known car model to know exactly where and how to assemble the component. Even though the constraints design is known, and the stress values are still high it could be possible to apply some localized reinforcements. This would represent a good solution but the use of a software with more powerful design tools could be preferred. High values of stress in correspondence of the boundary conditions and the displacement application point have to be expected because they are set as points and this let the values to be higher than in case of having distributed loads; the lack of knowledge about the real joint design does not allow to evaluate the proper stress distribution on the component. This limitation will affect the failure analysis of the component that will be described in the following.

3.5. Stiffness evaluation for the target design solutions

A detailed analysis to understand the components behavior has been done considering not only the final position reached during the deformation but also the deformation range from 0 up to 100 mm. This way it is possible to have a better idea about the force and therefore the stiffness variation during the loading.

The values have been computed considering 10 mm step variation and the results have been compared to the ones obtained during the test of the actual rear seat back in steel. The curves of force versus displacement are shown in Figure 3-73.

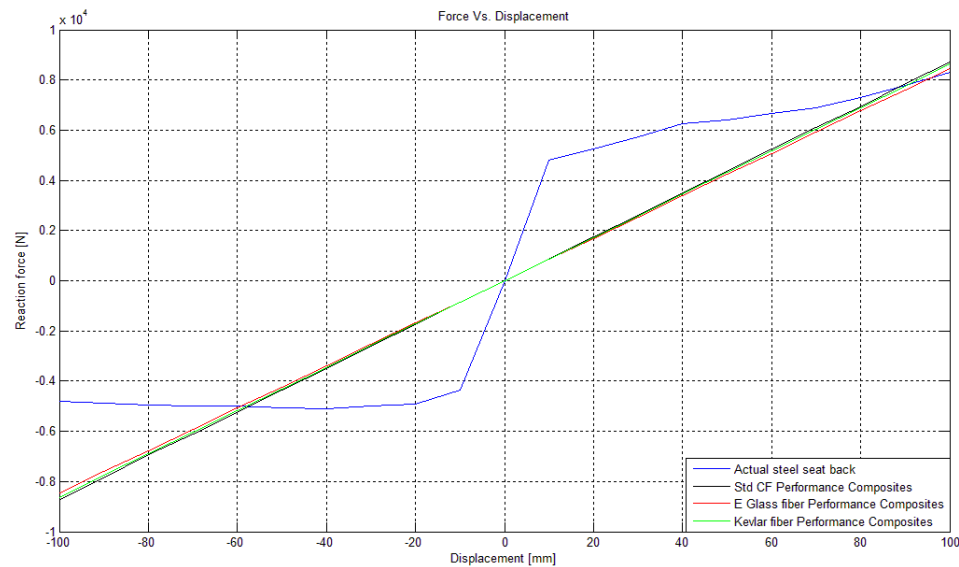


Figure 3-73: Force-Displacement trend for target design solutions compared to the current one

The three solutions have a slightly higher force magnitude than the actual steel seat back in considering the maximum displacement. It can be pointed out that the model presents a constant stiffness for all the displacement fields evident by the constant slope and linear behavior of the curves. In particular the stiffness values (K) are:

- ✓ $K_{\text{Steel}} = 83 \text{ N/mm}$
- ✓ $K_{\text{StdCF}} = 87.29 \text{ N/mm}$
- ✓ $K_{\text{Kevlar}} = 86.26 \text{ N/mm}$
- ✓ $K_{\text{E-Glass}} = 84.61 \text{ N/mm}$

CHAPTER IV

MATERIAL COSTS ANALYSIS AND COMPONENT PRICE ESTIMATION

In this chapter a brief explanation about the methods used to evaluate and estimate the components price will be provided. The starting point in order to achieve certain results consists of knowing all the prices related to fibers, matrixes and the processes involved in the production of pre-preg plies and the final component itself.

It is not easy to get exact price values since the costs have high variability according to several factors such as mechanical and physical properties of the materials and the production volume.

According to the information provided in the literature review section and some data provided by Fiat the costs assumptions are summarized as follows. For carbon fibers it has been assumed that the price range is from 33 to 110 \$/kg for aerospace-grade fibers with Young's modulus between 275 and 413 GPa while the price ranges from 15 to 30 \$/kg in case of standard-grade carbon fibers with elastic modulus from 220 to 250 GPa.

Unfortunately the fibers described in the analysis so far do not have the exact price values but the elastic modulus varies from 137.3 GPa for the weakest one that is the standard CF by Performance Composites up to 476.5 GPa for high-modulus carbon fibers by NPL, that have the best mechanical properties.

In order to assume a certain cost over a wider range of mechanical properties the known data of fiber cost per kilogram versus Young's modulus has been used to create a function that has been interpolated; this way it is possible to estimate a fiber cost for each value of elastic modulus.

The data has been interpolated with two functions; an exponential one in the range between 100 and 230 GPa and a quadratic one for Young's modulus values higher than 230 GPa. The quadratic function fits well the data only in the high range above 250 GPa. For this reason an exponential function has been used to fit the data in the lower range so that the costs can have more reliable estimate. The functions are plotted in Figure 4-1.

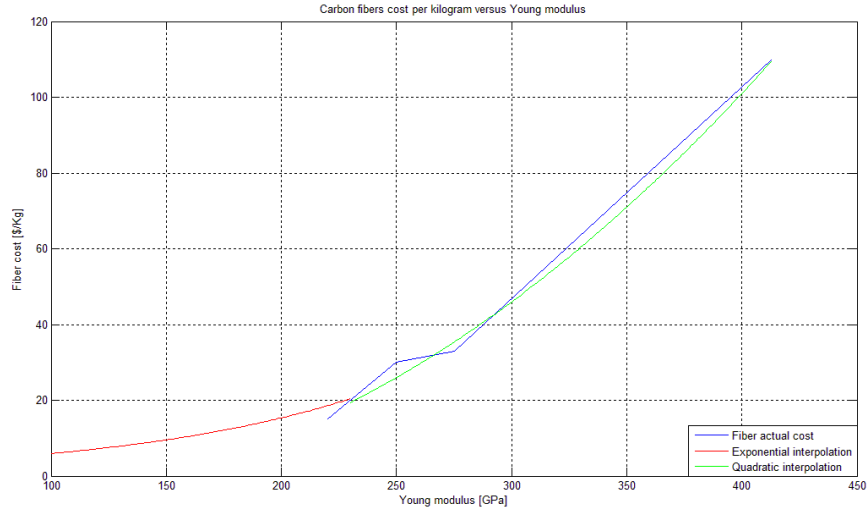


Figure 4-1: Interpolation of carbon fibers cost per kilogram as a function of Young's modulus

In the case of glass and Kevlar fibers it was not possible to apply the same procedure since the similar data trend was not available. It has been assumed a cost of 6.5 \$/kg for glass fiber with 80.5 GPa Young's modulus and a cost of 26 \$/kg for Kevlar fiber with elastic modulus of 123 GPa. The cost assumption has been done again considering the price as a function of the Young's modulus with the exception that the trend has been assumed to be linear. Fiber cost versus elastic modulus trend for Kevlar and glass fibers is presented in Figure 4-2.

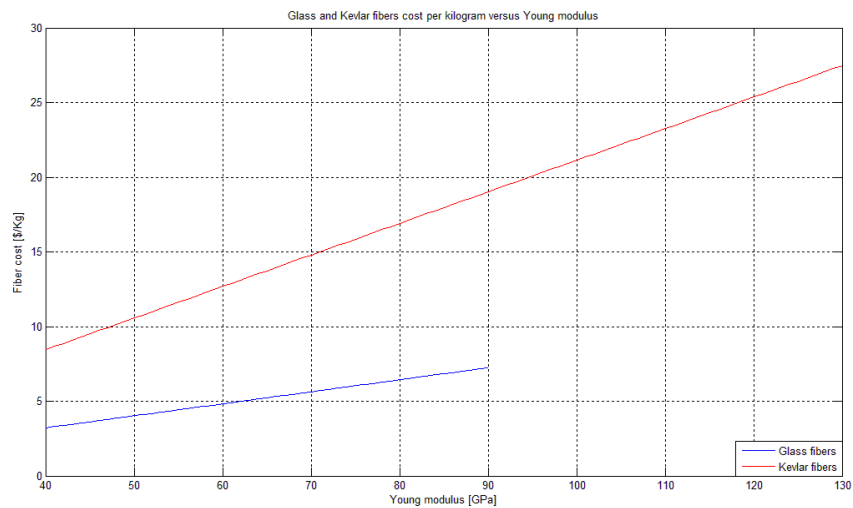


Figure 4-2: Glass and Kevlar fibers cost per kilogram as a function of Young's modulus

According to the assumptions presented above the carbon, glass and Kevlar fibers cost has been evaluated for the fibers in each composite material used to test the component and the results are provided in Figure 4-3.

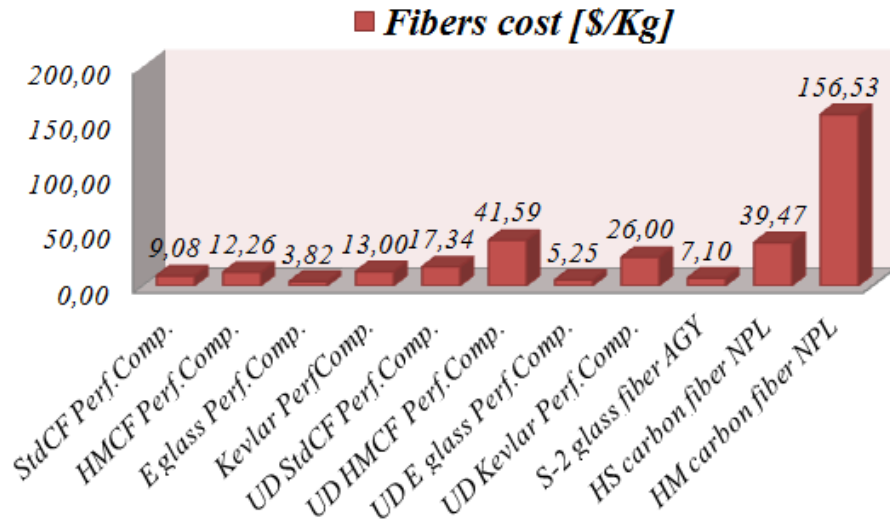


Figure 4-3: Fibers cost per kilogram estimation for the selected materials

As expected the highest costs are for carbon fibers with high modulus, followed by Kevlar and then glass fibers. E-glass fiber by Performance Composite has the lowest cost because of its very low Young's modulus, "S" glass fiber has a price almost double the E-glass one. A comparison between thermoplastic and thermoset resins cost is provided in Figure 4-4.

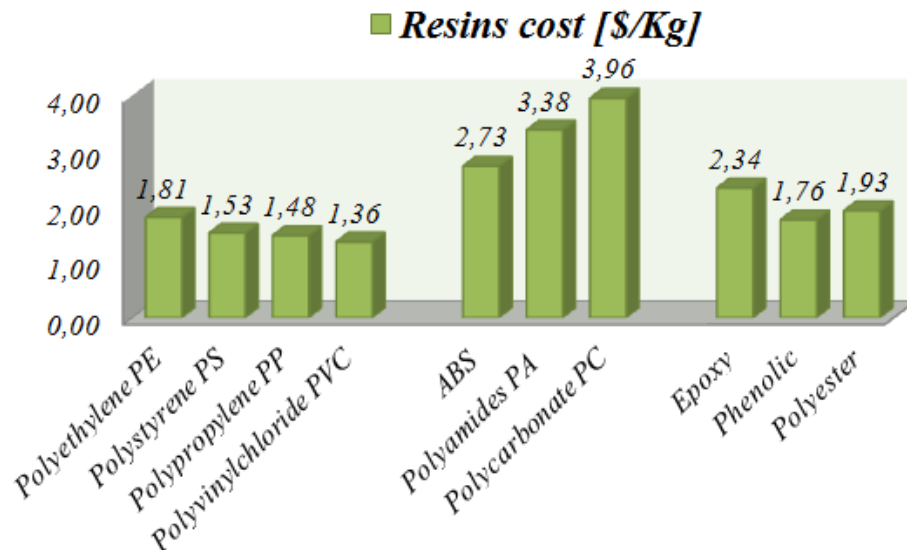


Figure 4-4: Thermoplastic and thermoset resins average cost per kilogram

The thermoplastic resin chosen is PVC as explained in the previous sections. The cost of the production of pre-preg plies is assumed to be associated with the manufacturing processes. A further distinction has also been made between composites with woven fabric fiber and composites with unidirectional fibers. It has been assumed an additional manufacturing cost of 15 % to composites with UD fibers and an addition of 30 % to composites with woven fibers since the fabric production requires one more step. According to these assumptions the composites costs have been evaluated and the values are shown in Figure 4-5.

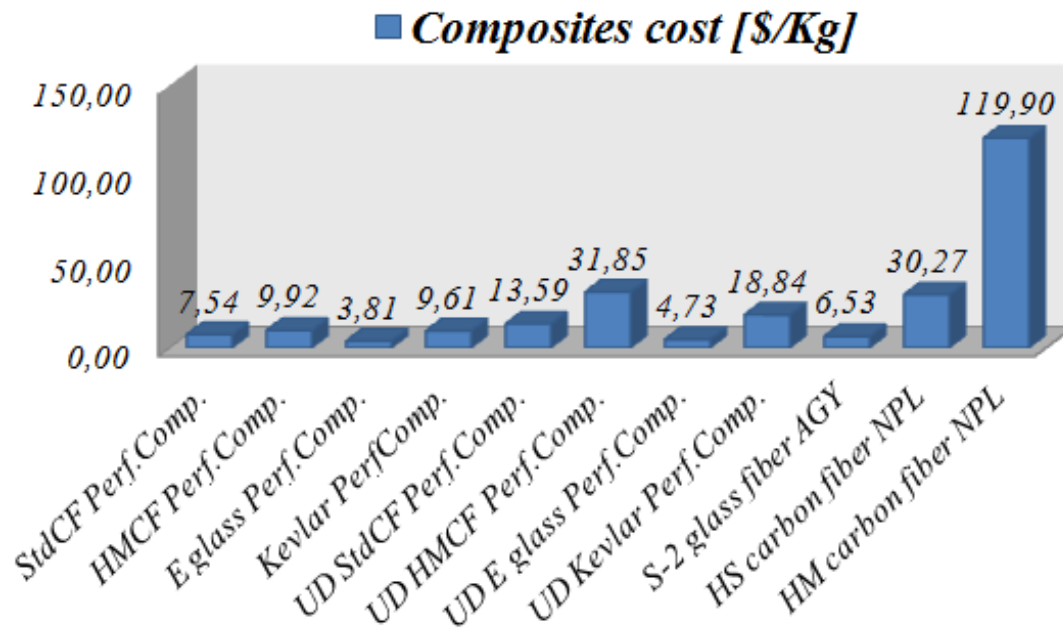


Figure 4-5: PVC thermoplastic composites cost per kilogram considering plies production

The cost trend is similar to the one described in fibers, since the matrix is the same for all the composites. The only difference is the fiber volume fraction that is 50 % for “fabric” composites and 60 % for composites with UD fibers. This effect is offset by the higher manufacturing cost for “fabric” products. With this data available and the known components weight, it is possible to estimate the cost of each of the proposed solutions. The analysis has been done only for the solutions presenting optimal weight and easiness of manufacturing since these aspects can be considered as the main project targets. The results are presented in Figure 4-6.

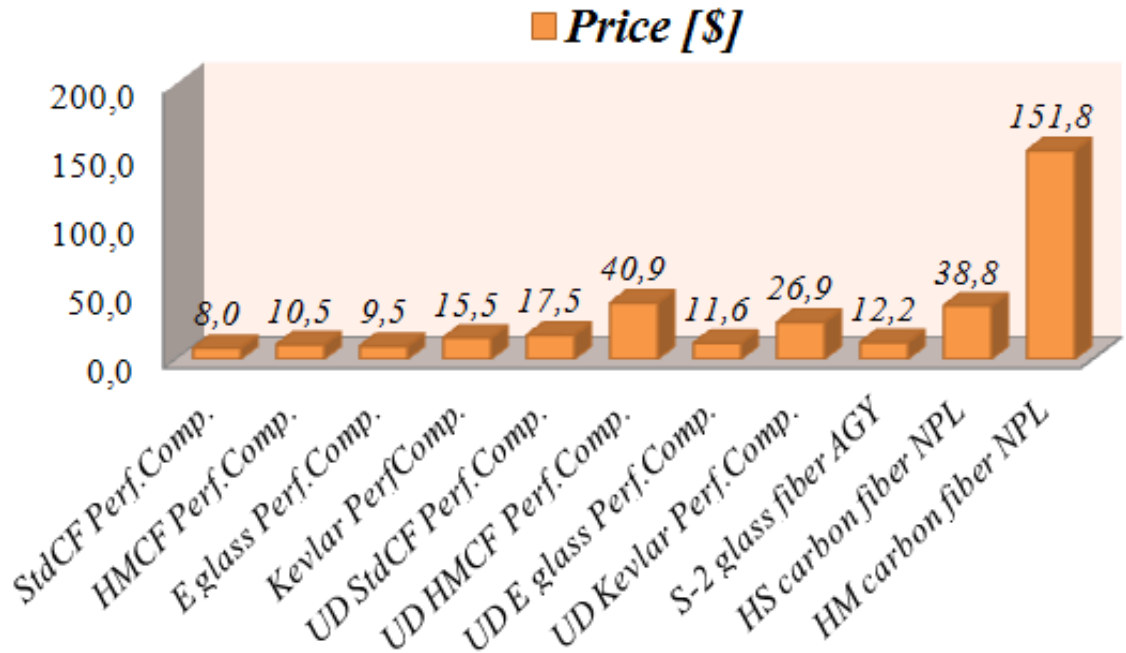


Figure 4-6: Component price estimation for each of the selected materials

The cheapest solution is provided by using standard CF by Performance Composites; it presents the best compromise of weight, mechanical properties and price among all the composites with carbon fibers as filler. The best solution with glass fibers as filler is given by E-glass fiber composite by Performance Composites while the best alternative by using Kevlar fibers reinforcement is given by yarn fabrics by Performance Composites. It can be pointed out that in all of the cases presented above the best results have been achieved having fabric fibers as reinforcement. The three best solutions presented will be analyzed in more details in the next section.

CHAPTER V

DELAMINATION AND FAILURE MODES OF COMPOSITE MATERIALS

5.1. Introduction to delamination

Delamination is one of the main failure causes for fiber reinforced composite materials due to the relatively low loading strength between laminas. This phenomenon can occur during manufacturing, transport, service etc. The first kind of delamination is induced on curved sections where both the normal and shear stresses can create a loss of inter-laminar adhesion and a crack initiation; the second category consists in abrupt section changes. Actually there is a third category that is related to the temperature variation and so to the different thermal expansion coefficients of matrix and reinforcement which can create contraction in the material during the curing process. During manufacturing the cutting of plies is one of the main delamination causes, while during service impact with other objects can reduce the material properties and lead to a crack formation. Delamination can arise inside the part or near the surface. Inner delamination reduces the load capacity of the structure and its flexural behavior. Near surface delamination represents a more complex scenario and does not influence the rest of the laminate deformation [47]. Figure 5-1 illustrates inner delamination for flat and curved sections.

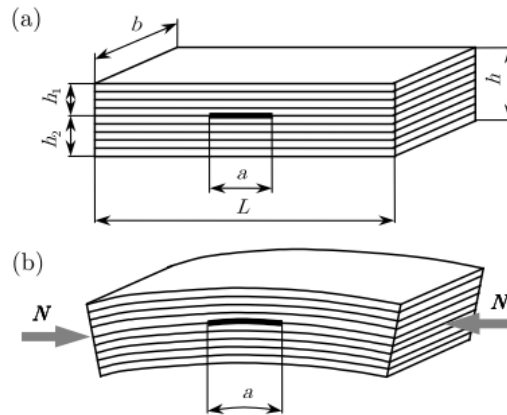


Figure 5-1: Inner delamination for flat (a) and curved (b) sections [47]

After initiation, delamination can propagate under static or fatigue loads inducing a noticeable loss of strength, stability and flexion capabilities of the component. This kind of failure is difficult to detect and particular attention has to be paid during the design.

Usually the stress concentration increases close to the edges or geometric discontinuities. The growth of inter-laminar crack is preceded by the formation of a damaged zone whose size and shape is influenced by the resin toughness and the stress state. Three kinds of failure modes can be distinguished. Mode I failure occurs usually in brittle systems and the damaged zone is relatively small and contains some micro-voids whose coalescence creates a growth in the crack advance. Sometimes this phenomenon can be preceded by the fiber-matrix debonding. During debonding fiber bridging or breakage can be observed. For ductile systems a plastic deformation is observed in correspondence of the crack tip before the propagation starts. Mode II and III consist in shear delamination of quasi-brittle systems. The crack originates at 45° with respect to the ply plane and propagates until reaching the fiber surface. These kinds of failure are of ductile type and just sometimes bring to a fiber debonding. Figure 5-2 shows the failure modes described above.

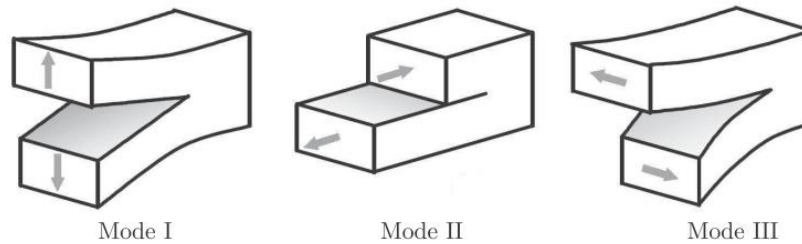


Figure 5-2: Illustration of delamination failure modes [47]

Figure 5-3 explains how in case of Mode II delamination the micro-cracks form, grow and create coalescence in between two different laminate plies in the resin rich area.

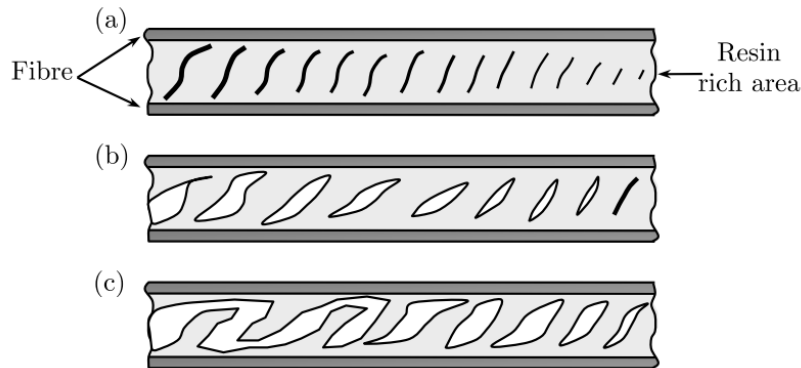


Figure 5-3: Mode II delamination crack formation (a), growth (b) and coalescence (c) [47]

The failure modes can be tested through dedicated devices. A double cantilever beam (DCB) system is adopted to evaluate Mode I failure while an end-notch flexure test is applied to analyze Mode II failure [48]. Figure 5-4 represents a DCB device, the load is applied perpendicularly to the plies surface and the length of the opening is evaluated.

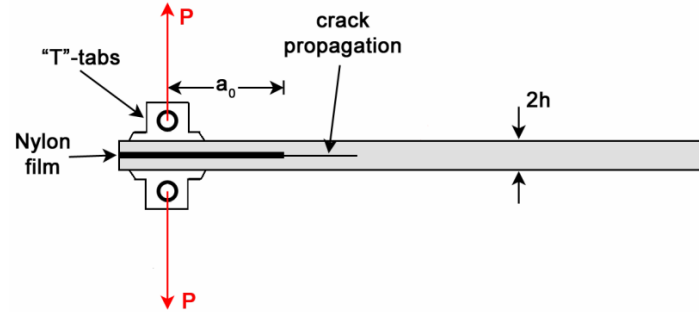


Figure 5-4: Schematic of a double cantilever beam test device [48]

Figure 5-5 shows an end-notch flexure test, the load is applied in the middle of the beam and the crack length is evaluated similarly to the previous case.

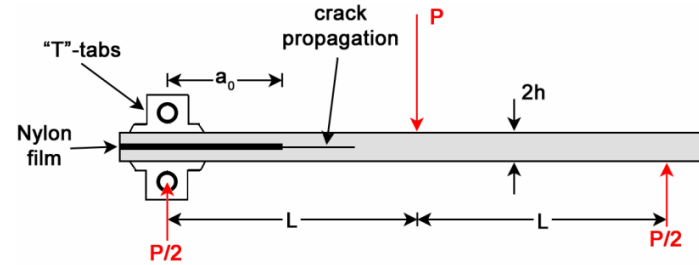


Figure 5-5: Schematic of end-notch flexure test device [48]

Figure 5-6 represents a schematic of a mixed mode bending apparatus with the applied loads and reactions.

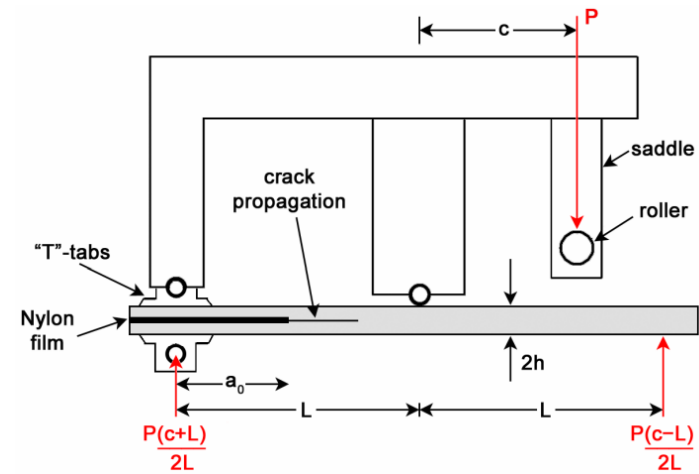


Figure 5-6: Schematic of a mixed mode test device [48]

5.2. Different approaches to delamination analysis

During the years several techniques have been proposed. In this section a review related to fracture mechanics and damage zone model will be provided.

5.2.1. Fracture mechanics approach

This model is based on linear elastic fracture mechanics and neglects the material non-linearities. The model has to be applied with an initial crack. Some models have been proposed to evaluate the stress energy rate released and nowadays it is hard to implement this model in a finite element numerical code. To predict crack propagation Virtual Crack Closure Technique (VCCT) is one of the most widely used procedures. It consists in assuming that the energy released during a crack formation is equal to the work needed to close the crack to its original length. The crack propagates when the energy rate per area is equal or higher than the critical value G_c . Analyzing nodal forces and displacement the energy release rates G_I , G_{II} and G_{III} can be computed for each of the three failure modes presented previously. In particular the value of each energy release can be computed by using the relations presented in Figure 5-7.

$$\begin{aligned} G_I &= \frac{1}{2b\Delta a} F_{cd}^y (v_c - v_d) \\ G_{II} &= \frac{1}{2b\Delta a} F_{cd}^x (u_c - u_d) \\ G_{III} &= \frac{1}{2b\Delta a} F_{cd}^z (w_c - w_d) \end{aligned}$$

Figure 5-7: Energy release rate for Mode I, II and III [47]

In the relations presented “b” corresponds to the specimen thickness, “a” is the length of the crack, F_{cd}^y , F_{cd}^x and F_{cd}^z are the nodal forces magnitudes in correspondence of nodes c and d in the three directions, u_c , v_c , w_c and u_d , v_d , w_d are the nodal displacements of nodes c and d along the three directions respectively. Figure 5-8 provides an illustration of the VCCT model.

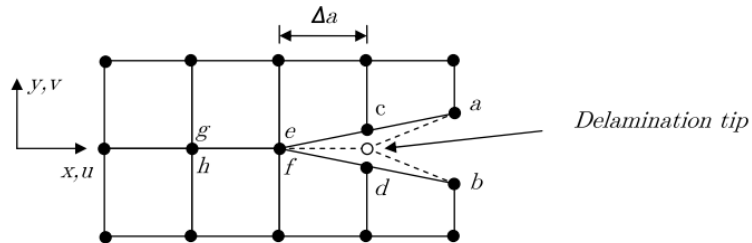


Figure 5-8: VCCT model finite element mode after crack propagation [47]

Once G_I , G_{II} and G_{III} values are known they have to be summed in order to obtain the total energy release rate G_T . Propagation occurs when total energy release rate is equal to the critical one and in particular:

$$G_T = G_c$$

$$G_T = G_I + G_{II} + G_{III}$$

The limit of this model is due to the absence of a method to consider and predict the crack initiation, and so only the crack propagation can be evaluated [47].

5.2.2. Cohesive or damage zone model

This model is based on the concept of the cohesive crack, it means that a cohesive damage zone is developed near the crack front. It considers traction and displacement jumps at the interface where a crack may occur. Figure 5-9 provides an illustration of traction slope versus displacement; the area under the curve corresponds to the energy release rate.

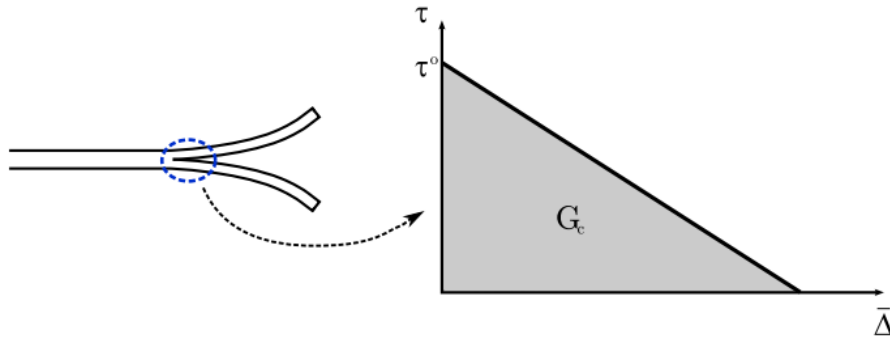


Figure 5-9: Traction in the cohesive zone ahead of the crack tip [47]

τ^0 refers to the maximum traction allowed before damage. When the area under the traction slope is equal to G_c the traction τ^0 is reduced to zero and a crack surface is formed. The advantage of this model consists in its simplicity and the opportunity to combine together crack initiation and propagation.

In case of pure mode loading the crack occurs when the traction values τ_I , τ_{II} , τ_{III} for Mode I, II and III are equal to their respective maximum interfacial strength τ_I^0 , τ_{II}^0 and τ_{III}^0 . The propagation instead is verified when the energy release rates G_I , G_{II} and G_{III} are equal to the critical values G_{Ic} , G_{IIc} and G_{IIIc} . For the mixed mode loading the procedure is similar, the difference lies in the fact that the traction and energy release rate values have to be considered together and complex functions have to be introduced.

Before implementing this method in a numerical code some modifications have to be applied, in particular a deformation zone with very high stiffness value has to be introduced before damage initiation. Figure 5-10 illustrates the modification applied to the traction curve in the numerical model.

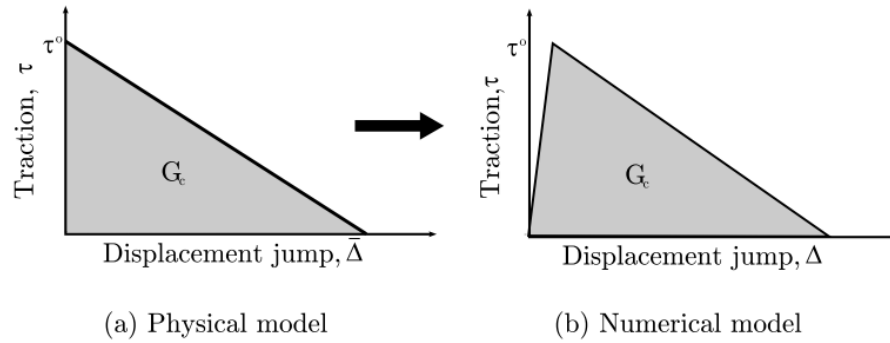


Figure 5-10: Comparison between physical and numerical cohesive model [47]

5.3. Analysis of fracture and debonding of seat back structure

In this section a general description of the fracture occurrence and location will be provided. Nowadays a deep knowledge exists related to fracture in materials with particle reinforcement, while not so much information is available for fiber reinforced composites. According to the tests results of many experiments on particle reinforced materials it has been noticed that the fracture of the particles near the surface is the source of crack nucleation and propagation under traction. Delamination activity occurs in correspondence of subsurface layers at a distance between 10 and 100 μm below the contact interface. This deformation is the cause of a stress intensification between the particles and the matrix and induces a noticeable change of the subsurface structure of the materials in contact thus bringing to a deep modification of mechanical properties, and as a consequence a reduction in performance. In case of Al-Si alloys many researchers observed that the vicinity of the particle/matrix interface is a point where cracks generate and decohesion can be observed. The presence of voids inside the stiffer particles induces an increase of stress concentration and then a crack nucleation is evidenced inside the matrix. Several kinds of surface damage can occur. The most common ones are interface debonding, that can be evaluated once the maximum shear stresses τ_{xy} are known, particle fracture, that can be evaluated through a fracture toughness model, and the last one refers to plastic deformation of the matrix in correspondence of the particles.

Interface debonding can be attributed to two mechanisms. A decohesion of the particles from the matrix along the interface or a fracture of the matrix in the close vicinity of the matrix/particle interface. In the case of needle like particles the main debonding occurrence is given by decohesion due to the high surface to volume ration in the particles. Continuous fibers can also be considered as a sort of needle like particles, this is one of the reasons why the failure in composites occurs usually at the interface between two different plies.

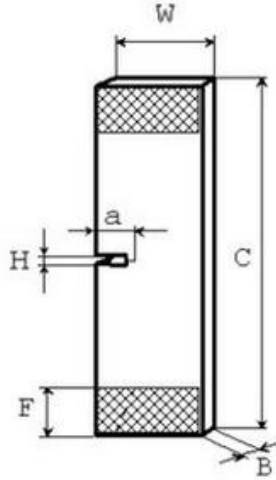
On the contrary, in case of rounded particles the dominant mechanism is the fracture of the matrix near the interface with particles. It has been proved that particles with smaller size have a higher interface threshold shear stress, and so they appear more difficult to debond. According to this, spherical shape particles are preferred in order to increase the material resistance [49].

In order to analyze the fracture inside the component the fracture toughness is considered the most important material property since it is a measure of the material resistance to either brittle or ductile fracture when a crack exists. A low value of fracture toughness means a brittle fracture and can be observed in ceramic materials; on the contrary, a high fracture value, as in the case of metals, refers to a ductile fracture. Several models exist to analyze the fracture, but the most diffused is the K_{Ic} model, which takes into account the plain strain and combines it to Mode I fracture mode. This means that in this occurrence it is supposed that the fiber breaks in composite materials, and the fracture plane is perpendicular to the fiber axis. This kind of failure can be classified as Mode I. In reality the 90 % of the fracture cases is due to Mode I, while Mode II and III are rarely observed. During the loading, since the component fibers are oriented at 45° and -45° , there are planes with alternating tension–compression loads. This induces bending within the structure. There is crack nucleation and subsequently fracture when the local stress intensity factor K_I in the section of the system exceeds the local threshold stress intensity factor K_{Ic} . The stress intensity factors, both actual and critical, can be evaluated according to the following expressions:

$$K_I = Y\sigma\sqrt{\pi a} \text{ (stress intensity factor in correspondence of a local section)}$$

$$K_{Ic} = Y\sigma_{tr}\sqrt{\pi a_c} \text{ (critical stress intensity factor)}$$

“Y” is a geometrical factor and its value is usually one, σ is the local stress, σ_{tr} is the threshold stress, “a” is the length of the fracture and a_c is the critical length of the fracture, that in case of fibrous reinforcement corresponds to the fiber diameter [50, 51]. K_{Ic} is a particularity of the material and this value is usually evaluated through experimental tests of molecular dynamic or pull-out test. An illustration of the specimen used during the test is provided in Figure 5-11.



SEN-T specimen, ($W = 30$ mm, $a = 10 + 1$ mm, $B = 2$ mm, $C = 110$ mm, $F = 15$ mm, $H = 1$ mm)

Figure 5-11: Illustration of single end-notched specimen and its dimensions [52]

From the experimental tests a relation to compute the stress intensity factor has been found and it is:

$$K_{Ic} = \frac{F_{max}}{BW} a^{1/2} f(a/W)$$

$$f(a/W) = 29.6 - 185.5(a/W) + 655.7(a/W)^2 - 1017(a/W)^3 + 683.9(a/W)^4 F_{max}$$

Where:

F_{max} : Maximum force in the force displacement graph

B : Thickness of the specimen

W : Width of the specimen

a : Total notch length

$f(a/W)$: Geometrical correction factor

In absence of specimen information or impossibility to conduct experimental tests, some graphs can be helpful to have an idea about the range of values for stress intensity factor as a function of the material adopted. One example is provided in Figure 5-12.

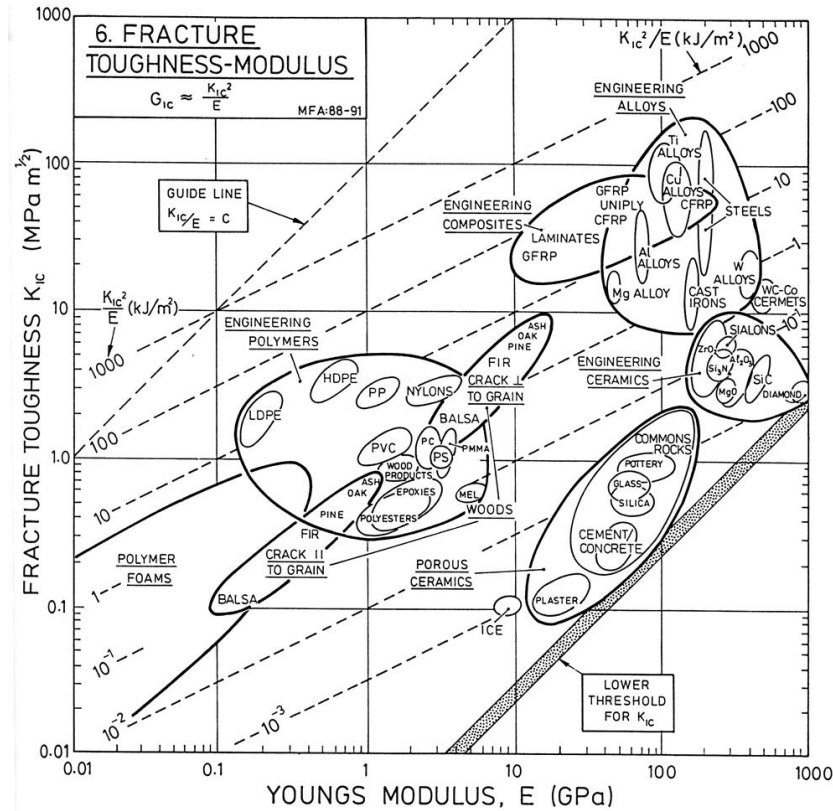


Figure 5-12: Fracture toughness as a function of Young's modulus for several materials [59]

According to Figure 5-12 a relation between Young's modulus, stress energy release and stress intensity factor can be noticed and in particular:

$$G_{Ic} = K_{Ic}^2 / E$$

Focusing the attention on engineering polymers it can be noticed that the stress intensity factor ranges from 20 to 90 MPa m^{1/2} with Young's modulus from 9 to 120 GPa. Glass fiber reinforced plastics are in the lower region while carbon fiber reinforced plastics have the highest values among engineering polymers. According to this information it is possible to do a simple evaluation of the fracture occurrence for the seat back model.

The analysis will be conducted for the three materials selected and presenting the best configuration in terms of mechanical properties, stress distribution and concentration and costs.

According to the Young's modulus of each material it can be assumed a certain range of critical stress intensity factor and compute the threshold stress value σ_{tr} as soon as the fiber diameter is known. In case of standard carbon fiber composite the Young's modulus is 70 GPa and so K_{Ic}^{StdCF} can range from 30 to 90 MPa m^{1/2}.

E-glass fiber composite instead has 25 GPa Young's modulus and so $K_{Ic}^{E-Glass}$ from 20 to 70 MPa m^{1/2} and Kevlar fiber composite with 30 GPa Young's modulus has K_{Ic}^{Kevlar} values from 25 to 80 MPa m^{1/2}. At this point it is necessary to know the diameter of the fiber a_c , since we consider the diameter as the crack critical length. According to the assumptions presented above, and having laminates with 0.5 mm thickness, it can be assumed that the fiber diameter is in the range between 0.3 and 0.5 mm. This means that the stress thresholds σ_{tr} considering the maximum range value of K_{Ic} are as follows:

$$\sigma_{tr}^{StdCF} = 2300 \text{ to } 2900 \text{ MPa if } K_{Ic}^{StdCF} = 90 \text{ MPa m}^{1/2}$$

$$\sigma_{tr}^{E-Glass} = 1800 \text{ to } 2300 \text{ MPa if } K_{Ic}^{E-Glass} = 70 \text{ MPa m}^{1/2}$$

$$\sigma_{tr}^{Kevlar} = 2000 \text{ to } 2600 \text{ MPa if } K_{Ic}^{Kevlar} = 80 \text{ MPa m}^{1/2}$$

These stress values are much higher than the ultimate tensile strength of the three materials that have similar values for both directions at 0° and 90° due to the fact that they are produced with woven fibers; and in particular:

$$UTS^{StdCF} = 600 \text{ MPa}$$

$$UTS^{E-Glass} = 440 \text{ MPa}$$

$$UTS^{Kevlar} = 480 \text{ MPa}$$

At this point in order to evaluate the occurrence of fracture we should consider the worst case scenario. The hypothesis is that the length of the crack is equal to the critical length and so $a=a_c$. With this assumption the comparison is no more between K_I and K_{Ic} , but local stresses σ are compared to threshold stresses σ_{tr} .

According to the stress analysis presented in the previous sections it has been noticed that the maximum loading condition on the component for the selected materials is reached applying the displacement in the negative direction and the maximum values of principal stresses are:

$$\sigma_{MaxPrinc}^{StdCF} = 3972 \text{ MPa}$$

$$\sigma_{MaxPrinc}^{E-Glass} = 1173 \text{ MPa}$$

$$\sigma_{MaxPrinc}^{Kevlar} = 1792 \text{ MPa}$$

Taking this values as reference it can be concluded that glass and Kevlar fiber composites have stresses lower than the minimum value for threshold stresses; carbon fiber composite has a much higher stress value that could bring to failure.

This hypothesis is verified only in case that the fiber crack length is equal to the fiber diameter, but in real situations this occurrence is not always valid and so it can be concluded that no fracture will occur.

A safety coefficient can be estimated for glass and Kevlar fiber composites considering the lower threshold stress value:

$$SC^{E-Glass} = \sigma_{tr}^{E-Glass} / \sigma_{MaxPrinc}^{E-Glass} = 1.54$$

$$SC^{Kevlar} = \sigma_{tr}^{Kevlar} / \sigma_{MaxPrinc}^{Kevlar} = 1.17$$

According to these results it can be concluded that glass and Kevlar fiber composites are more far from reaching fracture failure. A detailed analysis can be done considering the stress distribution according to the fiber orientation inside the material.

In order to perform this analysis it is useful to use Mohr's theory and build the stress circles starting from the stress values in the reference system directions S_{11} , S_{22} and S_{12} and then evaluating the stresses in the planes at 45° and -45° . The values obtained are much lower than the maximum principal ones presented above. This analysis can be applied to carbon fiber composite. Considering a plane oriented at 45° and -45° the results are:

$$\sigma_{45^\circ}^{StdCF} = 2540 \text{ MPa}$$

$$\tau_{45^\circ}^{StdCF} = 320 \text{ MPa}$$

$$\sigma_{-45^\circ}^{StdCF} = 1300 \text{ MPa}$$

$$\tau_{-45^\circ}^{StdCF} = 320 \text{ MPa}$$

According to these results it can be observed that the maximum normal stress $\sigma_{45^\circ}^{StdCF}$ value for 45° plane orientation is $\sigma_{45^\circ}^{StdCF}=2540 \text{ MPa}$, and that value is within the threshold stress σ_{tr}^{StdCF} range from 2300 to 2900 MPa. Considering the maximum value of threshold stress and comparing it to the maximum local stress along the fiber oriented at 45° a safety coefficient can be evaluated as follows:

$$SC^{StdCF} = \sigma_{tr}^{StdCF} / \sigma_{45^\circ}^{StdCF} = 1.14$$

The result is slightly lower than the one obtained with Kevlar fiber composite, and much lower than the one obtained with glass fiber composite, but, it has to be noticed that the hypothesis used in the previous cases refers to higher stress values since applying similar considerations to the previous cases the stress values would have been even lower, thus increasing further the safety coefficients for glass and Kevlar fiber composite.

The safety coefficient values for standard carbon fiber and Kevlar fiber composites are slightly higher than one. These values could appear low, but it should be considered that during the design phase many factors have to be considered at the same time and an optimal compromise between them has to be found. For example, it is possible to achieve a stiffer structure by increasing the amount of material, but so the weight and the costs. This discussion is especially valid for the aerospace sector, where safety coefficients lower than the ones obtained in this research are fully acceptable.

According to the fracture analysis presented, all three materials are not subject to composite fracture failure. In order to have a more detailed knowledge about fracture modes it is necessary to have precise information about material toughness properties, fibers diameter and final component design so that a proper stress distribution and concentration can be taken into account.

CHAPTER VI

CONCLUSIONS AND RECOMMENDATIONS

According to the data and information provided in the previous chapters it can be concluded that the design of a rear seat back using only composite materials is feasible. In contrast with all the solutions introduced by other companies with high volume production, the proposed solutions here do not apply steel reinforcing elements.

The research has been conducted focusing on thermoplastic materials and considering carbon, glass or Kevlar fibers as fillers, each of them presenting unique properties and able to meet the project requirements in terms of dimensions (550x550x30 mm), weight (3.1 kg) and structural resistance (83 N/mm).

Among the proposed and analyzed structures, only the corrugated design solution with an undulated panel in the middle and a closure rib running along the edges has been able to satisfy the desired targets; for this specific design the target constraints are satisfied with any performed of the proposed matrix and filler material.

Open corrugated structure and ribbed structure designs have shown to be unsatisfactory. A component optimization has been performed considering several combinations of thickness in the different regions and varying the fibers orientation inside the component. Furthermore a single design solution has been selected among all the materials adopted based on the stress concentration inside the component and the component price.

In order to evaluate the material cost, with known matrix cost and the fiber cost estimated, it has been assumed an additional 15 % to the material cost for composites with unidirectional fibers, and an additional 30 % for fabric composites. Putting together all this information three materials have been picked, each of them with a different filler. Standard carbon fiber composite by Performance Composites has the following properties:

$$\text{Weight}_{\text{StdCF}} = 1.06 \text{ Kg}$$

$$K_{\text{StdCF}} = 87.29 \text{ N/mm}$$

$$\text{ComponentCost}_{\text{StdCF}} = 8 \text{ \$/part}$$

E-glass fiber composite by Performance Composites instead has:

$$\text{Weight}_{\text{E_Glass}} = 2.49 \text{ Kg}$$

$$K_{\text{E_Glass}} = 84.61 \text{ N/mm}$$

$$\text{ComponentCost}_{\text{E_Glass}} = 9.5 \text{ \$/part}$$

Finally Kevlar fiber composite provided by the same company has:

$$\text{Weight}_{\text{Kevlar}} = 1.61 \text{ Kg}$$

$$K_{\text{Kevlar}} = 86.26 \text{ N/mm}$$

$$\text{ComponentCost}_{\text{Kevlar}} = 15.5 \text{ \$/part}$$

The results are collected in Figures 6-1, 6-2 and 6-3. Weight and stiffness results for all the three composites materials are compared to the current rear seat back design in steel.

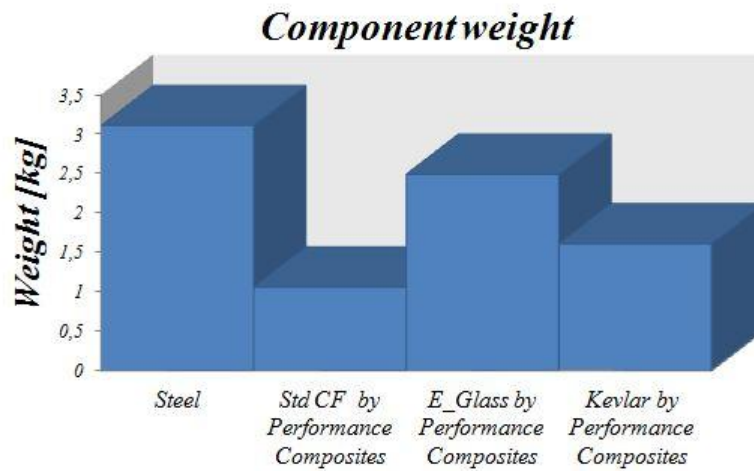


Figure 6-1: Component weight comparison between steel and composites

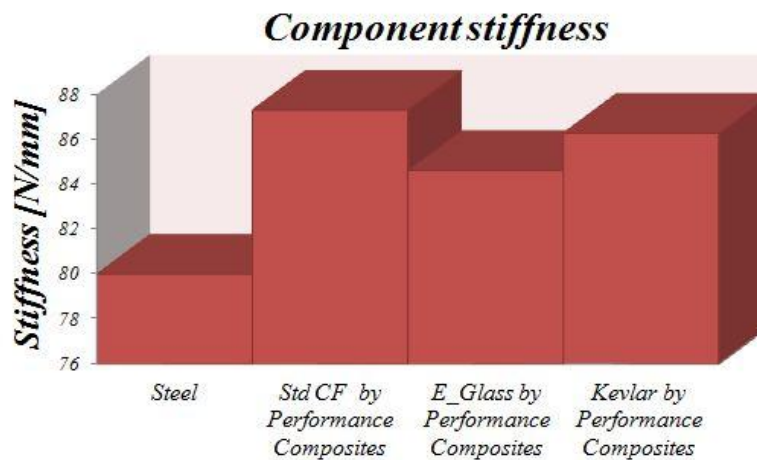


Figure 6-2: Component stiffness comparison between steel and composites

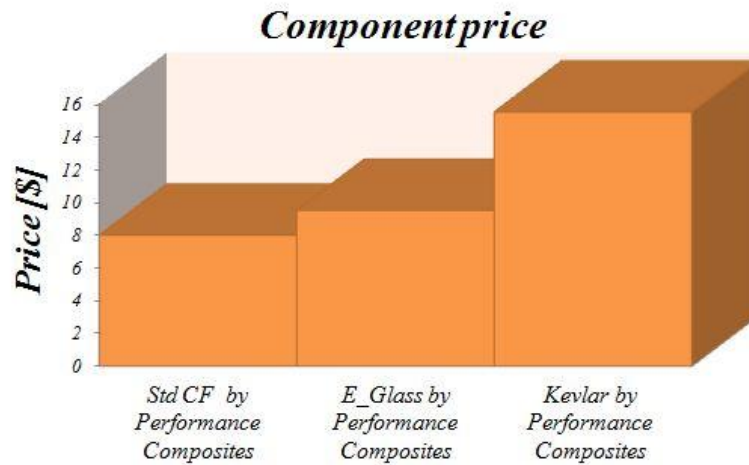


Figure 6-3: Component price comparison between carbon, glass and Kevlar fiber composites

It is interesting to notice that the three materials selected are produced as fabric and have close stiffness values.

As expected carbon fiber composite presents the lowest weight and the component cost is less than the one of Kevlar and glass fiber composite due to the higher material amount in the case of glass fiber composite and the higher fiber cost in the case of Kevlar fiber composite.

Considering the information presented above the best option is the one with carbon fibers; a further investigation has been done to evaluate the delamination aspects and the failure mode. It has been assumed that the fracture occurs as a consequence of the fiber breakage.

By using the fracture theory and knowing the fracture toughness coefficient for each material, once the maximum stress is computed inside the component and assuming a complete fiber breakdown, a safety coefficient has been computed and in particular:

$$SC^{\text{StdCF}} = 1.14$$

$$SC^{\text{E_Glass}} = 1.54$$

$$SC^{\text{Kevlar}} = 1.17$$

The safety coefficient results are better put in evidence in Figure 6-4.

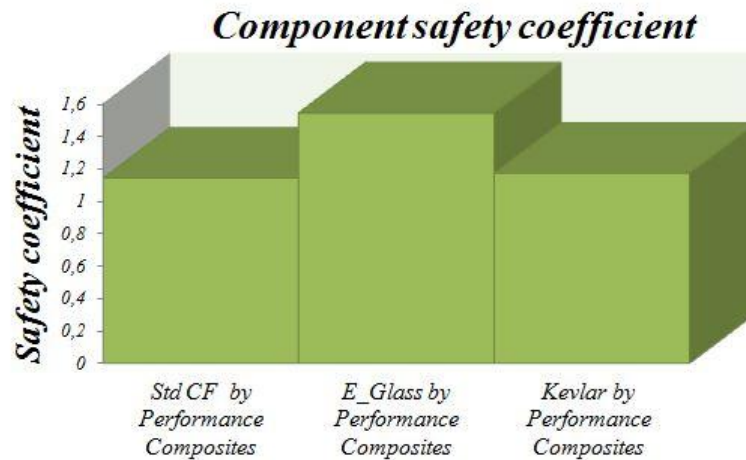


Figure 6-4: Safety coefficient comparison between carbon, glass and Kevlar fiber composites

It should be noted that glass fiber composite shows the best results in terms of safety coefficient. Considering all these aspects together, carbon and glass fiber composites provide the best results. However considering other aspects such as impact resistance or toughness, Kevlar fiber composite can present an optimal alternative though having a higher cost.

Furthermore, the manufacturing aspects have to be considered and the materials used can have a strong impact on the energy required or tooling wear. In this case study PVC resin has been selected as a matrix for optimal compromise between cost and mechanical properties.

Today there is not enough knowledge about how to manage it in composites manufacturing, and so PP or PE resins application is preferable even though at a higher cost; the mechanical response of the component will be slightly affected because the matrix mechanical properties are quite similar and the strongest effect is due to the fibrous reinforcement.

The manufacturing processes suitable for the component production are compression molding for the production of the flat, undulated and concave panels and melding, that is a novel process that allows to produce the parts independently and then the cycle is almost completed, the parts are joined together so that during the last phase of the cycle the resin cures and consolidates the components as a single piece.

In contrast, after compression molding, the several parts should be joined through adhesive bonding, mechanical fastening or other solutions. In order to select the best manufacturing process more information is required. Only after having a more detailed knowledge it is possible to identify the faster, cheaper and more reliable manufacturing process.

Specific consideration was given to the LCA and recyclability aspects; in order to do a life cycle analysis a huge amount of information is required before evaluating the CO₂ impact due to the component life. Today recyclability is not the major issue, especially for thermoplastic materials with carbon fibers, due to their optimal chemical stability during recycling processing. The only problem is the lack of an efficient recycling system and a capital investment from the companies is required to make it economically feasible. In conclusion it is evident that composite materials are one of the best alternatives for the future, but unfortunately there is not sufficient knowledge about the design, manufacturing and after life treatment.

The main causes can found in the lack of investments application and loss of confidence in the benefits that engineering polymers could bring in the replacement of the classical design based on steel solutions. As soon as these drawbacks are overcome through the efforts of engineers, technicians and companies it will be possible to see and appreciate the innovation in the everyday life.

APPENDICES

APPENDIX A

A guide to composites analysis in Abaqus environment

The software Abaqus allows to do simulations also on composite materials; the geometry can be imported from different CAD programs or created in the same program environment. The starting point consists in creating the component part in the section area appointed to the model, and more than one model can be created at the same time; the window is presented in Figure A-1 and illustrates how a model part is created and which are its properties.

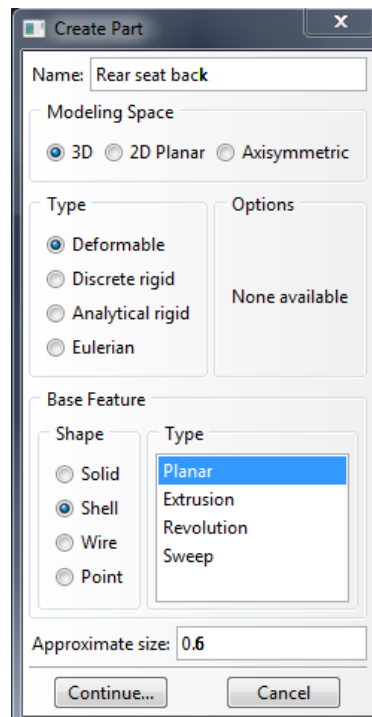


Figure A-1: Abaqus software part creation window

The user has to decide the part name, the modeling space, the type and the kind of shell. In this case study the model is built as 3D deformable, made by planar shells as illustrated in the previous figure; in the presented model extruded shell has been used at the same time. The approximate size is 0.6 m in order to respect the geometrical restrictions on the component design. Once the part is created it is possible to sketch the shell surfaces in order to create the desired component. In the features tree there is a collection of all the sketches history used to reach the final component design.

An example of sketch is provided in Figure A-2.

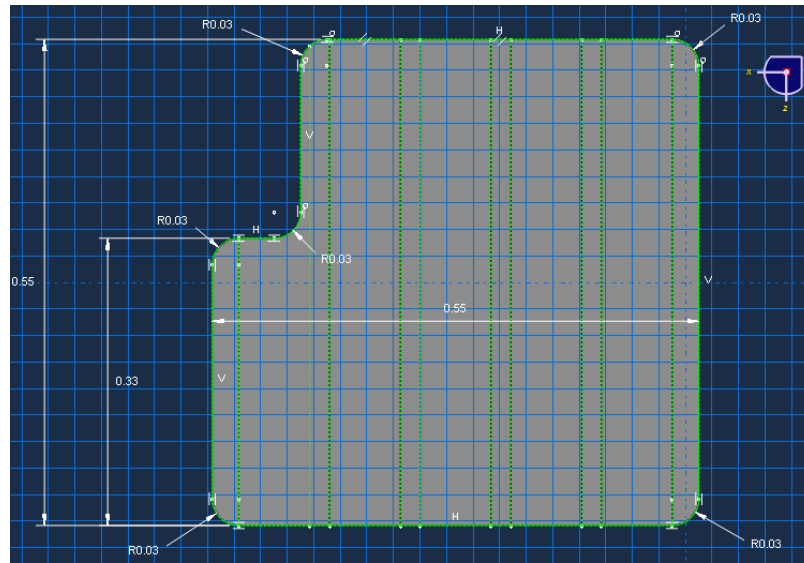


Figure A-2: Example of sketch drawing

An image of the final component design is provided in Figure A-3.

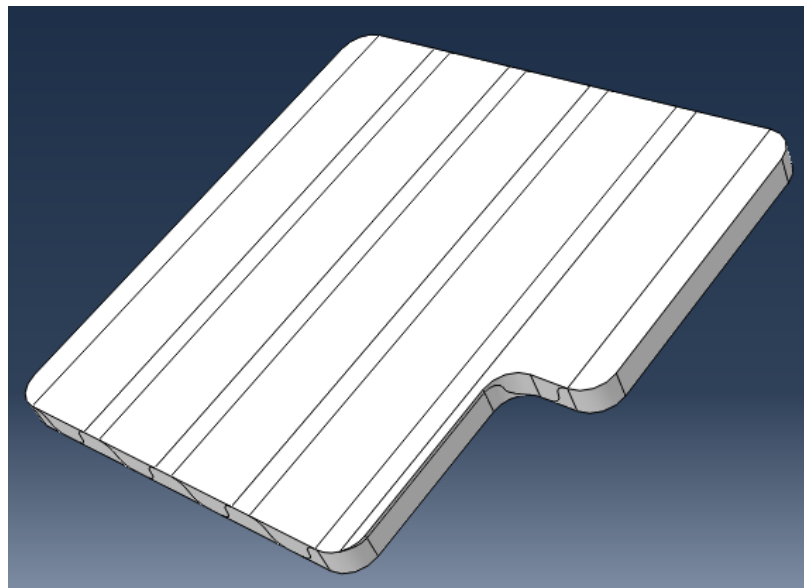


Figure A-3: Example of component design

The next step consists in defining the material properties and a new material can be introduced with the command “materials”. The input file consists of physical, mechanical, thermal, acoustical, electrical and other types of properties. For the project tasks it is enough to specify the mechanical properties and a collection of data types is presented in Figure A-4.

Name: CF composite
Description: Carbon fiber composite

Material Behaviors
Elastic

General Mechanical Thermal Other

Elastic
Type: Lamina
Use temperature-dependent data: ☐
Number of field variables: 0
Moduli time scale (for viscoelasticity): Long-term
No compression: ☐
No tension: ☐

Data

	E1	E2	Nu12	G12	G13	G23
1	85000000000	85000000000	0.1	5000000000	5000000000	2500000000

OK Cancel

Figure A-4: Composite material input data parameters

The composite material is created by selecting elastic mechanical behavior and lamina type; then all the parameters of elastic and shear modulus in Pa (Pascal) and non-dimensional Poisson ratio have to be provided. The data are not temperature dependent and the analysis takes into account both compression and tension. Once the material properties are known it is possible to create the component sections that allow the component to have different thickness in several regions and different constituent materials with different fiber orientation. The command window to create the section itself is presented in Figure A-5.

Create Section

Name: Composite Section

Category

☐ Solid
☒ Shell
☐ Beam
☐ Fluid
☐ Other

Type

Homogeneous
Composite
Membrane
Surface
General Shell Stiffness

Continue... Cancel

Figure A-5: Composite section creation command window

The options to pick are shell category and composite type; after that the lay-up can be created as shown in Figure A-6.

Name: FrontPanSec
Type: Shell / Continuum Shell, Composite
Section integration: ☒ During analysis ☐ Before analysis
Layup name:
Basic **Advanced**
Thickness integration rule: ☒ Simpson ☐ Gauss
☐ Symmetric layers

Material	Thickness	Orientation Angle	Integration Points	Ply Name
HM_NPL	0.0005	45	3	p1
HM_NPL	0.0005	-45	3	p2

Options:

Figure A-6: Composite lay-up definition during section creation

The part lay-up can be constituted by several materials with different thickness and fiber orientation angle thus allowing high variability in the component design. The section integration is performed during the analysis and Simpson integration rule is used. It is also possible to insert more data or considering them by default in the command window for an advanced analysis.

The created sections have then to be assigned to the desired parts inside the component by using the command “section assignment” opening the part folder tree. To assign a section the regions have to be picked on the component and the desired section has to be assigned to the selected areas as illustrated in Figure A-7.

Edit Section Assignment

Region
Region: (Picked)

Section
Section: FrontPanSec
Note: List contains only sections applicable to the selected regions.
Type: Shell, Composite
Material: HM_NPL

Thickness
Assignment: ☒ From section ☐ From geometry

Shell Offset
Definition: Middle surface

Figure A-7: Regions selection to assign the desired section

All the data are now available to create an instance under the command “assembly” present in the model tree; creating an independent mesh it is possible to have a mesh directly on it and in automatic way. An example of command window can be visualized in Figure A-8.

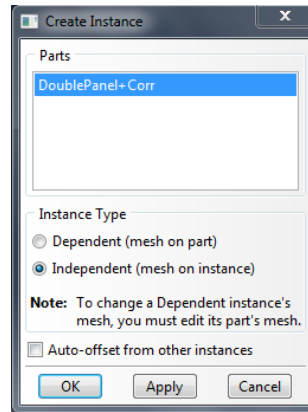


Figure A-8: Independent instance creation window

The next phase consists in creating a further step for the load condition in addition to the existing initial one. All the boundary conditions in terms of constraints and displacements or rotations can be applied to the load condition together with the load condition of the structure. In the command window it is also possible to specify the kind of analysis to be done, if static, dynamic, viscous, thermal and so on.

In the example provided in Figure A-9 the option static and general has been selected as can be seen in the following picture.

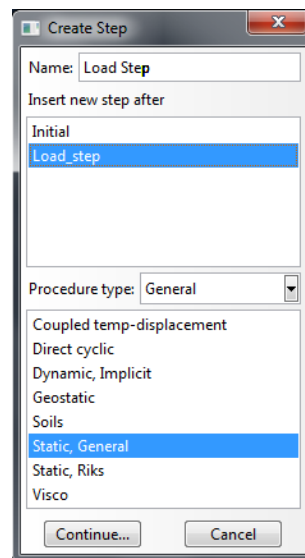


Figure A-9: Static load step creation command window

Before meshing the component the element size can be set through the commands “seed>instance”. It is also possible to use to command “seed” for edges but the procedures requires more time and the parts need to be selected each at the time. The approximate global size has been set to 0.01 m in order to have about 55 mesh elements on each edge. The minimum size factor has been set by default with value equal to 0.1. Other parameters are imposed by default and can be seen in Figure A-10.

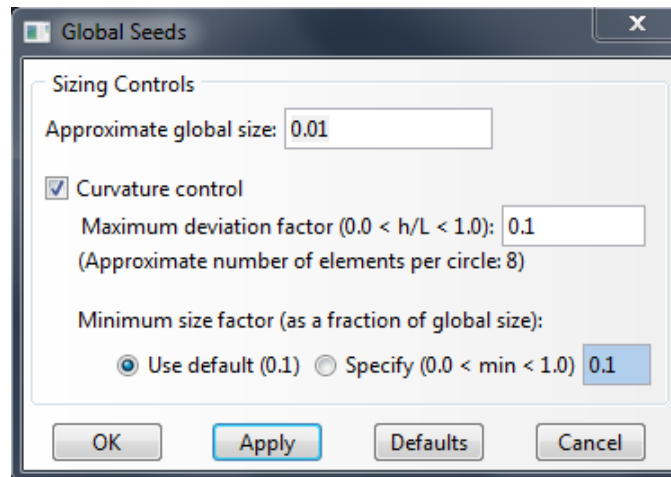


Figure A-10: Independent mesh “seed” command window

Before meshing, the mesh control can be set and the element shape is fixed as quad-dominated, free technique and advancing front algorithm using a mapped mesh where appropriate.

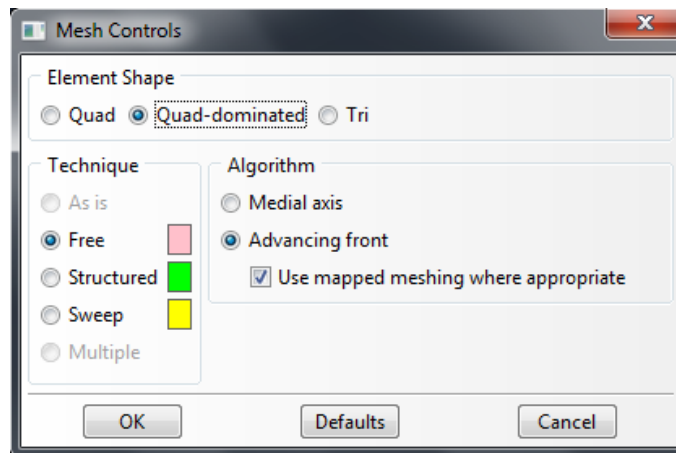


Figure A-11: Mesh control definition in terms of shape, technique and algorithm

The component can be meshed with standard elements having linear geometric order and Quad shape. All the options have been set by default and can be seen in Figure A-12.

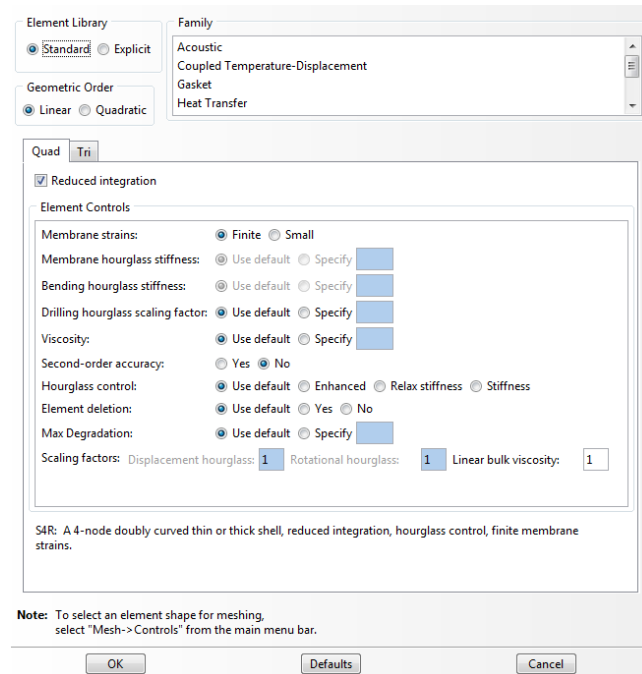


Figure A-12: Mesh elements definition default parameters

Once the parameters presented above have been set the component presents the following mesh shape as illustrated in Figure A-13.

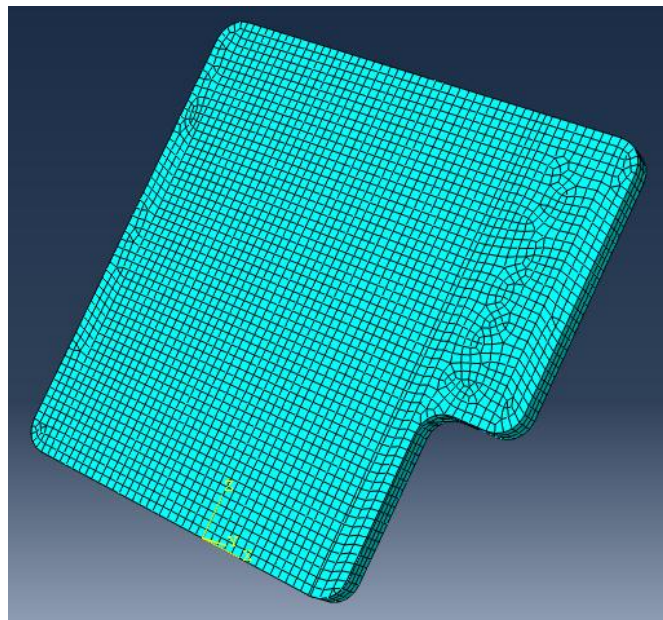


Figure A-13: Visualization of the component meshed with Quad elements

The boundary conditions can be introduced as rotations or displacements by selecting the mechanical category and have to be applied to the load step as explained previously; an example is provided in Figure A-14.

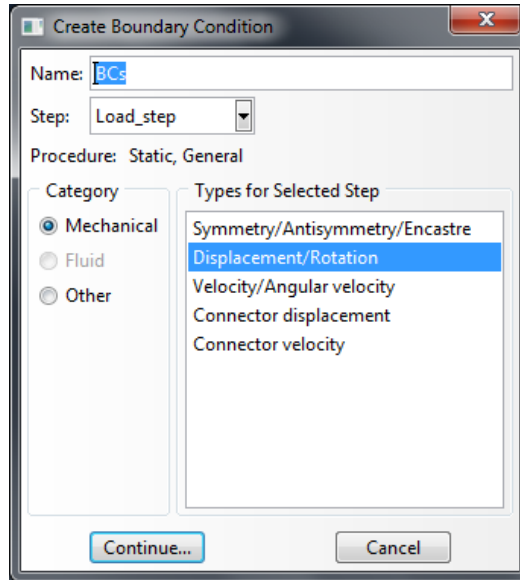


Figure A-14: Boundary conditions category and type definition command window

It is possible to impose the boundary conditions as symmetry/asymmetry/encastre, velocity/angular velocity, connector velocity or connector displacement. Then the degrees of freedom can be fixed as explained in the section regarding the model creation and the command windows for each of the boundary conditions (displacement, spherical joint and rotation hinge) can be visualized in Figure A-15.

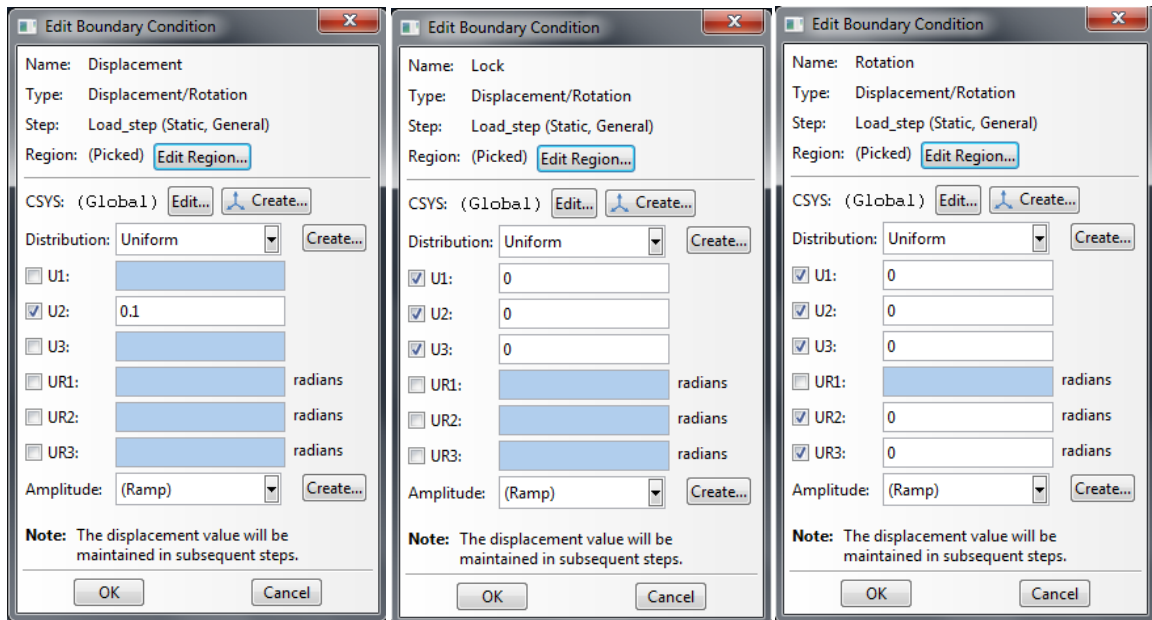


Figure A-15: Creation of boundary conditions selecting displacement and rotation

The boundary conditions are appointed to the desired area by using the command “edit region” and they can be applied on points, edges, lines, curves or surfaces.

In the project case it has been chosen to use just points in order to evaluate easier the reaction forces. Figure A-16 represents the component with all the constraints applied.

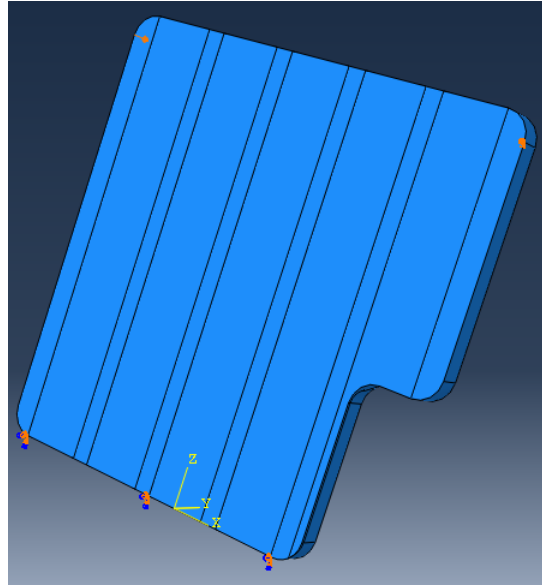


Figure A-16: Boundary conditions visualization on the component

The last step before running the simulation is to create a job, submit it and then visualize the output results. It is possible to relate each job to a particular model since the command is not included inside the model tree structure. Figure A-17 represents the job input window.

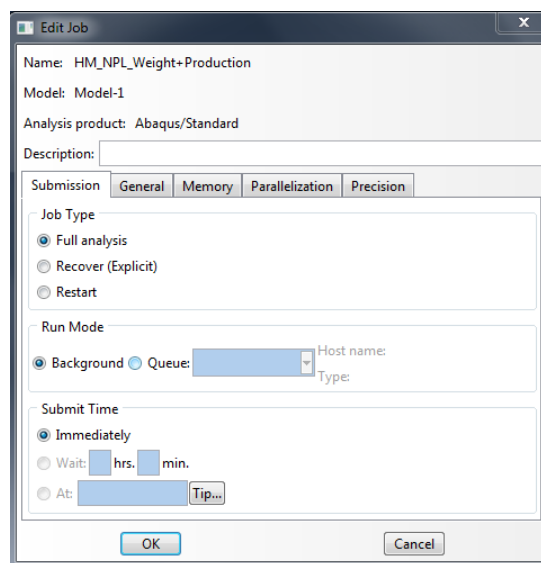


Figure A-17: Edit job command window

It is possible to change several parameters but in the example case all the data have been kept as default.

Switching to the results area it is possible to evaluate all the simulation output desired and specified with the command “field output request” present in the model tree.

The output options are stresses, strains, displacements/velocities/accelerations, forces/reactions, contact, energy, fracture/failure, thermal, electrical etc.

In the visualization mode the displacement field can be checked by asking the option U and selecting the magnitude value even if it is possible to know the deformation values in all the three directions U_1 , U_2 and U_3 along the x, y and z axis respectively.

The output values can be visualized on the structure with a color scale from red for the highest ones to dark blue for the lowest ones. It is also possible to have a numerical idea by comparing the colors with the numerical scale provided in the visualization area.

The component deformed shape appears as illustrated in Figure A-18.

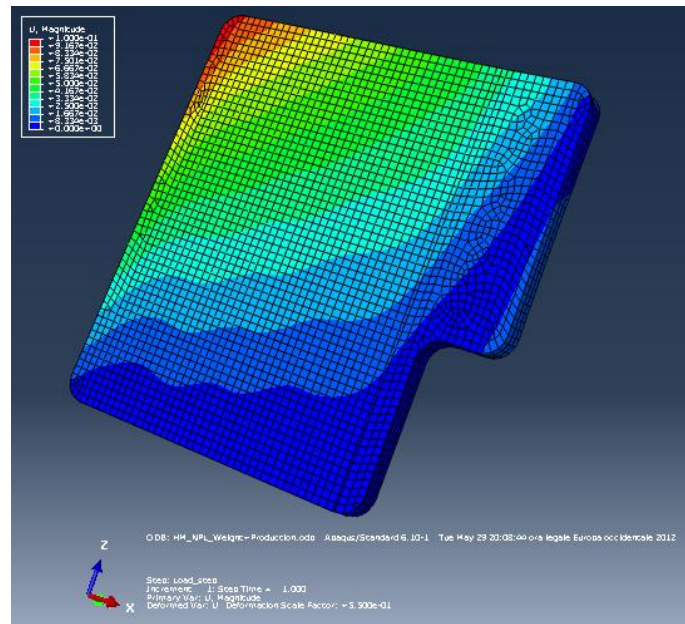


Figure A-18: Output visualization for displacement field

In order to know the force able to create 100 mm displacement the output RF allows to know the reaction forces magnitude on the whole structure. It is possible to visualize the force components RF_1 , RF_2 and RF_3 along the three axis direction and evaluate the values in each constraint point with the commands “tools>query” in order to apply the equilibrium on the structure. An example of query output window and reaction force distribution on the structure is presented in Figures A-19 and A-20.

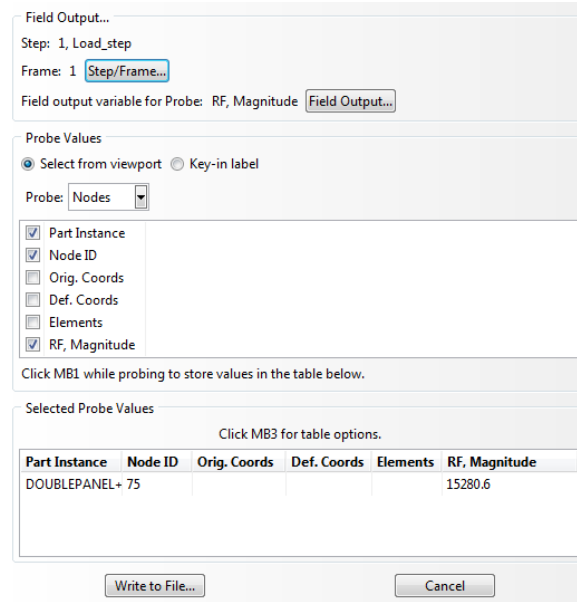


Figure A-19: Command window for output evaluation in correspondence of nodes

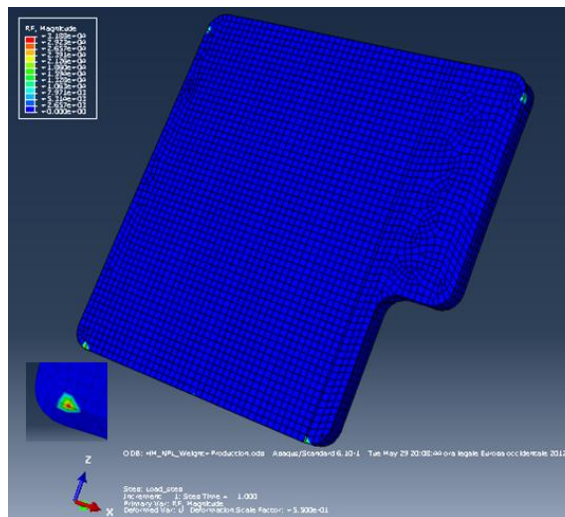


Figure A-20: Output visualization for reaction forces on the whole structure

As can be seen in Figure A-20 the forces are concentrated only in the selected boundary condition points while a uniform force distribution appears on the global structure. The force values provided by the program have no dimensions and the same occurs for the input related to geometrical dimensions and mechanical, physical, thermal, electrical and all the other properties. By using meters as dimensions during geometry construction, Pa (Pascal) for elastic and shear modulus, and kilograms for mass properties the force output dimension unit is Newton. Other output values can be investigated such as rotations, velocities, accelerations, concentrated moments, stresses, strains and so on.

REFERENCES

1. E. Mangino, J. Carruthers. "The future use of structural composite materials in the automotive industry". CRF.
2. G.S. Cole, A.M. Sherman (1995). "Lightweight materials for automotive applications". Elsevier science
3. R.A. Sullivan (2006). "Automotive carbon fiber: Opportunities and challenges". Journal of materials.
4. M. Kamiura (2008). "Toray's strategy for carbon fiber composite materials". Toray industries, Inc.
5. D.R. Cramer, D.F. Taggart (2002). "Design and manufacture of an affordable advanced-composite automotive body structure". EVS-19.
6. A. Polland. "Polymer matrix composites in driveline applications". GNK technology.
7. S. Pimenta, S.T. Pinho (2010). "Recycling carbon fiber reinforced polymers for structural applications: Technology review and market outlook". Elsevier Ltd.
8. B. Griffiths, N. Noble (2004). "Process and tooling for low cost, rapid curing of composites structures". SAMPE journal.
9. T. Corbett, M. Forrest. "Melding: A new alternative to adhesive bonding". Quickstep technology Pty Ltd.
10. R.J. Caspe, V.L. Coenen. "Through-thickness melding of advanced CFRP for aerospace applications". University of Manchester.
11. A. Ruegg, R. Ayer (2005). "Seating structures and other structural applications with locally unidirectional reinforced thermoplastic composites". Albert Weber GmbH, Germany.
12. S.Y. Yang, Y.C. Chen (1998). "Experimental study of injection-charged compression molding of thermoplastics". Advances in polymer technology.
13. S.C. Chen, Y.C. Chen (1999). "Simulations and application of injection-compression molding". Journal of reinforced plastics and composites.
14. T. Gutowski (2008). "Injection molding".
15. "Injection molding design guidelines". GE plastics.
16. (September 2004). "BASF has introduced a new, one-piece plastic seating structure that is quickly gaining commercial acceptance in the U.S. automotive industry". Jobwerx news, Michigan (U.S.A.).
17. "Case history: 3rd seat row". EATC.
18. J. Lester. "Seat back structures". Max forma plastics.

19. J. Zhang, S. He. "Lightweight stiffened composite structure with superior bending strength and stiffness for automotive floor application". Sir Lawrence Wackett Aerospace Research Centre.
20. L. Berger. "Program summary of the ACC automotive composites underbody". General Motors R&D.
21. C.W. Khanal (2010). "Manufacturing scenarios and challenges with a fabric SMC automotive underbody". USCAR, General Motors R&D.
22. L. Berger, C.W. Khanal (2010). "Material properties of a fabric sheet molding compound for a structural composite underbody". General Motors R&D.
23. H. Fuchs, E. Gillund. "Status of the composite underbody component and assembly structural test-analysis correlation". Multimatic Engineering.
24. Department of defense handbook (1997). "Composite materials handbook". Volume 3.
25. N.M. Barkoula, S.K. Garkhail (2009). "Fiber polypropylene composites effect of compounding and injection molding on the mechanical properties of flax fiber polypropylene composites". Journal of reinforced plastics and composites.
26. E.J. Garcia, B.L. Wardle (2008). "Joining pre-preg composite interfaces with aligned carbon nanotubes". Elsevier Ltd.
27. X. Li, G. Li (2011). "Optimization of composite sandwich structures subjected to combined torsion and bending stiffness requirements". Springer Science.
28. G. Alvino, A. Alloatti (2010). "Design of a composite material racing seat for formula SAE vehicle". Politecnico of Turin (Italy).
29. (February 2011). "BMW's MCV, the first mass-produced car with a carbon passenger cell". JecComposites.
30. (February-March 2010). "Interior parts go greener". Jec magazine.
31. (February 2011). "Audi and Voith form development partnership". JecComposites.
32. Elmarwritten (February 2011). "The European composite market 2008/2009". Jec Magazine.
33. (January 2011). "Daimler and Toray establish joint venture for manufacturing of automobiles parts". JecComposites.
34. K. Sehanobish (2009). "A vision for carbon fiber in the automotive market". High-performance composites.
35. J. Sloan (2012). "Automotive evolution or real revolution?". High-performance composites.
36. D. Brosius (2004). "Corvette gets leaner with carbon fiber hood". High-performance composites.

37. S. Black (2006). "Innovative Composite Design May Replace Aluminum Chassis". Composites technology.
38. S. Black (2010). "Life cycle assessment: Are composites "green"?". Composites technology.
39. P. Malnati (2010). "Interior innovation: The value proposition". Composites technology.
40. P. Malnati (2011). "Thermoplastic composites: Sustainable transports". Composites technology.
41. P. Malnati (2011). "Under the hood: Thermoplastics tackle tough jobs". Composites technology.
42. T. Robert (2004). "Manufacturing Processes Reference Guide". New York: Industrial P, Incorporated.
43. S. Kalpakjian, S.R. Schmid. "Manufacturing Engineering and Technology 5th Edition".
44. D.M. Bryce (1996). "Plastic Injection Molding: Manufacturing Process Fundamentals". SME, 1996.
45. D. Della Volpe (2008). "Modeling of water transport in sandwich composite structures for aerospace applications". "Federico II" University, Naples (Italy).
46. G. Belingardi, M.P. Cavatorta (2003). "Material characterization of a composite-foam sandwich for the front structure of a high speed train". Elsevier science Ltd.
47. A.T. Travesa (2006). "Simulation of delamination in composites under quasi-static and fatigue loading using cohesive zone models". Faculty of engineering, University of Girona (Spain).
48. P. Agastra (2004). "Mixed mode delamination of glass fiber/polymer matrix composites material". Montana State University, Bozeman.
49. V. Stoilov, J.F. Su. "Characterization of fracture and debonding of Si particles in AlSi alloys". Faculty of mechanical, automotive and material engineering, University of Windsor, Windsor, Ontario (Canada).
50. V. Stoilov, O. Rashwan (2012). "Numerical model of microstructure and fracture of coated aluminum alloys: A novel design approach". Faculty of engineering, University of Windsor, Windsor, ON, (Canada)
51. B.A. Miller (2002). "Overload failures, failure analysis and prevention". ASM Handbook Vol. 11 p. 671-699.
52. T. Czigany, J. Vad (2005). "Basalt fiber as a reinforcement of polymer composites". Periodica politechnica Ser. Mech. Eng., Vol. 49 pages 3-14.

WEBSITES VISITED

53. <http://engr.bd.psu.edu/rxm61/METBD470/Lectures/PolymerProperties%20from%20CES>
54. http://www.performance-composites.com/carbonfibre/mechanicalproperties_2.asp
55. http://www.agy.com/technical_info/graphics_PDFs/Advanced_Materials.pdf
56. http://www.kayelaby.npl.co.uk/general_physics/2_2/2_2_2.html
57. <http://www.substech.com/dokuwiki/punbb/upload/viewtopic.php?id=7>
58. <http://www.tech.plym.ac.uk/sme/MATS324/MATS324A2%20E-G-nu.htm>
59. <http://research.me.udel.edu/~dlburris/images/chart6.jpg>
60. http://alexpb.com/notes/wp-content/uploads/2007/12/compression_molding.png
61. http://alexpb.com/notes/wp-content/uploads/2007/12/transfer_molding.png
62. <http://www.custompartnet.com/wu/InjectionMolding>

VITA AUCTORIS

NAME: Gerardo Alvino

PLACE OF BIRTH: Atripalda, AV, (Italy)

YEAR OF BIRTH: 1988

EDUCATION: Scientific high school “Leonardo Da Vinci”, Calitri, AV, (Italy)
2002-2007

Politecnico of Turin, Facoltà di Ingegneria dell’Autoveicolo, TO, (Italy)
2007-2010 Bachelor degree

Politecnico of Turin, Faculty of Automotive Engineering, TO, (Italy)
2010-2012 Second level degree

University of Windsor, Faculty of Mechanical Engineering, Windsor, ON
2011-2012 Master of Applied Science